THE DISTRIBUTION OF STRESS-STRAIN RESULTANTS IN PRESTRESSED CONCRETE PORTAL FRAMES

by

Ashit Kumar Chatterji

A thesis submitted for the Degree of
Doctor of Philosophy
in the
Faculty of Engineering
of the
University of London

Imperial College of Science and Technology,
London

September, 1968

ABSTRACT.

The earlier part of this thesis deals with the testing of ten post-tensioned prestressed concrete I beams, according to an international testing programme of the European Concrete Committee. Under this scheme, the behaviour of ten simply supported beams were studied, under central point loads, to investigate the effects of the variation of the following parameters:-

1) the neutral axis depth,
2) the prestressing force
3) the spacing of binders.

The inelastic rotations observed in over-reinforced I beams, made it possible for the author to visualize that adequate inelastic rotations could be expected at highly over-reinforced critical sections to justify full redistribution of moments in a prestressed frame, provided that these sections were reinforced with an adequate quantity of binders.

The later part of this thesis deals with tests continued on post-tensioned prestressed columns and portal frames. Experimental evidence has been obtained to demonstrate the following points:-

1) An over-reinforced prestressed I-section is highly brittle; it is more brittle than a rectangular section having the same overall dimensions and the same quantity of reinforcement. It may prematurely fail by web buckling, before a frame attains the state of a complete collapse mechanism.

2) However, with an adequate quantity of binders, not only members having over-reinforced critical I-sections, but also heavily loaded columns, exhibit enough ductility to justify full re-distribution of moments in a frame.

The use of the effective 'EI' concept, in a non-linear analysis of prestressed concrete structures, has been discussed in Chapter V.

The possibility of a quick and effecient method for adjusting 'θ_{pi}' values as required in Baker's Limit design method, has been discussed in Chapter 7. A method of analyzing two span continuous prestressed beams, using Macchi's Imposed Rotation coefficient has been discussed in this chapter. Three continuous beams tested in the Cement and Concrete Association were analyzed by this method.

ACKNOWLEDGEMENTS.

The author wishes to thank Professor A.L.L.Baker for his invaluable supervision and guidance and encouragement.

He expresses gratitude to Dr. A.D.Edwards, for his assistance and sound advice, in planning the experiments and compiling the thesis.

He is grateful to Dr. C.W.Yu for his immense help in carrying out the test programme. He is also grateful to Mr. K. Newman for his assistance in the design of mixes and to Mr. R.W.Loveday for his suggestions in the design of the testing devices. He wishes to thank his friends and technicians in the laboratory for their co-operation and help.

He wishes to thank the Cement and Concrete Association for their valuable assistance and permission to use the 'Serius' computer installed in their premises. He is personally obliged to Dr. Cranston for his verbal communications, assistance and for lending his 'M-P-φ-θ programme to the author.

Finally, he is grateful to the Govt. of U.P., India, for the award of a loan and extension of leave to stay in this country, which made it possible for the author to complete this project.

CONTENTS

NOTATION.

DIMENSIONS.

x = distance measured from L.H. support of a beam.
 = length of a beam between supports
$2\ell_u$ = length of uncracked part of a simply supported beam subjected to a conc. load at centre.
$2\ell_c$ = cracked length of a simply supported beam subjected to a conc. load at centre.
Z = distance of critical section to point of contra-flexure.
b = breadth of a rectangular beam; flange width in I (beam.
b' = web width in I beam.
d = distance of the extreme fibre 2, from the C.G. of tendons

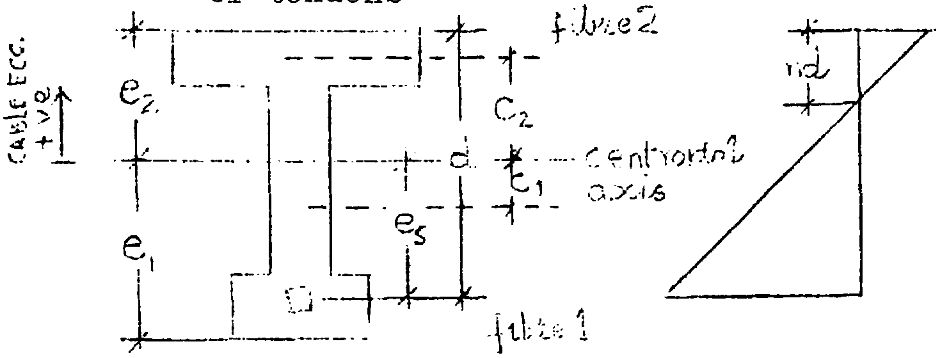

nd = depth of neutral axis from fibre 2 in general
n_1d = do. at the state L_1
n_2d = do. " " " L_2
td = depth of the compression flange in I beam.
A = gross X-sectional area.
I = moment of inertia
e_1 = distance of extreme fibre 1 from centroid.
e_2 = " " " " 2 " "
Z_1 = $\frac{I}{e_1}$ $Z_2 = \frac{I}{e_2}$
C_1 = distance of boundary of limiting zone from centroid measured in direction fibre 1.
C_2 = do from centroid measured in direction fibre 2.
e_s = eccentricity of cable from centroid measured positively towards fibre 2.
jd = lever arm
γnd = distance of extreme fibre 2 from the centre of compression.
D = overall depth of section.

Area of steel.

As = Area of steel in tension
A's = Area of steel in compression.
p = $\frac{As}{bd} \times 100$ (in rectangular beams).
p' = $\frac{A's}{bd} \times 100$

Area of steel (cont.)

p'' = percentage of lateral binders
$= \frac{\text{volume of binders per unit length}}{\text{effective volume of concrete bound}} \times 100$

$\omega = \frac{As}{bd} \cdot \frac{f_{su}}{C_c}$ (If the idealized stress strain curve of steel is used $= \frac{As}{bd} \cdot \frac{f_{s2}}{C_c}$)

Beam properties.

Ec = modulus of elasticity of concrete in general
Es = modulus of elasticity of steel in general.
E'I' = uncracked flexural rigidity
EI = cracked flexural rigidity at the state L_1
K , e.g. in $\frac{K}{CA}\int S_r S_s ds$ is a constant to account for the fact that shear stress distribution is not uniform in a section.
C = modulus of Rigidity

Strength of concrete, stresses and strains and stress block parameters.

C_c = standard 12" cylinder strength.
C_u = standard 6" cube strength.
$\bar{C}_c$ = maximum compressive stress in concrete in flexure as permitted in the Ankara stress block.
f''_c = do in Hognestad's stress block.
f_c = compressive stress in a concrete fibre in general
f_s = stress in tension reinforcement in general
f_{s1} = stress in tension reinforcement at L_1
f_{s2} = " " " " " L_2
f_{sy} = " " " " " at yielding or 1% offset strain*
f_{su} = max." " " " at rupture
e_c = compressive strain in concrete in fibre 2 in gen.
e_{c1} = " " " " " " " at L_1
e_{c2} = " " " " " " " " L_2
e_{cp} = prestress strain in concrete at the level of C.G. of tendons after losses at commencement of loading.
e_{2cp} & e_{1cp} = strains in concrete at fibres 2 and 1, due to prestress at commencement of loading.
e_{cs2} = increment in the strain in concrete at the level of C.G. of tendons, from the state of zero stress and strain, at L_2.
(i.e., from a state prior to application of prestress).
e_{cs1} = do at the state L_1
e_{sy} = strain in steel at yield or 1% proof stress
e_{s1*} = strain in steel at the state L_1
e_{s2} = strain in steel at the state L_2
e_{su} = maximum strain in steel at rupture.

* for under-reinforced beams $f_{s1} = f_{sy}$
$e_{s1} = e_{sy}$

Strength of concrete etc. (cont)

α = ratio of average compressive stress in concrete to C_c

γ = ratio of depth of effective compressive force in concrete to neutral axis depth.

Forces and Moments.

W = lateral load generally

m, M = bending moment generally

M^*, m^* = plastic moment of resistance generally

N = axial thrust generally.

M_{max} = max. B.M. attained by a critical section under test

M_1 = calculated B.M. at L_1

M_2 = " " " L_2

C = total compressive force acting on the area of concrete in a section.

T = total tension acting on the area of steel

$m_1 = \dfrac{M_1}{C_c bd^2}$, $m_2 = \dfrac{M_2}{C_c bd^2}$ — both for rectangular and I beams.

Deformations and parameters influencing inelasticity.

$K = \frac{1}{R}$ = curvature generally.

θ = total rotation in a beam between point of contraflexure and critical section

θ_p = permissible inelastic rotation at hinge on one side of critical section.

ℓ_p = equivalent plastic hinge length on one side of critical section

h_L = length of beam over which inelasticity occurs, on one side of critical section.

β = shape factor

K_1 = parameter for influence of steel in the expression for θ_p

K_3 = parameter for influence of concrete in the expression for θ_p

LIMITS OF THE BILINEAR AND TRILINEAR IDEALIZATION.

TriLinear.

L_{-2} = state of prestress only

L_{-1} = state of zero concrete stress adjacent to the position of the resultant of cable tensions.

L_{op} = state of ultimate concrete tensile stress at Fibre 1.

L_{1p} = yield state, the same as L_1 in bilinear idealization, excepting that cracked and uncracked flexural rigidity are accounted for in calculating rotations.

L_{2p} = ultimate state, the same as L_2 in bilinear idealization (the rotation at this stage is derived from the rotation at L_{1p}).

The corresponding moments at L_{-2}, L_{-1} and L_{op} are M_{-2}, M_{-1} and M_{op}.

BiLinear.

L_1 = yield state, i.e., at which cable attains .001 offset strain or mild steel attains yield strain, OR concrete attains .002 direct strain at Fibre 2, whichever is earlier.

The beam is assumed to be cracked throughout in calculating rotations.

L_2 = ultimate state, at which cable attains a strain of .01 * OR concrete attains the maximum permissible strain as discussed in the Ankara stress block, whichever is earlier.

* (In case of H.T. tendons, this is not defined and the criteria for the limiting strain in concrete has been used.)

MISCELLANEOUS.

In analysis of indeterminate structures.

n = number of statical indeterminacy

s = total number of critical sections where hinges may develop.

θ_i = the total discontinuity measured in radians at the i^{th} hinge, at all phases of loading, when a structure has been made statically determinate by the insertion of n hinge releases.

M_i = the ordinates of the diagram representing the distribution of bending moment when unit moment acts on the reduced structure at the i^{th} hinge.

M_k = - do - for unit moment at k^{th} hinge.

ds = a small increment of length in the direction of the frame members.

θ_{pj}, θ_{pi} = total plastic rotations at the critical sections j and i, assumed to be concentrated at the section. (A cracked modulus of rigidity = EI is assumed in the rest of the structure.)

M_o = the ordinates of the bending moment distribution when external load acts on the reduced structure.

$\bar{X}_k$ = restraint moment at the k^{th} hinge of the released structure.

θ'_{pi} = concentrated plastic rotation over a short length at the i^{th} hinge when an uncracked modulus of rigidity E'I', is assumed in the rest of the structure.

γ'_{pj} = concentrated plastic rotation over a short length at intermediate critical sections between the chosen releases, when an uncracked E'I' value is assumed.

CHAPTER 1

INTRODUCTION

1.1 Behaviour of a structure beyond the elastic limit.

An elastic analysis of any structure only ensures a factor by which the working loads may be increased before yield or inelasticity would occur at one of the critical sections of the structure. The effect of further increase in load cannot be determined by the elastic analysis.[39] The spread of inelasticity due to further increase of load causes a redistribution of moments. In other words, the bending moment at the section where yielding first occurs, rises at a much slower rate, and permits the application of further load till yielding occurs at a second point. A hinge action thus occurs at the section while the bending moment transmitted across it is practically constant. The structure finally collapses when sufficient number of hinges have developed to transform the structure into a mechanism.

1.2 Collapse load method for steel structures.

The redistribution of moments is possible only due to the existence of a nonlinear part in the constitutive relations of the material of which the structure is made. This does not create any serious problem in steel structures, because the moment curvature relationship can be idealized to an elastic-plastic behaviour (Fig. 1.1).

This idealization combined with the hypothesis that a plastic hinge can undergo rotations of any magnitude, led to the development of a simple plastic method of calculating collapse loads in framed structures, by J.F. Baker and his colleagues in Cambridge.[39]

1.3 A plastic design method for concrete structures.

In reinforced concrete and pre-stressed concrete structures, any idealization tends to be much more approximate. And in addition, a more serious limitation exists, which is the limited rotational capacities of the critical sections. This limitation in the ductility of concrete was recognised by Prof. A.L.L.Baker, and one of the main features of his simplified Limit design method is the checking and adjustment of rotations at the critical sections, within permissible limits.[6]

1.4 Idealization in prestressed concrete.

A bilinear idealization of the moment curvature or the moment rotation relationship, usually deviates considerably from the true behaviour of a prestressed concrete structural member. The latter exhibits a uniform stiffness until cracking, followed by a gradual decrease in stiffness until failure occurs, A trilinear idealization has been suggested for prestressed concrete[13] to recognize this behaviour.

1.5 The compatibility problem in plastic analysis.

The necessary conditions for analyzing a structure at the ultimate are:-

1) The conditions of statical equilibrium must be satisfied.
2) The continuity of the structure must be maintained at all points of the structure up to the point of collapse.
3) The ultimate load carrying capacity of a particular section has to be determined vis-a-vis, the stress strain characteristics of both concrete and steel; the usual assumption made in this connection is that plane sections remain plane up to the limit of collapse.

The most difficult part of the problem is to be able to comply with the rapidly changing moment deformation characteristics in the inelastic range.

In an 'n' times statically indeterminate structure, which has been made statically determinate by introducing 'n' hinge releases, the following equation represents the discontinuous rotation at the i^{th} hinge.

$$\theta_i = \int M_i K ds \quad \text{—— 1·1}$$

An idealized bilinear moment curvature relation is shown in Fig. 1.2.

Sawyer [45] pointed out that the total curvature at a point, could be broken up as the sum of an elastic and a plastic effect (shown as k_E and k_p in this diagram).

From 1.1,

$$\theta_i = \int M_i K_E ds + \int M_i K_p ds$$

Assuming that the total plastic effect in the neighbourhood of a critical section is equivalent to a concentrated rotation at that point, (i.e., $\theta_{pj} = \int K_p ds$, for values of j from $1 \cdots S$ where S is the total number of critical sections we obtain

$$\theta_i = \int M_i \frac{M}{EI} ds + \sum M_i \theta_{pj}, \; j = 1 \cdots S$$

The bending moment M, at a section of the structure can be assumed to be the algebraic sum of the moment caused by the external loads acting on the reduced structure with n releases, and the moments at that section caused by the restraints at the releases.

In other words

$$M = M_o + \sum \overline{X}_K M_K$$

$$\therefore \; \theta_i = \int \frac{M_i M_o}{EI} ds + \sum \overline{X}_K \int \frac{M_i M_K}{EI} ds + \sum M_i \theta_{pj}, \; j = 1 \cdots S \qquad \text{------ } 1.2$$

1.6 <u>Baker's method of analysis.</u>

Baker, in his simplified Limit design approach,(6) suggests a method to find out a possible solution to the problem when the structure develops only 'n' plastic hinges at the chosen releases. The plastic rotations at the remaining s-n hinges, at this stage are therefore zero. The section properties of the members are chosen in such a way that hinges are likely to form at the chosen points, and not in between them. An advantage is taken of the fact that the moment of resistance of concrete sections can be easily altered by adjusting the area of the steel, without substantially changing the flexural rigidity and therefore the elastic stress resultant distribution.

Now the value of M_i at the i^{th} critical section is unity and at all other releases, it is zero. Also remembering that there is no plasticity excepting at the n releases, equation 1.2 reduces to

$$\underset{=0}{\theta_i} = \int \frac{M_i M_0}{EI} ds + \underbrace{\sum \overline{X}_K \int \frac{M_i M_K}{EI} ds}_{\text{for continuity}} + \theta_{pi} \qquad \text{—— 1.3}$$

An important feature of the proposed method is that $\overline{X}_1$, $\overline{X}_2$ etc, can be chosen in such a way that the values of θ_{pi} are within safe prescribed limits. The problem of compatibility set forth in equation 1.3 has to be satisfied at all the 'n' hinges.

Yu, Poologasoundranayagom and Tokarski [40,41,42] carried out a considerable work in these lines and suggested practical methods of choosing the $\overline{X}$ values and adjusting the θ_{pi} values. The check on serviceability conditions is done by adjusting the θ_{pi} values to zero. Nowhere in the structure, the elastic bending moment so found must exceed a value which may give rise to excessive cracking.

1.7 Difficulties of the Simplified Limit Design Method.

Baker seeks one of the possible solutions when the structure is still statically determinate. The

Uniqueness theorem applicable to steel structures at the state of collapse, is not applicable at this stage.

It is also not certain that a compatible solution exists at all, for the position and direction of assumed hinges. Amarakone [2] has recently shown that the influence coefficient characteristics of the assumed hinge system must satisfy certain conditions in order that the system may be suitable for inelastic compatibility analysis.

Although Baker has considerably simplified the problem, yet the fact remains that even with the above simplifications, the adjustment of rotations present a considerable difficulty which has not yet been successfully overcome. The published graphs in the Concrete Series design booklet, [42] can be used in conjunction with a particular bending moment distribution assumed in preparing these graphs. Designers have to draw their own curves if they want to improve upon the bending moment distribution. The difficulty lies in the fact that the rotation at a particular section can only be adjusted by altering the bending moment distribution which in turn, affects the rotations at other hinges. Further to check on the serviceability condition, it is necessary to adjust the rotations approximately to zero. This itself is a difficult task and amounts to solving a number of simultaneous equations by trial and error.

Synopsis of author's work.

1.8 The author in his investigations has made an attempt to find out the extent to which the ductility of concrete can be improved, under adverse conditions by the use of closely spaced binders. He has also suggested a method which would reduce the adjustment of rotations from a trial and error procedure to a systematic direct method, in those cases where a standard pattern of building construction is followed.

Brief summary of next chapter.

1.9 In the next chapter, the basic ideas of a limit design have been discussed in greater detail and the necessity of a correlated result obtained from a large number of tests carried out on simple beams, as suggested by C.E.B. has been explained. Computation charts for calculating the idealized limits, obtained with the help of a digital computer, have been presented.

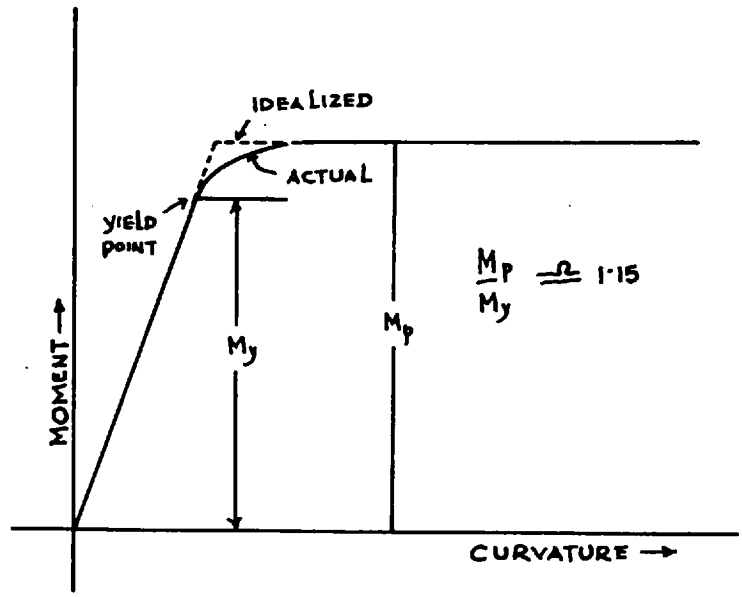

FIG 1.1

MOMENT CURVATURE IDEALIZATION (STEEL STRUCTURE)

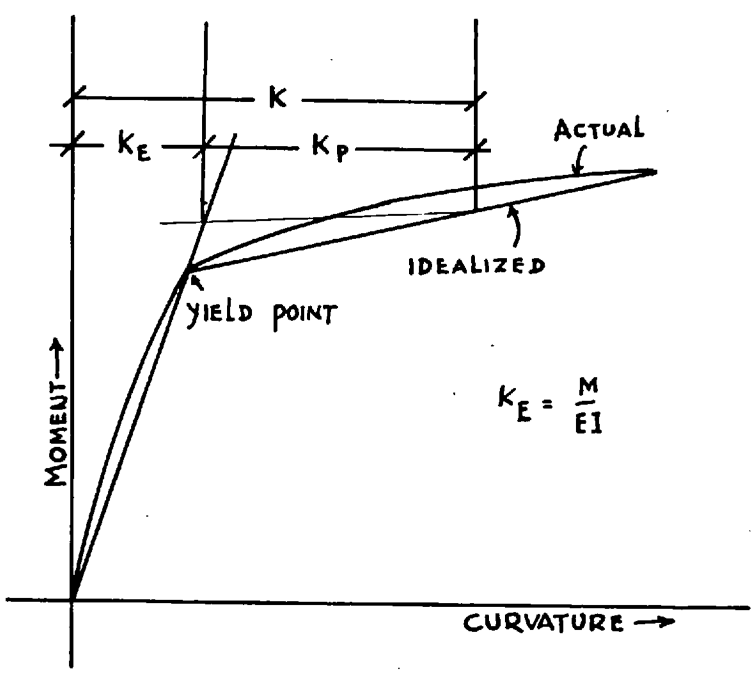

FIG 1.2

POSSIBLE BILINEAR IDEALIZATION IN REINFORCED CONCRETE

CHAPTER 2.

INELASTICITY IN SIMPLE MEMBERS.

2.1. Influence of steel and concrete in the non linear behaviour of structural concrete.

When a stress resultant, such as bending moment, at a critical section is plotted against the corresponding strain resultant such as 'curvature' at the section or the rotation of the member as a whole, we observe that at a particular stage the curve becomes non-linear with decreasing stiffness, with increasing moment. This inelastic behaviour is primarily due to the non-linear part of the stress strain curve of the material of which the section is composed. (Figs.2.1 and 2.2.) Thus, the stress-strain curves of both steel and concrete have their influences. The under-reinforced beam develops large curvatures due to the yielding of the steel, and in case of mild steel, the moment rotation curve of such a beam can be idealized to an elasto plastic behaviour. The load deformation characteristic of an over-reinforced member, however, follows more closely the pattern of the stress strain relation of concrete, which does not have a sharp yield point.

2.2 Moment curvature relationship - its difficulties.

The knowledge of a moment curvature pattern which can be applied to all the sections of a member, is necessary if the load deformation characteristics of the structure are required. Assuming that the stress-strain curves of concrete and steel are given, a section of known properties, must have a unique position of neutral axis for a given bending moment, so that the following basic requirements are fulfilled.

1) The strain in the extreme fibre in concrete and the strain in steel* are proportional to their distances from the neutral axis.

2) Total tension = Total compression.

3) Moment of all the internal forces about the centroid = applied moment.

The curvature can thereafter be calculated from the relation

$$\frac{1}{R} = K = \frac{e_c}{nd} \quad \ldots\ldots\ldots\ldots\ldots\ldots(2.1)$$

A theoretical moment curvature relation therefore exists satisfying the above criteria. Unfortunately the moment curvature relationship actually followed by a section of a loaded member is influenced by other factors not included in this criteria and the theoretical relation so obtained may not be of significant practical value.

A considerable amount of work on the stress-strain curve of concrete under flexure has been done, the most significant being that due to Hognestad and that due to Rusch. These curves give a very good estimate of the plastic moment, but usually they do not give a correct picture of the neutral axis and the strain in the extreme fibre, in the neighbourhood of the ultimate load. Baker and Amarakone suggested an improvement in this respect in a paper presented to the Hyperstatic symposium of the E.C.C. at Ankara in Sept. 64, which was also

* In case of prestressed structures, the increment of strain in concrete at the level of the steel, from a condition of zero strain, must be considered.

discussed in the Institute of Structural Engineers, London, on 30th March 1965.[11] The stress block recommended in this paper gives a fair estimate of the ultimate strain, but the estimate of the position of the neutral axis is still poor. Further research has recently been completed at the Imperial College in this direction.[47]

We observe that the prediction of a correct moment curvature relationship, based on theory alone has not yet been possible. The situation is much worsened by the fact that all the sections of a frame member do not obey the same moment curvature relationship. This is due to bond slip, local concentration of cracks, suspected arch action, or any other cause, which is not fully understood. In a series of tests on reinforced concrete beams, subjected to a central point load, Edwards observed that sections which were away from the critical section, yielded at a bending moment lower than the yield moment at the critical section.[25] A tied arch action (Fig.2.3) may be one of the causes responsible for an increase in steel stresses towards the supports, causing yielding of the steel earlier than anticipated. Edwards has further pointed out that if the moment curvature relation has a drooping portion, it is not possible for other sections near the critical, to follow the same route, unless reductions are noticed in the curvatures at those points with a consequent total reduction in the deflection, when a beam is sustaining a lower load after the peak value.

In the case of prestressed concrete beams, it was found by the author that the sections which are slightly away from the critical section, are actually stiffer. This was due to a tendency of concentration of cracks at the critical section. Increased curvatures near the cracks in prestressed concrete have been observed by others. Bennet pointed out in the 2nd Congress of the Federation Internationale held in Amsterdam in August and September 55, that it appeared probable that the deformation of a prestressed beam was brought out mainly by severe curvatures in the vicinity of cracks, rather than uniform curvature.[19]

An analysis made on the basis of an experimental moment curvature relation has therefore to be used with caution. Perhaps an upper and a lower bound can be fixed for the purpose of analysis, based on a considerable number of tests.

2.3 Moment Rotation characteristics of structural members.

As seen above, the relation between the applied moment and the curvature attained, is not a function of the section properties only. It has been realized by the C.E.B. that the moment rotation relationship, which gives an integrated deformation diagram of the member as a whole, is much more useful. Guyon also suggested the investigation of a moment rotation relationship of a plastic hinge.[29] A rotation between the end supports, obtained from a test conducted on a simply supported beam, takes into account the effect of the variation in the flexural rigidity throughout the member and evaluates the expression $\frac{M}{EI}$ ds along the length of the beam. It is possible to use this integrated rotation in the analysis of a frame, a member of which is subjected to a similar bending moment distribution between points of contraflexure. The moment rotation curves also directly give an idea of the amount of the plastic rotation possible at the critical section of a particular member.

2.4 C.E.B Programme - author's task in the schedule.

The C.E.B. planned an extensive programme of testing a large number of beams so that safe empirical values of the available hinge rotations were obtained from sufficient statistical data. Bannerr[14] first observed that the most influential parameter in determining the value of the plastic rotation, is the depth of the neutral axis at ultimate. In the first five I beams tested by the author, which are described in the next chapter, an attempt was made to study the influence of the neutral axis in case of prestressed beams. This was achieved by changing the amount of reinforcement. The next five beams were devoted to the study of the influence of the prestressing force, and lateral binding in the compression flange.

2.5 Development of equations for calculating Idealized limits.

The stress block in concrete under compression.

The distribution of stress in a cross-section under a flexural effect, has been the subject of extensive research. As the distance of the point of observation, measured from the neutral axis increases, the strain increases linearly, but not the stress. Assuming that all the concrete fibres obey the same stress-strain law, (which is not true due to a difference in the rate of straining at the level of each fibre) the distribution of stress can be plotted against the distance from the neutral axis from a typical stress-strain curve of concrete. This distribution is known as the stress-block.

The stress block suggested by Hognestad, Fig. 2.4, gives an estimate of the ultimate moment for unbound concrete. In fact the moment at the ultimate is very little affected by the assumed shape of the stress block, because a change in the stress block is accompanied by a compensating change in the lever arm. However, a refinement to the above was felt necessary, to permit more correct evaluation of the strain values, and the position of the neutral axis at ultimate. The stress block suggested by Baker at Ankara, Fig. 2.5, is a considerable improvement in this respect and has been adopted by the author in all computations in this thesis.

Derivation of expressions for α and γ at L_2

The Ankara stress block mainly differs from the previous blocks in the respect that it permits the use of strains in concrete higher than .0035, according to the formula

$$e_2 = .0015\ (1 + 1.5p'' + (0.7 - 0.1p'')\ \frac{1}{n_2}) \ldots\ldots 2.2$$

e_2 therefore depends on the neutral axis and the percentage of lateral binding.

It also permits a little reduction in the maximum flexural stress for large values of the neutral axis, according to the formula

$$\frac{\bar{C}_c}{C_c} = 0.8 + \frac{0.1}{n_2}$$

(An upper limit of 1.00 is operative for small values of n_2).

Let qd be that part of the neutral axis in which a strain of .002 is attained. (Fig. 2.6) The stress block is parabolic up to this point.

$$q = \frac{.002}{e_c}.n \quad , \quad \text{if } k = \frac{.002}{e_c} \quad , \quad q = kn$$

$$s = n - q = n(1-k)$$

$$\text{Now } \alpha = \frac{\frac{2}{3}q + s}{n} = \frac{2q + 3s}{3n} = \frac{2kn+3n-3kn}{3n} = 1-\frac{k}{3} \text{ ---2.3}$$

$$\gamma = \frac{\frac{s^2}{2} + \frac{2}{3}q\ (s+\frac{3}{8}q)}{n} = \frac{(1-k)^2/2+ \frac{2}{3}k(1-k+\frac{3}{8}k)}{1-k/3}$$

$$= \frac{6+6k^2-12k+8k-5k^2}{12-4k} = \frac{k^2 -4k+6}{12-4k} \text{ ....2.4}$$

α and γ at L_1

For over-reinforced sections, when e_{c1} is limited to .002, $\alpha = 2/3$ and $\gamma = 3/8$

For an under-reinforced section, the state of L_1 will be reached when the steel attains an offset strain of .001 ($e_{c1} < .002$)
Bremner(14) has shown that α and γ, are given by the following expressions for $e_{c1} < .002$

$$\alpha = \frac{e_{c1}}{.002} - \frac{1}{3}\left(\frac{e_{c1}}{.002}\right)^2 \text{...............2.5}$$

$$\gamma = \frac{4 - e_{c1}/.002}{12\left(1 - \frac{e_{c1}}{3x.002}\right)} \text{.................2.6}$$

Equations for strain compatibility (in prestressed concrete.)

Strain Compatibility at L_2

Let e_p be the resultant strain in steel due to prestress after losses, at the time when the application of external moment has to commence. Fig 2.7 (a and b).

Assuming perfect bond, the net change in the strain in concrete at the level of steel, due to applied moment since commencement of loading at stage L_2,

$$= e_{cs2} - (-e_{cp}) = e_{cs2} + e_{cp}$$

The final strain in steel at ultimate is given by $e_{s2} = e_p$ + change in strain in concrete at the same level.

$$= e_p + e_{cp} + e_{cs2} \quad \ldots\ldots\ldots\ldots\ldots\ldots \; 2.7$$

Fig. 2.7 (b), represents changes in the concrete strain due to applied load, from a datum which is the state of zero stress and strain in the section (i.e., from an unloaded state, when prestress was absent).

$$\text{Now} \quad \frac{e_{cs2}}{e_{c2}} = \frac{1-n}{n}$$

Equation 2.7 therefore reduces to

$$e_{s2} = e_p + e_{cp} + e_{c2}(1-n)/n \quad \ldots\ldots\ldots\ldots \; 2.8$$

Strain Compatibility at L_1

In the state L_1, the strain in concrete at top fibre is given by the equation

$$e_{c1} = (e_{sy} - e_p - e_{cp}) \frac{n}{1-n} \ldots\ldots\ldots\ldots \; 2.9$$

Where e_{sy} is the strain in steel if it reaches 0.001 proof stress before concrete reaches .002.

The Equilibrium Equations.

In a cracked section it is not possible to consider the effects of prestress and the applied moment separately, and add their effects to get the final distribution of stresses. This is because the section properties assume new values in the cracked state, i.e., the concrete no more takes any tension and the condition of a constant flexural rigidity does not exist. The principle of superposition no longer applies, because the linearity of the relationship between an applied force and the deformation, is destroyed. The applied bending moment and thrust have to be considered simultaneously with the cable forces in the equilibrium equations, which are as follows:

1) In case of pure bending, Fig 2.8(a)

$$C = T^* \quad \ldots\ldots\ldots\ldots \quad 2.10$$

i.e., the total compression in the area of concrete = total force in cables.

2) In case of bending + axial thrust, Fig 2.8(b).

$$C = T + N^* \quad \ldots\ldots\ldots\ldots \quad 2.11$$

In this case the total compression is a sum of the components,

i) that caused by the tension in the cables and

ii) that due to the external load.

Fig 2.9 (a and b) shows the cross-sections of a rectangular and and I-beam. The position of the neutral axis and the stress-block are also shown.

The total compression in a rectangular section is given by the equation

$$C = \alpha\, \bar{\sigma}_c \text{ bnd} \quad \ldots\ldots\ldots\ldots \quad 2.12$$

* In case of reinforcement in the compression zone, suitable modification in the value of C has to be done.

In case of an I-section, if C_1 be the total compression in the rectangular area of width 'b' and depth 'nd', and C_2 be the compression in the shaded area

$$C = C_1 - C_2$$

$$= \alpha \bar{C}_c \, bnd - \alpha' \bar{C}_c (b-b')(n-t)d \quad \ldots\ldots\ldots \quad 2.13$$

where α corresponds to the stress block of depth nd and α' " " " " " " " $(n-t)d$, between the neutral axis and the bottom flange.

2.6 Advantages of a bilinear idealization.

Consider a simply supported reinforced concrete beam subjected to a point load at the centre. Let the moment curvature relation of the critical section be as shown in Fig 2.10(a), in which the actual behaviour is replaced by an idealized bilinear relation OL_1L_2. Now, assuming for the sake of argument that this M/K relation holds good for all sections, a curvature distribution along the length of the beam can be arrived at, due to the linear variation of the moment, as shown in Fig 2.10(b), when the moment L_2 is reached by the critical section. This curvature distribution can be replaced by two straight lines CD and DA, corresponding to OL_1 and L_1L_2 respectively.

Imagine an isolated span AB of length 'l' of a continuous beam (Fig 2.11). It can be shown that the end slopes φ_A and φ_B are given by the expressions[14]

$$\varphi_A = \int \left(\frac{l-x}{l}\right) k\,dx \quad \ldots\ldots\ldots\ldots \quad 2.14$$

$$\varphi_B = \int \frac{xk\,dx}{l} \quad \ldots\ldots\ldots\ldots\ldots \quad 2.15$$

The conditions of compatibility at supports of the continuous beam will be satisfied if 'φ_B' of span 'i' is equal and opposite to 'φ_A' of the adjacent span 'i + 1'.

The assumption of an idealized moment curvature characteristic, tremendously facilitates the calculation of the angles 'φ_A' and 'φ_B'.

Take the case of the simply supported beam Fig. 2.10(a and b). The rotation in half of the beam can be deduced from the area of the curvature diagram which now consists of two triangles BCE and AED.

In a continuous beam φ_A and φ_B in the i^{th} span, can be determined by obtaining the moment of all such triangular areas about the supports, which is in fact a method to evaluate the integrals given by equations 2.14 and 2.15. In reinforced concrete beams, the points D and E are usually close enough to justify a further simplification to the effect that the plastic rotation represented by the area of the triangle AED is concentrated at the critical section.

The Bilinear idealization in such a case has a horizontal ceiling and represents an elasto-plastic behaviour. An elasto-plastic framed structure with such an idealization, can be analyzed in the intermediate phases between the structure being completely elastic and the structure being completely plastic, by using the elastic equations, to determine the concentrated hinge rotations, provided the value of the flexural rigidity used is that attained by the member at the State L_1 (equation 1.3).*

* Baker recommends that the flexural rigidity of a member at L_1 be calculated at the potential hinge in between the chosen ones(5).

2.7 Calculation of limits L_1, L_2 in a moment rotation curve.

It has been stated that it is more practical to obtain a moment rotation curve from an experiment rather than the corresponding moment Curvature r ation.

The calculation and plotting of the theoretical idealized limits at L_1 and L_2 will now be discussed with respect to a moment rotation curve. The simplfied bilinear idealization proposed by Baker for R.C.C. members, is shown in Fig.2.12. Fig. 2.14 shows the possible bilinear and trilinear idealization in prestressed members (discussed in detail in 2.8).

Limits L_1 and L_{1p}. (L_{1p} in trilinear idealization Fig.2.14)

A critical section attains this state when either of the following conditions is satisfied.

i) The steel reaches the yield point. In case of cold worked steel and high tensile tendons, when no sharp yield point exists, the steel is assumed to yield at an offset strain of .001.

ii) A strain of .002 is achieved at the extreme fibre of the concrete.

Moment at L_1 - M_1 (and at L_{1p} in case of trilinear idealization.)

The method of calculating M_1 is one of trial and error and the steps adopted are as follows:-

1) Assume a depth of neutral axis and calculate e_{c1} from a known value of steel strain. In case of prestressed concrete use equation 2 .9. Check that e_{c1} is less than .002. Find α and γ from equations 2.5 and 2.6.

2) Calculate the total compression in concrete using equations 2.12 or 2.13. Check that the equilibrium is satisfied according to equations 2.10 and 2.11. If not, alter the value of N.A. and repeat.

3) If the final value of the nautral axis obtained by the above process is such that e_c exceeds .002, then use the value of .002 as the guiding factor for e_c , and calculate the forces in the tendons in each trial. (Use of an idealized stress-strain curve for the steel is recommended.)[10]

4) M_1 is then found by taking moments of all the forces about a convenient point.

<u>Rotation at L_1</u> (Bilinear idealization).

The rotation at L_1 is obtained by dividing the area of the moment diagram by the flexural rigidity calculated at the limit L_1. (i.e. beam is assumed to be cracked throughout.)

Consider again the simply supported reinforced concrete beam subjected to a point load at the centre. The curvature distribution in its half span is shown in Fig. 2.13.

$$\text{The rotation at } L_1 = \tfrac{1}{2} \times \frac{M_1}{EI} \times l$$

$$= \tfrac{1}{2} \frac{e_{c_1}}{n_1 d} \cdot l$$

It may be noticed that the calculated rotation at L_1 represented by the triangle ABC, is greater than the actual rotation obtained from the ~~shaded~~ area ABC bounded by the curved line. Burnett[15] objected to this and suggested that an equivalent EI value should be used and an ordinate BA' be calculated, such that the area of the triangle A'BC is equal to the ~~shaded~~ area ABC bounded by the curved line. If this is done, the point L_1 shall lie on the actual moment rotation curve in Fig. 2.12. This is not of sufficient importance in R.C.C. but in prestressed concrete members, the disparity between the actual curve and the point L_1 is significant. This has been taken care of in the suggested tri-linear idealization(13).

Moment at L_2 - M_2 (and at L_{2p} in trilinear idealization).

The method is basically the same and the steps are:-

1) Assume a tentative value of neutral axis. Calculate the ultimate strain from equation 2.2.

2) Calculate the values of α and γ from equations 2.3 and 2.4.

3) Calculate the total compression from equations 2.12 or 2.13.

4) Calculate the force in the tendons using equation 2.8 and an idealized stress-strain relation. Check whether the equilibrium equation 2.10 or 2.11 is satisfied. If not repeat with another value of the neutral axis.

5) Finally, calculate M_2 by taking moments of all forces about the centroid.

Rotation at L_2 (Bilinear idealization).

The total rotation at L_2 is the sum of the rotation at L_1 and the inelastic rotation which in the case of simply supported beams is $2\ \theta_p$ where θ_p is given by the following equation:-

$$\theta_p = 0.8\,(e_{c2} - e_{c1})k_1k_3\left(\frac{Z}{d}\right) \text{ [11]} \quad \ldots\ldots\ldots\ 2.16$$

$k_1.k_3$ is usually taken as .5

A set of computation curves for use in the design of rectangular beams, have been prepared by the author, vide graphs 2.1 to 2.7, to calculate the limits at L_1 and L_2. Effects of various parameters such as type of steel, the degree of prestressing force and the quantity of laterial binders, have been considered. The digital computer was used and a typical flow diagram will be found in appendix 1.

2.8 Idealized limits in the moment rotation curve of a prestressed concrete member.

Baker has suggested a trilinear relation for prestressed members,[10 & 13] in addition to the usual bilinear idealization, Fig.2.14. The limits of this idealization are calculated as follows.

Limit L_{-2}

This is the state before any external moment is applied. The point O' is the origin of reference, if it is desired to find the resultant bending moment at the critical section, in the uncracked state. The ordinate OO' represents the bending moment due to the prestressing force in the tendons, which is opposing the applied moment. The length OL_{-2} is the negative rotation between supports due to the prestressing force.

Limit L_{-1}

This limit corresponds to an applied moment, when the concrete at the level of the resultant of tendon forces, attains a zero stress. Such a state will not usually be attained in the uncracked stage, in beams designed to be tested in the laboratory, due to the difficulty in keeping the centre of gravity of the tendons at a low level. This state is therefore of not sufficient importance in present context.

In drawing Fig. 2.14, it has been assumed that a simply supported prestressed concrete beam having uniform cable eccentricity, is subjected to a central point load. The bending moment diagram due to the prestress is a rectangle, while the applied moment diagram is triangular. At a stage when the applied moment at the critical section is equal to OO', the corresponding rotation caused by the external force is only half of OL_{-2}. This accounts for a steeper slope of $L_{-2}L_{-1}$.

Limit L_{op}.

At this stage, concrete fibre 1 is just going to crack under flexural tension. The method of calculating the cracking moment has been explained in section 3.9.

Limit L_{1p}

The moment at this limit is the same as at L_1. The rotation however, has to be calculated with due regard to the cracked and uncracked values of the flexural rigidity in different parts of the beam, as shown in Fig. 2.14. The author has suggested a satisfactory method of doing this in section 3.11.

Limit L_{2p}

The moment at L_{2p} is the same as at L_2 and the rotation is the sum of the calculated rotation at L_{1p} and the inelastic rotation $2\theta_p$ obtained from equation 2.16.

2.9 Computational difficulties of the trilinear Idealization.

For the sake of simplicity, consider a 3 span continuous Reinforced concrete beam subjected to point loads shown in Fig 2.15(b), in which a trilinear moment curvature relation as in Fig 2.15(a), is applicable at all sections, for analysing the beam. The inelastic rotations shown by the shaded areas, now considerably extend away from the critical sections and can no longer be assumed to be concentrated at the hinges. The calculation of 'φ_A ' and 'φ_B' involve the determination of the moment of the shaded areas about the supports.

It is evident that this is much more difficult and includes many more triangular areas, than when the idealization is bilinear. For each trial value of the distribution of moments satisfying equilibrium conditions, an enormous work has to be done before the incompatibilities at the supports can be determined. If there are a number of spans, a computer is required.

In prestressed concrete members, where in addition to this, the deformations of the structure due to cable forces have also to be taken into account, a trilinear idealization is hardly of any use to the practical designer.

2.10 Use of a moment rotation characteristic in structural analysis.

In the 'Report by Research Committee' on 'Ultimate load design of concrete structures'(49), published in the proceedings of the Institute of Civil Engineers, Feb. 62, a method has been suggested regarding the use of the moment rotation characteristics of a short inelastic length at a critical section of an R.C.C. member, (shown in Fig. 2.16).

The author has to point out that it may be necessary in a rigorous analysis to omit the simplified assumption that hinge rotations are concentrated at critical sections. In such a case it is not easily seen how the moment rotation characteristics measured between the points of supports of simply supported beams, give sufficient information to solve the compatibility problem in a frame.

The author feels that attempts to obtain a moment curvature relationship which could be used in a rigorous analysis yielding realistic results, need not be given up at this stage.

It is true that in most cases, the experimental curvatures obtained from strain gauge readings, when integrated over a length of the beam, do not fully account for the difference in slopes at the ends of this length. It is also true that the moment curvature relationship has its numerous difficulties, as discussed in 2.2.

An investigation to solve these difficulties may be useful in understanding the basic behaviour of the structure. On the other hand, an attempt to use a moment rotation characteristic in a rigorous analysis, may not give results up to expectations.

2.11.

The results of the ten beams, tested by the author in connection with the C.E.B. programme, which form the basis of the further work in this thesis, are discussed in the next chapter.

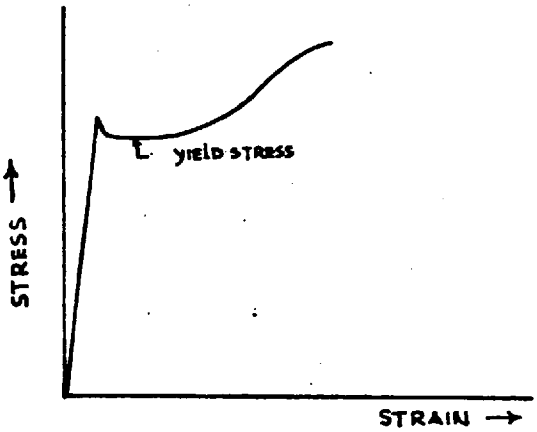

FIG 2·1

STRESS STRAIN CURVE — MILD STEEL

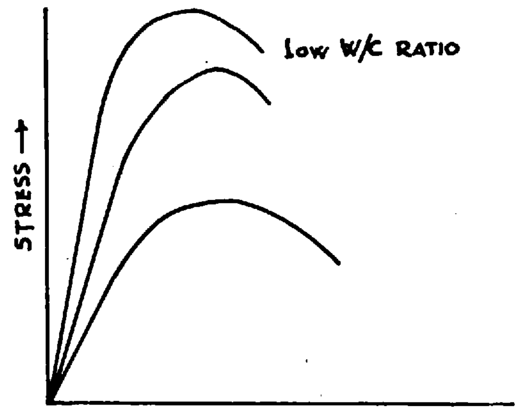

FIG 2·2

STRESS STRAIN CURVE - CONCRETE IN FLEXURAL COMPRESSION

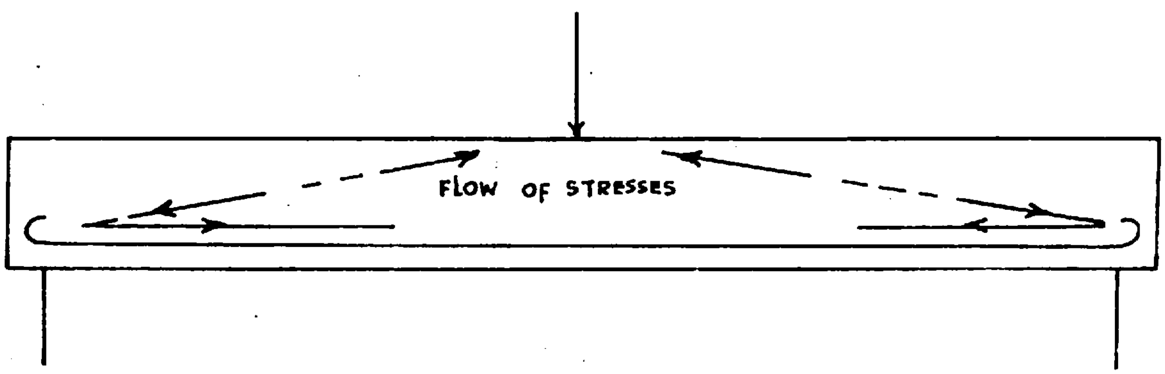

FIG 2·3

SUSPECTED TRUSS OR TIED ARCH ACTION IN A BEAM

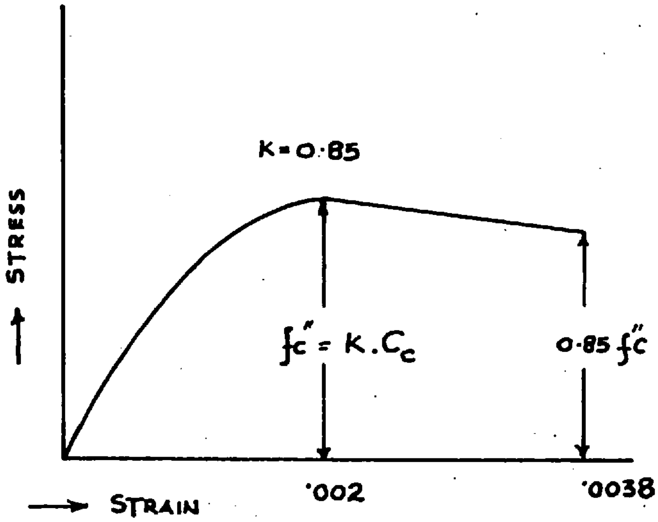

FIG 2·4

STRESS BLOCK - HOGNESTAD

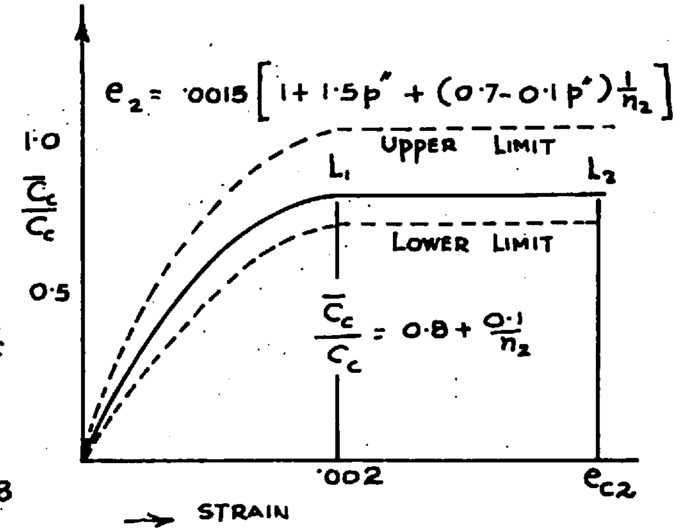

FIG 2·5

STRESS BLOCK - 'ANKARA'

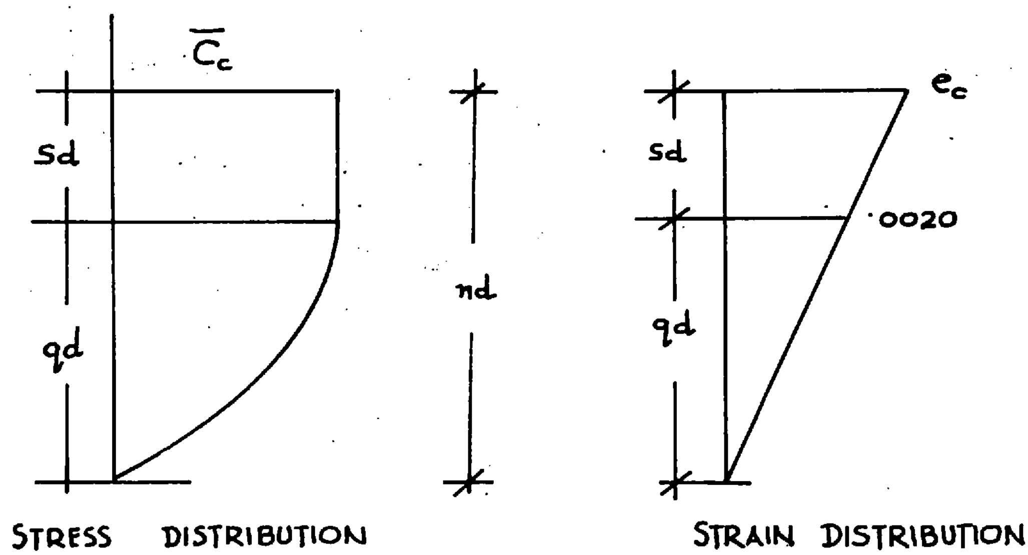

FIG 2·6

DISTRIBUTION OF STRESS AND STRAIN ACROSS A SECTION UNDER FLEXURAL COMPRESSION

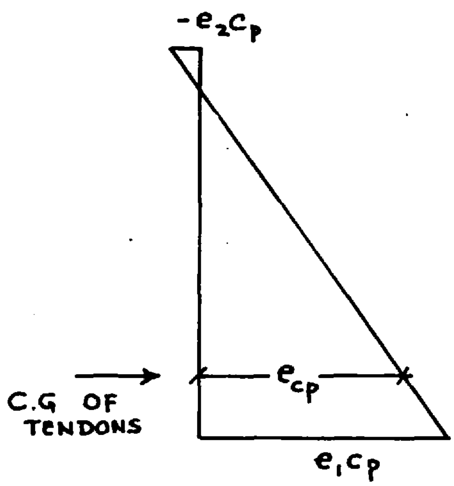

FIG 2·7 a

STRAIN DISTRIBUTION DUE TO PRESTRESS AT COMMENCEMENT OF LOADING

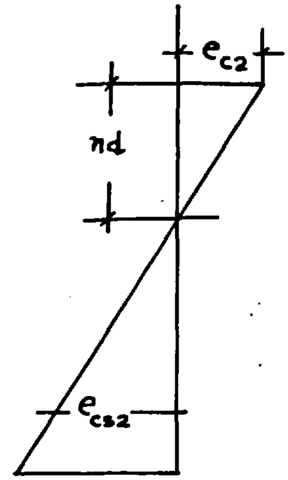

FIG 2·7 b

STRAIN DISTRIBUTION AT L_2

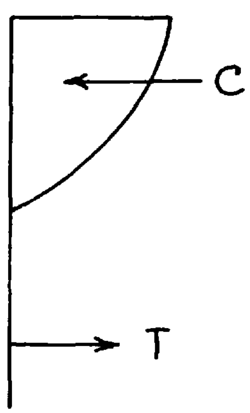

FIG 2·8 a

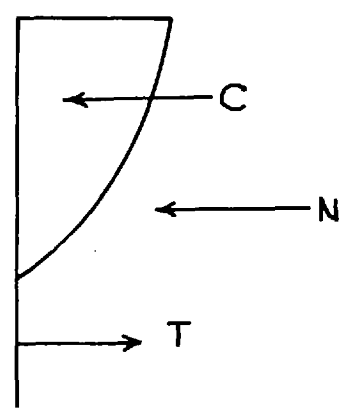

FIG 2·8 b

FORCES TO BE CONSIDERED FOR EQUILIBRIUM

(a) SIMPLE FLEXURAL BENDING (b) BENDING AND AXIAL THRUST

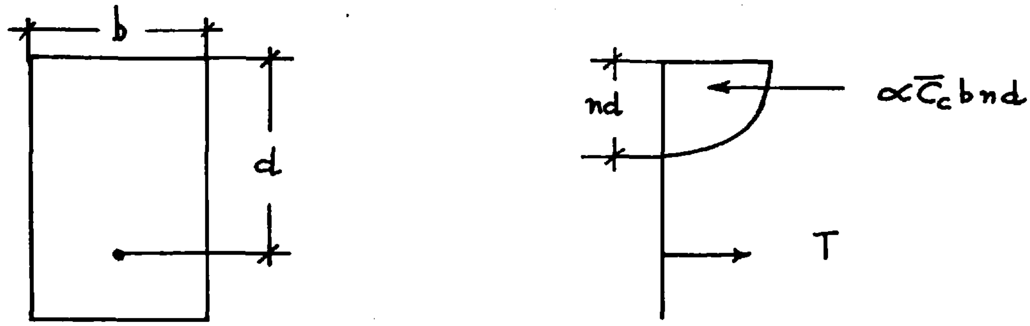

FIG 2·9 a

STRESS BLOCK IN A RECTANGULAR X-SECTION

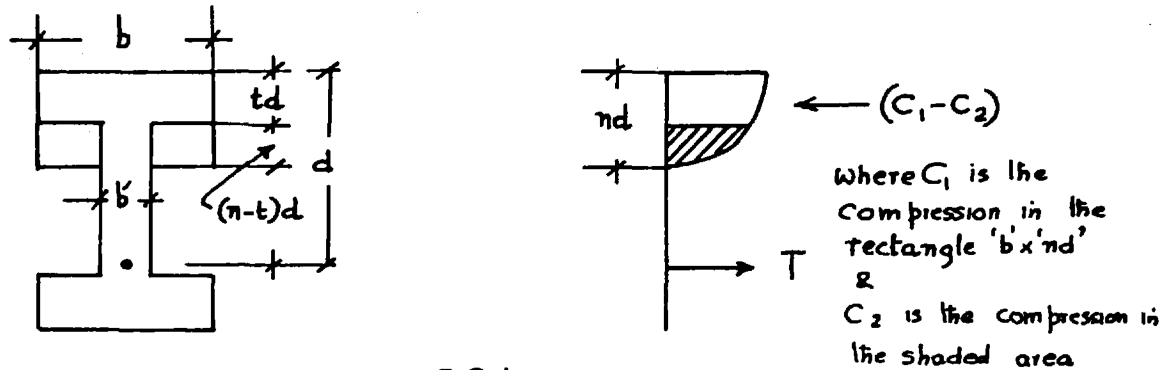

FIG 2·9 b

STRESS BLOCK IN A I- SECTION

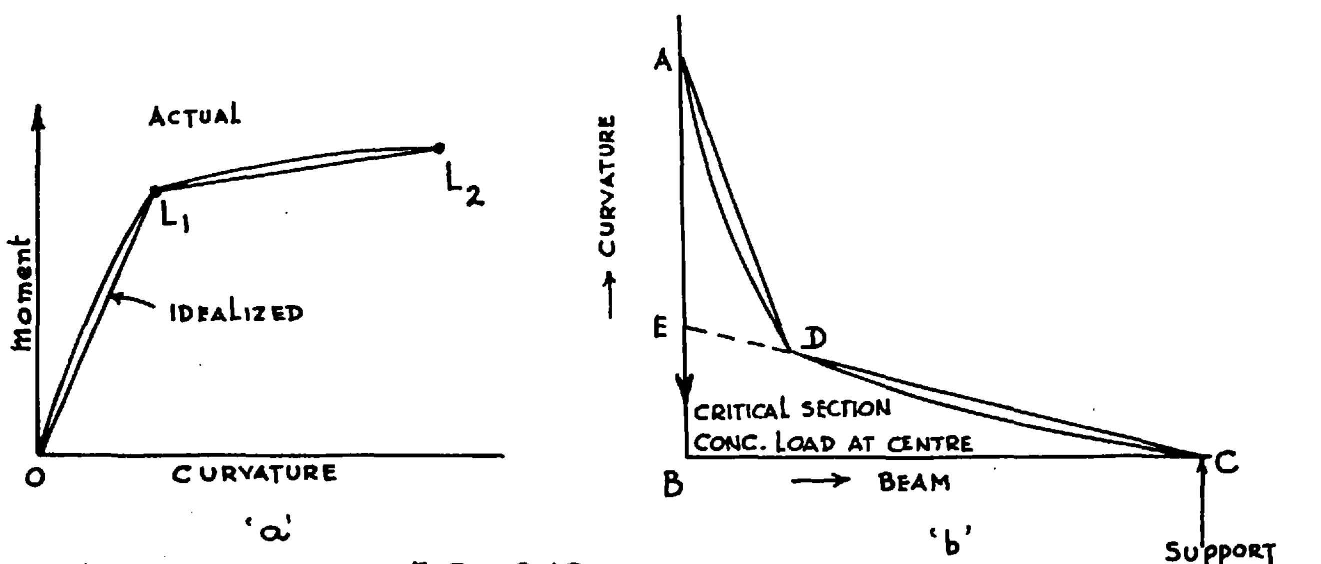

FIG 2·10

'a' SHOWS M/K RELATION FOR CRITICAL SECTION

'b' SHOWS CURVATURE DISTRIBUTION ALONG HALF LENGTH OF A S-SUPPORTED BEAM

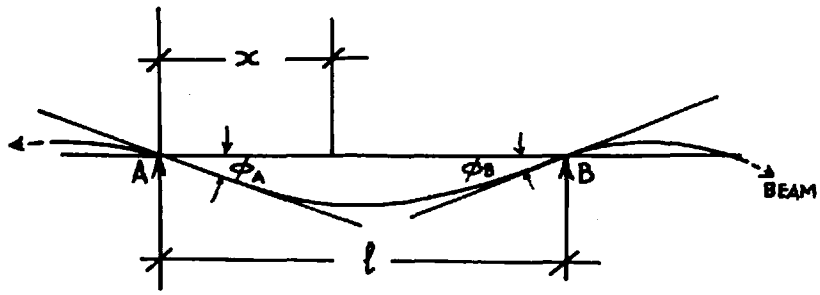

FIG 2·11

AN ISOLATED SPAN OF A CONTINUOUS BEAM

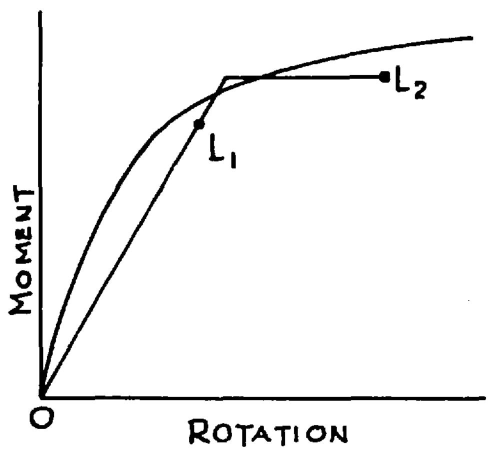

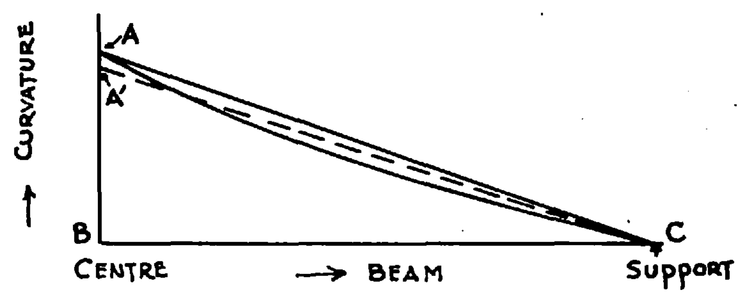

FIG 2·12

FIG 2·13

MPLIFIED BILINEAR IDEALIZATION FOR R.C.C.

CURVATURE DISTRIBUTION AT L_1

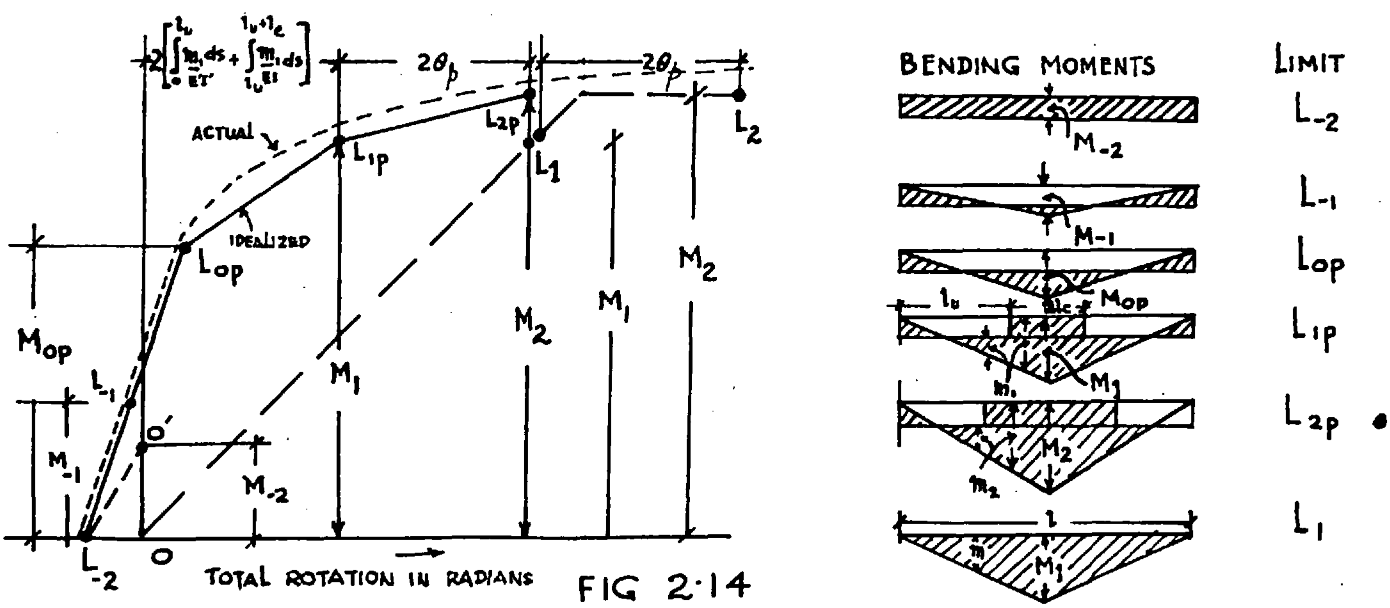

FIG 2·14

-ILINEAR AND TRILINEAR IDEALIZATIONS PROPOSED FOR PRESTRESSED CONCRETE

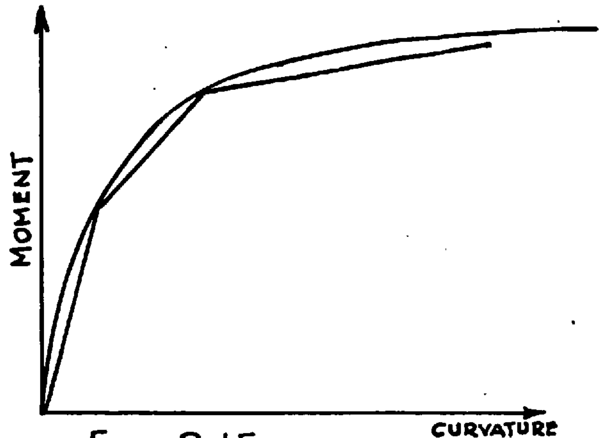

FIG 2·15 a

TRILINEAR MOMENT CURVATURE RELATION

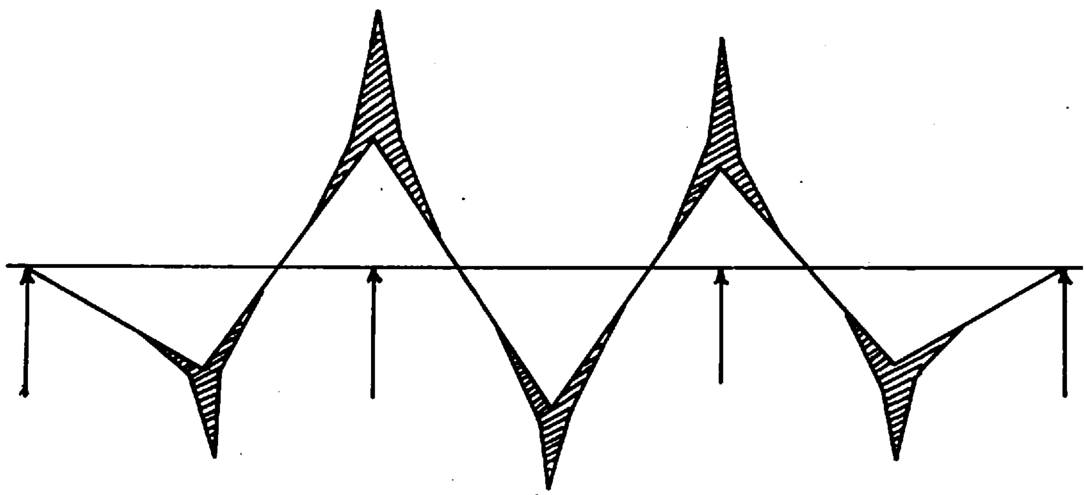

FIG 2·15 b

THREE SPAN CONTINUOUS BEAM SUBJECTED TO POINT LOADS

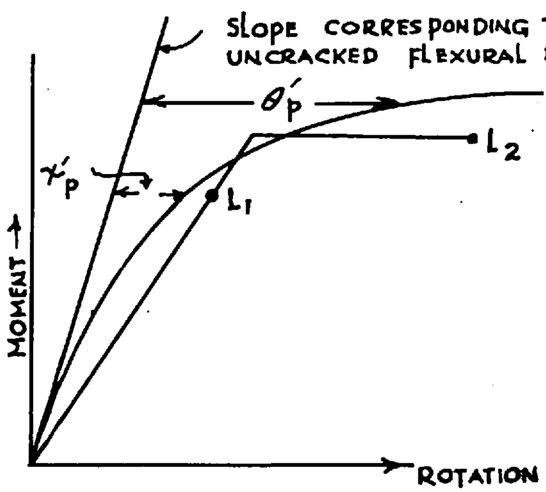

FIG 2·16

MOMENT ROTATION CHARACTERISTICS OF A SHORT LENGTH WHICH IS PLASTIFIED

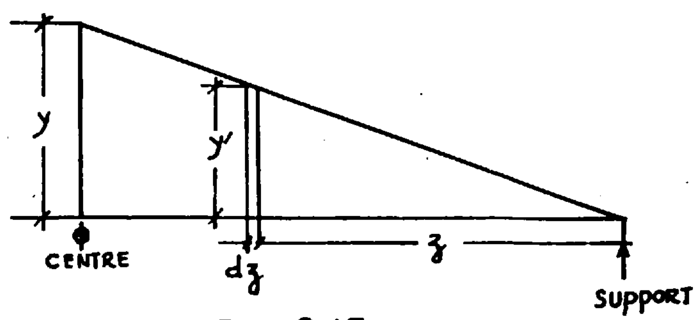

FIG 2·17

INTEGRATION OF AN AVERAGE MOMENT CURVATURE RELATION

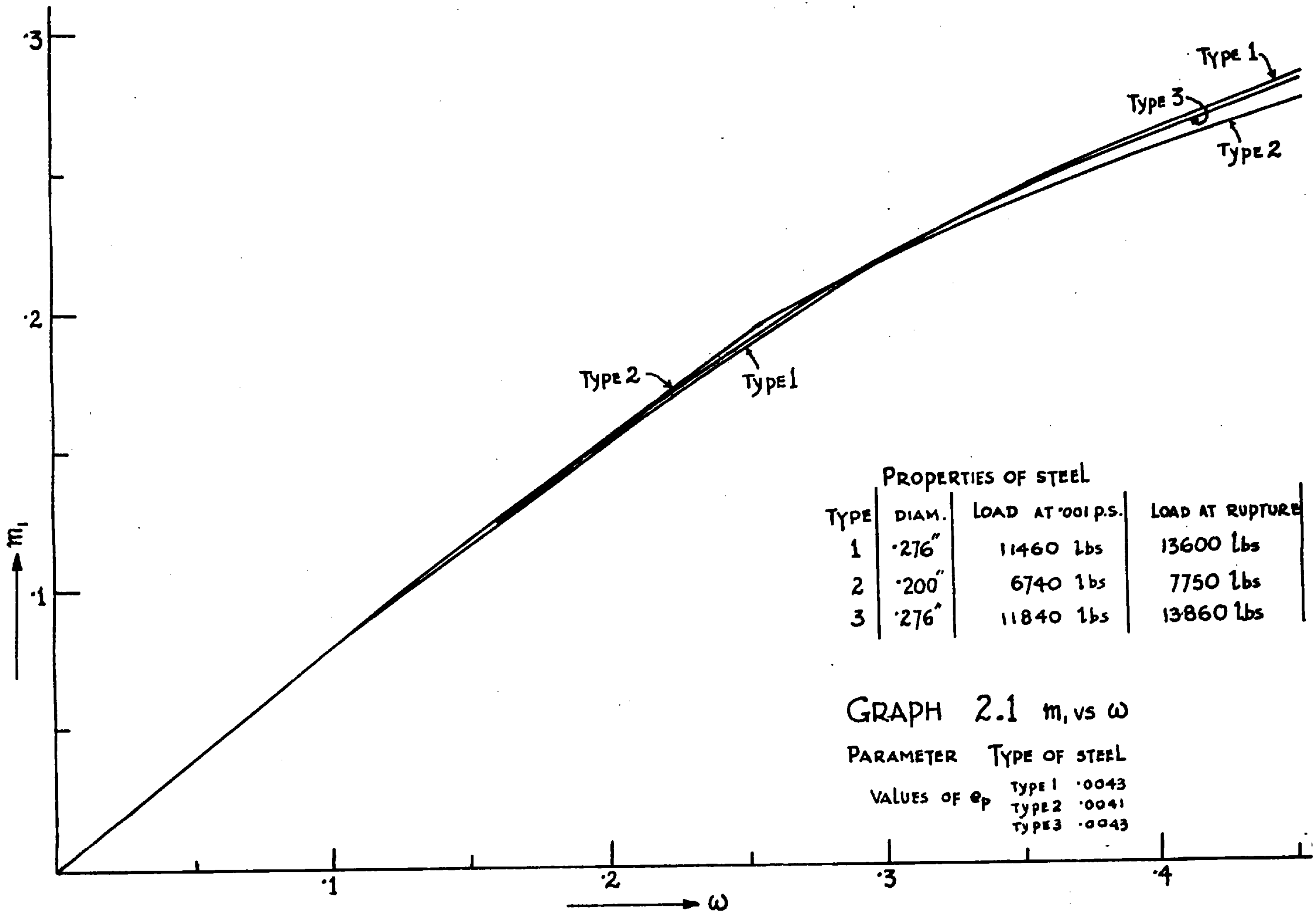

PROPERTIES OF STEEL

TYPE	DIAM.	LOAD AT ·001 P.S.	LOAD AT RUPTURE
1	·276"	11460 lbs	13600 lbs
2	·200"	6740 lbs	7750 lbs
3	·276"	11840 lbs	13860 lbs

GRAPH 2.1 m_1 vs ω

PARAMETER TYPE OF STEEL

VALUES OF e_p TYPE 1 ·0043
TYPE 2 ·0041
TYPE 3 ·0043

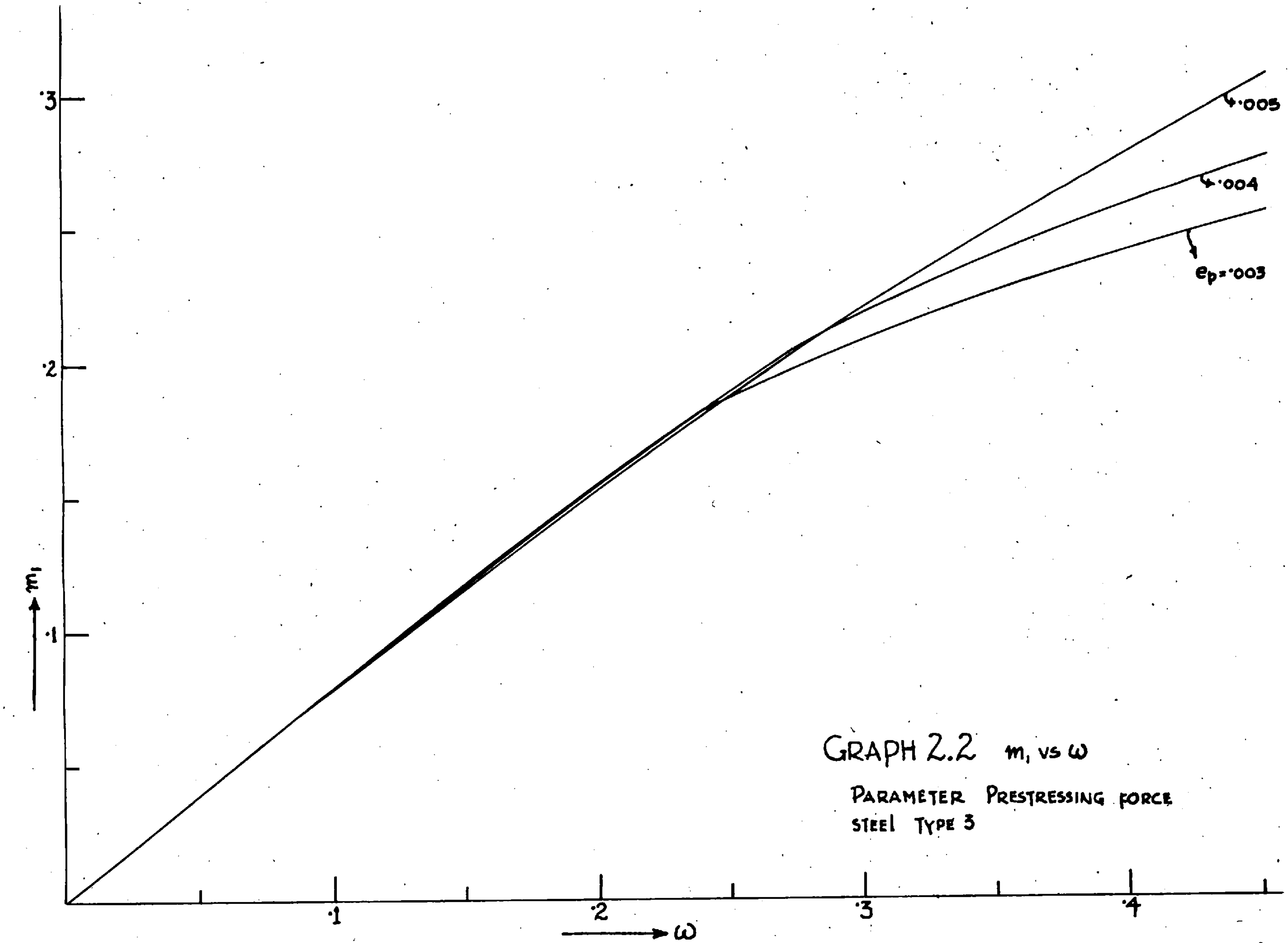

GRAPH 2.2 m_1 vs ω

PARAMETER PRESTRESSING FORCE
STEEL TYPE 3

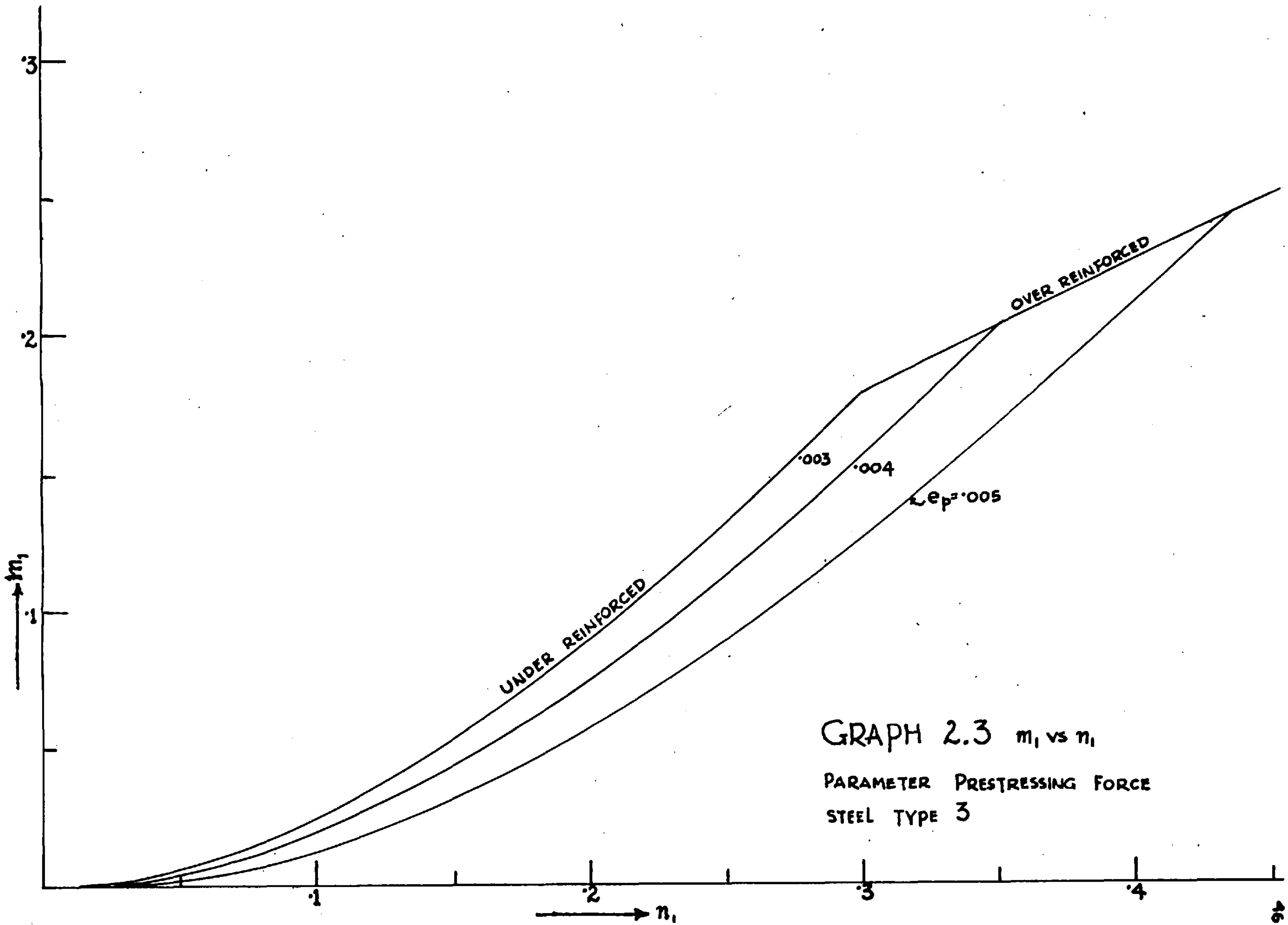

GRAPH 2.3 m_1 vs n_1

PARAMETER PRESTRESSING FORCE

STEEL TYPE 3

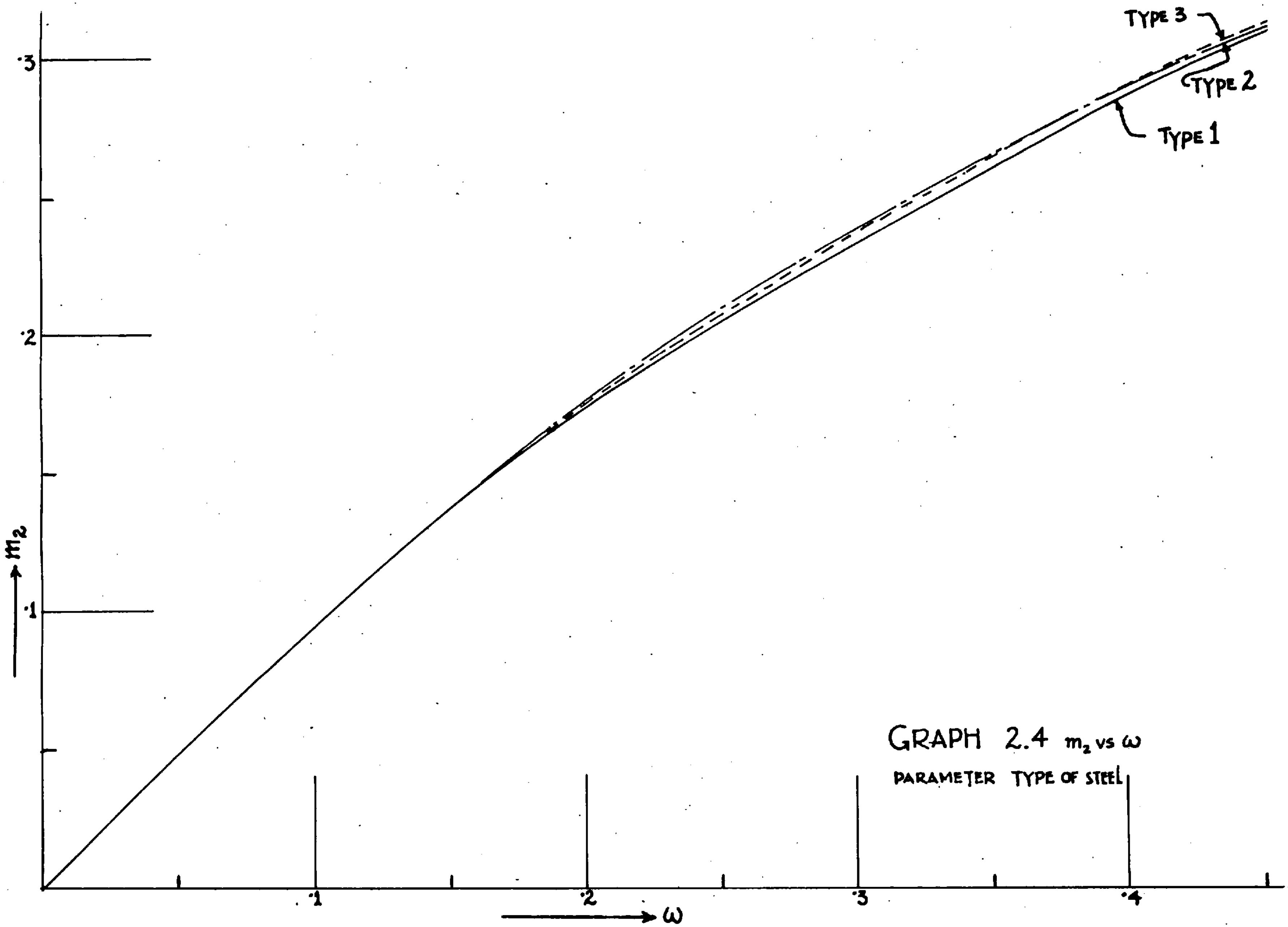
TYPE 3
TYPE 2
TYPE 1
·3
·2
·1
m_2
·1
·2
·3
·4
ω
GRAPH 2.4 m_2 vs ω
PARAMETER TYPE OF STEEL

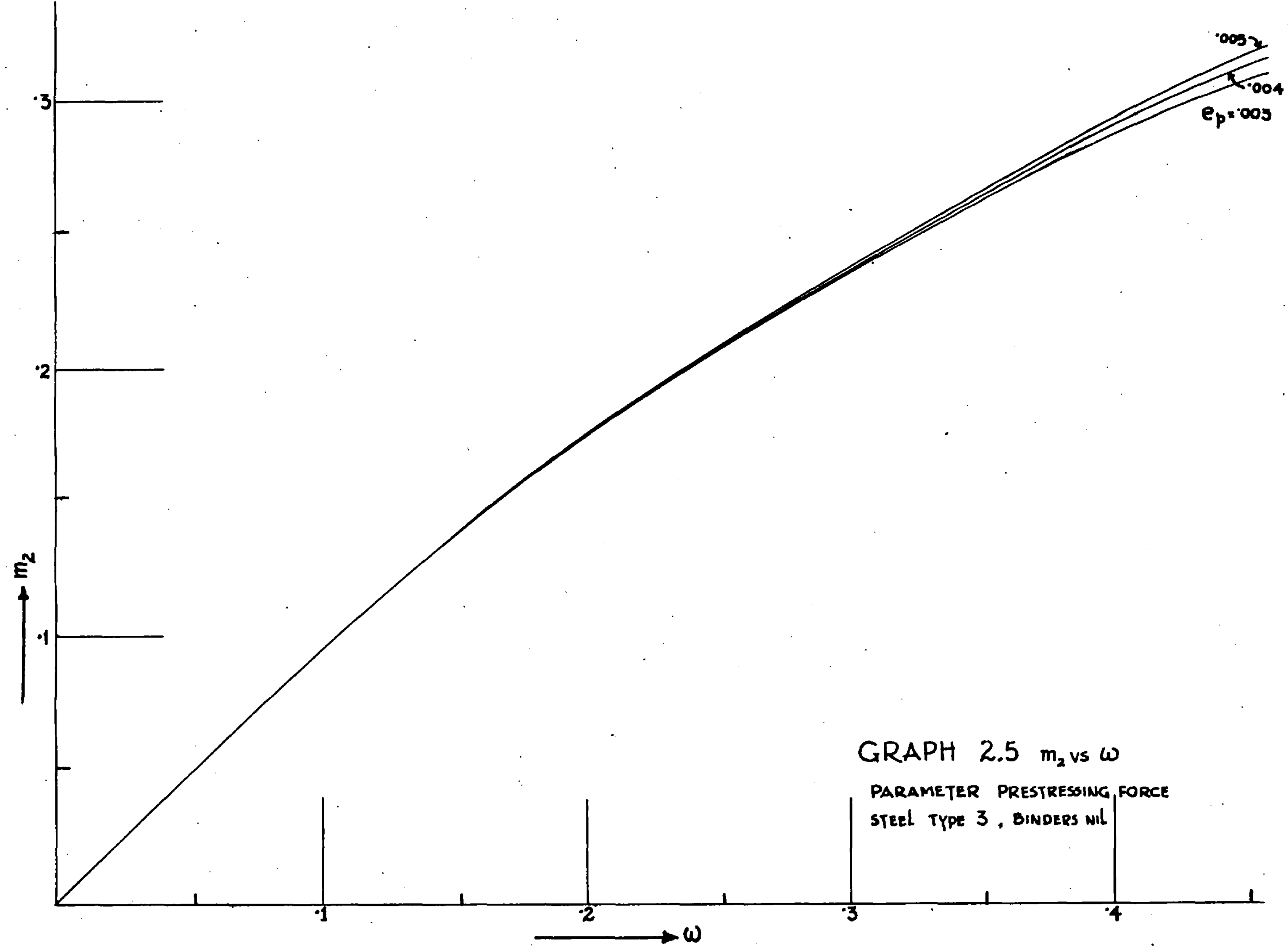

GRAPH 2.5 m_2 vs ω

PARAMETER PRESTRESSING FORCE

STEEL TYPE 3 , BINDERS NIL

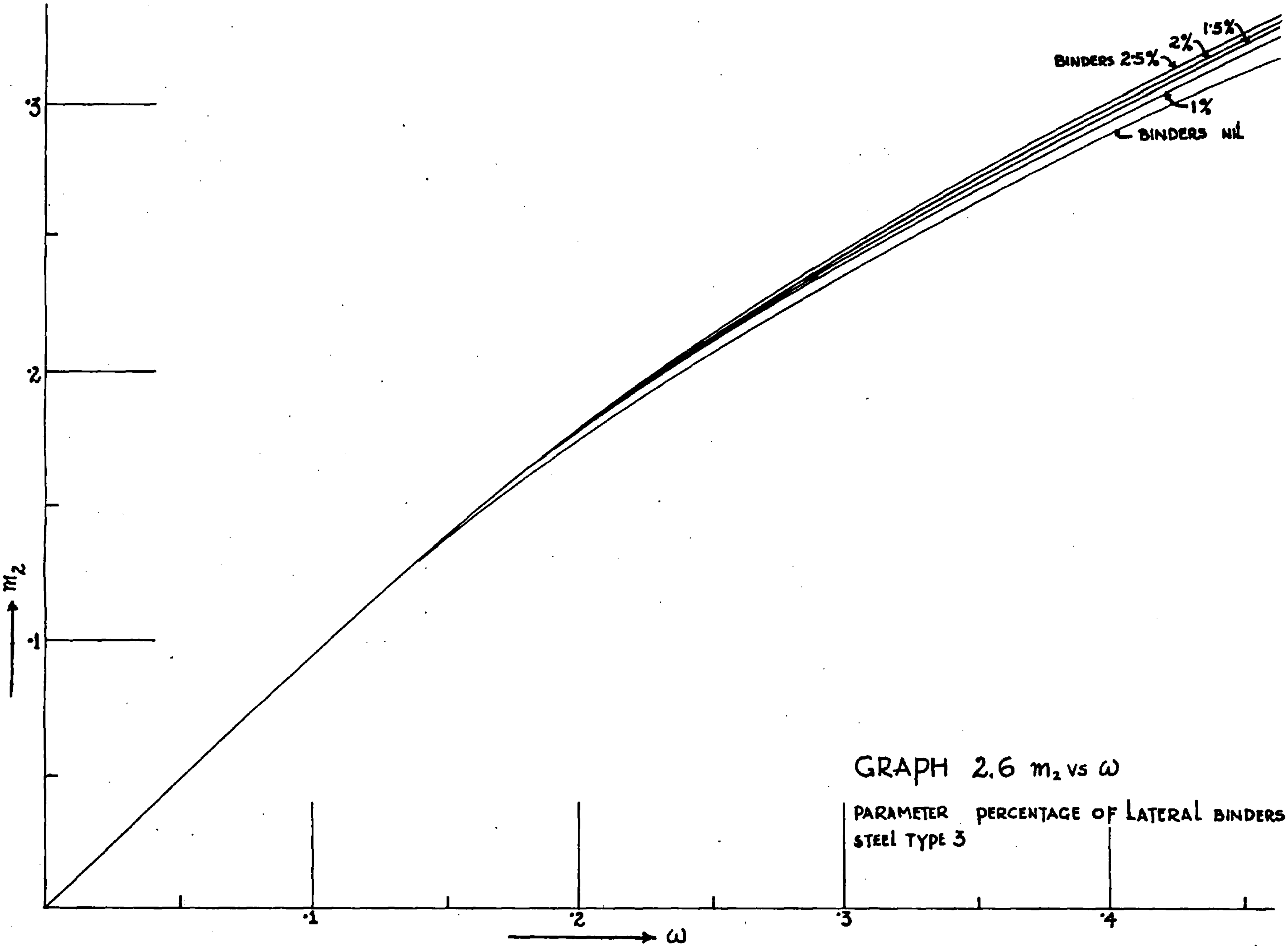

GRAPH 2.6 m_2 vs ω

PARAMETER PERCENTAGE OF LATERAL BINDERS
STEEL TYPE 3

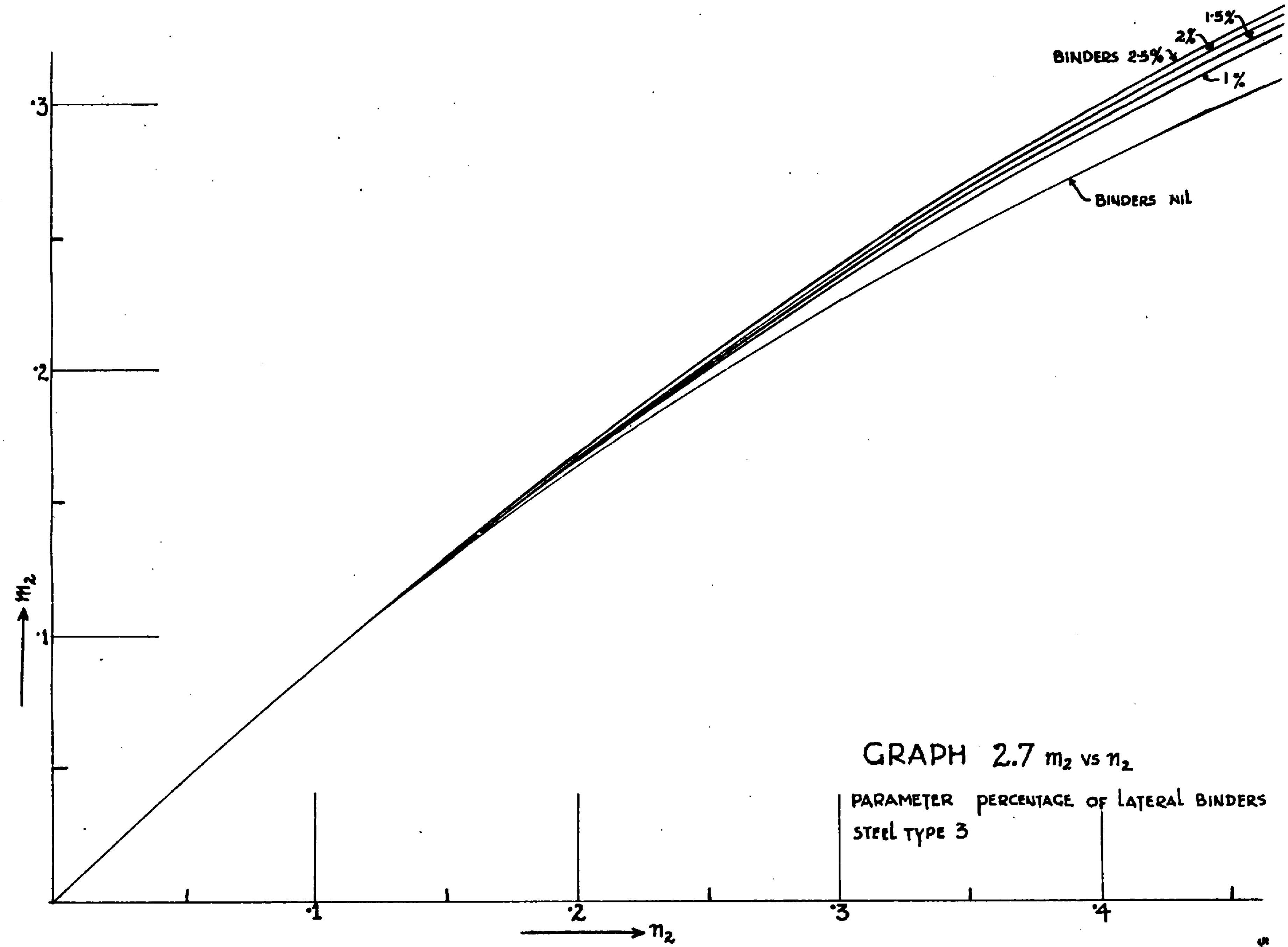

1·5%
2%
BINDERS 2·5%
1%
BINDERS NIL
GRAPH 2.7 m_2 vs n_2
PARAMETER PERCENTAGE OF LATERAL BINDERS
STEEL TYPE 3
·3
·2
·1
m_2
·1
·2
·3
·4
n_2

CHAPTER 3.

MOMENT ROTATION CHARACTERISTICS OF POST-TENSIONED PRESTRESSED CONCRETE BEAMS.

3.1 Object

The discussion in this chapter relates to ten simply supported beams subjected to central point loads, and tested in accordance with the C.E.B. programme. In the first five beams labelled as 1 to 5, the percentage of steel was varied from .173 to .865 calculated on the rectangular area represented by bxd. Thus a wide range between a highly under-reinforced and a fairly over-reinforced case was covered. In beams 6 and 7, the prestressing forces were 40% and 33% of the ultimate value. The percentage of steel was the same as for Beam No. 3 in which the prestressing force was 50% of the ultimate. Beams 3, 6 and 7 therefore form a set in which the effect of various degrees of prestressing force on the ultimate load and the rotations was studied. Beams 8, 9 and 10 had the same percentage of steel as the over-reinforced beam No.5, but were provided with various percentages of lateral binders in the compression flange. This series was chosen to study the effect of binders, after it was noticed that Beam No. 5 had a sudden brittle failure in the neighbourhood of the ultimate load, without undergoing any appreciable plastic rotation. The properties of the beams are summarized in Table 3.1.

3.2 Beam details.

All beams were of I-section having 6" flange width and 8" overall depth. The span between the centres of end supports was 82". The reinforcement details are given in fig. 3.1. The eccentricity was kept constant throughout the length of the beams in all the cases. The main reinforcement consisted of high tensile wires of .276" diameter, manufactured in Great Britain by Richard Johnson and Ne phew Ltd. Two different consignments were used , as indicated in Table 3.1. Each had slightly different characteristics. The corresponding load extension graphs were supplied by the firm and were verified in the laboratory. (figs 3.2 to 3.4)

2 NOS ¼" diam. mild steel bars were used for holding stirrups in all the beams. The corresponding stress-strain curve (supplied by J.G.C. Chinwah)(18) is shown in fig. 3.5.

Ordinary portland cement was used throughout. The course aggregate was irregular Thames River gravel of ¾" maximum size and the fine aggregate was also from the same source. For the sake of convenience, the fine aggregate was separated into two different sizes in the laboratory viz $\frac{3}{16}$" - 25 and 25 down.

The absorption capacity and sieve analysis of aggregates were determined in co-operation with J.G.C. Chinwah and are shown in Tables 3.2 and 3.3.

3.3. Concrete Mix.

The desired 6" cube strength at 28 days, was

6,000 lbs/square inch. The design was based on Road Note No. 4.[50] It was noticed that for a given W/C ratio, the experimental strengths obtained by previous workers were higher than that indicated by Road Note No.4 as shown below.

6" cube strength

W/C	As per R.note No.4	practical values.	Factor	Av. Factor.
Bremner[14]				
.53	4900 (28 day strength)	6700	1.37	
.56	4500 "	5800	1.30 (neglect)	
.59	4100 "	5500	1.34	1.35
Dastur [24]				
.45	4400 (12 day strength)	6000	1.37	
.64	2640 "	4000	1.50 (neglect)	

The target strength of 6000 lbs/square inch was divided by a factor of 1.35 before using the tables of R. note No.4. The following proportions were found to be satisfactory for combining the C.A. and the F.A. This gave an overall grading which was close to No.3 of the Road Note 4.

Course aggregate = 60 lbs.

Fine aggregate = 40 lbs (consisting of 28 lbs. of $^{3}/_{16}$" -25, and 12 lbs. of 25 down).

The grading of the combined aggregate when mixed in the above proportions is shown in Figs. 3.6 to 3.8.

The aggregate cement ratio was 6.00 and the effective water cement ratio was .55. A summary of the mix design shall be found in Appendix 2.

3.4 Batching, mixing, casting and curing.

The volume of the beam and the control specimens dictated that the casting of each beam be done in two batches. To avoid segregation, the order in which the constituents of each mix was weighed in a 200 kg weigh batcher , is as follows:

Fine aggregate 25 - $^{3}/_{16}$"
Fine aggregate 25 down.
Cement
Course aggregate.

The water was weighed separately on a weighing balance. A horizontal pan mixer was used. Dry mixing was usually carried on for two minutes before water was added, and the mixing continued thereafter for further three minutes.

The following control specimens were cast with each beam.

	Mix 1	Mix 2	Total
6" cubes	2	4	6
6" x 12" cylinders	1	2	3
4" x 4" x 20" flexural beams.	3	0	3

The aim of the above arrangement was to obtain more specimens for compression tests from the second batch of mix, which was used in the top of the beam, and specimens for flexural tests from the first batch.

The shuttering used was of steel with timber insets to reduce the thickness of the web. The shuttering permitted the use of two 'kango' hammers, one on each side of the shuttering for vibration. The control specimens were vibrated on a vibrating bench .

After the casting, the beam and the control specimens were cured under wet hessian and polythene for 24 hours. Thereafter the side shuttering was stripped off and they were cured for a further period of six days under the same conditions. The beam and the specimens were then cured in air under the controlled conditions of the laboratory until testing. The constant temperature and the humidity maintained were 68°F and 60% respectively.

3.5 Testing Frame.

The beams were tested in a 50 ton testing frame (Figs. 3.9 and 3.10). The bearings at the supports were located on two concrete pedestals. In the first five beams, the bearing at one end did not permit lateral movement and the loading was done via a proving ring having hinges at its points of contact with the jack and the beam. This permitted tilting of the proving ring while lateral movement took place at the free roller end. The arrangement was unsatisfactory as it induced secondary lateral forces in one half of the beam, which in its turn influenced the pattern of the shear cracks to a considerable extent. The loading arrangement was therefore altered in testing the remaining beams. The load was transmitted vertically through a load cell, rigidly screwed onto the ram of the jack. A spherical ball seating was provided where the load cell came into contact with the loading platten which in its turn was holding the beam by friction. The beam was provided with rocker cum roller bearings at both the ends and was free from all lateral restraints. This arrangement considerably improved the pattern of cracks in subsequent beams. No instability was encountered.

In all the beams, oil was pumped into the jack by means of an electric pump and hence the rate of loading at the different stages, could be controlled.

3.6 Instrumentation.

The method adopted for measuring rotations and recording strains was precisely the same as initiated by Bremner. Clinometers consisting of a .0001" micrometer head and a 10 second level tube, were mounted on the top of the beams at several places including the supports, to record the changes in the slopes. 4" demountable Demec gauges were used throughout to record strains. The layout of the Demec points was so arranged that differences in strains could be recorded every 1" apart near the critical section. The deflected profiles of the beams were also obtained by using .001" dial gauges underneath the beam. The layout of the clinometers, Demec points and the dial gauges are shown in Fig. 3.11 to 13.

3.7 Testing Procedure.

The loading procedure recommended by the committee XI of the C.E.B., states that an increase from zero load be made up to 60% of ultimate in steps of 15% and thereafter the ultimate load be attained in steps of 5%. Near the ultimate the strain at the extreme fibre is not allowed to exceed ·0007 for each step. The time for each step is 15 minutes, 5 minutes for applying the load and 10 minutes for taking readings.

Now, during the time taken for recording readings, there are two alternatives. Either the load or the deformation may be kept constant. The former is difficult to achieve and would mean the application of a constant oil pressure against a falling resistance due to creep. Edwards (25) achieved this by balancing the oil pressure by dead weight. An Amsler machine with a constant load maintaining device was available in the laboratory at a later date. The measurement of rapidly changing strains in the plastic phase is a problem in this system.

The second alternative is very nearly attained by shutting the oil supply as close as possible to the jack. The jack ram is thereby locked and provided the falling backward pressure of the deflected beam does not alter the deformation of the loading device appreciably, and provided the testing frame is sufficiently rigid to cause an inappreciable amount of flow of energy from the frame to the beam during this period, the deflection at the point of application of the load may be assumed to remain constant. The load cell used in Beams 6 - 10, is better suited for this method and the increase in the deflection of the beam during the time when the valve was kept shut in these beams, was much less noticeable than in the case of beams where a proving ring was used.

3.8 Prestressing and Grouting.

The C.C.L. single wire system was used for prestressing. Usually after 14 days of casting, the tendons were post tensioned using a Mark I C.C.L.

jack at one end. In beams 1 to 5, the tendons were left within the duct tubes at the time of casting, with the leads of the electrical strain gauges partially embedded in concrete. Later on, all tendons were introduced in the duct holes at the time of prestressing, and the strain gauge leads were taken out of the beam, through vents provided for grouting near the supports. The latter was accomplished by using wire hooks (see Fig. 3.14). As strain gauges were only used to measure the prestressing level, by using the load extension graphs, there was no particular disadvantage in using them near the ends in case of beams. An attempt was made to use two tendons in the central duct tube, in case of beams 2, 4 and 5. This was unsatisfactory from the point of view of friction and it also led to the rupture of the gauges in some cases, whence the degree of prestress was assessed by noting the oil pressure at the pump and measuring the extension.

Grouting was carried out soon after prestressing, by means of a high pressure hand pump. In case of Beams 1 to 5 the grout was injected through holes built in the end plates (Fig. 3.15). In beams 6-10, special vents provided access to the duct tubes for grouting. Both arrangements were satisfactory. High alumina cement was used for the grout and the water cement ratio was .375. Aluminium powder (CABCO Grout Additive) was used to nullify the shrinkage of grout, according to the maker's specifications.

The dates of casting, prestressing, grouting and testing are given in Table 3.5. Laboratory conditions did not permit a strict uniformity to be observed in all cases. Due regard was taken of this fact in calculating shrinkage and creep losses.

V_u = ultimate shear force

V_c = cracking shear force

A_V = X-sectional area of shear steel

d = effective depth of section

S = spacing of shear reinforcement

f_y = permissible stress in shear reinforcement in tension

3.9 Brief Summary of Calculations.

(a) Shear reinforcement.

The shear reinforcement was calculated according to the formula

$$V_u - V_c = {}^5/_4 \, A_v \frac{d}{s} \cdot f_y \quad \ldots\ldots\ldots\ldots\ldots\ldots \quad 3.1$$

This empirical formula was suggested by Hernandez[30], who tested a number of simply supported prestressed beams subjected to a system of two point loading. This formula was found to be satisfactory for all the beams tested by the author. The cracking moment and the corresponding shear force V_c was calculated by a process of successive iteration, taking into account the increase in the force in the tendons at the time of cracking (vide appendix 3). The permissible flexural tensile stress in the extreme fibre was taken as 500 lbs/ square inch in these calculations, as found from tests on flexural beam specimens.

The cracking moment calculated according to the following formula suggested in Illinois Bulletin No. 452, was very close to the results obtained by the above method.

$$M_c = f_t \, bd^2 \sqrt{\frac{b'}{b}} \left(1 + \frac{F_{sc}}{A_c f_t}\right) \quad \ldots\ldots\ldots\ldots \quad 3.2$$

M_c = cracking moment

f_t = permissible tensile stress in concrete in extreme fibre under flexure.

b = top flange width.

b' = web thickness.

A_c = area of X-section

F_{sc} = prestressing force.

(b) <u>Stresses in Anchor zone</u>.

The stresses were assessed according to the procedure suggested by Y. Guyon[28] in conjunction with the published tables on page 516 of his book. The effect of each tendon was first calculated at various heights and depths of the zone. The total effect of all the tendons was then taken into account and a reasonable average stress was assumed to find out the area of the mild steel which was provided in the shape of a cage (Vide appendix 4).

The calculation of the bearing pressure on the end plate was done according to the following formula suggested by Guyon, based on the French Code of Practice (B.A.45 formula).

$$\text{Allowable pressure} = 0.4\ Cu\ k \left[4 - 5\sqrt{a/A} + 2\,a/A \right] \quad \ldots 3.3$$

where Cu = cube strength

k = increment factor for hoop reinforcement (taken as 1)

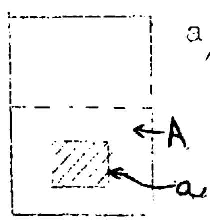

a/A = Area of bearing plate / a fictitious distribution area centred upon the bearing.

(c) <u>Losses in prestressing force</u>.

The force in the tendons at the time of testing is less than to which they are initially stressed at the jack end, before transfer. The causes for this reduction are:-

1. slip at anchorage during transfer
2. friction due to curves and bends in the tendons
3. creep and relaxation of steel.
4. elastic losses - which occur in all tendons which are subject to the effect of subsequent tensioning of one or more wires
5. losses due to shrinkage
6. losses due to creep.

The loss due to the anchorage slip depends on the personal factor of the man who does the hammering. Consistent results are obtained only after experience. An allowance of 1000 lbs. was found to be satisfactory for a .276" tendon.

As the tendons were straight, no allowance was made for loss due to friction.

The loss due to creep and relaxation of steel was minimized by keeping the wires under tension for 5 mins. before locking off.

The losses due to elasticity, creep and shrinkage were calculated in accordance with the formulae suggested by Evans & Bennett [26].

The calculated values are given in Table 3.6. Typical calculations will be found in Appendix 5.

(d) Rotations and moments at limits L_1, L_2, L_{1p} and L_{2p}.

Typical calculations for Beam No. 4 will be found in Appendix 6. It may be noted that the tendons were initially stressed before transfer to a state which is beyond the initial straight portion of the stress-strain curve. Further, the wires were maintained at that load for some time. The resultant stress in the tendon after transfer was therefore found from strain values in conjunction with a path not obtained by retracing the load extension curve originally followed, but by unloading along a straight line parallel to the initial part of the forward journey.

3.10 Historical development of the length of the plastic hinge.

Figure 3.16 (a and b) represents a simply supported R.C.C. beam with a concentrated load at the centre. The bending moment distribution is shown by the triangle ABC. AEOFC represents the curvature distribution on some scale. E and F are points on the curvature diagram, corresponding to the moment M_1 at which significant inelasticity occurs. There is a sharp rise in the curvature of the beam in the zone between E & F. The length EF is the inelastic zone.

If it is assumed that the same moment curvature relation holds good at all points of the beam, we get the following expression for half of the plastic rotation

$$\theta_p = \beta \frac{l}{2} \left[1 - \frac{M_1}{M_2}\right] \left[\frac{1}{R_2} - \frac{1}{R_1} \cdot \frac{M_2}{M_1}\right] \quad \ldots\ldots 3.4$$

where β is a shape factor.

W.W.L. Chan obtained this expression in his thesis(17) in a slightly different form.

C.E.B., proposed to replace the term '$\beta \frac{l}{2}\ (1 - \frac{M_1}{M_2})$' by an equivalent plastic length 'l_p' having a constant curvature as shown in figure 3.17.

$$\therefore \quad \theta_p = l_p \left(\frac{ec_2}{n_2 d} - \frac{ec_1}{n_1 d} \cdot \frac{M_2}{M_1}\right)$$

A further simplification is achieved by assuming that

$$n_2 d = n_1 d \times \frac{M_1}{M_2} \qquad (14)$$

and we get the following expression

$$\theta_p = l_p \times \frac{ec_2 - ec_1}{n_2 d} \quad \ldots\ldots\ldots\ldots\ldots\ldots\ldots\ldots 3.5$$

C.E.B. recommended that l_p may be obtained empirically and proposed the formula

$$\frac{l_p}{d} = k_1\ k_2\ k_3\ \left(\frac{z}{d}\right)^{1/4} \ldots\ldots\ldots\ldots\ldots\ldots\ldots\ldots 3.6$$

where k_1 is a parameter which depends on the quality of steel.

k_2 " " " " " on axial load.

k_3 " " " " " on concrete.

Z is the distance between the point of contraflexture and the point of maximum moment.

Bremner[14] found that the length of the plastic hinge 'l_p' did not remain constant with varying percentages of one particular type of steel, but it was primarily a function of the neutral axis. He attributed this to a decrease of the shape factor. (Vide discussion on beams 1, 2, 5 - chapter IX of his thesis.)

The omission of n_2 in the denominator in the expression for θ_p as suggested by Baker at Ankara vide equation 2.16, is a recognition of the fact that the length 'l_p' is primarily a function of the neutral axis depth.

Amarakone[1] suggested that in the under-reinforced beams, the presence of a steeper strain gradient across the section, between the neutral axis and fibre 2, was responsible for the higher strains noticed in the extreme fibre in such cases. The higher strains in their turn, cause higher localized rotations, which tend to decrease the total length of the hinge. Soliman[47] has further confirmed that the presence of a steep horizontal gradient corresponding to a low value of $\frac{Z}{d}$, causes larger concentrated rotations at the hinge. This is quite contrary to the expectation that inelastic rotations would be smaller if the plastified length of the beam is reduced by shortening the value of 'Z', as indicated by equations 3.5 and 3.6.

According to Soliman θ_p in case of pure bending is given by the following expression:-

$$\theta_p = 0.0125\lambda - 0.005 \qquad \ldots\ldots\ldots\ldots\ldots \quad 3.7$$

where $\lambda = 1 + 0.8\, q'' + \dfrac{1-n_2}{0.5+n_2} + \dfrac{4d}{(1+n_2)Z}$

and q" (a factor which determines the properties of transverse binders)

$$= \left(1.4\,\frac{A_b}{A_c} - 0.45\right) \quad \frac{A''_s\,(S_o-S)}{A''_s.S + 0.0028\,BS^2}$$

note: A''_s = X-sectional area of binders.
B = breadth OR .7 × depth of the bound CONCRETE, WHICHEVER IS THE GREATER.
S = spacing of binders, S_o = 10"
A_b/A_c = ratio between bound area and the total area under compression.

3.11 Discussion on the tests carried out by the author.

Moment rotation curves in respect of the ten beams tested by the author are presented in graphs 3.1 to 3.10. These curves have been plotted according to the method suggested by Baker(11) and as explained in Chapter 2. The effect of the uncracked modul.s of flexural rigidity was taken into account as explained in 3.11. The state of L_{-1} was found to be above the cracking limit L_{op} and has been omitted in the graphs. Curvatures plotted along the length of the beams 1 to 5 are shown in graphs 3.12 to 3.14. They exhibit a general spread of the plastic length as the percentage of steel is increased. This is in accordance with Brember's observations.

The deflection profiles of Beams 1 to 5 will be found in graphs 3.15 and 3.16

Crack patterns are shown in plates 3.1 to 3.5

Beams 1, 2, 3, 6 and 7 are under-reinforced.

Beam 4 is nearly balanced.

Beams 5, 8, 9 and 10 are over-reinforced.

The following observations were made by the author.

(a) Effect of the uncracked modulus of flexural rigidity.

Rotations calculated at the limit L_1 are far in excess of the experimental values of the corresponding point.

The calculated rotations at L_{1p}, by the method suggested below, are fairly close to the experimental values and are adequate for the purpose of a Trilinear idealization.

The method used to take into account the stiffness of the uncracked length, when calculating rotations at L_{1p} is as follows. The method is approximate in view of the fact that it assumes a uniform 'El' value in the cracked zone.

Fig.3.18 shows the distribution of bending moments at L_1, which is typical for simply supported beams uniformly prestressed by tendons at constant eccentricity, and subjected to a central point load.

Let the uniform moment due to prestress be M_p

$$\frac{a}{b} = \frac{M_p}{M_c - M_p} \quad \text{from which} \quad a = l_u \cdot \frac{M_p}{M_c} \;\&\; b = l_u\left(1 - \frac{M_p}{M_c}\right)$$

$$\text{Now} \quad l_u = \frac{l}{2} \times \frac{M_c}{M_1}, \quad \therefore a = \frac{l}{2} \cdot \frac{M_p}{M_1} \quad \text{and} \quad b = \frac{l}{2} \cdot \frac{M_c - M_p}{M_1}$$

Rotation between A and B (taking uncracked flexural rigidity as E'I')

$$= \frac{1}{2} l_u \times \frac{M_c}{E'I'} - \frac{l_u M_p}{E'I'} = \frac{l}{2\,E'I'} \cdot \frac{M_c}{M_1}\left(\frac{M_c}{2} - M_p\right)$$

$$= \frac{l}{E'I'} \frac{\left(M_c^2 - 2M_cM_p\right)}{4M_1}$$

Rotations between B & C (assuming a uniform cracked flexural rigidity of EI calculated from the state L_1 at the critical section).

$$= \left(\frac{\ell}{2} - \ell_{ck}\right)\frac{M_1 + M_c}{2EI}$$

$$= \frac{\ell}{2}\left(1 - \frac{M_c}{M_1}\right)\frac{M_1 + M_c}{2M_1 R_1} = \frac{\ell}{4R_1}\left(1 - \frac{M_c^2}{M_1^2}\right)$$

The total rotation between the end supports

$$= 2\left[\frac{\ell}{4R_1}\left(1 - \frac{M_c^2}{M_1^2}\right) + \frac{\ell}{E'I'}\frac{(M_c^2 - 2M_cM_p)}{4M_1}\right]$$

$$= \frac{\ell}{2R_1}\left(1 - \frac{M_c^2}{M_1^2}\right) + \frac{\ell}{2E'I'M_1}(M_c^2 - 2M_cM_p) \quad \text{—— } 3.8$$

The second term may be only 5% of the total rotation and may be neglected in some cases.

If we compare equation 3.8 with the expression $\frac{L}{2R_1}$ which is the rotation obtained by assuming a cracked EI value throughout the beam, for the limit L_1, in a bilinear idealization, we observe that an approximate value of the increased stiffness at L_{1p} is obtained by dividing the cracked EI value at L_1 by the factor $(1 - \frac{M_c^2}{M_1^2})$, provided M_c is small compared to M_1.

All rotations calculated for plotting L_{1p} in graphs 3.1 to 3.10 are in accordance with equation 3.8.

(b) Effect of lateral binders.

The danger of an unbound over-reinforced section is obvious from graph No. 3.5. The beam has a brittle failure even before the rotation at the limit L_1 is attained. The maximum bending moment is also less than that the calculated value at L_1. Practically no plastic rotation is available. A considerable improvement is gained in the values of rotations as well as the maximum moment, by the use of a small amount of binders (compare graphs 3.5 and 3.8). With a closer spacing of binders such as used in Beam No. 10, the rotation characteristic is highly ductile and resembles an under-reinforced member. In fact the limitation in the permissible extension of the jack prevented sufficient deformation to be applied to Beam No. 10, to be able to plot the falling part of the curve. The available rotation in this case is about 2½ times the calculated value.

In prestressed concrete structures, a critical section may become undesirably over-reinforced, due to linear transformation. Guyon[28] recognised the fact that the efficiency of redistribution of moments may depend on the way in which a linear transformation is effected. According to him 'Transformations which cause the cable to be very close to the compression surface will reduce the efficiency'. The use of lateral binders will be advantageous where it is necessary to leave a section over-reinforced after such a transformation.

In the discussions which took place in the meeting held in the Institute of Structural Engineers, in March 65, when the 'Ankara' paper was presented by Baker and Amarakone, it was pointed out that an approach similar to the limit design method of steel structures, might also be applicable in case of R.C. structures, provided recognition was given to the falling part of the moment rotation curves.

Lagrange[32] has also commented that better redistribution would take place in prestressed members under similar circumstances. Pietrzykowski[40] however, observed that heavily loaded columns were highly brittle and exhibited a tendency to sudden failure with a sharp fall in their moment carrying capacity. The results obtained by the author in case of over-reinforced beams, indicated that perhaps highly brittle columns might also be made to behave as ductile members, by the use of binders. The later part of this thesis is devoted to this problem.

(c) Crack pattern and moment curvature relationship near the critical section.

The pattern of cracks in all the beams shows that there is a tendency of the formation of a large crack near the critical section. This is very much pronounced in the under-reinforced beams. Perhaps bond slip is a major factor. Although the complete investigation into the causes of this behaviour is beyond the scope of this thesis, it may be pointed out that Raina[43] obtained similar results in case of pretensioned beams which did not have any un-tensioned mild steel reinforcement.

The moment curvature curves for sections which are slightly away from the critical section, were plotted in case of beams 3, 4 and 5 vide graph 3.11. The nature of these curves imply an increase of stiffness towards the supports. The formation of a large crack in the centre may be directly responsible for this. The method of plotting these curves from the curvature distribution diagrams, is explained in Appendix 7.

(d) Comparison of the true moment rotation curves as experimentally obtained, with the theoretical idealizations according to the recommendations of the Ankara paper.

In comparing the actual results with the idealized limits, it is necessary to assess a point on the actual curve which corresponds to the actual yielding behaviour of the beam. This has been done as follows:-

1) Where the maximum moment attained by the beam is not widely different from the calculated moment at L_2, the actual yielding behaviour of the beam has been assessed from the state when a moment equal to that calculated at L_1 is attained by the beam. The observed θ_p has been assessed from this point.

2) Where the maximum moment attained by the beam is appreciably different from this calculated moment at L_2 (Beam No.5), the actual θ_p has been measured from the state when a strain of .002 was attained by the extreme fibre of concrete in compression.

It will be found from graph 3.5 that the expression suggested by Baker at Ankara for calculating θ_p, ______ is not satisfactory in case of an over-reinforced beam without binders and is it recommended that the use of the above formula may be permitted in conjunction with a minimum specified percentage of lateral binders in all over-reinforced cases. The minimum quantity recommended is .75%.

It was also observed that this expression only partially accounts for the increase in rotations that is possible by the use of binders.

The following modification based on empirical results is suggested to take a better advantage of the use of binders.

$$\theta_p = .4(e_{c2} - \epsilon_{c1}) \frac{Z}{d} \left\{ 1 - .1 \frac{p''}{p''_{min}} + .1\left(\frac{p''}{p''_{min}}\right)^2 \right\} \ldots 3.9$$

where $p''_{min} = .75$

p'' = actual percentage of binders.

Finally it was also observed that although the Ankara stress block gave a fair estimate of the ultimate strains, it failed to assess the position of the neutral axis with a fair degree of accuracy. Table 3.7 gives the actual values of the neutral axis and strain attained in Beams 1-10, against the calculated values. Further research has been done recently in this respect.[47]

(e) Effect of altering the prestressing force.

The comparison of graphs 3.3, 3.6 and 3.7 shows that a wide variation in the prestressing force (from 50% to 30% of ultimate) does not materially alter the moment of resistance of the beam, but a lower prestressing force considerably increases the plastic rotations. The cracking moment also drops significantly by lowering the prestress.

3.12. The next chapter is an introduction to portal frames which is the main subject of study in this thesis. Moment rotation characteristics of column members with high axial loads have also been discussed.

TABLE 3.1

SHOWING CHARACTERISTICS OF 10 PRESTRESSED AND POST TENSIONED BEAMS.

BEAM NO.	b	b'	d	D	C_c p.s.i.	Ultimate stress in tendons fsu k.s.i.	Pre-stressing stress in tendons. fp k.s.i.	ω
1	6"	2.25"	5.75"	8.00"	4775	228.0	117.5	.0825
2	"	"	"	"	5360	"	121.5	.1470
3	"	"	"	"	4640	"	114.0	.2550
4	"	"	"	"	5040	"	127.5	.3120
5	"	"	"	"	4960	"	127.0	.3970
6	"	"	"	"	5360	"	91.5	.2550
7	"	"	"	"	5200	"	75.3	.2550
8	"	"	"	"	5450	232.5	126.0	.3680
9	"	"	"	"	5450	"	126.0	"
10	"	"	"	"	5450	"	126.0	"

BEAM NO.	p"	m_{max} $\left(=\frac{M_{max}}{c_c bd^2}\right)$	$2\theta_1$ Calculated	θ_b Calculated.	$\frac{m_1(act)}{m_1(cal)}$	$\frac{m_2(act)}{m_2(cal)}$	$\frac{\theta_b(act)}{\theta_b(cal)}$
1	-	.098	.0303	.026	.95	1.03	1.8
2	-	.157	.0305	.018	1.00	1.095	3.00 approx. if rotations are counted up to .95 M_{max}.
3	-	.216	.0345	.0118	.91	1.035	1.35
4	-	.262	.0323	.0077	.96	.99	.65
5	-	.276	.0288	.0057	.94	.885	.875
6	-	.175	.0416	.0123	.92	.95	1.30
7	-	.182	.0470	.0118	.92	.967	1.67
8	.625*	.319	.0328	.0100	1.05	1.04	1.00
9	1.25	.333	.0328	.0142	1.10	1.12	1.65
10	2.5	.344	.0328	.0185	1.07	1.10	3.00

* Only in the compression flange.

TABLE 3.2

ABSORPTION CAPACITY.

	COARSE AGGREGATE	FINE AGGREGATE
SPECIFIC GRAVITY	2.65	2.65
ABSORPTION	1.20	1.00

TABLE 3.3

SIEVE ANALYSIS OF AGGREGATES

(a) SAND 25 downwards Weight of sample 1000 gms.

Sieve No.	Wt. retained (gms.)	Wt. passing (gms.)	% passing
7	1	999	99.9
14	5	994	99.4
25	11	983	98.3
52	771	212	21.2
100	186	26	2.6
PAN	26	0	0
	1000		

(b) SAND $^3/_{16}$" to 25 Weight of sample 1000 gms.

$^3/_{16}$	4	996	99.6
7	223	773	77.3
14	319	454	45.4
25	269	185	18.5
52	163	22	2.2
100	20	2	.2
PAN	2	0	0
	1000	-	-

continued .

TABLE 3.3

(c) ¾" down C.A. Weight of sample 3000 gms.

SIEVE NO.	Wt. retained. (gms)	Wt. passing (gms)	% passing.
¾"	30	2970	99.0
⅜"	2940	30	1.0
3/16"	30	0	0
	3000		

N.B. In each case, the weight retained is the average of three readings.

TABLE 3.4

STRENGTH OF CONTROL SPECIMENS.

BEAM NO.	(1) Av. Cube Strength.	(2) Av. Cylinder Strength.	Ratio 2/1	Av. Strength in flexural tension.
1	5970	4200	.7	528
2	6700	4275	.635	535
3	5800	4275	.74	500
4	6300	4440	.7	495
5	6200	3970	.64	500
6	6700	4690	.7	530
7	6500	4550	.7	500
8	6800	4760	.7	520
9	6800	4760	.7	520
10	6800	4760	.7	520

Note: Av. cylinder is rather low due to capping difficulties.

TABLE 3.5
SCHEDULE OF CASTING PRESTRESSING AND GROUTING AND TESTING.

BEAM	Date of Casting	Prestressing Date	Prestressing period after casting	Grouting	Testing Date	Testing Period after pre-stressing	Period after casting.
1	3. 6.64	18.6.64	15	19.6.64	7.7.64	19	34
2	12. 6.64	26.6.64	14	8.7.64	15.7.64	19	33
3	26.6. 64	10.7.64	14	20.7.64	1.8.64	22	36
4	9. 7.64	5.8.64	27	7.8.64	14.8.64	9	36
5	24. 7.64	19.8.64	26	24.8.64	29.8.64	10	36
6	26.11.64	22.12.64	26	22.12.64	1.2.65	41	67
7	2.12.64	29.12.64	27	30.12.64	8.2.65	41	68
8	9.12.64	13.1.65.	35	13.1.65	13.2.65	31	66
9	17.12.64	19.1.65	33	20.1.65	21.2.65	33	66
10	8. 1.64	10.2.65	33	10.2.65	6.3.65	24	57

TABLE 3.6
SUMMARY OF LOSSES.

BEAM	WIRE NO.	Losses in lbs. due to Elasticity	Shrinkage.	Creep of concrete	Creep of steel	SKETCH.
1	1	0	50	80	300	1
2	(1	110	50	160	300	1 2
	(2	0	50	160	305	
3	(1	200	50	200	320	1
	(2	120	50	200	250	2
	(3	0	50	310	320	3
4	(1	320	25	240	325	1 2
	(2	210	25	230	320	
	(3	115	25	350	335	
	(4	0	25	360	340	3 4
5	(1	415	25	255	330	1 2
	(2	330	25	255	330	
	(3	300	25	365	335	3
	(4	125	25	450	335	
	(5	0	25	450	330	4 5

REMARKS.

1) The number shown in the sketch also indicate the sequence of prestressing.

2) The following data was taken from Concrete Research Magazine No. 40 Vol.14.

cont...

TABLE 3.6 REMARKS cont.

a) Specific creep factor for Beams 1, 2 and 3, which were tested after about 20 days of prestressing = 140×10^{-9}. Ditto for Beams 4 and 5 = 110×10^{-9}.

b) For calculating shrinkage losses, the difference between shrinkage strains at 14th and 34th day was taken for Beams 1 to 3, and the difference between the 26th and 36th day was taken for Beams 4 and 5.

3) Losses in Beams 6 and 7 were mainly derived from Beam No.3, by altering the prestressing force.

4) An average loss of 1000 lbs. per wire was estimated in Beams, 7, 8 and 9, as derived from Beam 5.

TABLE 3.7

Actual Values of e_{c2} and n_2 against calculated values using the Ankara stress block.

BEAM NO.	n_2 Calculated	n_2 Observed.	e_{c2} Calculated	e_{c2} Observed.
1	.115	*.088 at L.S.11	.01	*.0039 at LS 11
2	.155	*.12 at L.S.12	.0075	*.0048 at LS.12
3	.245	.16	.0057	.0092
4	.335	.25	.0045	.0057
5	.445	.386 at L.S.12 just before brittle failure.	.004	.0041 at LS.12
6	.21	*.18 at L.S.12	.0060	*.01 at L.S.12
7	.215	*.18 at L.S.12	.0060	*.011 at LS.12
8	.3675	.35	.0055	.0069
9	.361	.33	.0070	.0081
10	.356	*.33 at L.S.15	.0085	*.01 at L.S.15

REMARKS.

* Observation could not be recorded in these cases at the ultimate stage, due to spalling.

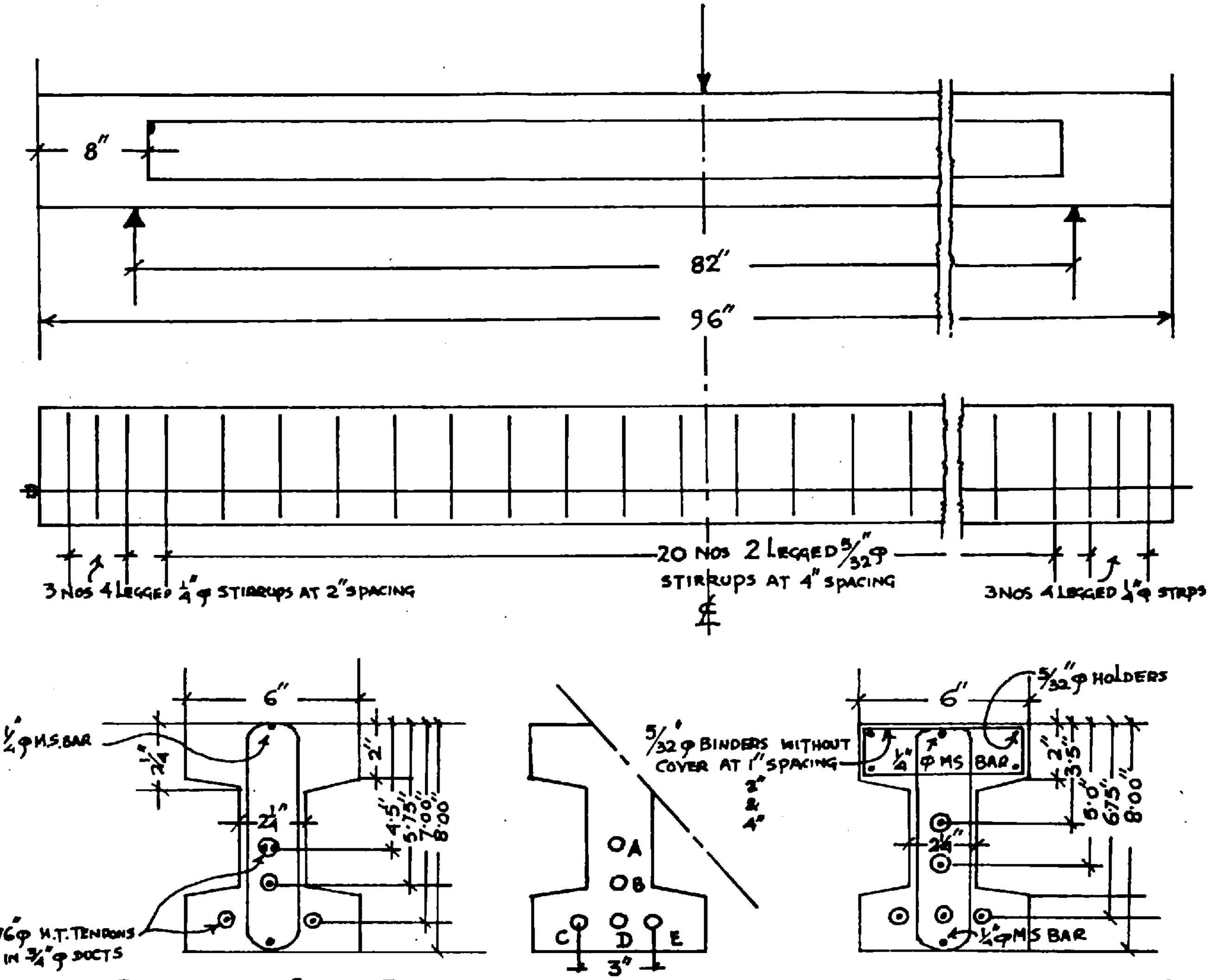

CROSS-SECTION BEAM 5 GENERAL LAYOUT CROSS-SECTION BEAMS 10, 9 & 8

6"×8" I SECTIONS

TABLE OF REINFORCEMENT

	BEAM 1	BEAM 2	BEAM 3	BEAM 4	BEAM 5
A	NIL	NIL	1 BAR, ·276" φ	2 BARS, ·276" φ	2 BARS, ·276" φ
B	1 BAR, ·276" φ	2 BARS ·276" φ	1 BAR, ·276" φ	NIL	1 BAR, ·276" φ
C	NIL	NIL	NIL	1 BAR, ·276" φ	1 BAR, ·276" φ
D	NIL	NIL	1 BAR, ·276" φ	NIL	NIL
E	NIL	NIL	NIL	1 BAR, ·276" φ	1 BAR, ·276" φ

REMARKS

BEAMS 6 & 7 HAVE THE SAME REINFORCEMENT AS BEAM 3

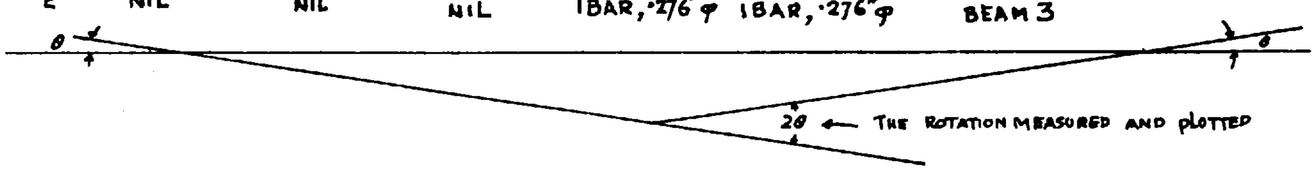

FIG 3.1

DETAILS OF REINFORCEMENT IN BEAMS 1 TO 10

PRESTRESSED POST TENSIONED BEAMS TESTED IN IMPERIAL COLLEGE (GROUTED) BEAMS 1 TO 10

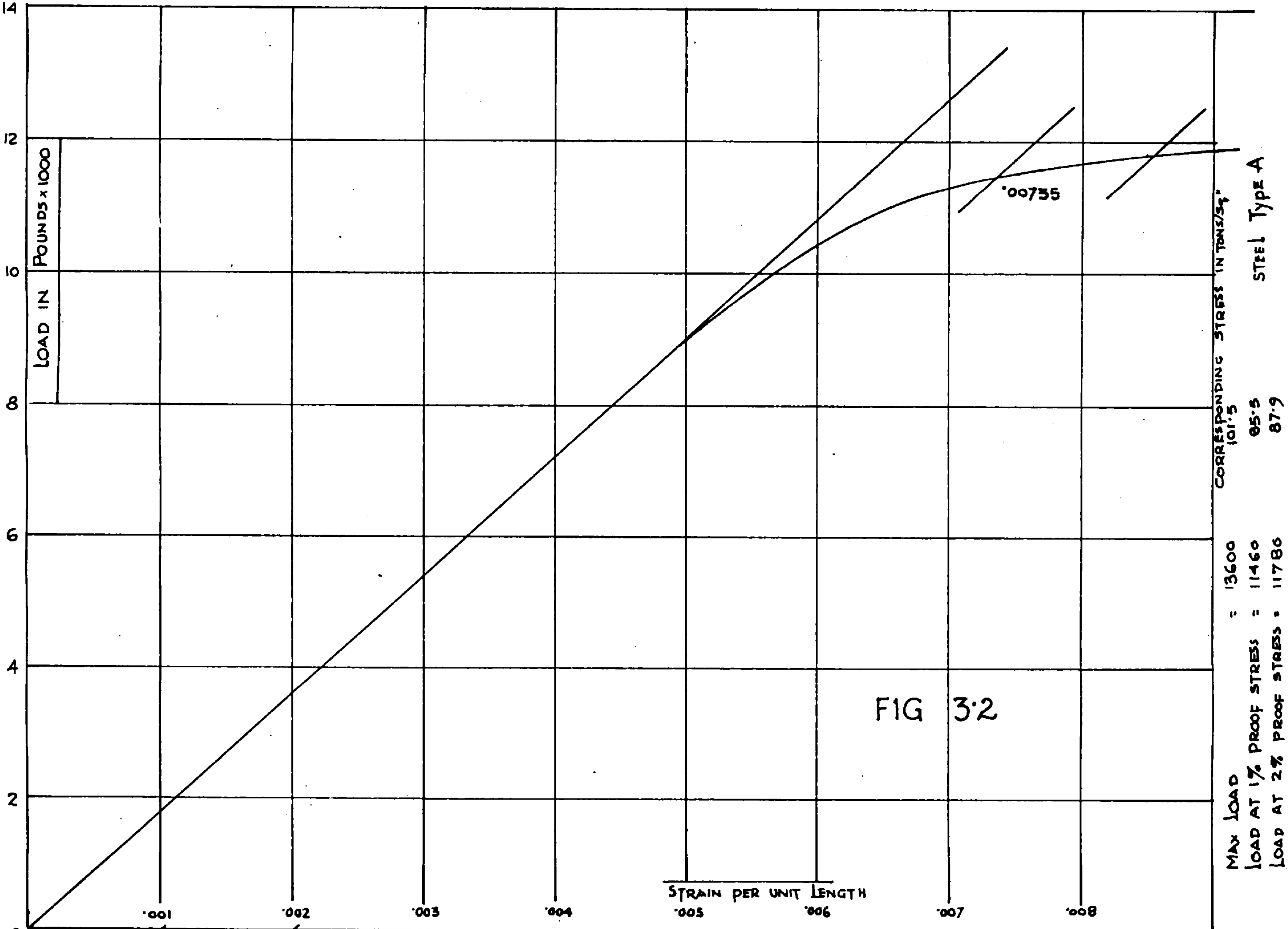

FIG 3·2

LOAD VS STRAIN CURVE FOR ·276" φ INDENTED TENDONS USED IN BEAMS (1–7)

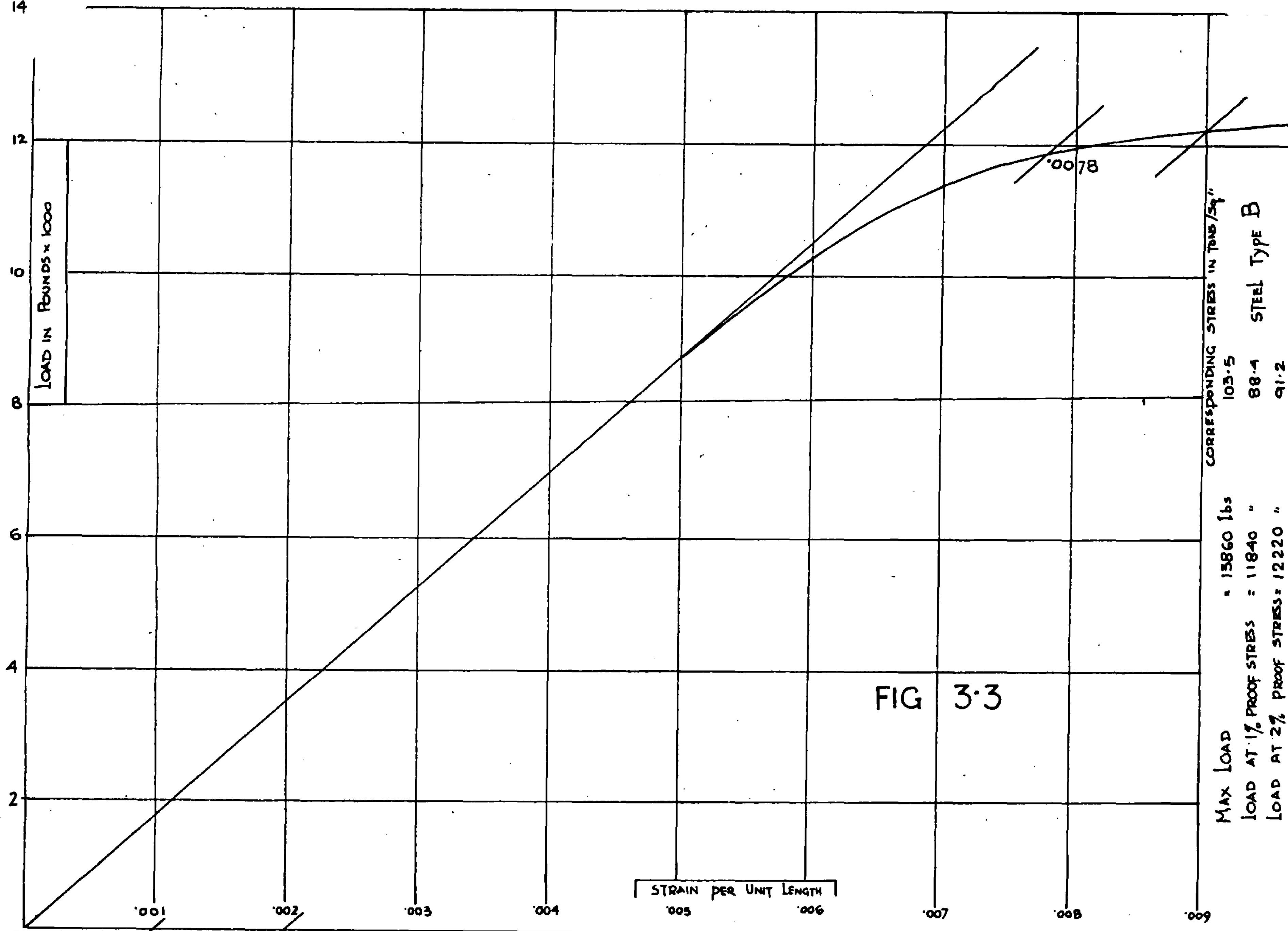

FIG 3·3

MAX LOAD	= 13860 lbs	103·5
LOAD AT 1% PROOF STRESS	= 11840 "	88·4
LOAD AT 2% PROOF STRESS	= 12220 "	91·2

CORRESPONDING STRESS IN TONS/Sq"

STEEL TYPE B

LOAD VS STRAIN CURVE FOR ·276" φ INDENTED TENDONS USED IN BEAMS (8-10)

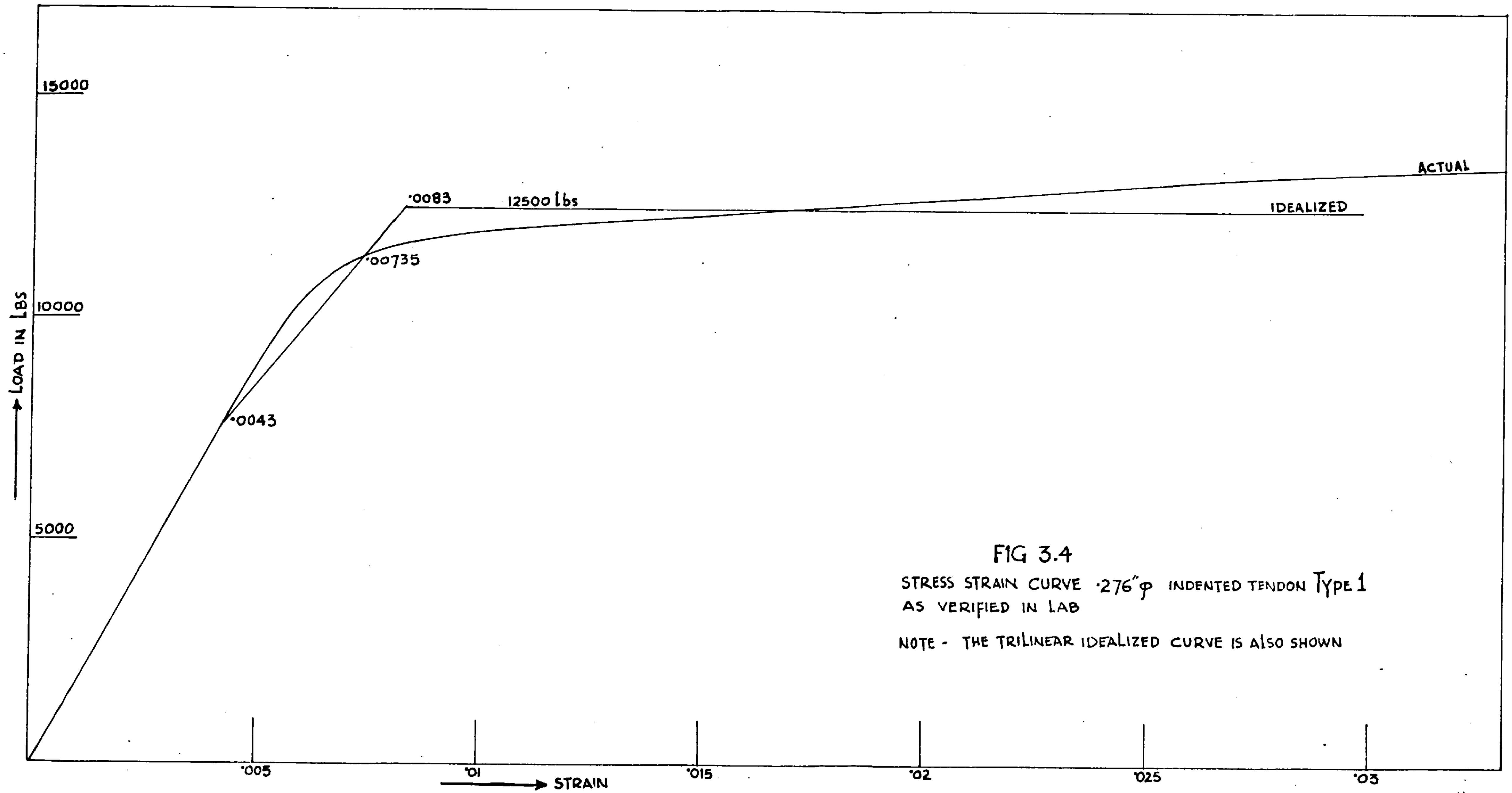

FIG 3.4

STRESS STRAIN CURVE ·276″φ INDENTED TENDON TYPE 1
AS VERIFIED IN LAB

NOTE - THE TRILINEAR IDEALIZED CURVE IS ALSO SHOWN

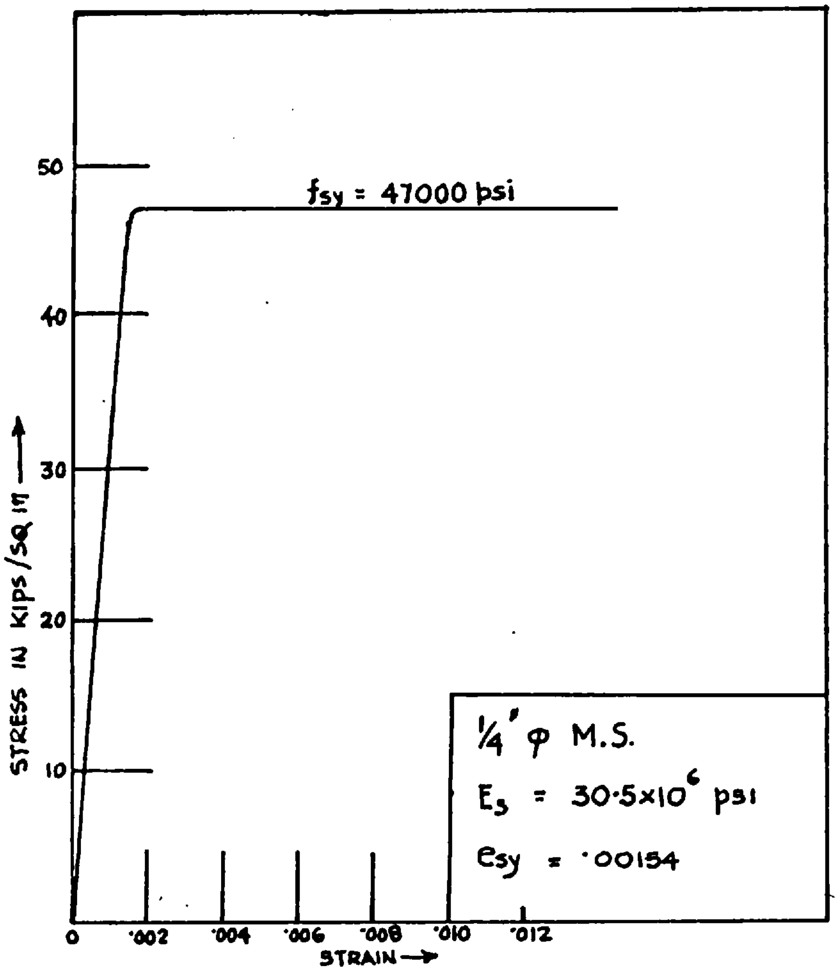

FIG 3.5

STRESS STRAIN CURVE OF MILD STEEL BARS

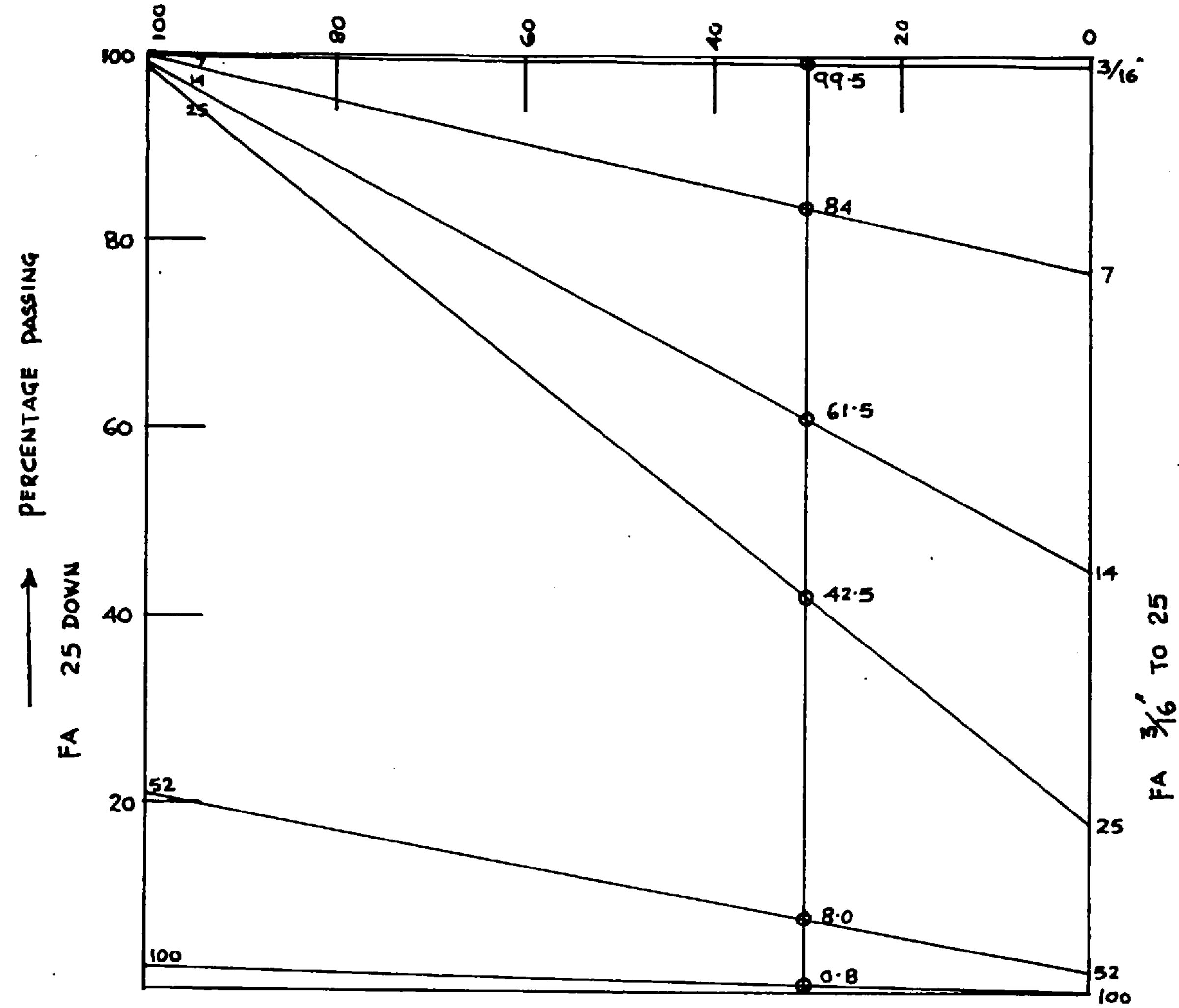

FIG 3.6

COMBINING THE FINE AGGREGATE

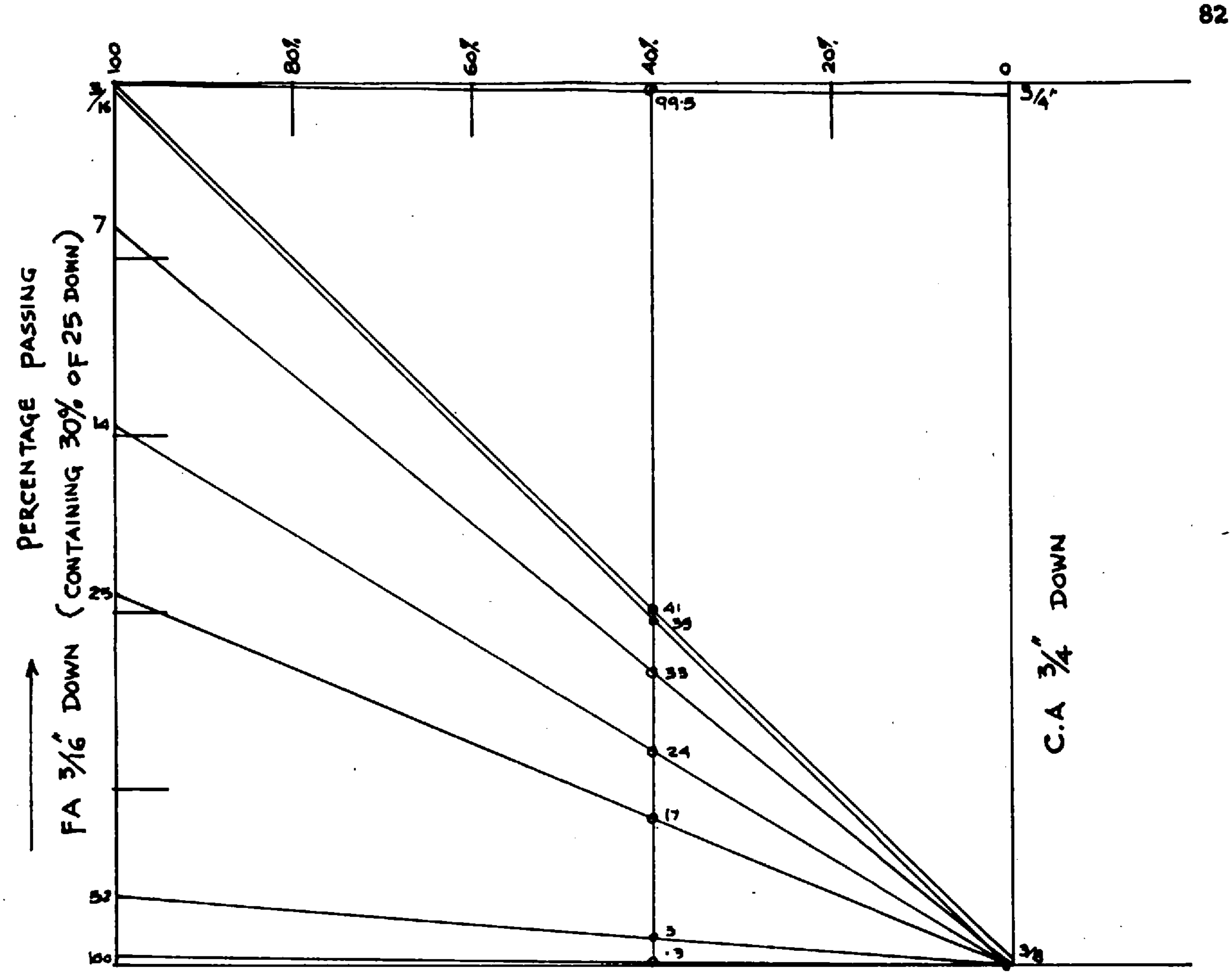

FIG 3.7
COMBINING THE FA WITH CA

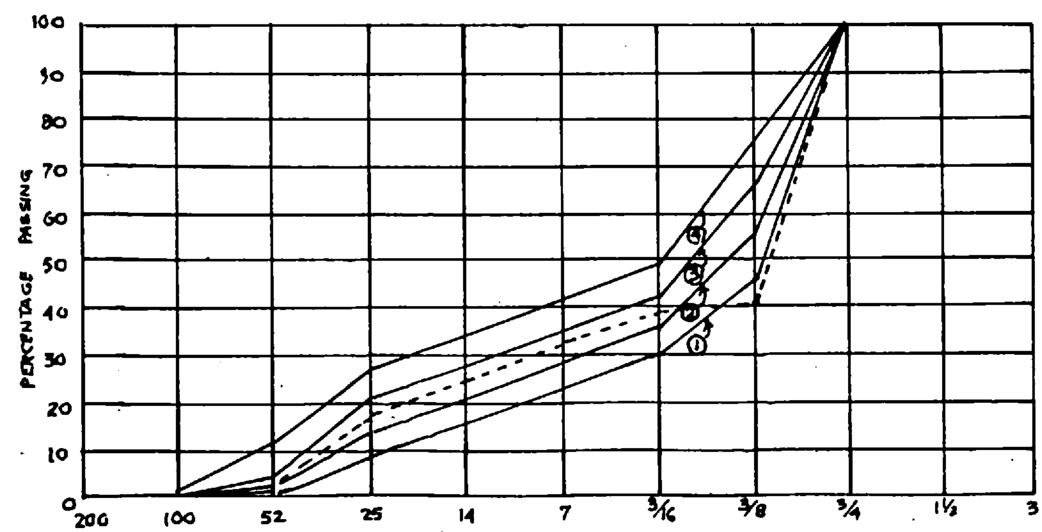

FIG 3.8

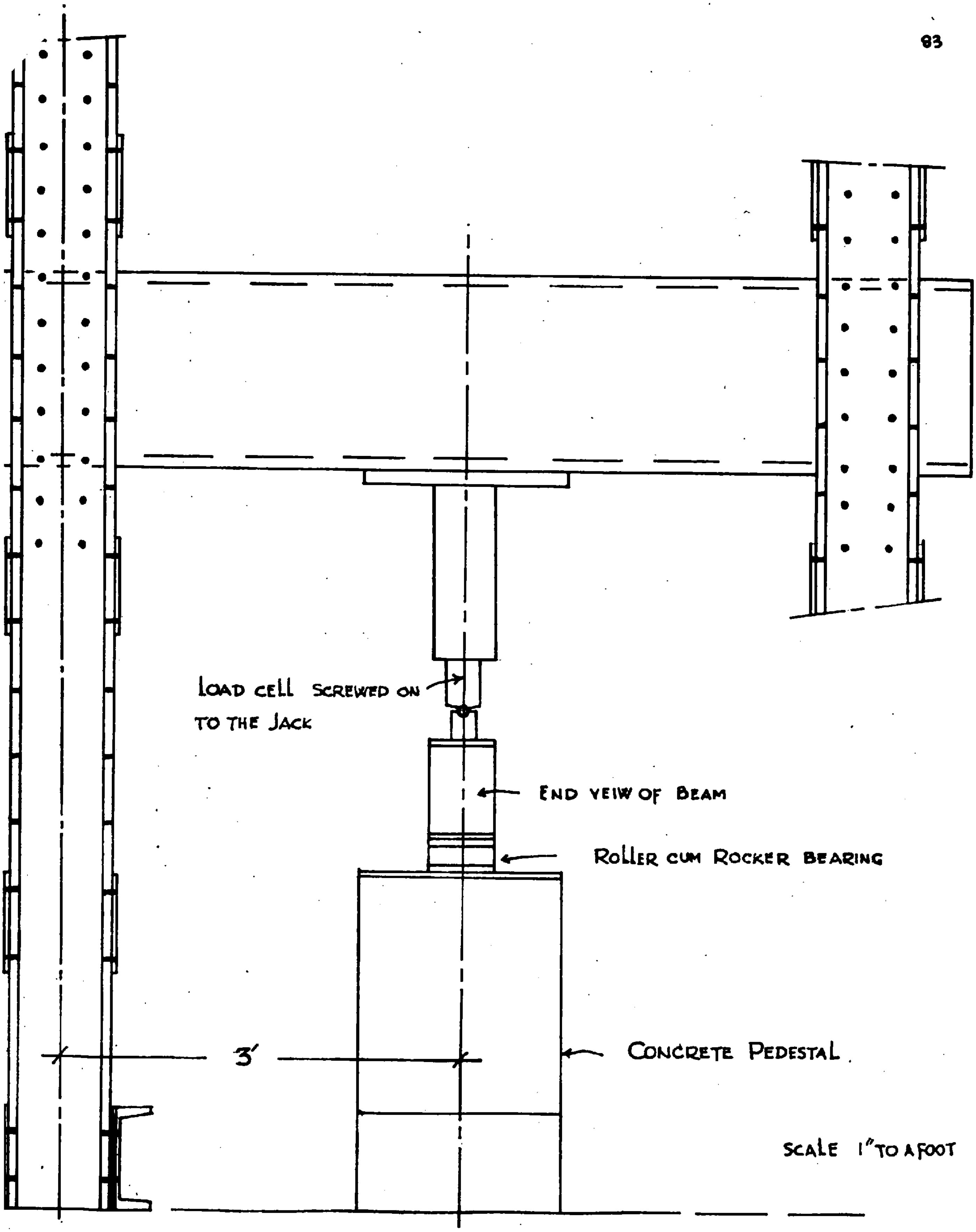
LOAD CELL SCREWED ON TO THE JACK
END YEIW OF BEAM
ROLLER CUM ROCKER BEARING
3'
CONCRETE PEDESTAL
SCALE 1" TO A FOOT

FIG 3.9

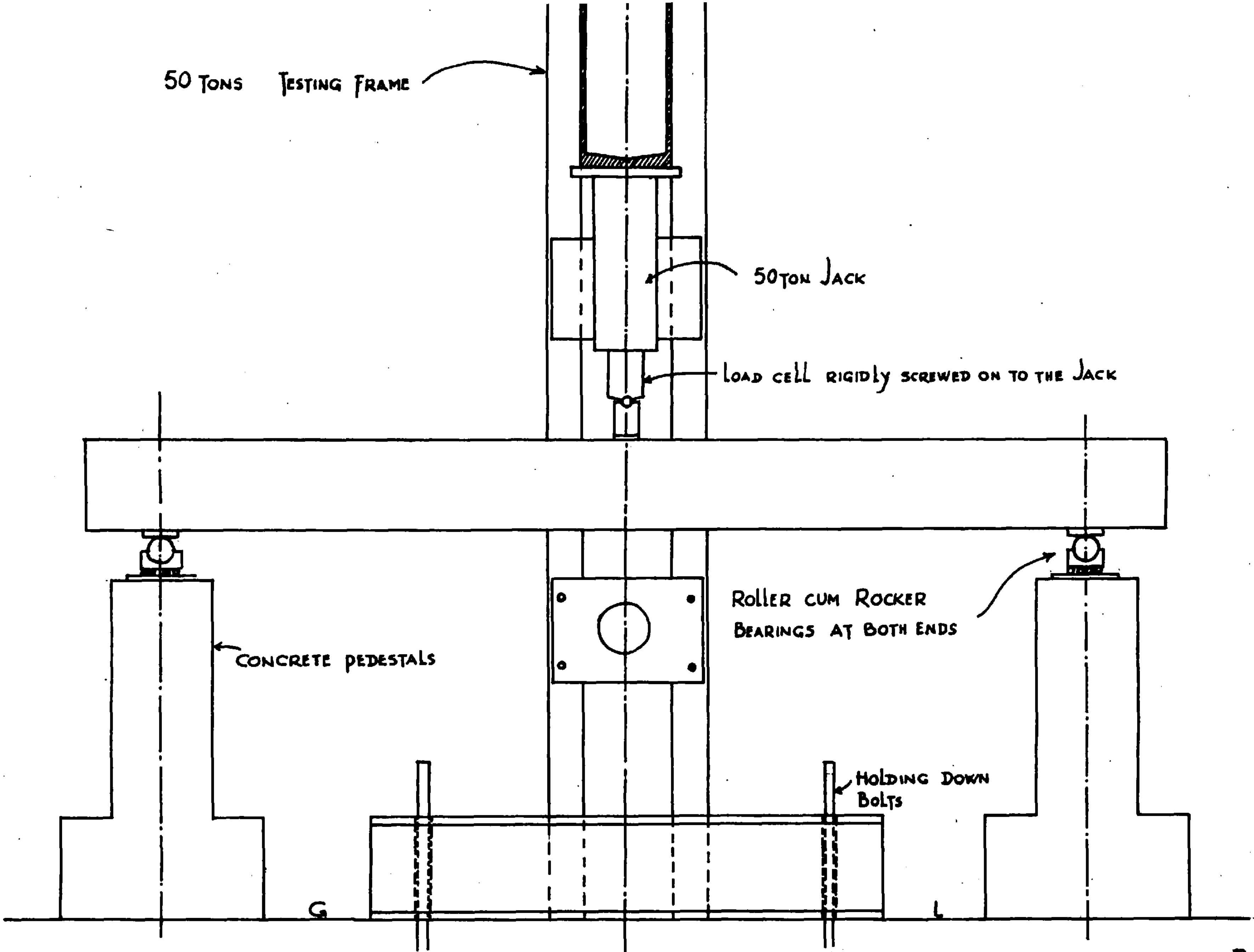
50 TONS TESTING FRAME
50TON JACK
LOAD CELL RIGIDLY SCREWED ON TO THE JACK
ROLLER CUM ROCKER
BEARINGS AT BOTH ENDS
CONCRETE PEDESTALS
HOLDING DOWN
BOLTS
G
L

FIG 3.10

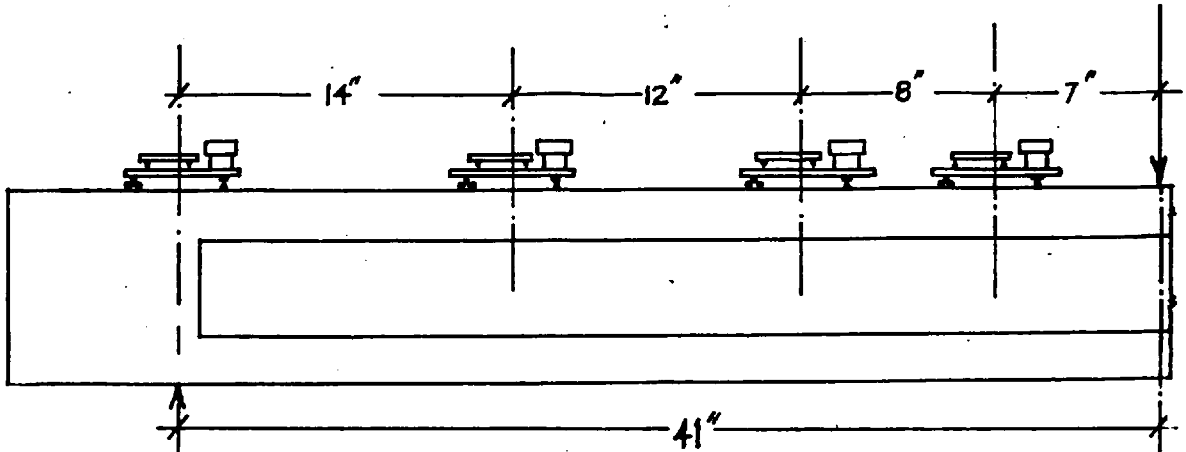

FIG 3.11

Layout of Clinometers

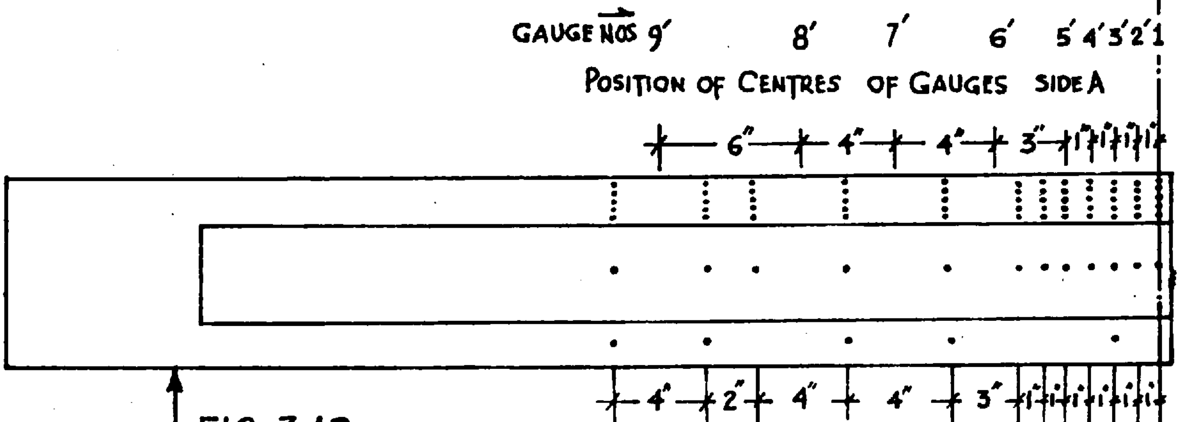

FIG 3.12

Layout of Demec points

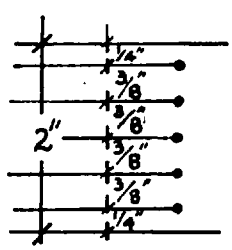

Detail of Demec points in the Top Flange

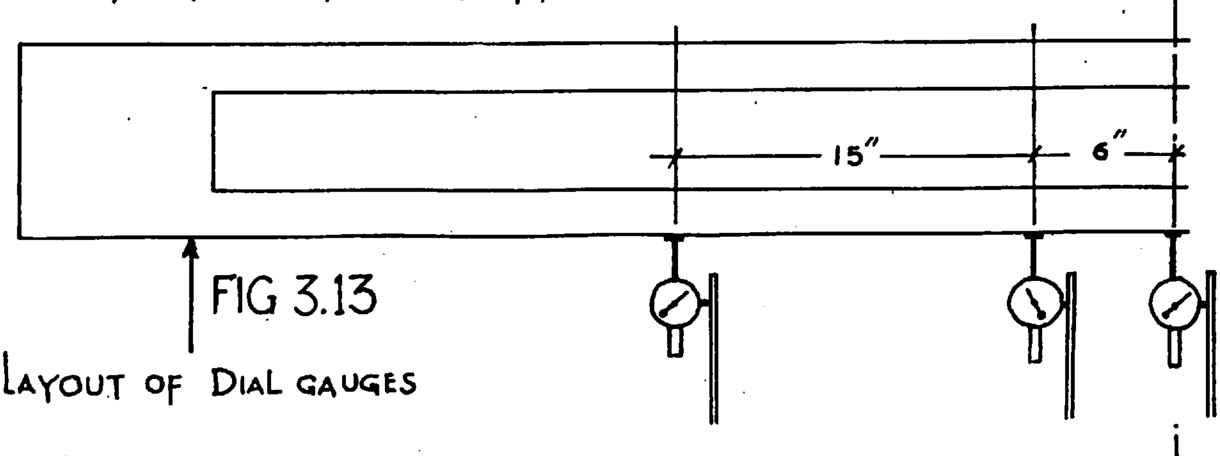

FIG 3.13

Layout of Dial gauges

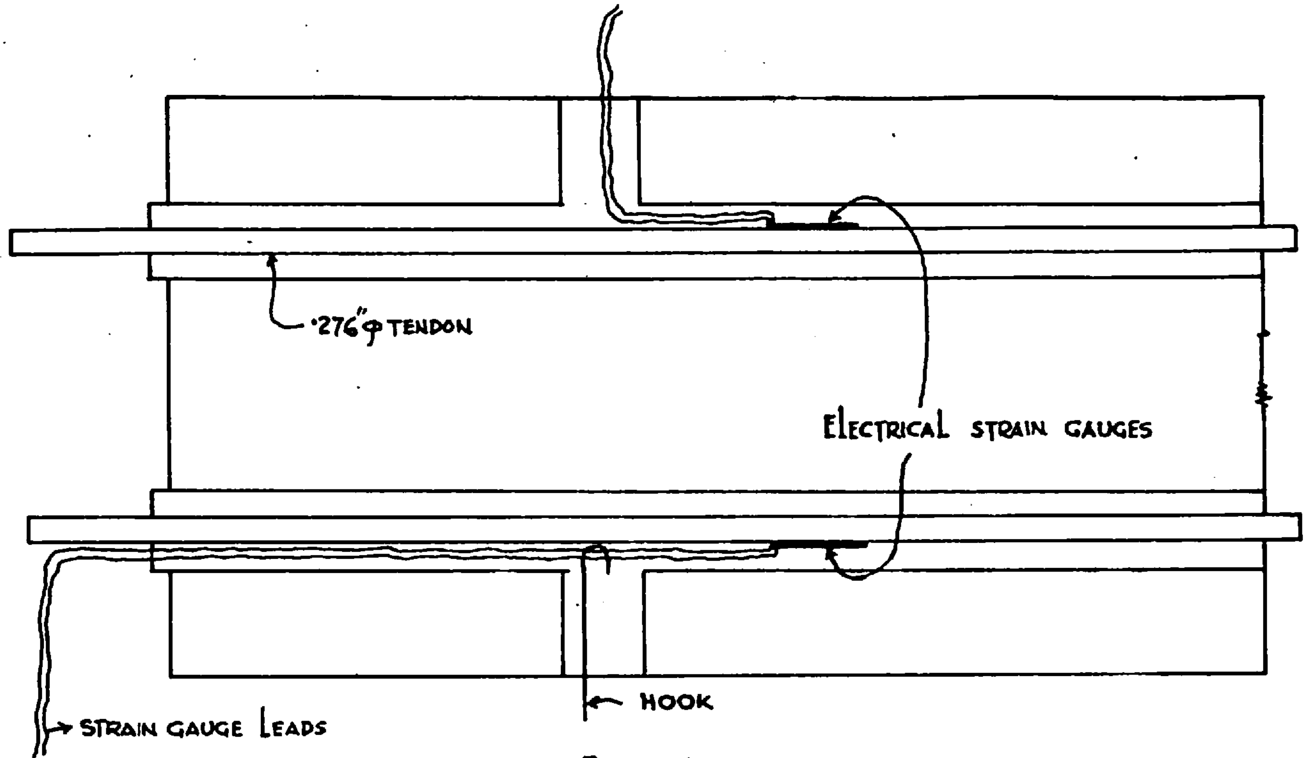

FIG 3.14

DETAIL OF GROUTING THROUGH SIDE VENTS

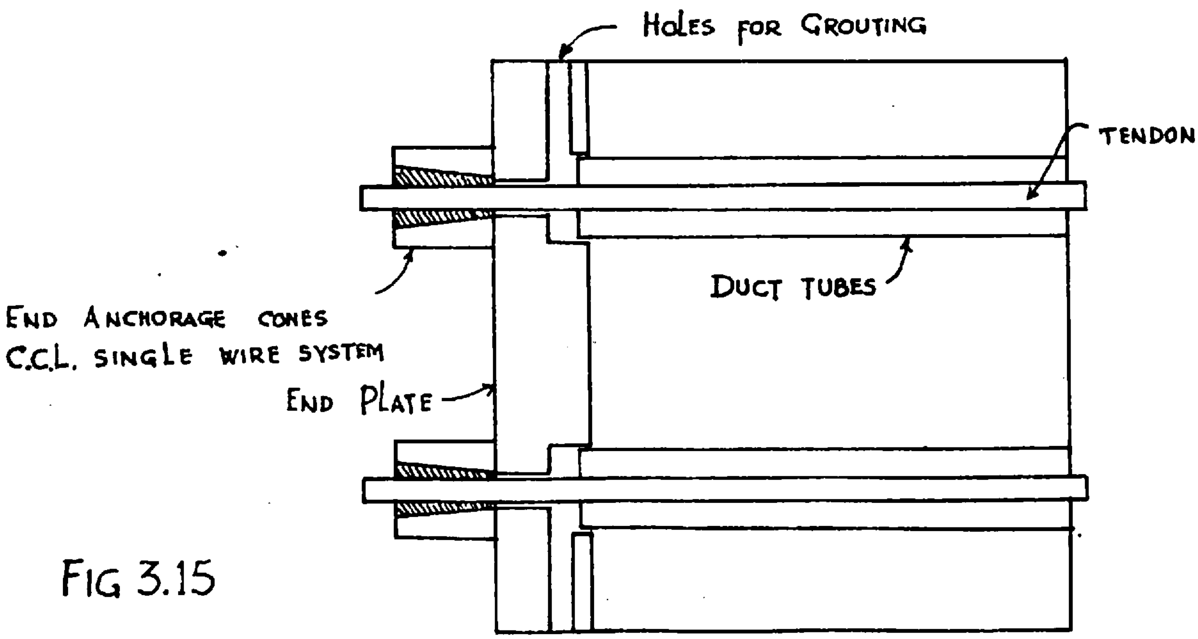

FIG 3.15

DETAIL OF GROUTING THROUGH END PLATE

SECTIONAL PLAN OF END OF BEAM

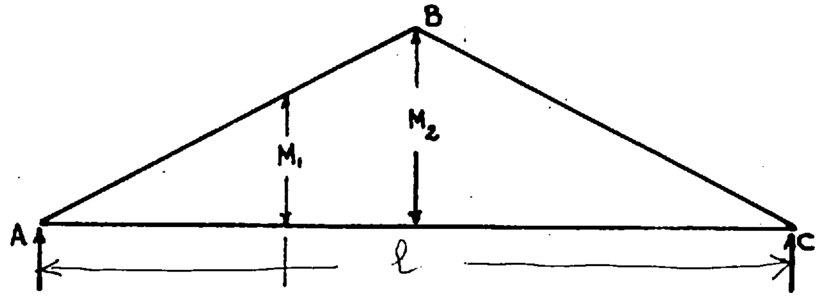

FIG 3.16 a

DISTRIBUTION OF BENDING MOMENT IN S-SUPPORTED BEAM WITH CONCENTRATED LOAD AT CENTRE

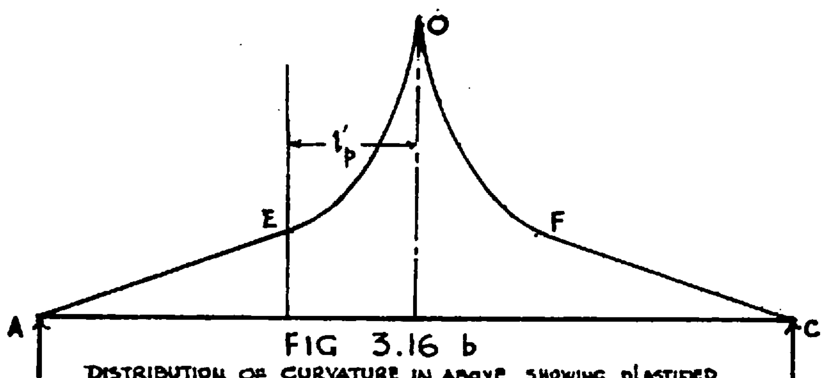

FIG 3.16 b

DISTRIBUTION OF CURVATURE IN ABOVE SHOWING PLASTIFIED LENGTH l_p'

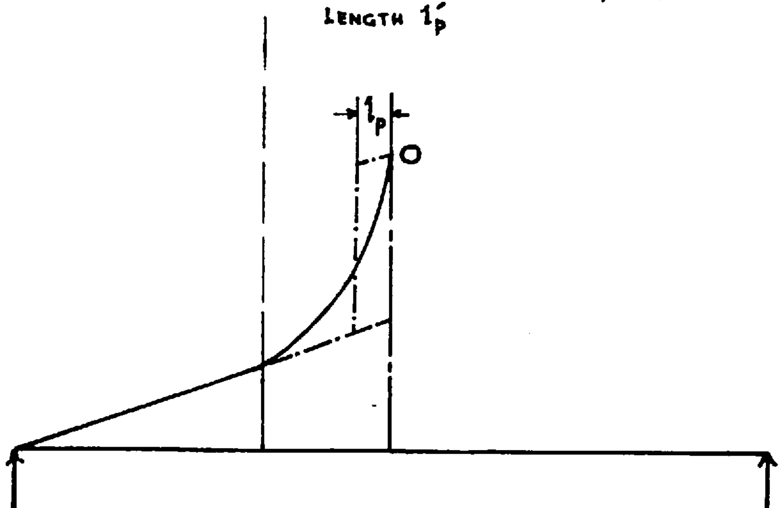

FIG 3·17

SHOWING EQUIVALENT PLASTIC HINGE LENGTH l_p HAVING UNIFORM CURVATURE

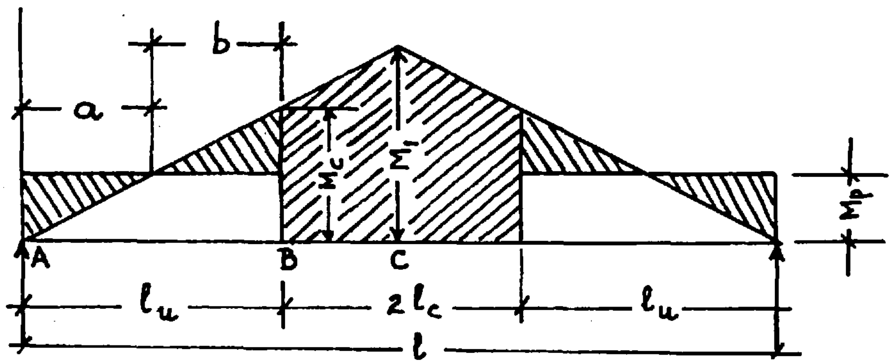

FIG 3·18

SHOWING ZONES OF CRACKED AND UNCRACKED FLEXURAL RIGIDITY IN A PRESTRESSED CONCRETE BEAM HAVING CABLES AT CONSTANT ECCENTRICITY AND SUBJECTED TO A POINT LOAD AT CENTRE

NOTE l_u DENOTES ZONES OF UNCRACKED EI'

$2l_c$ IS THE ZONE OF CRACKED EI

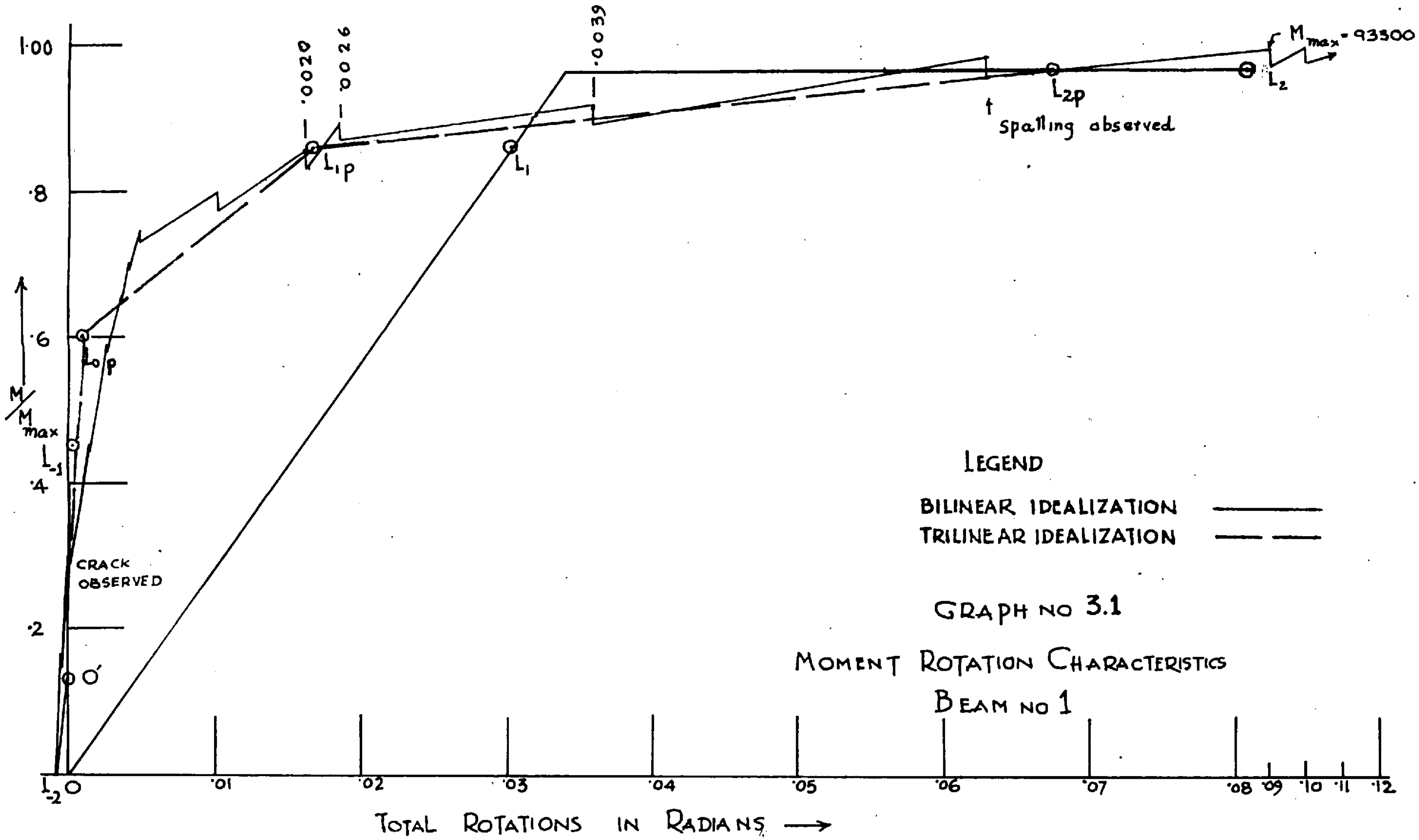

GRAPH NO 3.1

MOMENT ROTATION CHARACTERISTICS

BEAM NO 1

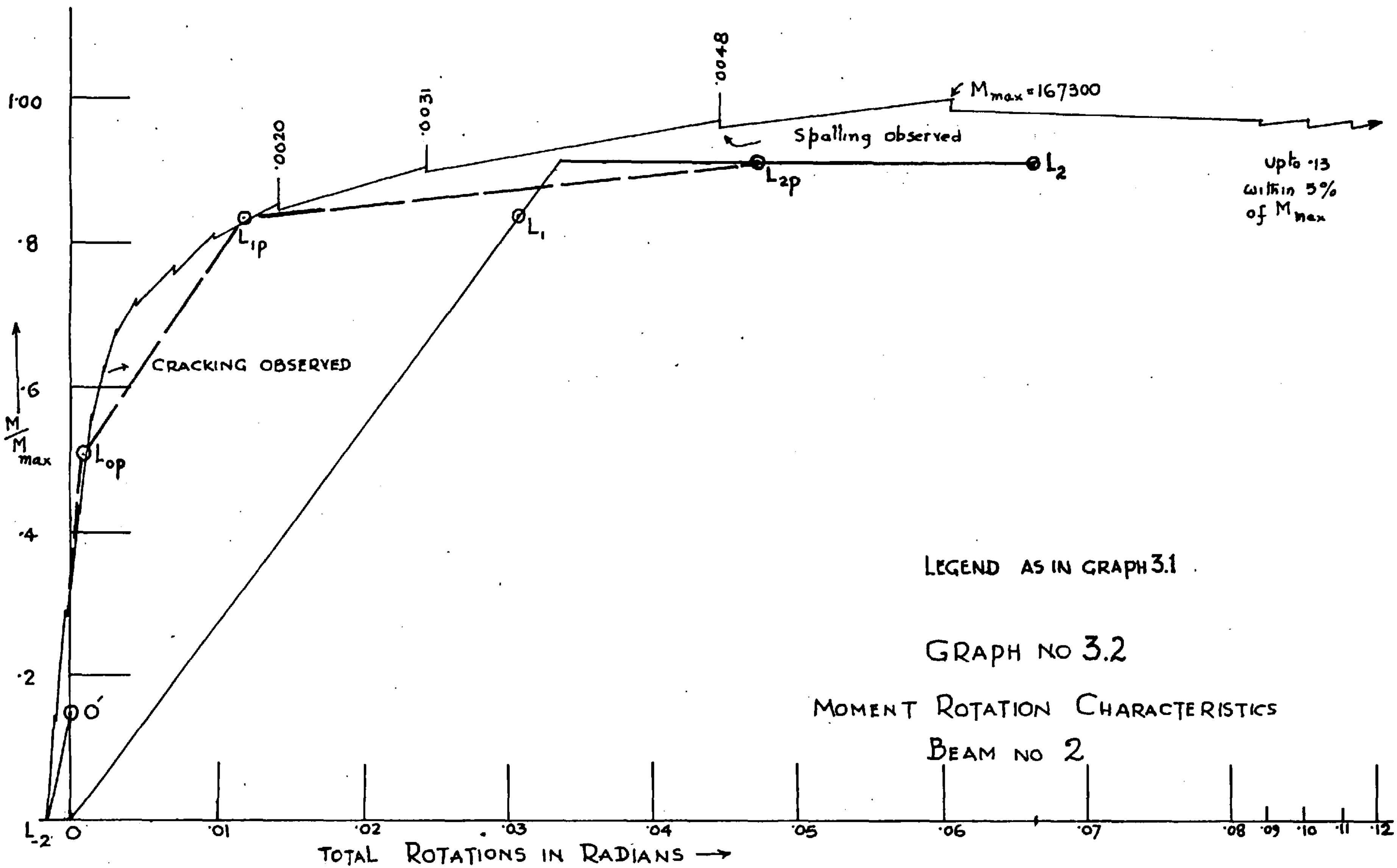

GRAPH NO 3.2

MOMENT ROTATION CHARACTERISTICS

BEAM NO 2

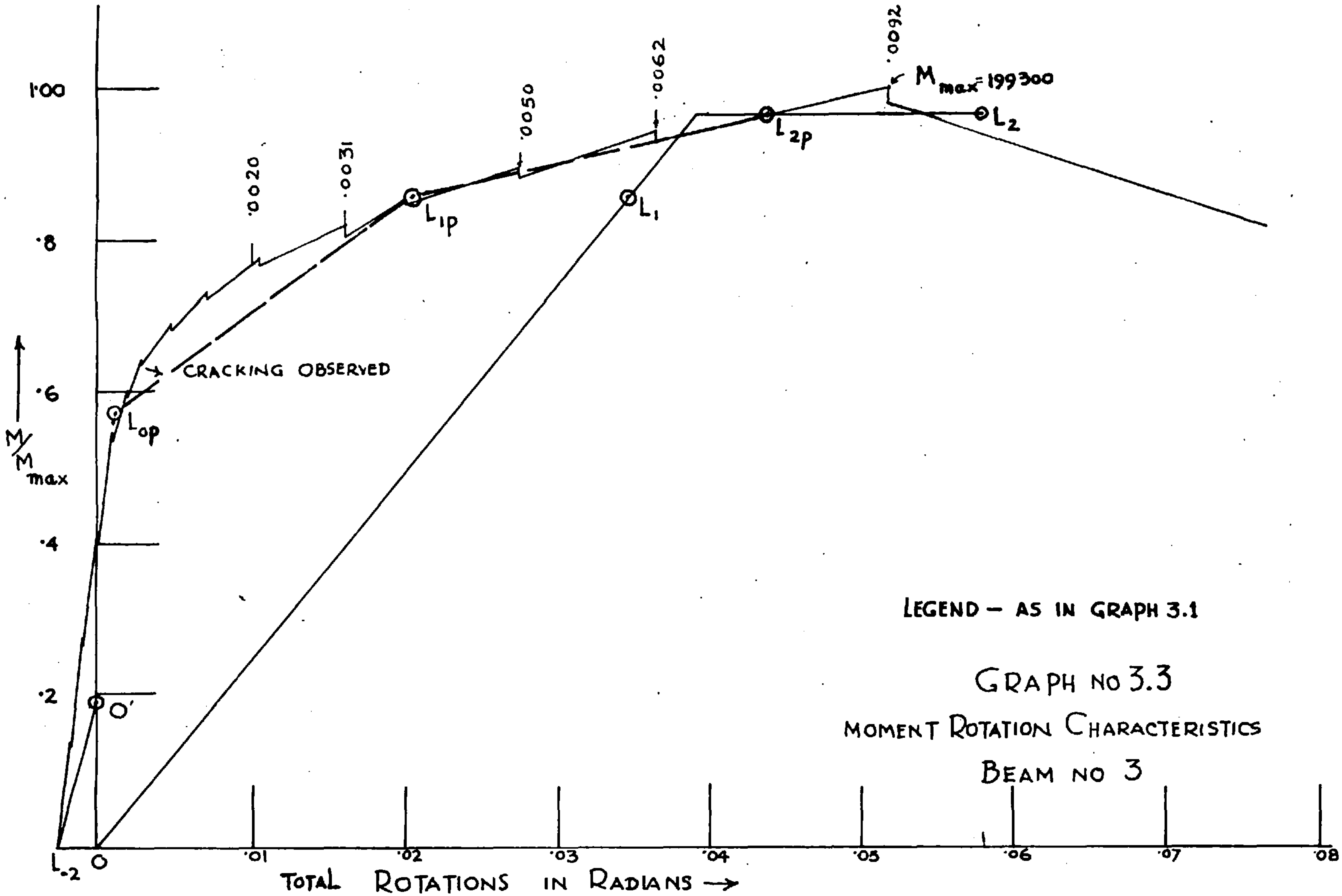

LEGEND – AS IN GRAPH 3.1

GRAPH NO 3.3

MOMENT ROTATION CHARACTERISTICS

BEAM NO 3

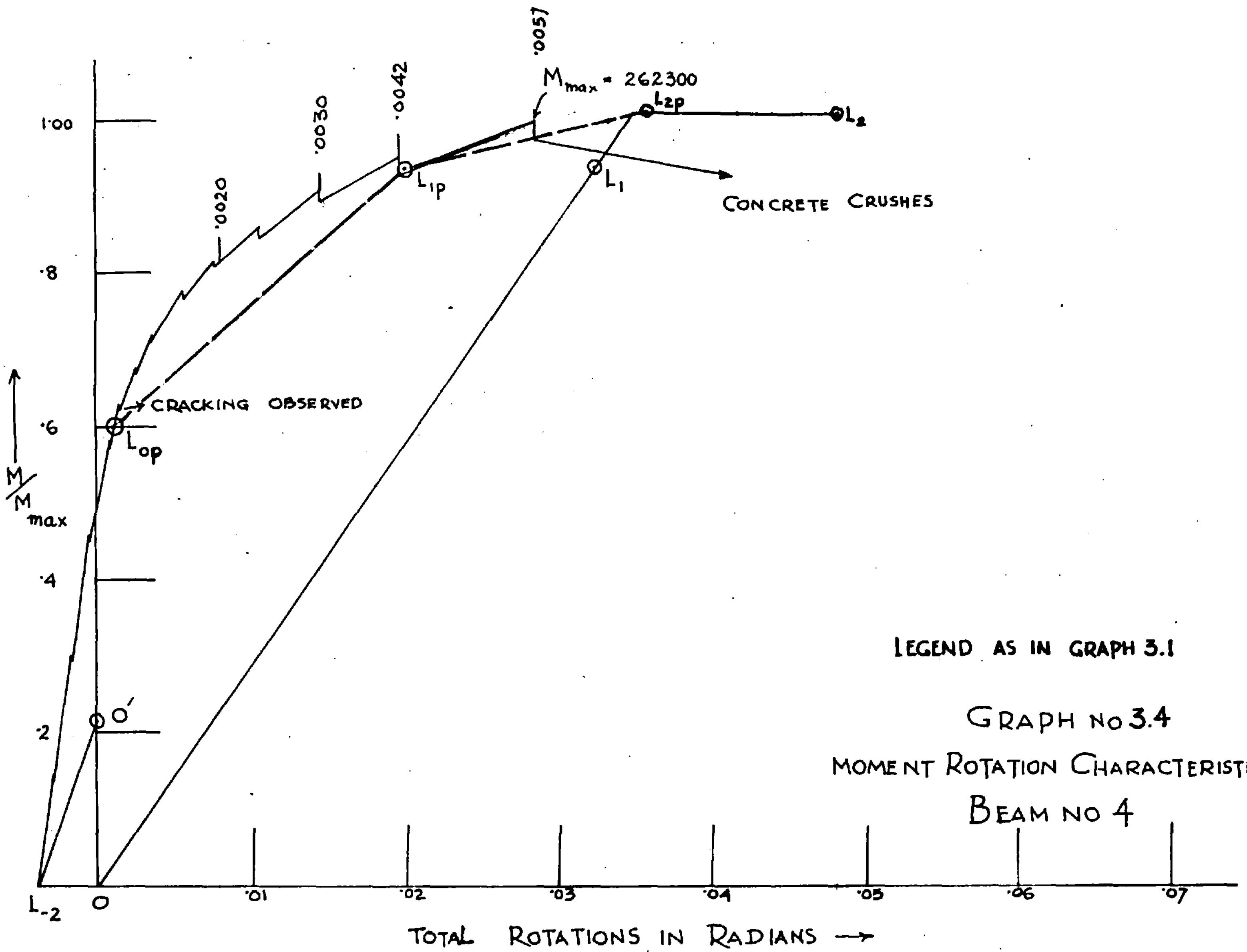

LEGEND AS IN GRAPH 3.1

GRAPH NO 3.4

MOMENT ROTATION CHARACTERISTICS

BEAM NO 4

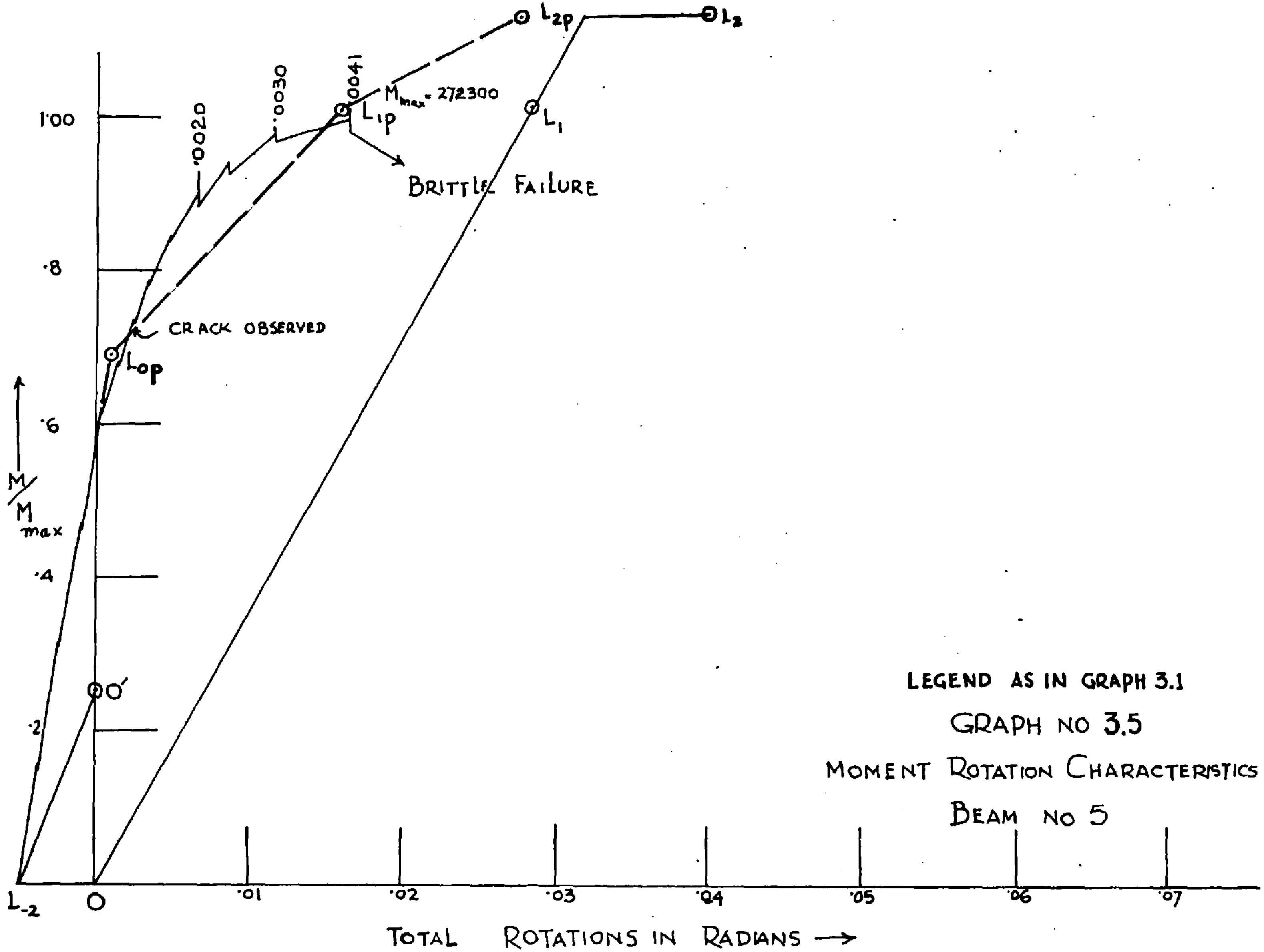

LEGEND AS IN GRAPH 3.1

GRAPH NO 3.5

MOMENT ROTATION CHARACTERISTICS

BEAM NO 5

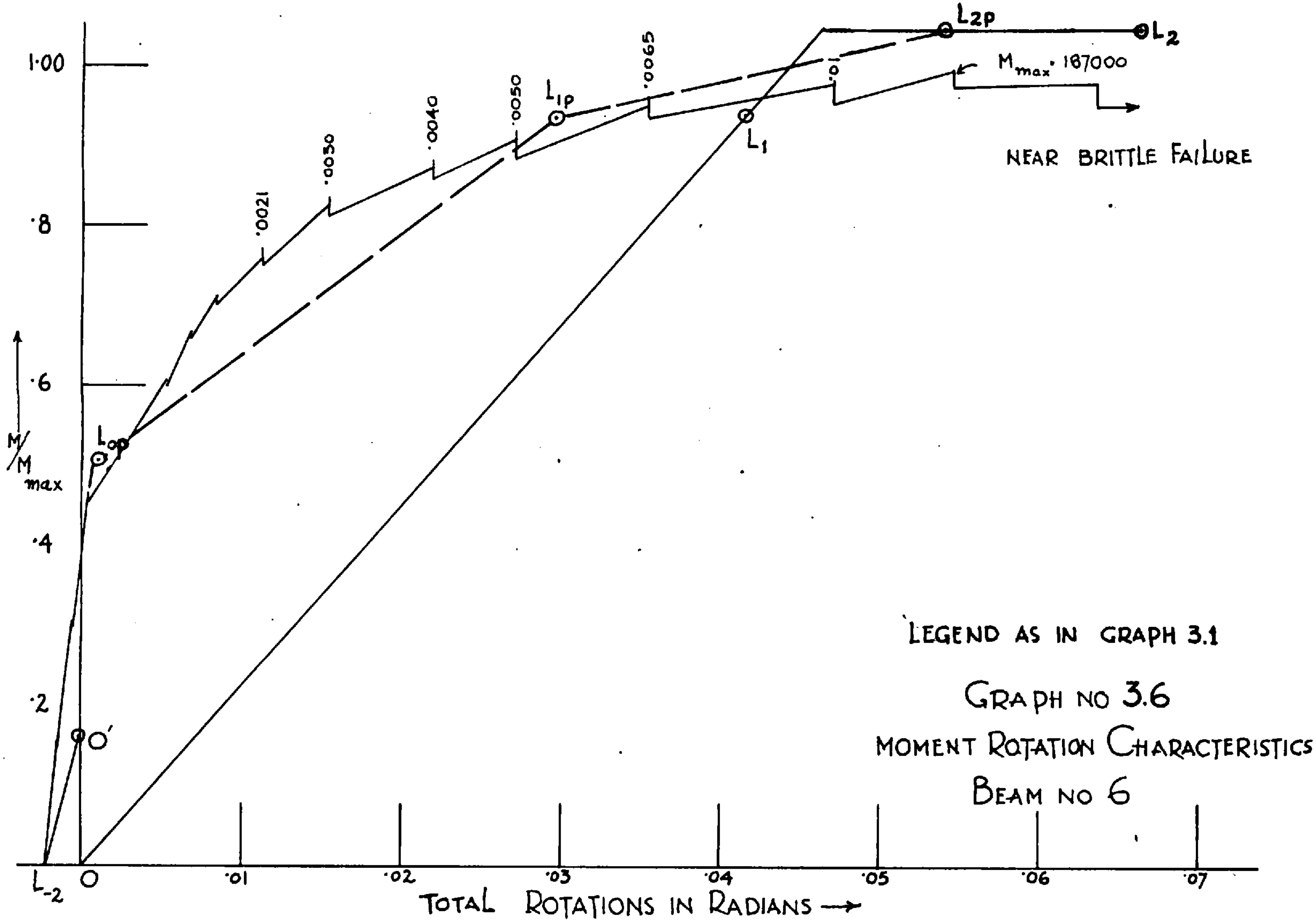

GRAPH NO 3.6
MOMENT ROTATION CHARACTERISTICS
BEAM NO 6

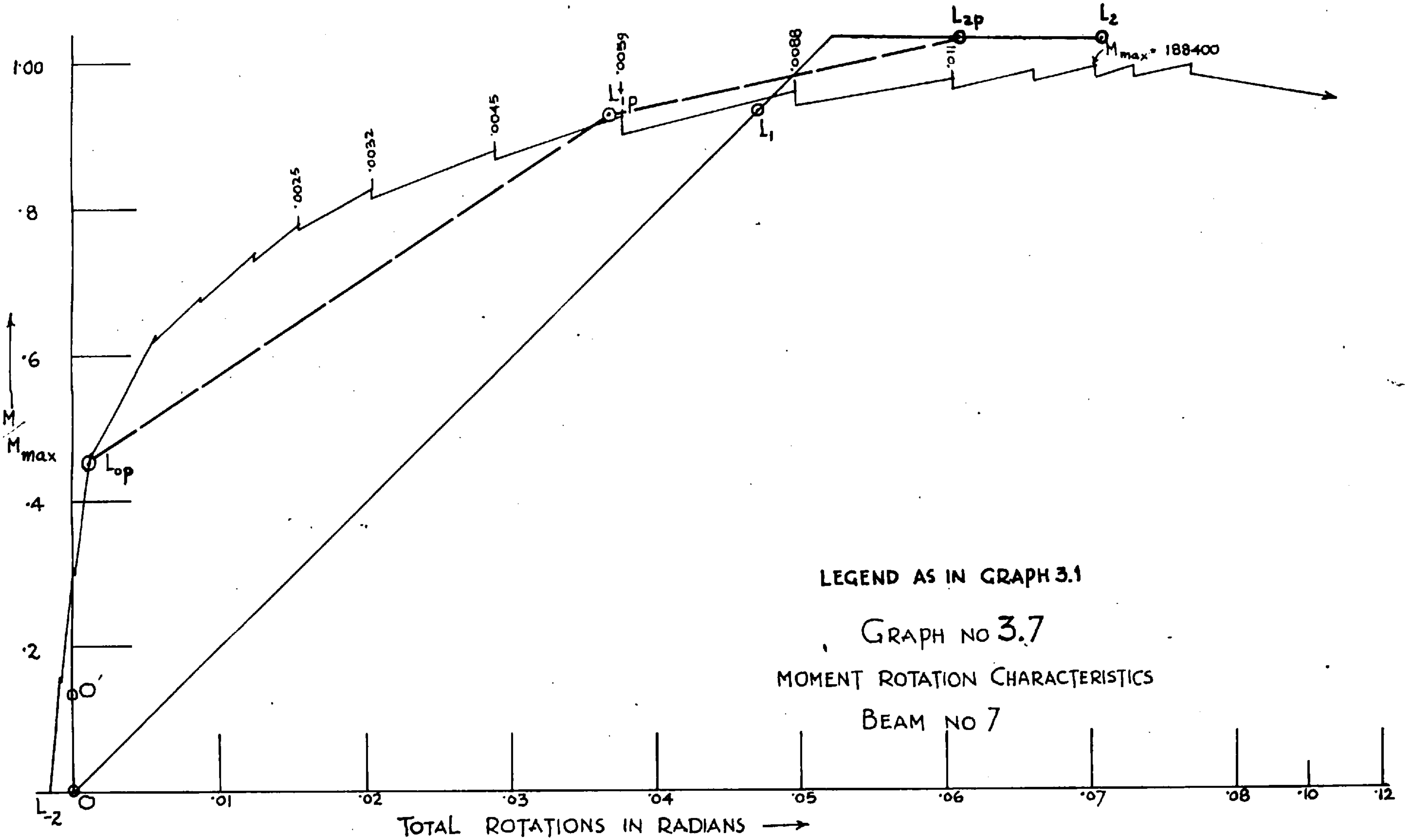

LEGEND AS IN GRAPH 3.1

GRAPH NO 3.7

MOMENT ROTATION CHARACTERISTICS

BEAM NO 7

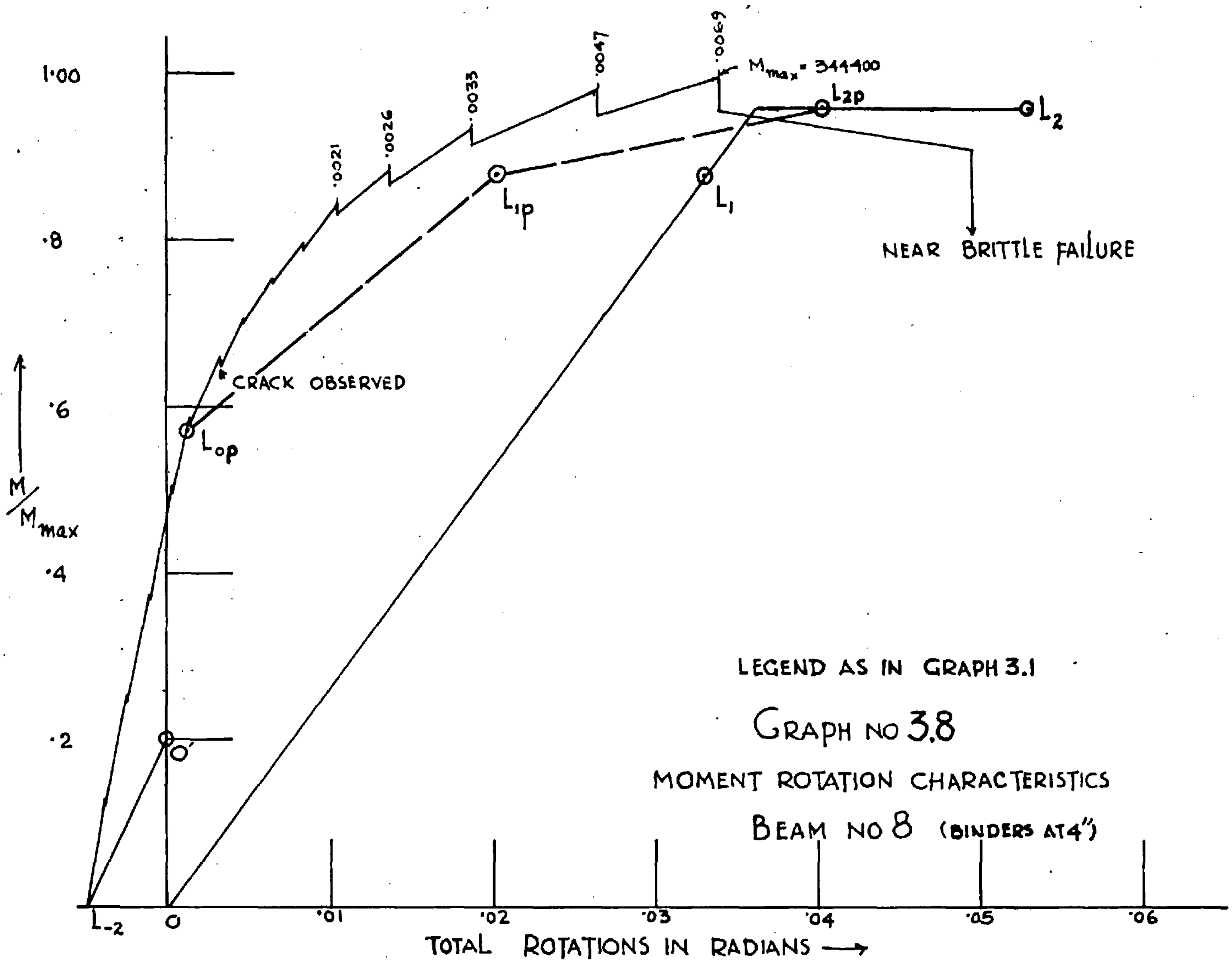

LEGEND AS IN GRAPH 3.1

GRAPH NO 3.8

MOMENT ROTATION CHARACTERISTICS

BEAM NO 8 (BINDERS AT 4")

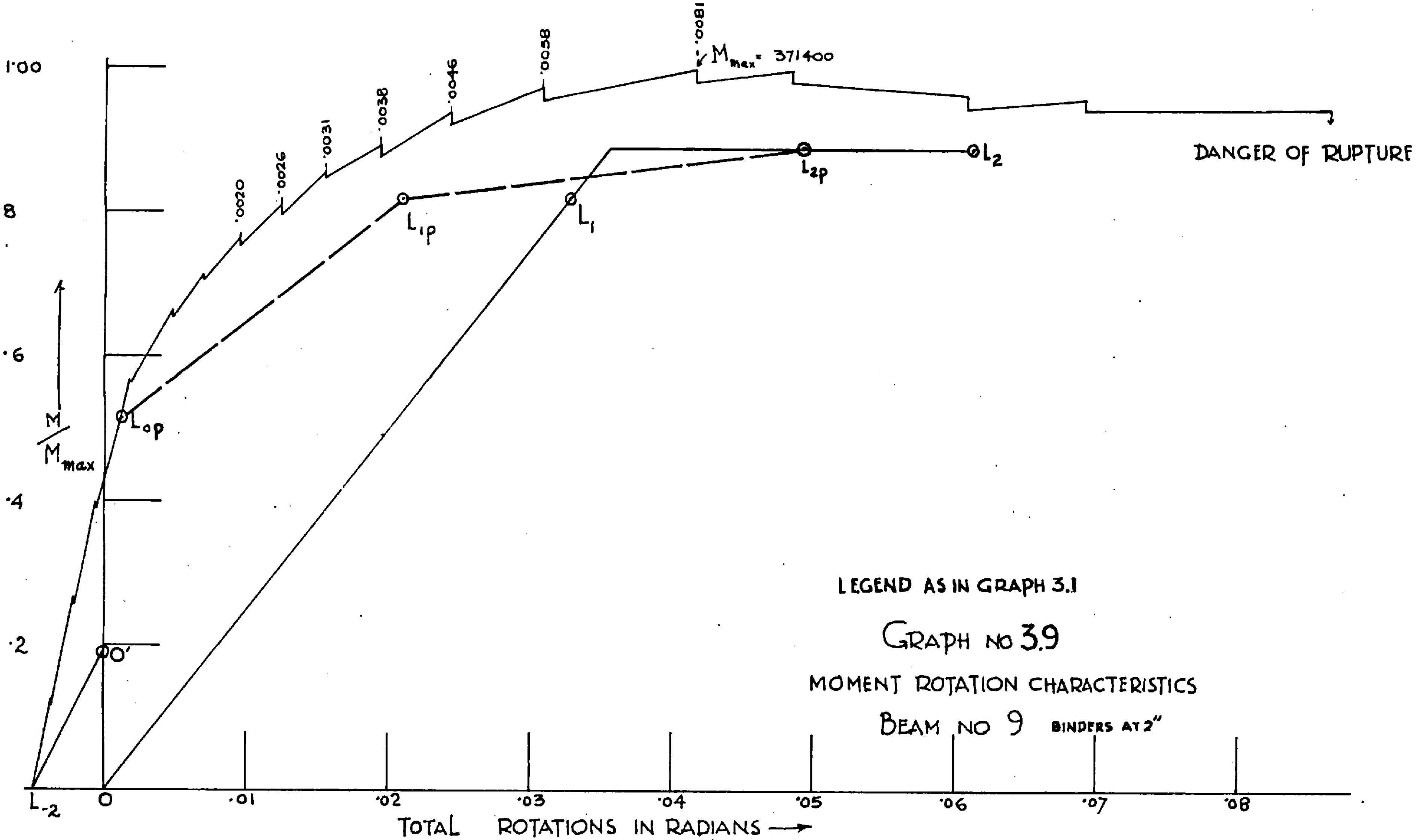

GRAPH NO 3.9

MOMENT ROTATION CHARACTERISTICS

BEAM NO 9 BINDERS AT 2"

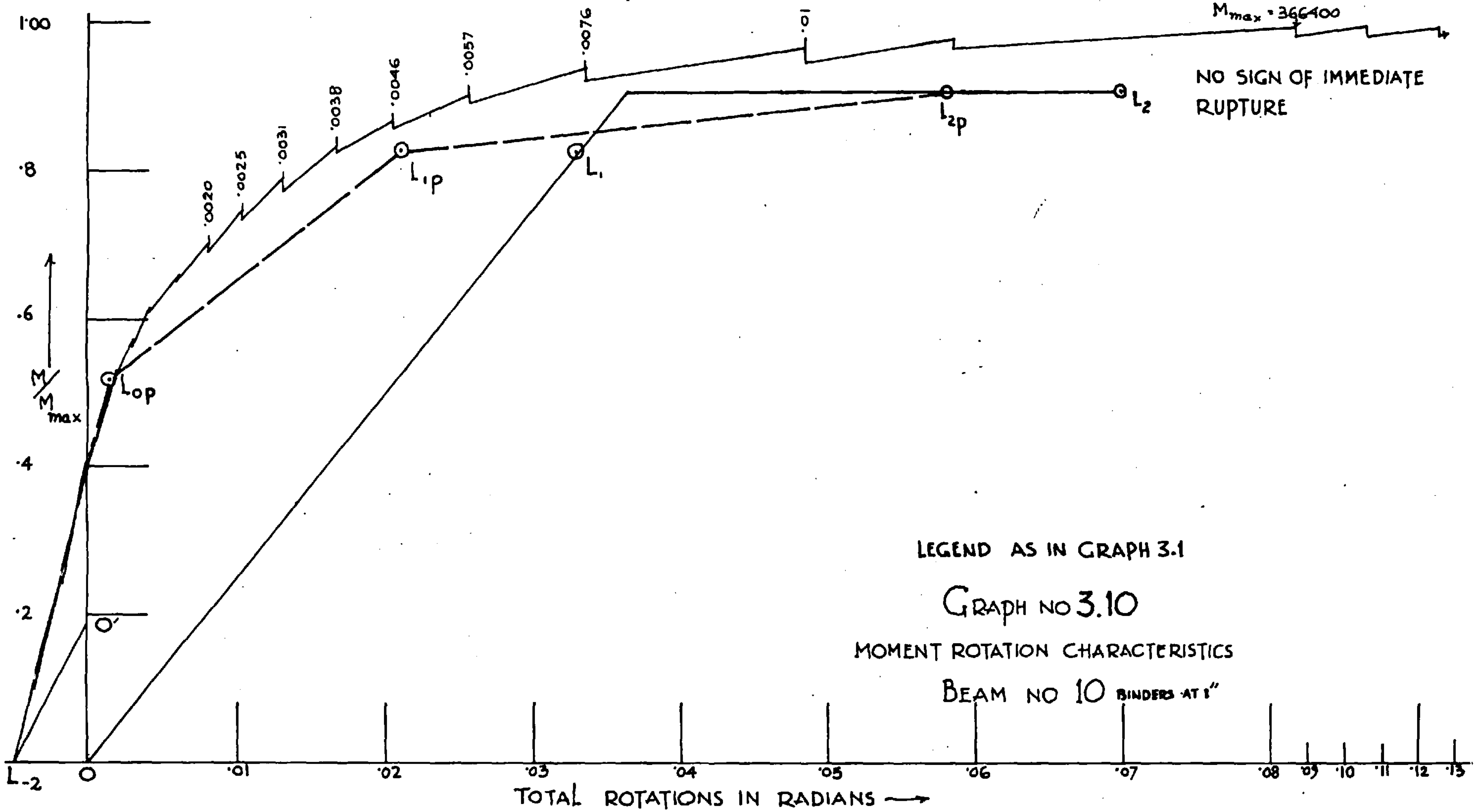

LEGEND AS IN GRAPH 3.1

GRAPH NO 3.10

MOMENT ROTATION CHARACTERISTICS

BEAM NO 10 BINDERS AT 1"

GRAPH 3.11

EXPERIMENTAL RELATIONS BETWEEN MOMENT AND CURVATURE AT DIFFERENT X-SECTIONS

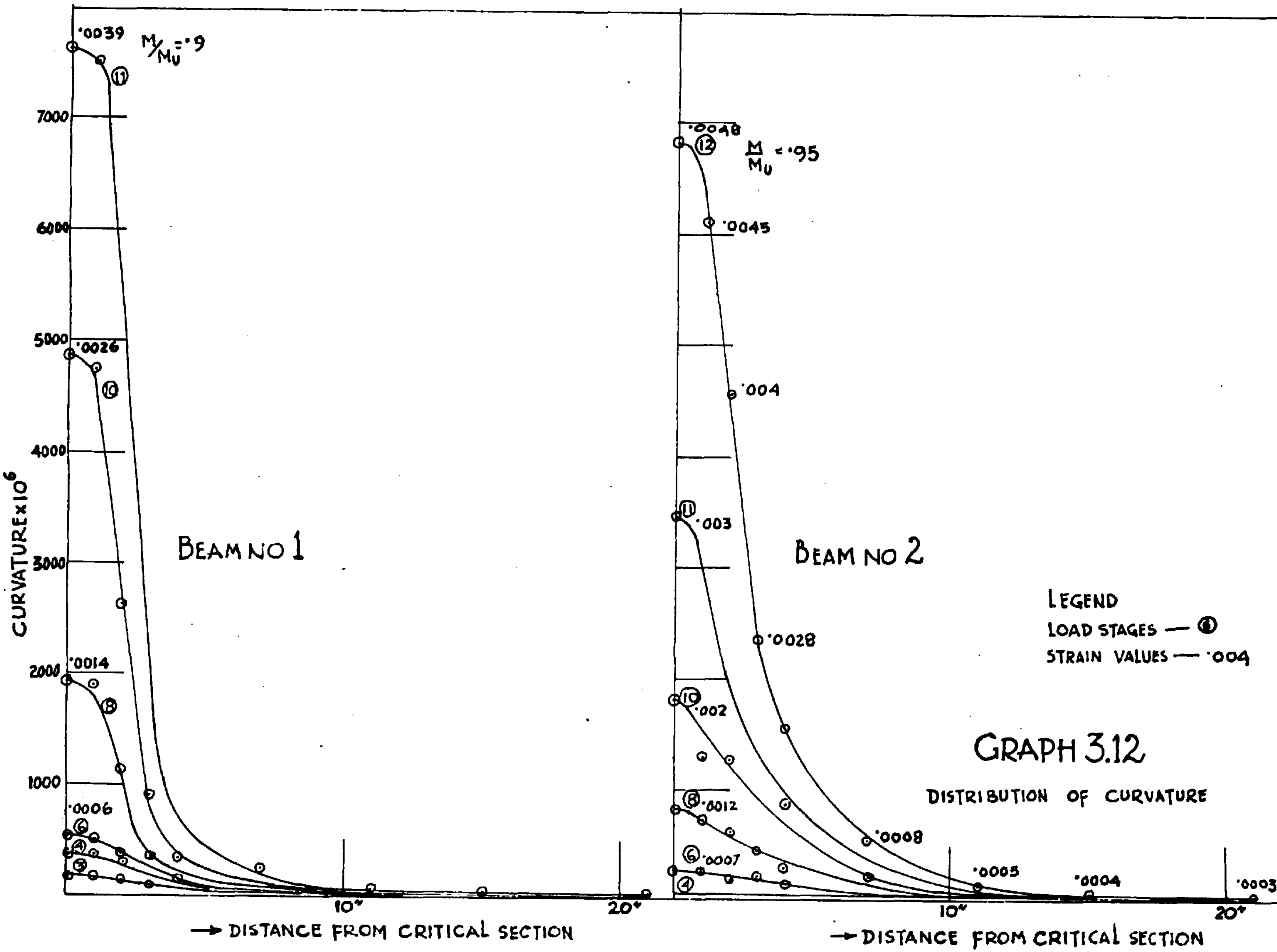

GRAPH 3.12

DISTRIBUTION OF CURVATURE

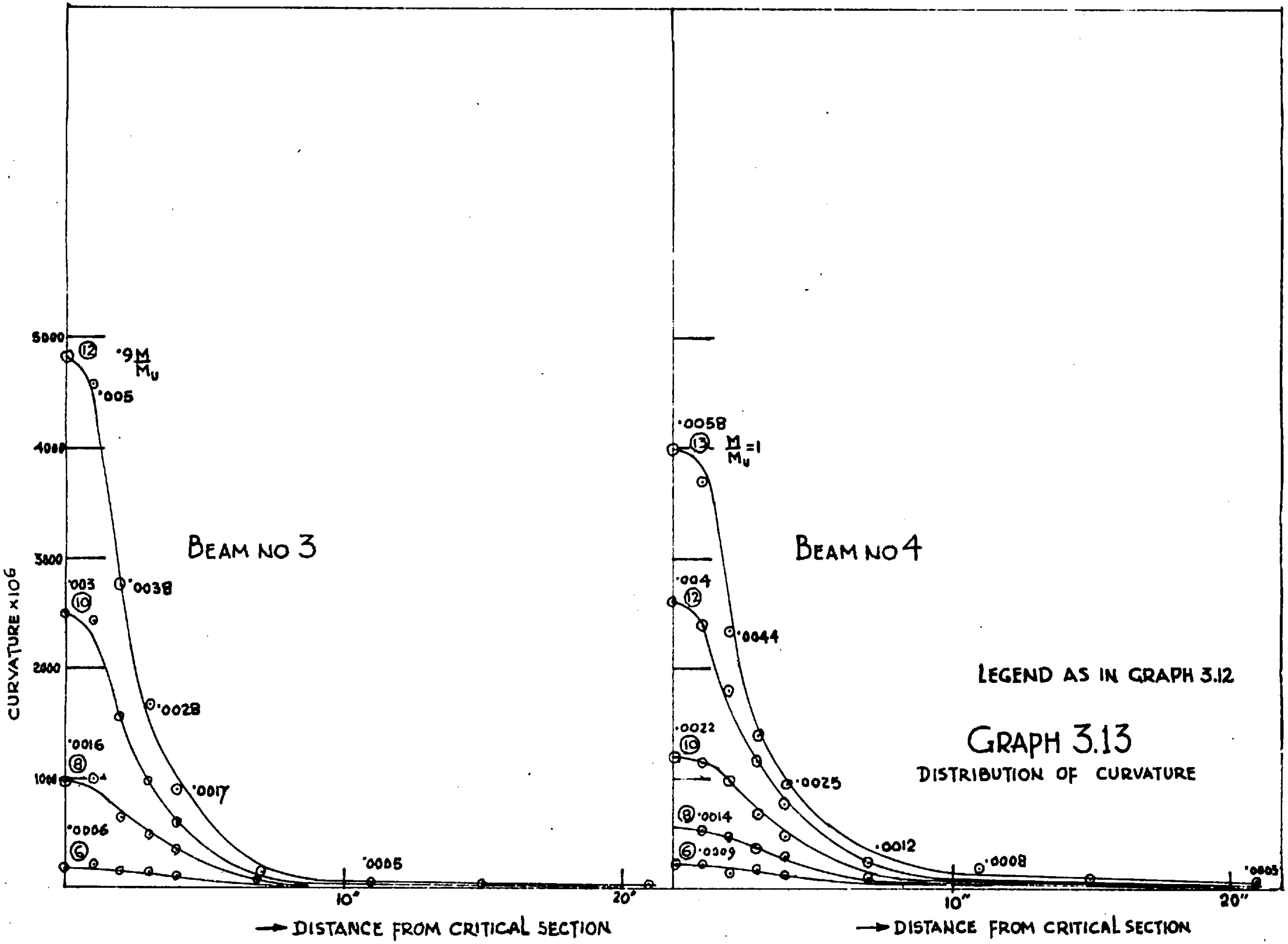

GRAPH 3.13
DISTRIBUTION OF CURVATURE

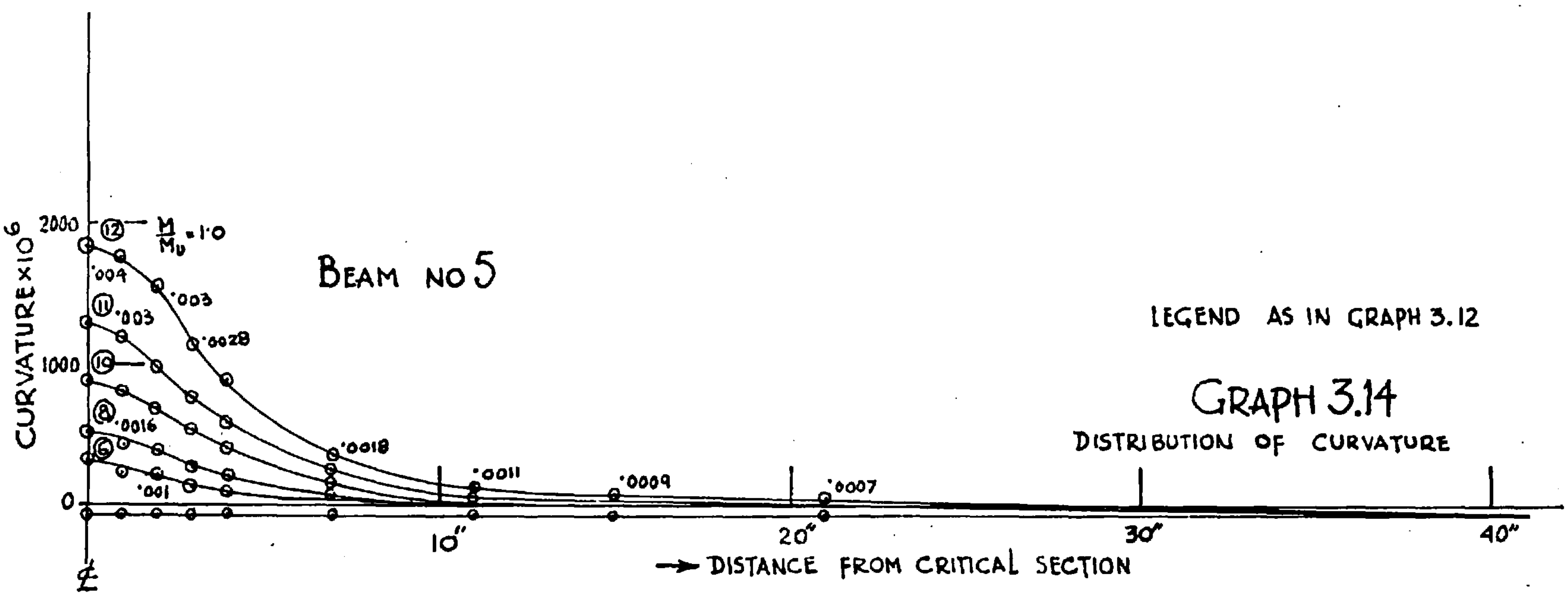

LEGEND AS IN GRAPH 3.12

GRAPH 3.14
DISTRIBUTION OF CURVATURE

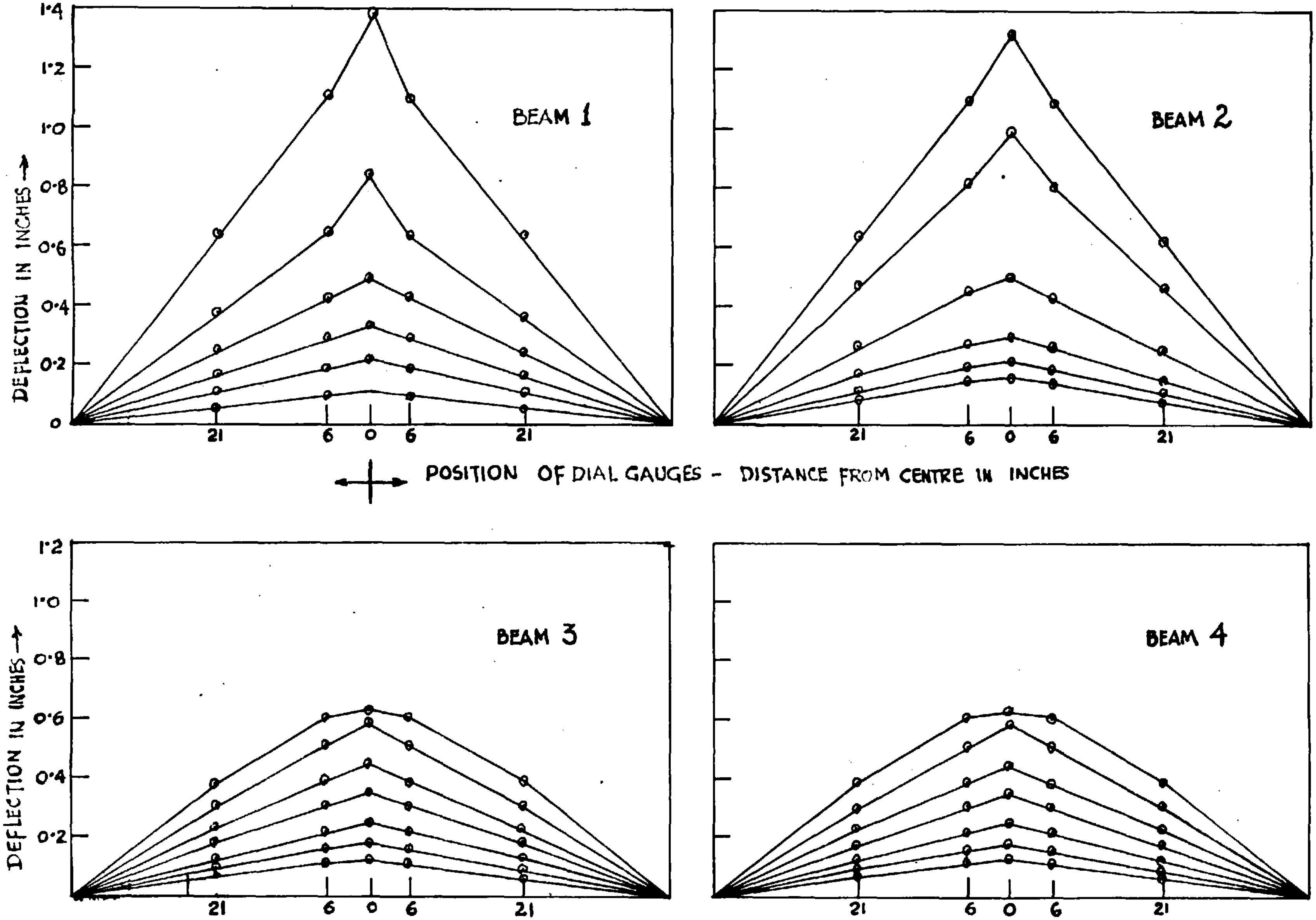

GRAPH 3.15

DEFLECTION OF BEAMS

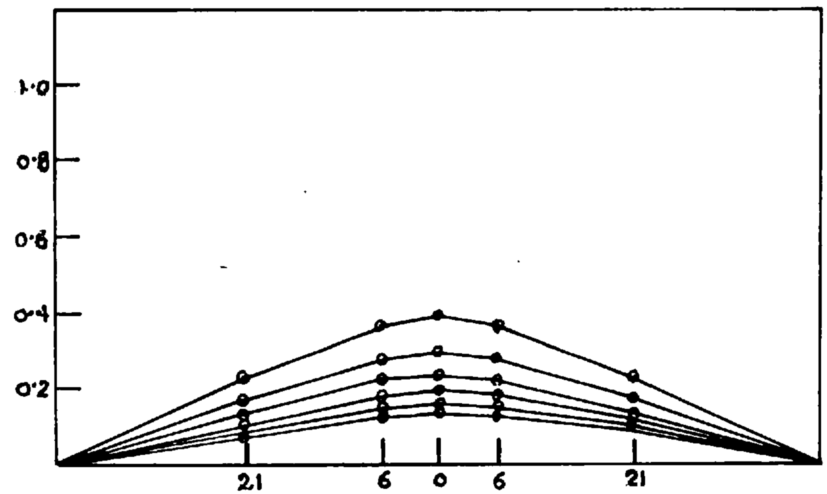

GRAPH 3.16

DEFLECTIONS BEAM NO 5

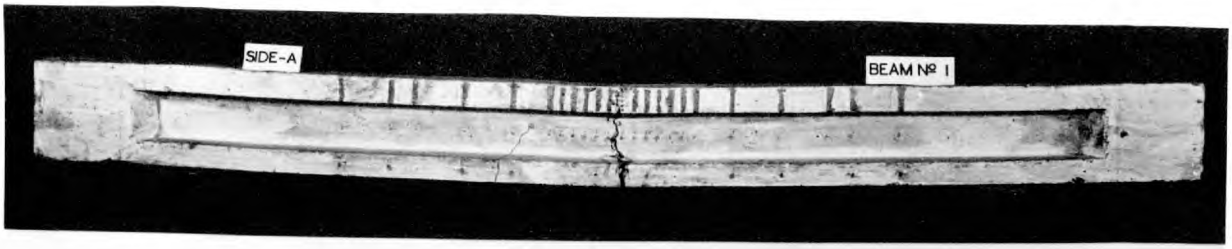

Plate 3.1 Beams 1 & 2 after failure

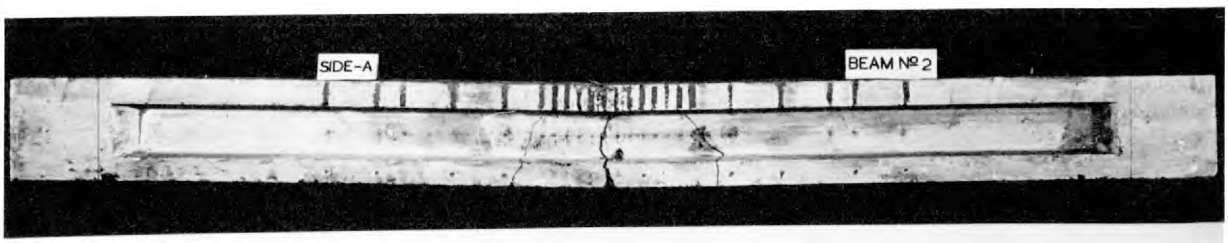

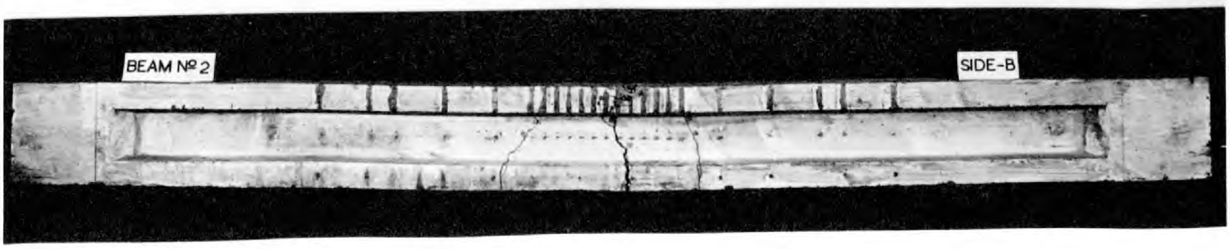

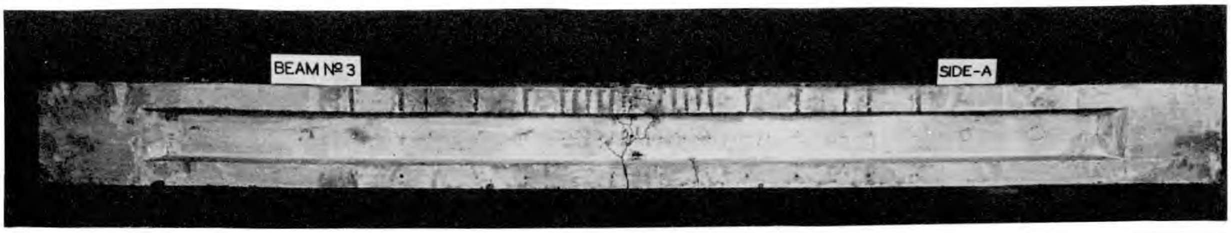

Plate 3.2 Beams 3 & 4 after failure

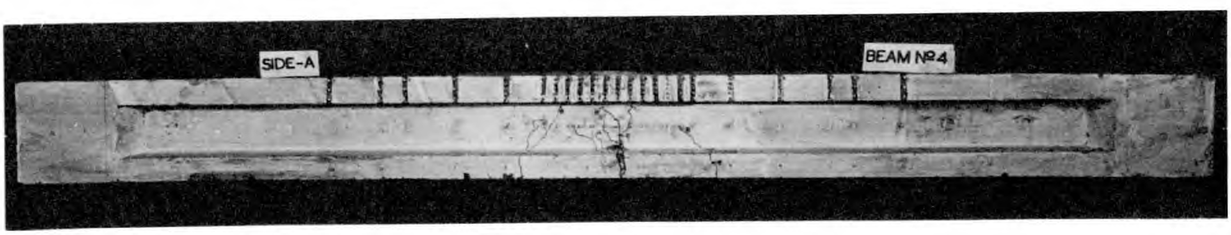

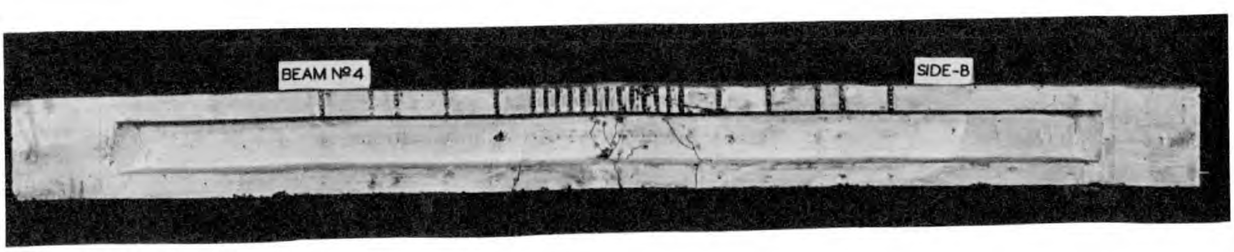

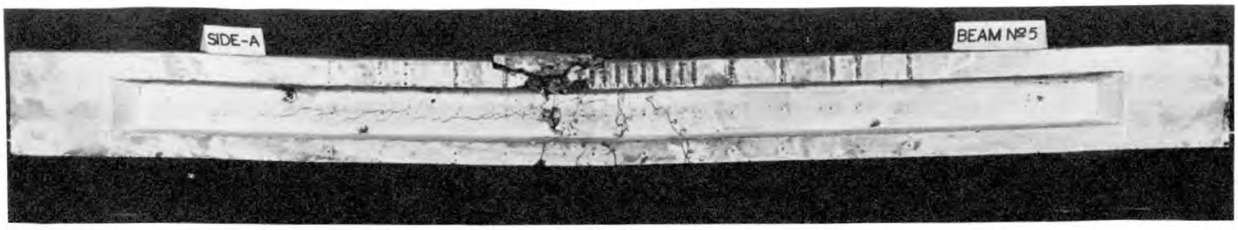

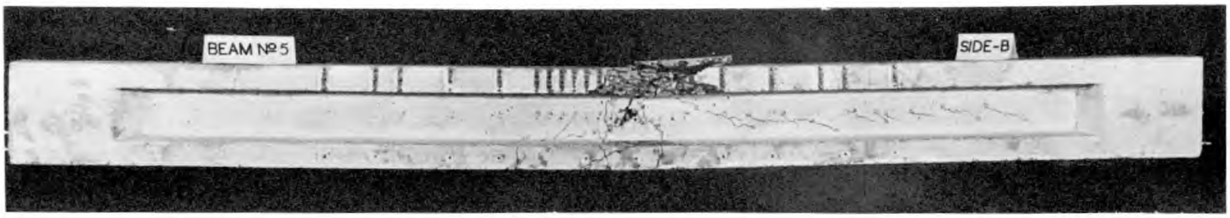

Plate 3.3 Beams 5 & 6 after failure

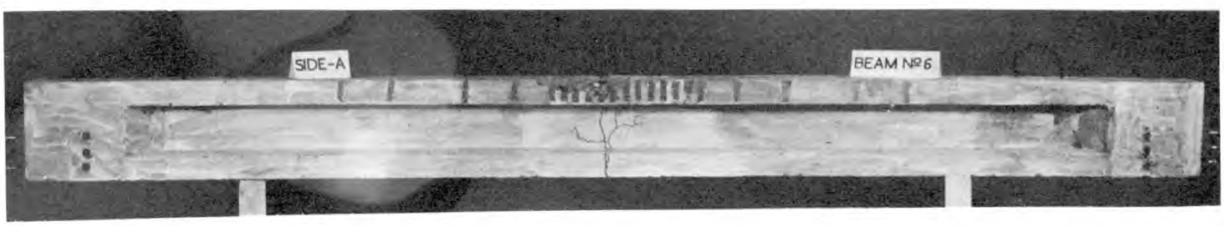

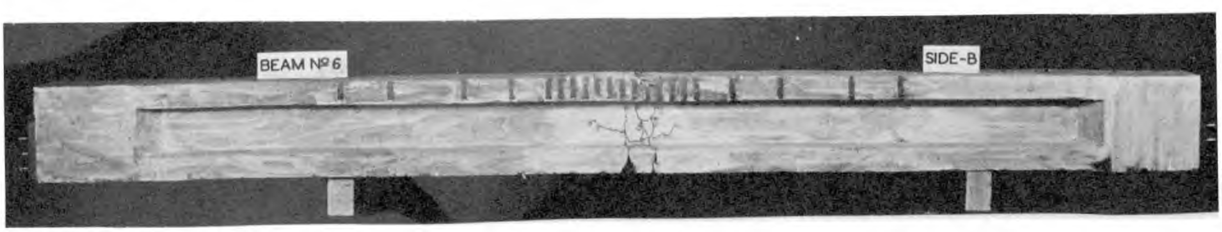

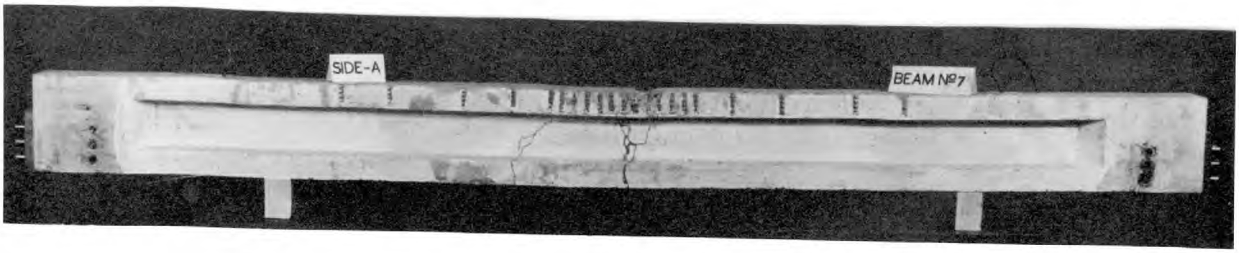

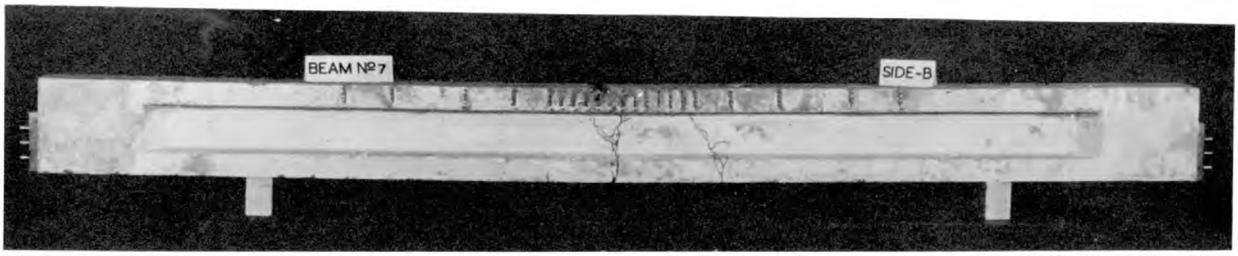

Plate 3.4 Beams 7 & 8 after failure

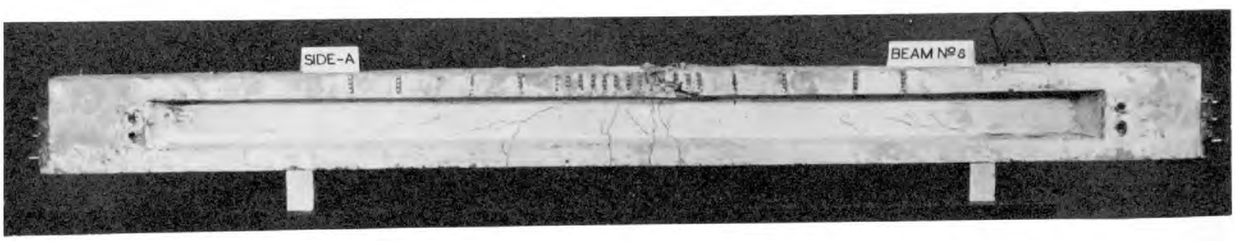

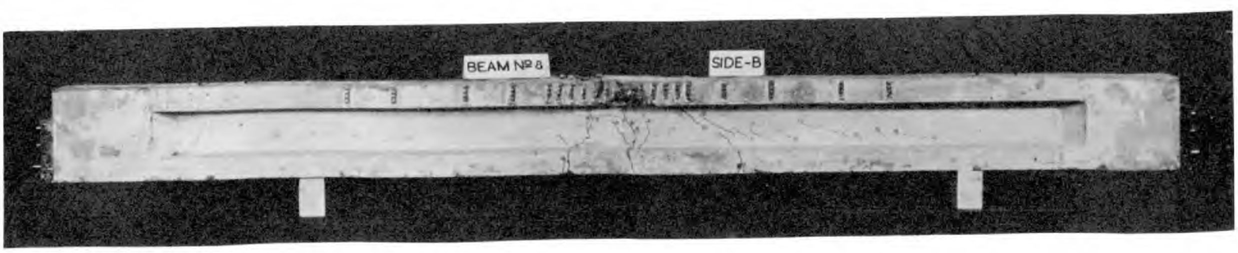

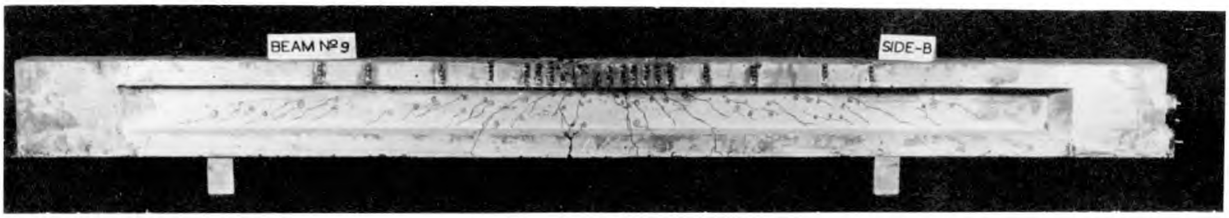

Plate 3.5 Beams 9 & 10 after failure

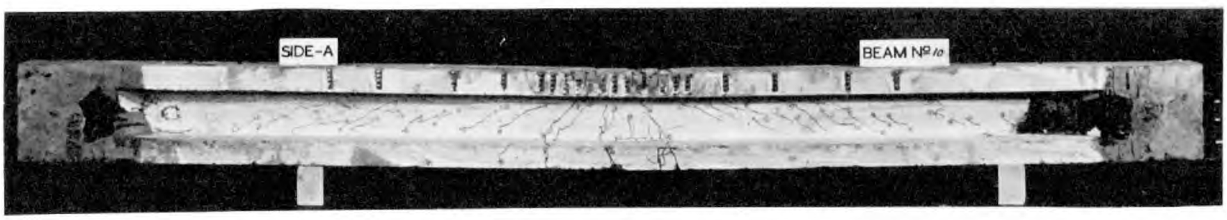

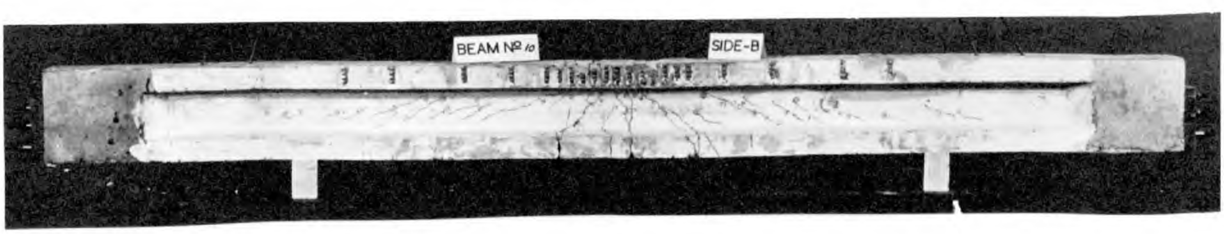

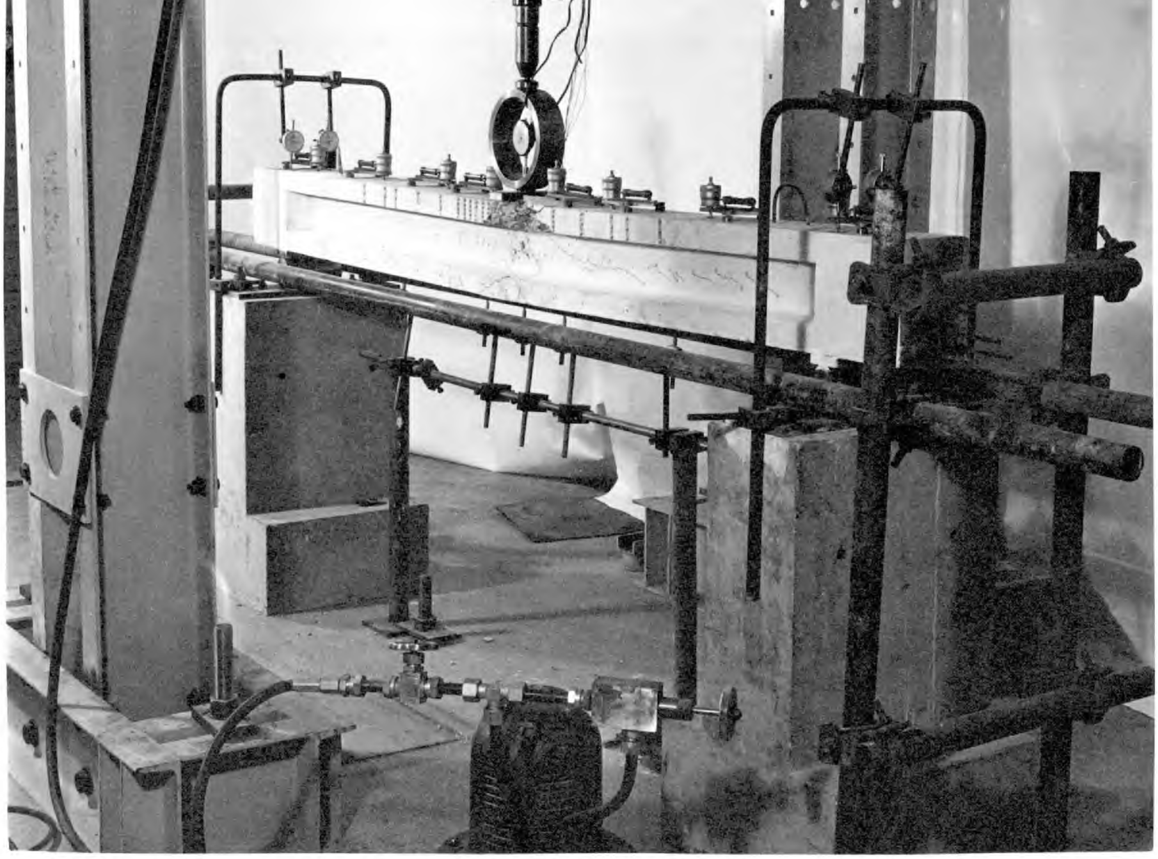

Plate 3.6 Test arrangement for beams 1 to 5 with Proving ring

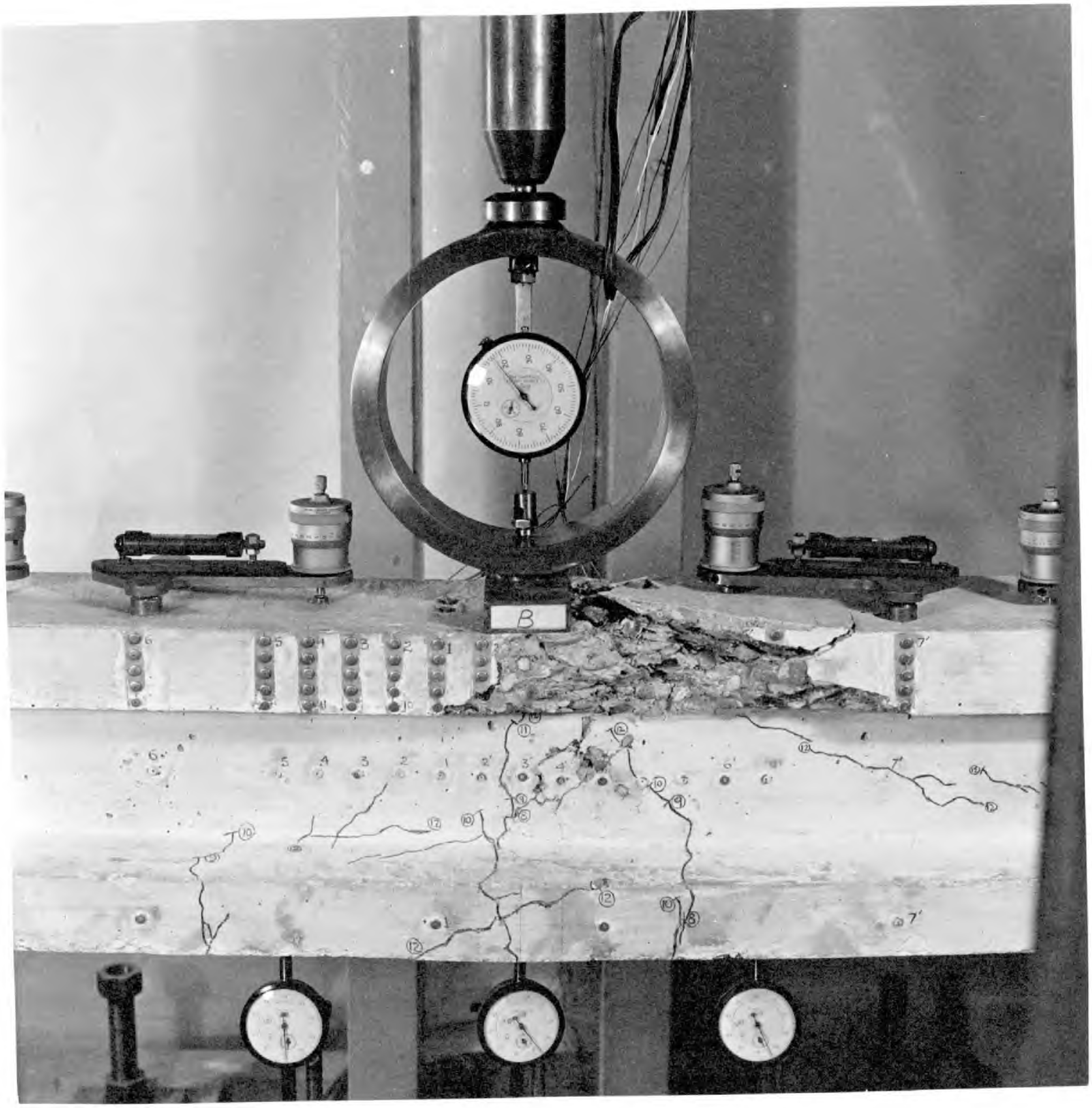

Plate 3.7 Close up veiw of Beam 5 side B after crushing

CHAPTER 4.

AN INTRODUCTION TO PRESTRESSED CONCRETE PORTAL FRAMES.

4.1. History of Tests on Portal Frames.

Prestressed portal frames have not been tested as widely as prestressed continuous beams. Out of the few tests performed, those done by La Grange(32) and Pietrzykowski(40) are notable.* La Grange concluded from his tests in the Cambridge University, that better redistribution of moments could be achieved if recognition was given to the falling branch of a load deformation characteristic. Pietrzykowski carried out tests on three prestressed concrete ring portals, in the University of Southhampton. He concluded that the condition of full redistribution did not, in general, occur in prestressed concrete structures. In his frames, the columns were heavily loaded to simulate conditions similar to those which occur in the lower storey of a building frame.

The incomplete redistribution in Pietrzykowski's frame could be attributed to the brittleness of the heavily loaded columns. All over-reinforced members are also brittle. The author has found that a brittle failure can be successfully overcome by the use of closely spaced binders. The ductility introduced by properly spaced binders is so effective that full redistribution may be ensured in the true sense (i.e. without any reduction of moments at the plastic hinges), and the necessity of the use of falling branches for better redistribution, may be dispensed with.

*Recently more research has been done on prestressed portal frames (25 and 27).

Three fixed footed portal frames were tested by the author to demonstrate the use of binders to obtain full redistribution. The first two frames had over-reinforced members and they were identical, except for the fact that one of them had closely spaced binders at critical sections, while the other had no binders. The third frame had heavy axial loads on both columns. It was similar to Pietrzykowski's frame but it was reinforced with closely spaced binders throughout the length of its members. The results of the tests are discussed in Chapter 6.

4.2 A review of the paper presented by Baker and Amarakone, at a joint meeting of the Cement and Concrete Association, The Institute of Civil Engineers, The Institute of Structural Engineers and the Reinforced Concrete Association, held on 30.3.65.

The contents of this paper were similar to those presented by the authors at the Ankara meeting of the C.E.B., held in September 1964.

The philosophy of limiting plastic rotations in concrete structures, as propounded by Baker, was severely criticized by many. Jones thought that experiments on moment rotation characteristics were not carried far enough. He said that if one tested steel beams with a very flat plastic curve, depending on where people stopped the test, there would be a very wide distribution of results. As regards continuous concrete structures, he thought that many of the hinges would be on the falling branches of the rotation curves, which should be taken into account.

Cranston agreed that there would be some cases where one would have to check rotations. He pointed out that if a reduction of moment of 10% could be tolerated, the rotations would be doubled. He further said that one of the alternatives to avoid brittle failures, was to let a part of the structure remain below the limit L_1, even under the ultimate loads (for example, at hinges of columns subjected to heavy axial loads). Such an approach, he said, had been advocated for the design of columns in multi-storeyed steel frames where a plastic design was used to proportion the beams.

The work taken up by the author has to be viewed in the light of the above discussion. The author has to point out that it is not necessary to consider the falling branches in order to increase rotations in brittle members, provided binders are used at a suitable spacing.* The use of binders can be extended to heavily loaded columns, provided the expense of using binders throughout the full length of the columns (see page 116) is justified. However, if it is preferable not to permit rotations in column hinges and to keep part of the structure elastic, for the sake of economy, the author has pointed out a method in Chapter 7 of doing so, by adjusting 'θ_{pi}' values to zero, at hinges where plastic rotations are undesirable.

4.3 Details of the tests proposed by the author.

As already stated, three fixed footed portals were the main subject of study by the author. The aim of the investigation was a study of the distribution of stress and strain resultants in the

*In fact it is extremely doubtful whether the falling branch technique will really help in obtaining a higher load factor, in really brittle cases.

portals in the neighbourhood of the ultimate load to demonstrate the effectiveness of lateral binders.

Before testing the frames, it was considered necessary to investigate the moment rotation characteristics of prestressed members subject to axial loads. A pilot project was initiated to determine the moment rotation characteristics of members similar to those to be incorporated in the frames.

4.4 Details of the Pilot project.

Two members representing the columns of Frame No. 3, were tested in a rig devised by Soliman[47]. The dimensions, the reinforcement, the properties of the mix and other details of these columns were kept as close as possible to those proposed for the two columns of the actual frame.

In the tests an attempt was also made to keep the distribution of moments in the columns similar to that which would occur at ultimate load of Frame No. 3, assuming complete redistribution of moments. The position where the tie bar was connected to the brackets clamped at the end of the specimens (plate 4.1) was altered, so that the value of 'Z' was different in the two specimens. This was done ~~so that~~ as the actual distribution of moments in the two columns of Frame 3 might not be exactly identical.

It may be noted that under conditions of equal moment being applied at both the ends of the specimen, the plastic rotation is concentrated at the weaker end of the two. (The other end remains at the state L_1.) The difference in the readings between the clinometers fixed to the top and the bottom brackets is the desired plastic rotation. The rotation between the hinge and the point of contraflexure was also measured by recording the change in the slope of a mirror fixed as near as possible to the point of zero moment. The change in the slope of the mirror was recorded by observing the change in the readings of an illuminated scale as seen through a fixed telescope, and using the principle that the rotation of the mirror is half of the angle of turning of a ray of light reflected by the mirror.

Additional moments caused by the change in the geometry of the specimen were also accounted for. The displaced position of the critical section was assessed by noting the rotation at the end of the specimen, and assuming that the specimen was rigid between the point of application of the vertical load and the critical section. This was a reasonable assumption because the specimens were of considerably higher stiffness at the ends and there was a sharp change in the section of the specimen, where the critical section was situated.

The results are presented in Graphs 4.1 and 4.2 and Fig. 4.1. A slight increase in plastic rotation was observed in Col. 1, in which the slope of the bending moment diagram was steeper than that in Col. 2. Similar observations were made by Mattock[20] and Soliman[47]. It was concluded from the graphs that closely spaced binders did increase plastic rotations considerably, in heavily loaded columns, provided binders were continued in their entire lengths, to prevent a brittle failure in between the critical sections, induced by additional moments due to change in the geometry of the structure. The fact that the use of binders in the entire length of a column is expensive, cannot be ignored and perhaps the advantage gained by designing fully plastic, heavily loaded columns, is in most cases, more than offset by the increased cost. The use of binders is, however, a useful device to avoid brittle failure in cases where rotations in column hinges cannot be avoided.

4.5 Stress resultants in a portal frame by the elastic theory.

Any statically indeterminate structure can be analyzed by either assuming the forces or the displacements, as the unknowns. The solution is obtained by solving the resulting linear algebraic equations. In the discussions which follow in this thesis, the method of analysis and the notation used, are the same as used by Morice[36]. In case of fixed footed portals, there are three unknowns and the linear equations are of the following form:-

$$\left.\begin{aligned} f_{11} x_1 + f_{12}x_2 + f_{13}x_3 &= - U_1 \\ f_{21} x_1 + f_{22}x_2 + f_{23}x_3 &= - U_2 \\ f_{31} x_1 + f_{32}x_2 + f_{33}x_3 &= - U_3 \end{aligned}\right\} \quad \ldots . \; 4.1$$

which can also be expressed as $F x = -U$, in abbreviated notation

where F is known as the flexibility Matrix.

In order to follow a step by step analysis involving the successive formation of plastic hinges, it is more convenient to choose the unknowns as moments at critical sections, where plastic hinges are expected to form. The elements f_{11}, f_{12}, f_{13}, represent rotations at hinge No.1, due to unit moments applied respectively at hinges 1, 2 and 3. These elements have been derived by different authors, by different methods. For our discussions we shall restrict ourselves to the principle of virtual work as used by Baker.[10 and 4]

The derivation of the stress resultants will be found in Appendix 8.

4.6 The secondary effect of the prestressing force and the concordant cable.

The act of prestressing a structure causes each section to undergo deformation (in the case under consideration, axial deformation and bending deformation). If these deformations are considered to be acting on a statically determinate form of the structure, then discontinuities are created at, and corresponding to the releases.

The chosen profile of the tendons in a structure is said to be concordant, if the discontinuities at releases caused by the prestressing forces are nil. In such a case no secondary reactions are induced in the structure, because no forces are required at the releases to restore continuity in the structure. The centroid of the resultant thrust at all sections, therefore, lie at the centroid of the applied force in the tendons.

Let $U^p{}_1$, $U^p{}_2$, $U^p{}_3$, denote the hinge deformations in the fixed footed portals under discussion, due to the prestress alone. $U^p{}_{1,2,3}$ are product integrals taken all round the structure and are given by the following expressions

$$U^p_1 = \int \frac{m_1 \, m_p}{EI} ds + \int \frac{n_1 \, n_p}{EA} ds + k \int \frac{s_1 s_p}{CA} ds$$ (this term is small and may be neglected.)

etc. for 2 and 3.

where m_1, n_1, s_1 are the ordinates of the moment, thrust and shear diagrams all round the structure, due to unit moment at hinge No. 1

and m_p, n_p and s_p are similar ordinates due to the prestress.

The conditions for concordancy are given by

$U^p_{1,2,3} = 0.$

In a fixed footed portal, subjected to a system of loads as proposed for the author's tests, there are 5 critical sections where suitable values of eccentricities have to be assigned, (assuming that at the corners, the column and the transom have the same eccentricity.). Having satisfied the above 3 conditions to attain concordancy, enough scope is usually left in the choice of eccentricities to satisfy the requirements of the ultimate moment of resistance required at the critical sections.

In Frames 2 and 3, the ultimate moments of resistances at the bottom of the left foot, had to be increased by the use of mild steel bars, in spite of the above freedom of choice.

Calculations for finding the concordant cable will be found in Appendix 9.

4.7 Collapse load of the proposed frames.

An estimate of the collapse load can be made by the rigid plastic theory. Just before collapse, the structure is still statically determinate, but is about to change to a mechanism. At an intermediate stage of loading, when the structure is statically indeterminate, but has a degree of indeterminacy less than the initial value, the distribution of stress resultants can be conveniently determined, if it is assumed that the 'EI' value of the members having a uniform X-Section, remain constant between the hinges. Such calculations for intermediate stages are given in appendix 10.

The ratio of the vertical and the sway loads in all the frames was ~~so~~ 1:1. It was chosen so that the collapse would occur under a combined mechanism except in frame 3, where an over complete mechanism failure was contemplated. Pietrzytowski's frames also failed by an over complete mechanism, see details in appendix 11.

4.8 Calculation of rotations at collapse and intermediate stages.

The rotation at a hinge, at any stage of loading, can be obtained by calculating the integral of the products of the ordinates of the bending moment diagram under the given loads, and the bending moment diagram obtained by the application of a unit moment at the hinge, taken all round the structure, provided no closing of hinges has taken place andsubject to the conditions explained in the next paragraph. These integrations can be conveniently carried out, if a uniform 'EI' value is assumed to exist between the hinges. The calculated rotations are then the angular discontinuities at the hinges. Care must, however, be exercised in choosing the release hinges so that just before collapse, when the structure is still statically determinate, the calculated rotations are of the correct sign to correspond with the induced redistribution moments.

An example of the above conditions not being satisfied, has been given in appendix 12. In this case the last hinge to form was first established by a step by step analysis. The principle of contragredient relations was used to obtain zero rotation at the last hinge, in the manner set out by Munro.[38]

4.9 Summary of analysis of portal frames by Linear methods.

Three portal frames were analyzed by the author prior to the actual tests. The results of such an analysis by the linear theory, including the distribution of stress resultants in the elastic phase, and also their distribution in the reduced elastic phase, assuming a constant 'EI' value between the hinges and an elastic-plastic moment curvature relationship with angular discontinuities at hinges, have been determined. Rotations at the state of collapse and intermediate stages have been calculated. It was ensured that the chosen release hinges were the ones where plastic hinges would form.

An attempt has been made in the next chapter to analyze prestressed concrete sections in the cracked phase.

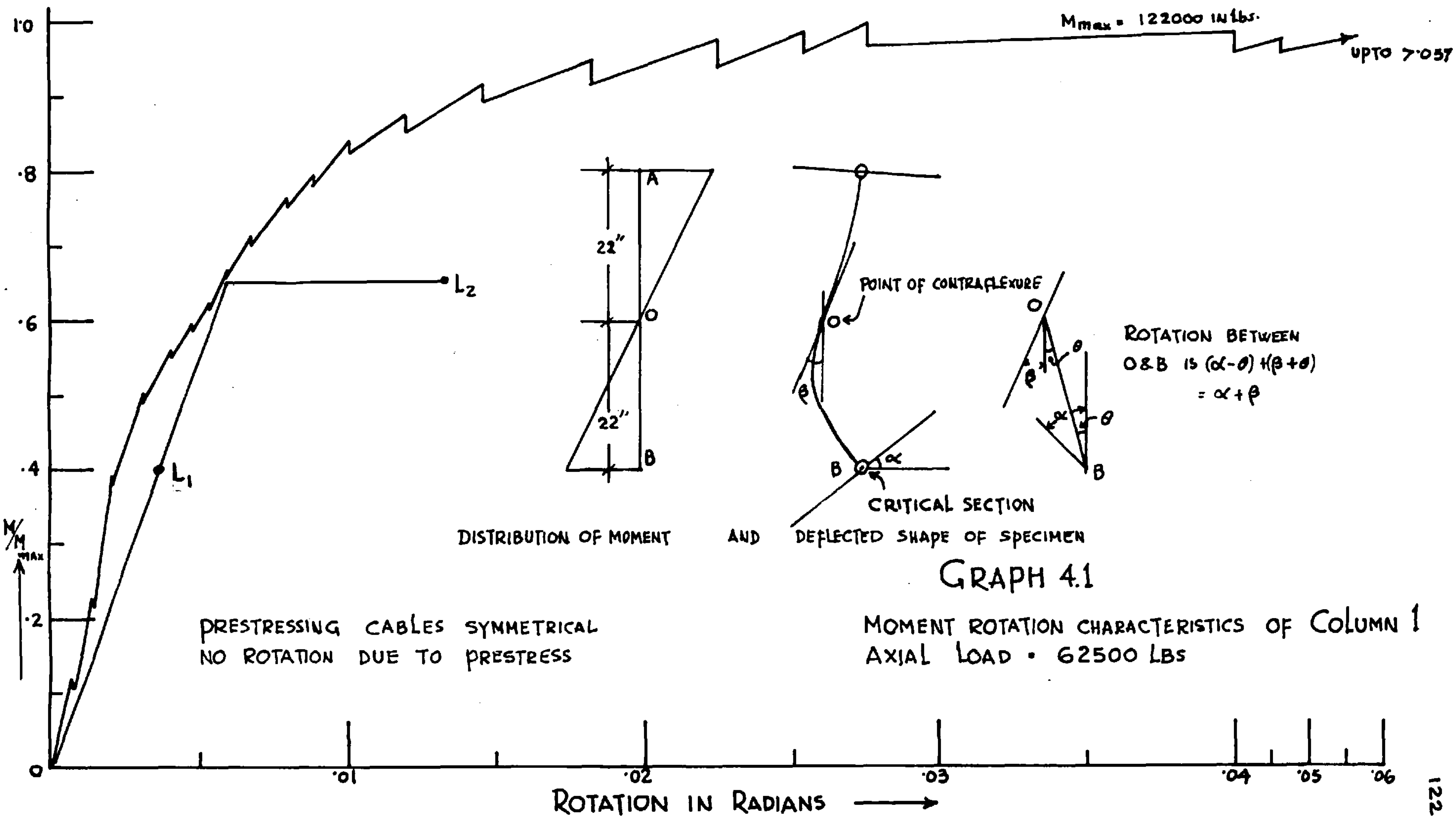

GRAPH 4.1

MOMENT ROTATION CHARACTERISTICS OF COLUMN 1
AXIAL LOAD = 62500 LBS

PRESTRESSING CABLES SYMMETRICAL
NO ROTATION DUE TO PRESTRESS

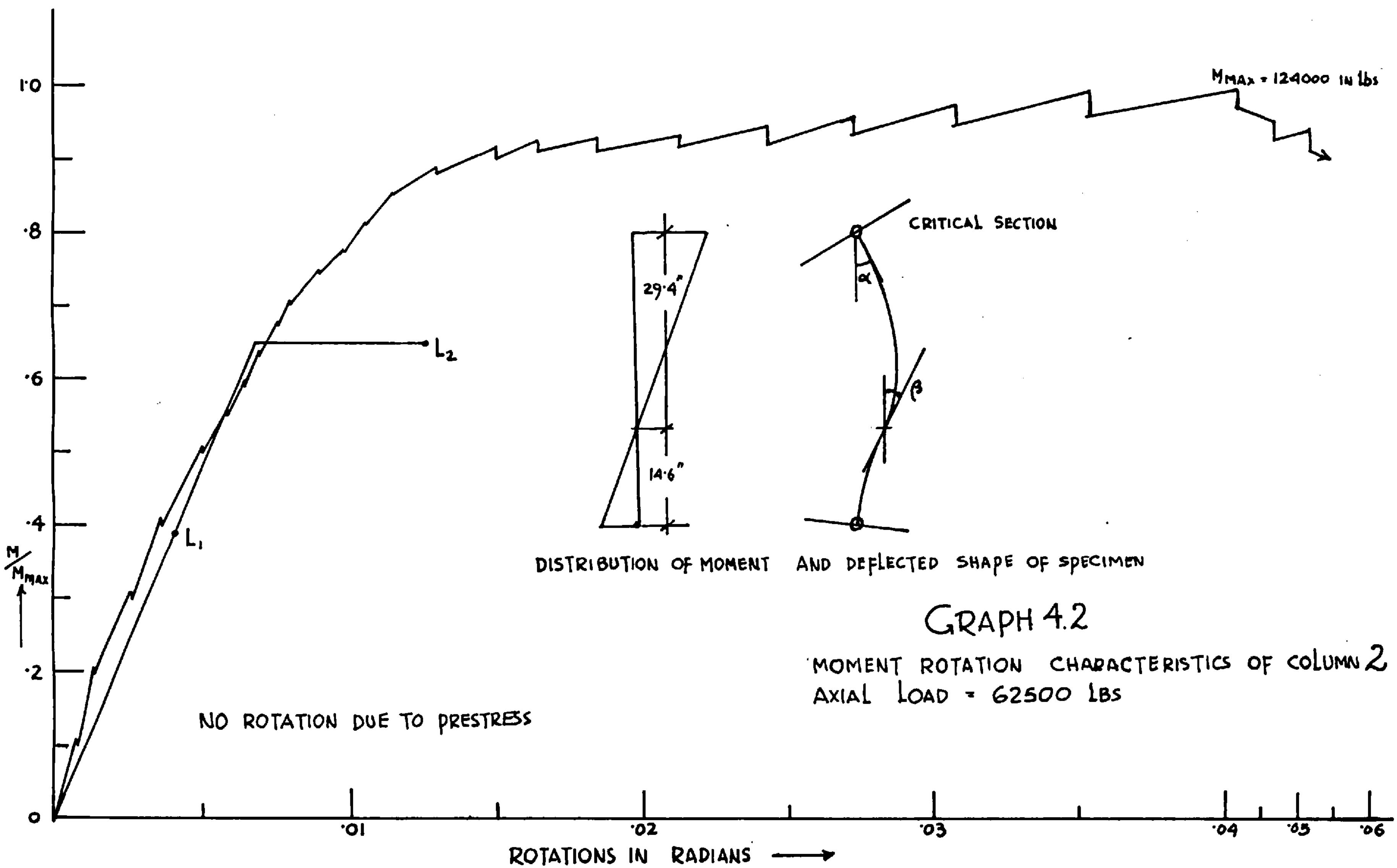

GRAPH 4.2

MOMENT ROTATION CHARACTERISTICS OF COLUMN 2
AXIAL LOAD = 62500 LBS

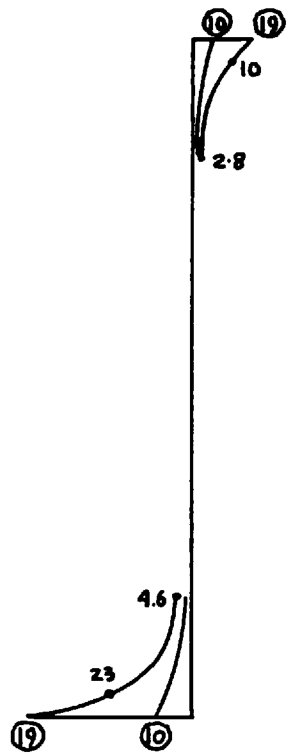

LEGEND

FIGS IN CIRCLE ARE LOAD STAGES

FIGS WITHOUT CIRCLE ARE CURVATURE $\times 10^4$ UNITS

AT LS 19 $M = M_{max}$

AT LS 10 $M = \cdot 75 M_{max}$

FIG 4.1

DISTRIBUTION OF CURVATURE IN COL 1

SCALE 1CM TO 6″

1CM REPRESENTS 20×10^4 UNITS OF CURVATURE (1/INCH)

Plate 4.1 Test apparatus for columns under heavy axial load

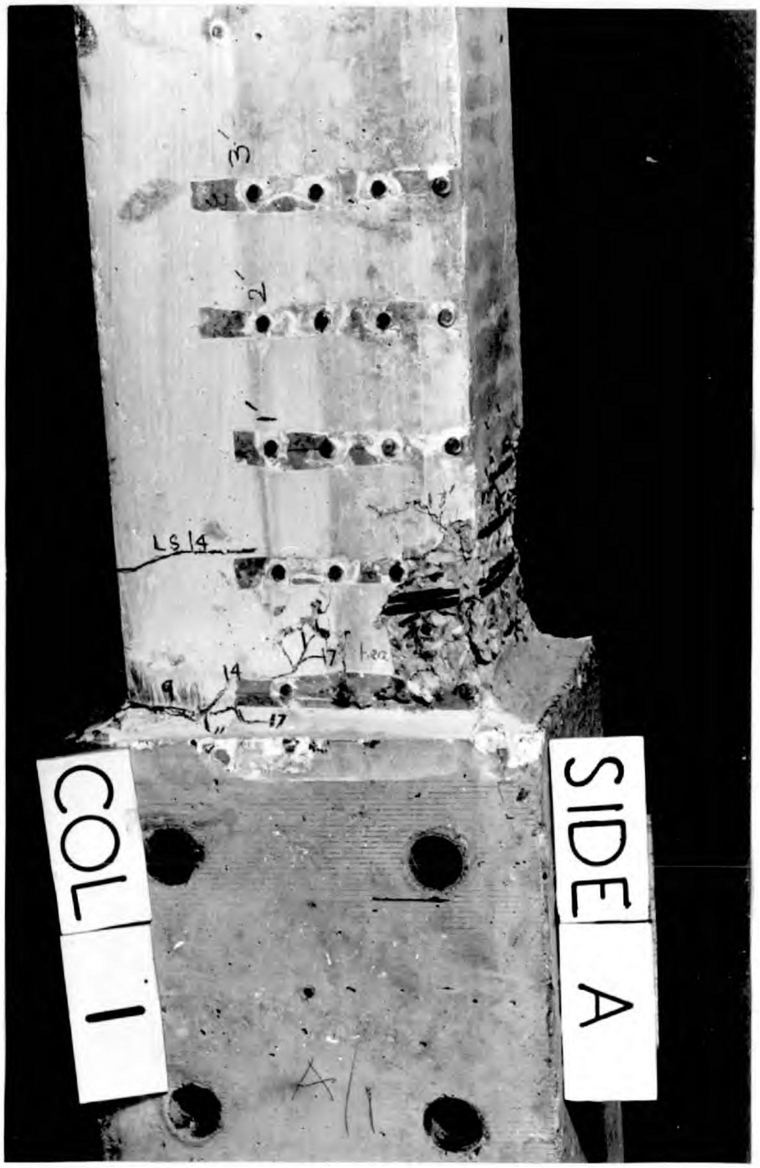

Plate 4.2 Hinge at the bottom of column 1

Plate 4.3 Hinge at the top of column 2

CHAPTER 5.

ANALYSIS OF PRESTRESSED CONCRETE SECTIONS IN THE CRACKED PHASE.

5.1 INTRODUCTION.

An analysis of a structure depends on the proper knowledge of the behaviour of its sections. A cracked prestressed concrete section behaves in a manner similar to that for reinforced concrete. Edwards(25) has discussed in detail the path of the moment curvature relationship of a prestressed section in various phases of loading, unloading and reloading. The object of this chapter is to study how the flexibility matrix method of analysis can be applied to cracked prestressed sections. A computer programme for deriving the theoretical moment curvature relationship has also been developed.

5.2 Centroid of a cracked section.

Before proceeding further, it is necessary that a suitable definition be given to the centroid of a cracked section in the inelastic phase. Certainly the geometric centroid of the entire area of the section is not a satisfactory substitute for the point through which the true axis of the member to which the above section belongs, may be assumed to pass. The internal geometry of the entire structure is governed by the position of centroids at the critical sections in the neighbourhood of the ultimate load. Edwards(25) has shown that the effect of the change in the internal geometry is significant. From an analogy drawn from the methods used in elastic analysis, an effective centroid of the section may be defined to be the point where the axial load may be increased by an infinitely small amount, without causing a change in the curvature of the section.

The curvature depends on the properties of the section and the stress-strain curves of its elements. It is also a function of the applied moment, the axial load and its line of action. For a particular section, the section properties and the stress-strain curves are constant. The curvature can then be expressed by the following equation:-

$$K = f(M, N, x) \quad \ldots\ldots\ldots\ldots\ldots\ldots\ldots\ldots \quad 5.1$$

where K is the curvature

M is the applied moment

N is the axial thrust

x is the distance of the line of action of N from the extreme fibre (see Fig. 5.1).

If the axial load N, passes through the effective centroid,

$$\frac{\partial K}{\partial N} = 0$$

The value of 'x' is therefore determined from the equation

$$\frac{\partial f(M, N, x)}{\partial N} = 0 \quad \ldots\ldots\ldots\ldots\ldots\ldots\ldots \quad 5.2$$

The author has not attempted an analytical solution of equation 5.2 for a prestressed section. Instead, he has shown in Appendix 13, by a computer analysis, using Cranston's M-P-Ø-θ Programme [22], & the Serius Computer of the Cement & Concrete Association that a real value of 'x' exists for a section in a reinforced concrete member, which satisfies the above equation.

5.3 Flexibility matrix of a cracked prestressed concrete structure.

In para. 4.5 of chapter 4, it was stated that the equations governing the continuity of a structure at the releases, can be expressed as:-

$$FX = -U$$

'U' is a column matrix, the elements of which are obtained by integrating the sum of the products of ordinates of the stress resultant diagrams due to the applied loads on the released structure, and ordinates of diagrams due to unit restraints at the releases. In prestressed structures 'U' must include similar integrals in respect of the stress-resultant diagrams obtained by treating the pre-stressing forces as external loads. It was further shown in Chapter 4, that if the cable were concordant, these additional terms due to the prestressing forces, are zero.

The distribution of stress resultants in the structure is given by the following set of equations (assuming that there are only 3 unknowns).

$$m_t = m_o + m_1X_1 + m_2X_2 + m_3X_3$$

$$s_t = s_o + s_1X_1 + s_2X_2 + s_3X_3$$

$$n_t = n_o + n_1X_1 + n_2X_2 + n_3X_3$$

where

m_t, s_t, n_t are the total moment, shear and thrust, acting at a section which are to be resisted by internal forces including those set up by the prestressing force in the tendons.

m_o, s_o, n_o are the stress resultants at the section, due to external loads on the released structure (prestressing forces are not considered here as external forces).

$m_{1,2,3}$, $s_{1,2,3}$, $n_{1,2,3}$, are the stress resultants at the section due to unit restraints acting at releases 1, 2 and 3,

and $X_{1, 2, 3}$, are the actual restraints at releases 1, 2, 3 and include parasitic reactions.

The above set of equations can be expressed as

$$x_t = x_o + HX \quad \ldots\ldots\ldots\ldots\ldots\ldots\ldots\ldots \quad 5.3$$

where $H = \begin{pmatrix} m_1 & m_2 & m_3 \\ s_1 & s_2 & s_3 \\ n_1 & n_2 & n_3 \end{pmatrix}$

$x_t = \begin{pmatrix} m_t \\ s_t \\ n_t \end{pmatrix} \qquad x_o = \begin{pmatrix} m_o \\ s_o \\ n_o \end{pmatrix}$ and $X = \begin{pmatrix} X_1 \\ X_2 \\ X_3 \end{pmatrix}$

In order to determine X, the stiffness of the sections must be known at all points of the structure. Baker has suggested that an equivalent 'EI' value given by tan Ø in Fig. 5.2, which is compatible with the value of 'm_t' may be used in the cracked zones of the structure. The integrals $\int \frac{m_p m_k}{EI}\, ds$ has then no significance in the cracked zones and must be omitted in the evaluation of the matrix 'U_k', for the k^{th} release.

Similarly if the value of 'EA' as suggested by the author in Appendix 14, is used in the analysis, the integral $\int \frac{n_p n_k}{EA} ds$ must also be omitted in the cracked zone.

Thus the equivalent 'EI' approach may be used for a non-linear numerical analysis of a structure by the flexibility method. In this case, when the structure has been loaded into the non linear phase, a simulated elastic structure can be established in which the secant 'EI' values are so defined that under the total required load the correct deformation characteristics are obtained.

5.4 A computer programme to derive the moment curvature relationship of a prestressed section.

Cranston[22] has produced a refined computer programme to find the moment curvature relationship of a cross-section. The section is broken up into small strips and different stress-strain relations can be assigned to each strip. These strips are small enough to make the assumption valid that they are uniformly stressed. The programme can deal with an axial load acting at any specified point of the X-section.

The calculation involves an initial proposed value of strain in the axis of the load. Corresponding to a given value of curvature, the strain distribution across the section is then determined. The compressions and tensions are calculated in the strips and if their algebraic sum differs from the axial load by a quantity which is smaller than that specified, the value of the moments is calculated corresponding to the given value of curvature.

The method seeks values of moments for given values of the curvature. Since the curvature continually increases even for decreasing values of the moment after the peak has been reached, it is possible to trace the falling branches of M-K relations. (Two values of moment are impossible for one value of curvature.) Local dips are also faithfully recorded.

N. Somes [46] has produced a programme for prestressed concrete members, in which the real root of a cubical equation is sought by the programme.

The programme produced by the author is based on a systematic trial and error method in which a technique sometimes called the Artillery Technique, has been used. The position of the neutral axis is gradually raised from the bottom fibre towards fibre 2. For each position of the neutral axis proposed, the strain value at the top fibre is continuously increased from a nil value, till the compression in the concrete calculated according to the stress block presented by Baker at Ankara, is nearly equal to the sum of the tension in the tendons, (taking into account changes in tension, caused by changes in concrete strains at the level of tendons) and the axial thrust, if any. This method is particularly suitable for prestressed concrete where the tendons have a tension to start with. Both moment and curvature are calculated when the above condition is satisfied. Calculation of such values for a range of values of the neutral axis, enables the 'M-K' relation to be traced out.

The programme can also calculate the curvature for a given value of moment. In this case the calculated moment is compared with the given value, for continually decreasing values of the neutral axis, and the curvature is calculated when both the values of the moments are nearly equal.

The Artillery technique is used at each stage when a change is proposed, either in the position of the neutral axis, or in the value of strain at the top fibre. In other words, the area under preview is first scanned by the computer in larger intervals. The computer then enters into a finer mesh by retreating backwards when it finds that the desired condition has been satisfied in the larger strides.

The only condition to be satisfied at each chosen position of the neutral axis is that the compression is greater than the sum of the tension and the axial thrust. The accuracy of the calculated moment has been ensured by entering into finer meshes, such that the position of the neutral axis is determined correctly up to three decimal places. The disagreement between the forces across the section from the point of view of equilibrium, is then negligible.

One of the advantages of this technique is that there are no convergence difficulties. The programme is, however, not designed to deal with falling branches. It was thought that the necessity to deal with a falling branch would not arise in the frames in which all plastic hinges were ductile. The Flow diagram of the programme is shown in Appendix 15.

The programme has been used to evaluate $M-\phi$ relations at critical sections of Frame No.2. An attempt has been made in the concluding chapter, to calculate discontinuous rotations at hinges, by using a Trilinear idealization derived from these results.

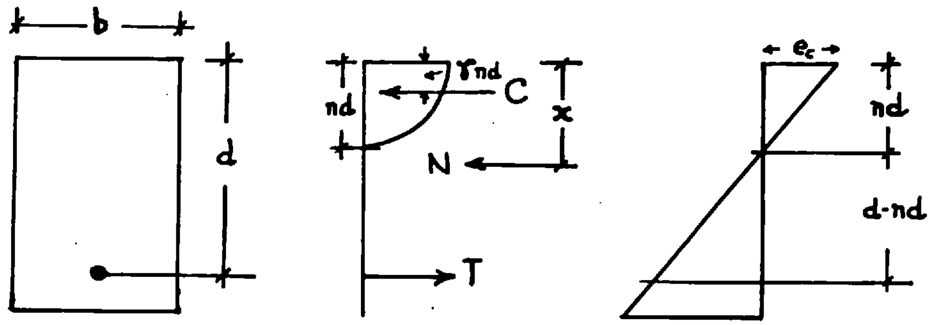
b
d
nd
γnd
C
x
N
T
e_c
nd
d-nd

FIG 5.1

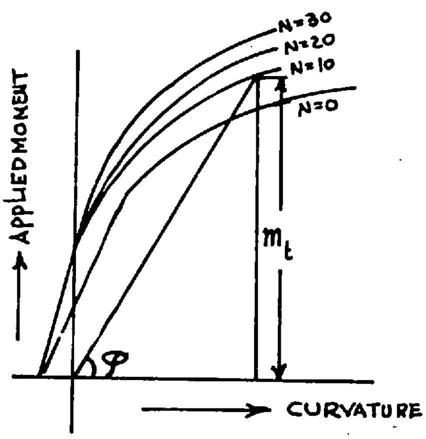
N=30
N=20
N=10
N=0
APPLIED MOMENT
m_t
φ
CURVATURE

FIG. 5.2

CHAPTER 6.

TESTS ON PRESTRESSED CONCRETE PORTAL FRAMES WITH FIXED FEET.

6.1. Object.

The object of these tests was to establish the following:-

1) Laterally unbound concrete is highly brittle. In cases where the rotational capacity of hinges depends on the ductility of concrete (e.g., over-reinforced beams), a failure may suddenly occur in a framed structure without warning, at a load considerably lower than the rigid plastic failure load of the frame.

2) Properly spaced lateral binders improve ductility in concrete adequately, to ensure full redistribution of moments in a framed structure by formation of plastic hinges, even in heavily loaded columns. Pietrzykowski[40] has shown that the condition of full redistribution does not exist in similar frames with unbound concrete.

A continuous beam was not chosen as a field of study to establish the possibility of a brittle failure, because the amount of rotation needed for full redistribution is rather low in a continuous beam. This is illustrated in Fig. 6.1. Consider a system of point loads being applied to a continuous beam or a portal frame having equal moments of resistance (m) at all critical sections.

A two span beam which is the worst case for redistribution of moments amongst continuous beams subjected to central point loads, needs a rotation of $\frac{ml}{12EI}$ at the support hinge, while a portal frame in an extreme case, subjected to a vertical and sway load as shown in Fig.6.1, needs a rotation of $\frac{ml}{EI}$ at hinge No. 1.

6.2 Frame details.

General details are given in Fig. 6.2. The transom span and the column height of the frames were 9' and 4½' respectively, allowing for the tolerance which was necessary to permit repeated use of the shuttering. Frames I and II were identical, excepting for details of shear reinforcement and lateral binders. The transom in these two frames was of 6" x 4" I section with a 1¼" wide web, while the columns were of rectangular section, 5¾" x 4" in size. This facilitated the placing of concordant cables with varying eccentricities. The moments of inertia of the transom and the columns were the same.

In Frame No. 3, the X-section of all members was rectangular, and of dimensions 6" x 4". This frame closely resembled Pietrzykowski's Ring portal No. GK[40].

Indented tendons of .276" and .2" diameters were used for prestressing. The tendons of .276" diameter were of the same type as used in Beams 8-10, described in Chapter 3. The idealized load extension characteristics of .2" diameter tendon used in the columns of Frame 3, are shown in Fig.6.3.

6.3 Concrete Mix.

The concrete mix was the same as used in the design of a prestressed concrete pressure vessel tested in the Imperial College and in the investigation of creep properties associated with it (3). The mix had a high workability of 2" - 3" slump, but the shrinkage and creep properties aimed at, was representative of normal concrete.

The coarse aggregate was Thames river gravel of ⅜" max. size. The aggregate cement ratio was greater than 3.0 to minimize creep and shrinkage and the sand content was restricted to a ratio of 30% by weight of total concrete.

The details of the mix used are as follows:

Aggregate cement ratio	3.75
Sand percentage by weight	30% of total aggregate.
Water cement ratio	.564 (total),
	.500 (effective).

The grading of the aggregate is given in the following table:-

	Percentage passing.						
Size of Sieve.	⅜	3/16	7	14	25	52	100
River gravel ⅜-3/16"	99	2	0	0	0	0	0
Sand 3/16"-100	100	100	91	75	54	13	2

6.4 Design - general details.

As discussed in 4.7, all the three frames were designed to fail under the combination of an equal vertical and a horizontal load. In frame No. 3, the position of the vertical load was, however, a quarter span away from the centre of the transom towards the right hand column, (i.e. $\frac{3}{4}^{th}$ span away from the point of application of the sway load). Excepting for the sway load, this arrangement was the same as followed by Pietrsykowski[40], in his frame No. GK. The necessity of the sway load has been explained later on.

In frames 1 and 2, in which the position of the tendons varied from point to point, it was necessary to find an envelope of maximum moments of resistance, to ensure that a premature development of hinges would not occur at a wrong place. This was done by writing a computer programme. The envelope as applicable to Frame 2, is shown in Fig. 6.4. It takes into account the contribution of mild steel in calculating the moment of resistance where necessary. A cracking moment envelope which takes into account the effect of increase in the prestressing force and which is based on a flexural tensile strength of 500 lbs/sq.inch, was also calculated by the computer programme and is shown in this diagram. It was ensured that during prestressing, a tensile stress of more than 200 lbs/sq. inch was not exceeded anywhere in the frames.

A preliminary calculation of moments at L_1 and L_2, in which the effect of the axial loads are neglected, show that all critical sections in Frames 1 and 2 are over-reinforced - vide Table 6.1. Plastic rotations predicted by Baker's theory and those required for full redistribution are also shown in this table. It can be easily seen from this table that Frame No. 1 was designed to fail at the foot of the right hand column for want of ductility at that point.

Frame No. 3 Vs Pietrzykowski's frame GK.

The properties of the X-sections of the two frames have been compared in Table 6.2. The necessity of an additional side sway load in the author's Frame No. 3 is explained below.

Practical considerations did not permit the use of jacks beyond 30 ton capacity, and these were planned to operate almost at their maximum capacity. The axial loads in the columns were in the region where a lower moment of resistance would be obtained by increasing the axial loads. During the experiment, it was therefore not possible to ensure, by increasing the axial loads, that hinges would form in the columns. The side sway load was introduced to force at least two hinges at the feet of the columns, before collapse. If only a vertical load were applied at the quarter point as was done by Pietrzykowski, failure might have taken place by a beam mechanism with all the three hinges in the beam itself. The purpose of the experiment would then have been defeated.

The side sway load also increased the amount of rotation needed at the top of the right-hand column for full redistribution of moment. A step by step analysis shows that the rotation required at this point at the time of failure by the beam mechanism under a vertical load only, would have been $\frac{1.166mh}{EI}$, against a value $\frac{3}{2}\frac{mh}{EI}$ required under the combined mechanism of failure proposed by the author. However, in the actual experiment, an advantage of this fact could not be taken to demonstrate the greater ductility of columns, as the hinge did form in the beam itself.

An attempt was made to have equal moments of resistances in all the frames at all critical sections.

Shear Reinforcement.

Shear reinforcement was provided in all the frames, according to the recommendations of Leonhardt[33]. 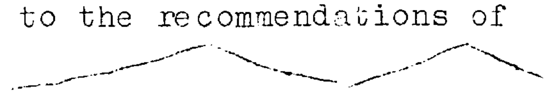

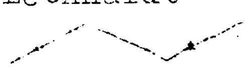 . In Frame 1 the shear reinforcement was in the shape of bars bent in a zig-zag fashion, lying in the plane passing through the longitudinal axis of the members* In this way the presence of any transverse reinforcement which might have an influence on the confinement of concrete was avoided. In Frame 2, two legged stirrups were used in the conventional way, in conjunction with lateral binders at 1" spacing. In case of the transom, these binders were in the compression flange. (See Fig. 6.5 for details.)

* A system introduced by Edwards.

The pedestals of the frame.

An extra care was taken to design the reinforcement in the pedestals. Four legged stirrups of ⅜" cold worked bars were used at 2½" spacing in the pedestal of Frame No. 3, to take care of the heavy shear caused by the self equilibrating system of axial loads acting on it.

6.5 Casting details.

The frames were cast in one piece in a timber mould lying on the floor. The level of the floor had a maximum deviation of .1". To minimize the possibility of alterations in dimensions due to the repeated use of the formwork, the vertical shuttering on the inner side was braced by angle iron struts - (plate 6.1). In addition to this, a short piece of a hollow square tubing of 1" width, was partially introduced into each pedestal through holes left in the side shuttering, at the time of casting. The protruding ends of the tubings were then connected together by two angle irons introduced between them. A strut parallel to the transom was thus formed between the pedestals which helped the feet to remain at a fixed distance until the time of the testing, when the connecting angle irons were disengaged.

The front faces of the pedestals (which were horizontal and facing upwards at the time of casting) were also connected together by a 5" x 3" angle iron. Necessary bolts for this purpose were lightly tapped into the concrete when it was still wet, after the casting was over. This prevented the twisting of the feet during transport and lifting. Nine, 6" control cubes were cast and cured as far as possible under the same conditions as existed for the main specimen.

The frames were partially prestressed up to 75% of the desired final values to take up handling stresses during lifting and transporting. The prestressing was done while the frame was still lying on the floor on its bottom shuttering. In frames 1 and 2, in which the transom was of I section, foam polystrene was used in short lengths at each end of the bottom shuttering under the transom, to form the projection which was needed to give the desired shape of an I section. This prevented the sticking of the bottom shuttering to the specimen, at the time of prestressing. The prestressing was done systematically in two stages, covering all the members so that excessive stresses and cracking was avoided at all stages. Enough length of bars were left at the stressing ends to enable the operation of restressing to be taken up at a later date. The prestressing force was measured by using a tiny load cell of 5 tons capacity at the rear of the jack. (i.e. between the body of the jack and the grip used behind the jack.)

6.6 Test Rig.

The general arrangement of the testing frame is shown in Fig. 6.6. The rig was first developed by Edwards. Later on, the reaction measuring dynamometers (described in 6.8), to which the pedestals were clamped, were developed by Gupta[27]. The vertical load was applied through a jack of 4 tons capacity and was measured by a load cell screwed into the jack. The load was transmitted to the transom through a ball and socket joint on the top of a 1½" wide loading platten. The sway load was applied through a jack of 10 tons capacity and the load was measured by a similar load cell. In this case, the loading platten rested on tiny rollers designed to move in vertical grooves cut onto the face of a mild steel bridge, which covered the end anchorage.

The vertical load always remained at the centre of the transom due to an ingenious hydraulic system devised by Edwards.

The movement of the transom was transmitted through a dummy jack, touching the right-hand corner of the portal frame, to an exactly similar jack clamped to the test rig on the left-hand side of the point of application of the vertical load, by the displacement of oil in the hydraulic system connecting the two jacks. When the system was sealed against leakages after carefully bleeding out air pockets, the movement of the rams of both the jacks were equal to the movement of the transom. The jack at the left-hand side of the test rig, was mechanically coupled to a horizontal plate holding the main vertical jack. This plate was capable of sliding forward, due to the presence of a set of rollers introduced between itself and a bearing plate welded to the rig. The vertical jack therefore, always moved by an amount equal to the movement of the transom, and remained at its centre.

Great care was taken in aligning and fixing the pedestals to the reaction measuring dynamometers. The base plates of the dynamometers were firmly fixed to the floor.

A tubular scaffolding independently connected to the floor, provided a framework to which transducers* were connected, for the purpose of recording deflections.

Another independent platform was provided for watching cracks without disturbing the potentiometers.

6.7 Application of axial loads to columns in Frame 3.

It was an implied condition of introducing a sway load in this frame, that the jacks used for applying the axial loads, must also move freely with the frame. It was impossible to provide this movement by the method that was adopted for the jack used for applying a point load to the transom. Not only was there not enough space in the test rig, but also such a system would have overloaded the reaction measuring dynamometers at the base of the pedestals. A self-equilibrating system was therefore chosen, such that the reaction was absorbed by the pedestals. Four mild steel bars of 1¼" diameter were chosen to provide the necessary tension and adequate stability in the system. Each bar was connected to a hinge both at the top and the bottom. Full details are shown in Figs. 6.8 & 6.9

* A transducer is very similar to a potentiometer.

Holl-o-Ram jacks of 30 tons capacity were used for applying the axial loads. A 2¼" thick plate was screwed onto threads specially cut on the outer circumference of the jacks. Knife edge bearings which gave the necessary freedom of rotation to the top of the tension bars, were fixed on this plate. Similar bearings were provided underneath rectangular cross pieces, which passed through grooves provided in the pedestals at the time of casting. Each jack rested on a cylindrical hinge attached to a base plate at the top of the column. The latter also acted as the end plate for the anchors of the prestressing cables and was thus fixed in position.

Both jacks were fed by the same hydraulic system. It was originally contemplated that the load in the jacks would be maintained by an Amsler Cabinet having a load maintenance device. Unfortunately, a cabinet capable of delivering an oil pressure of about 8500 lbs/sq.in. and suitable leads to take this pressure, necessary to develop the required load in the jacks, was not available. A hand pump was used instead, with leads of steel tubing, except for short lengths of rubber tubing, needed to provide flexibility at suitable points. These rubber tubings were guaranteed for a pressure of 5000 lbs/sq.inch, but they behaved satisfactorily under the required pressure.

The loads transmitted by the jacks were primarily controlled by an oil pressure gauge attached to the pump. Any fall in the oil pressure was recouped from time to time. The exact load acting on each column was, however, recorded by four strain gauges fixed at the centre of each tension bar, as if each bar were a load cell. Although it was not practical to use these eight load cells to control the loads on the two columns, yet they provided an accurate method of measuring the actual loads. The axial load aimed at was 62500 lbs. The readings of the strain gauge fixed to the vertical bars indicated that the actual load in the column was 60000 $\pm$ 1500 lbs.

Each tension bar was connected to the housing containing the knife edges, by means of threads which were clockwise at one end and anti-clockwise at the other. A nut was welded to the bar to permit the use of a spanner, which could under the above arrangement, either shorten or lengthen the bar, by turning it one way or the other. To ensure a uniform stress on the column, a partial load was first applied and the tension bars were then tightened or loosened by a systematic trial and error, to give equal strain readings on all the four faces of the columns, as recorded by a 4" demountable Demec gauge. It was then checked that on the application of the full load, the strains on opposite faces did not differ by more than 10%. If this was not attained, the column was unloaded and the process was repeated.

6.8 Instrumentation.

Fig. 6.7 shows the position of electrical strain gauges and clinometers. In all, 66 gauges were used on each face of the frame. Strains were recorded by the Solartron data logger, which could record strains at the rate of two channels per second and could deal with a maximum of 200 channels. Deflections were also recorded by this instrument. There was a change in the solartron reading when a deflection occurred, due to the corresponding change of resistance in the transducer. A correlation between the readings of the solartron, and standard changes in length occurring at the tip of the transducers, was first obtained by using a micrometer screw gauge.

Only clinometer readings were recorded manually. The clinometers were the same as previously used for measuring rotations in beams and columns.

The readings of the load cells fixed to jacks and the readings derived from the strain gauges fixed to the legs of each reaction dynamometer, were also recorded by the 'Solartron'.

Brief description of the reaction measuring Dynamometers.

The dynamometers which were used under the pedestals to measure the stress resultants at the foot of the columns, consisted of three tripods under each pedestal. Each tripod had three sensitive legs. On each of these legs, electrical strain gauges were attached to form the four arms of a wheatstone bridge. The layout of the tripods under the pedestals is shown in Fig.6.7 The top plate of a dynamometer was connected to the three tripods underneath it by a ball and socket system at the top of each tripod. The vertical and horizontal load acting at the centre of this hinge above each tripod is given by the equation:-

$$\begin{pmatrix} V \\ H \end{pmatrix} = \begin{pmatrix} K_{11} & K_{12} \\ K_{13} & K_{14} \end{pmatrix} \begin{pmatrix} \xi_1 \\ \xi_2 \end{pmatrix}$$

where 1) V and H are the vertical and the horizontal loads.

2) $\begin{pmatrix} K_{11} & K_{12} \\ K_{13} & K_{14} \end{pmatrix}$ is the calibration matrix.

3) ξ_1 is the increment in readings in leg 1 and ξ_2 is the average increment in legs 2 and 3. } per unit load.

A typical calibration matrix was of the order

$$\begin{pmatrix} .5 & 1 \\ -.37 & .37 \end{pmatrix}$$

If it is assumed that ξ_1 and ξ_2 can be assessed to 1 division on the solartron, the vertical load at the top of each tripod has a sensitivity of 1.5 lbs.

6.9 Erection.

The frames were lifted in the partially prestressed stage and transported to the Test Rig by the laboratory crane. Finally, they were lowered on the top plates of the dynamometers. The frames were then carefully centered and the pedestals were firmly clamped to the dynamometers by means of steel plates running across the top of the pedestals and holding down bolts on both sides, connecting these plates with the top plate of the dynamometers.

6.10. Prestressing and grouting.

Table 6.3 shows the date of casting, the dates of application of full prestress and grouting and the average cube strength attained on the day of testing.

The frames were first of all partially destressed, so as to retain approximately 25% of the final prestressing force in each member. This was done in a systematic and controlled sequence so that the danger of cracking was avoided at all stages. Complete destressing might have resulted in shrinkage cracks. Unfortunately the frames were tested after more than a year from the date of casting and such a possibility existed.

After recording the readings of the legs of the dynamometers, the tendons were fully re-stressed with the help of a re-stressing stool. The XL grips were released and relocked in position after removing the shims which were used in the first instance when stressing was done in several stages.

Grouting was done immediately after full prestressing. When this was not possible, the first available opportunity was taken to complete this operation. Columns were grouted from bottom upwards. The grout was of the same consistency as used in the beams and columns previously described. Grouting was successfully done through holes provided in the end anchorage plates.

6.11. Test procedure.

The rigid plastic collapse load of the frame was recalculated, using the crushing strength of 6" cubes, found one day before the test. Incremental loads in intervals of 10% were applied, using the load maintaining device of the Amsler Cabinets. After attaining about 80% of the collapse load, or as soon as the formation of the second hinge was noticed, the load maintaining device was abandoned. Thereafter the frame was allowed to deflect under specified deflections measured both vertically and horizontally. An attempt was made to proceed in increments of 10% of the values of deflections attained at the time when the constant load maintaining device was abandoned. An excellent control could be exercised on the behaviour of the frame by following this method, because both the increments in loads and deflections could be observed in the panel of the data logger by the person who was controlling the experiment. It was possible to follow the plastic behaviour of the frame in this way in 15 to 20 stages. A constant ratio of the loads of course, could not be maintained. In fact, in order to minimize the effect of creep and to keep the deflections at a fairly constant level, one or both of the loads had to be decreased at some stages.

6.12 Test Results.

The punch encoder of the solartron gave the output in the form of a five hole punched tape. A computer programme was written to read and process this information and to print out the extreme fibre strain, the curvature and the neutral axis depth at chosen points of the structure, followed by values of the applied loads, deflections of the structure, and the moment and reactions at the foot of the columns, as deduced from the readings of the reaction dynamometers.

6.13 Behaviour of individual frames.

Frame 1.

This was the first frame tested by the author. As already discussed, it had all the potentialities of a brittle failure.

Cracks first appeared in the right hand column under the transom and also immediately above the joint with the pedestal when both W_V and W_H were about 2300 lbs. Pimpling of concrete appeared on the compression surface corresponding to these cracks, when W_V and W_H reached the values of 3704 and 3654 lbs.

Beyond this stage the load maintaining devices in the Amsler loading cabinets were abandoned and an attempt was made to let the frame deform under controlled deflections. A vertical deflection of .6" and a horizontal deflection of .7" was recorded up to this stage. In the next load stage, an increment in the deflections by about 10% was aimed at. An increase in the vertical load at this stage exhibited signs of immediate collapse (i.e. more pimpling, accompanied by a creaking noise). The side sway load W_H was therefore first increased, whence it was found necessary to simultaneously decrease the vertical load slightly. The vertical and the horizontal loads recorded at the end of this operation were 3524 lbs and 3694 lbs respectively, while the vertical and the horizontal deflections were .66" and .76".

An attempt to repeat the process to achieve a further increment of 10% in deflections, resulted in a violent brittle compression failure (see plate 6.25) and the experiment had to be abandoned. There was no shear distress. It will be seen that the maximum load at the time of failure was about 75% of the rigid plastic collapse load (4800 lbs. neglecting axial loads). No cracking or pimpling was noticed at the foot of the left-hand column.

Frame No. 2.

This frame was identical to Frame No. 1, except for the fact that it had lateral binders on either side of the critical sections, which extended up to a point where the maximum moment was half of the maximum moment at the critical section.

The first crack appeared at the toe of the right-hand column, when both W_V and W_H attained a value of about 2200 lbs. As the load was increased the hinge in the transom exhibited a distinct ductility and when W_V and W_H were approximately 3500 lbs. each, the tensile crack at this hinge was growing without apparently showing any signs of pimpling at the top. Pimpling of concrete was first noticed at the foot of the right-hand column when both W_V and W_H were 3840 lbs. (approx.) In the transom hinge, pimpling was noticed when W_V and W_H were 4400 lbs. each. By this time a plastic hinge had developed at the foot of the left-hand column. The frame was entering the stage of a collapse mechanism. The load maintaining devices in the loading cabinets were shut off and the frame was allowed to move further under controlled deflections.

As the transom hinge exhibited somewhat less ductility than the other hinges, it was again the sway load which was first manipulated to obtain the desired increments of deflections. This resulted in W_H attaining somewhat higher values than W_V. The latter remained constant for a while, followed by a reduction in its value. e.g. W_H was 4608 lbs. when W_V was 4432 lbs. and thereafter W_H was 5800 lbs when W_V was reduced to 4037 lbs.

Finally, the frame collapsed at W_H = 6093 lbs and W_V = 3622 lbs, by forming a 5^{th} hinge in the transom at a distance of approximately a quarter of the transom span from the left-hand column. At this point, the moment of resistance of the transom was not enough to cope with the applied moment due to termination of binders in the top flange and the termination of M.S. bars at the bottom. The failure was obviously due to the fact that the frame was not designed for such a combination of loads.

The deflections at the time of collapse were 1.39" under the vertical load and 2.44" measured horizontally at the point of application of the sway load, (approximately twice the vertical deflection and three times the horizontal deflection obtained in Frame 1.)

The ductility resulting from the use of the binders in the flange of the I beam is clearly demonstrated in this experiment. (See plates 6.3-7-8-9)

Frame 3.

This frame represented a lower storey frame of a tall building. An incremental load on the columns was unnecessary because in an actual building the forces due to the wind load would come into play in the columns of a lower storey, when they were already under heavy loads due to the dead load alone.

Before starting the main test, both the columns were fully loaded. The resulting direct stress was about 2600 lbs/sq.inch. The frame was then subjected to an incremental vertical load, accompanied by an equal incremental sway load. The axial loading device was perfectly stable. A compensation was made at each load stage to account for the fact that the inclination of the axial load continually changed. This was done by increasing the side load by an amount equal to $P\frac{\delta_H}{\ell}$

where P = axial load

δ_H = horizontal deflection

ℓ = length of column

note:- $\frac{\delta_H}{\ell}$ was assumed to be equal to the inclination of the tie bars.

Cracking was first observed as anticipated at the top of the transom near the right-hand corner of the frame.

Crushing of concrete was first observed at the toe of the right-hand column when W_V was 4378 lbs. and W_H was 4746 lbs. This was the indication of the fact that the first plastic hinge had formed at this point. Tensile cracks also appeared under the vertical load at this stage.

Crushing of concrete was noticed at the bottom of the transom at the right-hand corner of the frame when W_V was 4690 lbs. and W_H was 5117 lbs. This was the second hinge to form and it was in the beam and not in the column.

The third hinge formed at the foot of the left-hand column when W_V was 5622 lbs. and W_H was 6077 lbs.

The 4^{th} and the last hinge needed to transform the frame into a mechanism, formed under the vertical load at the load stage when W_V was 6328 lbs. and W_H was 6529 lbs. It was possible in this frame to continue with the load maintaining device up to this stage. The order of formation of the hinges was the same as predicted by the step by step analysis.

After this stage the loads continued to rise apparently due to a strain hardening behaviour, while the frame continued to deform under specified deflections, until W_V and W_H attained the values of 7370 lbs. and 7160 lbs. respectively. Thereafter a gradual reduction in the loads was observed. The experiment was terminated when the sideways deflection attained the value of 2.36" and the values of W_V and W_H were 6770 lbs and 6300 lbs. i.e. still within 10% of the maximum values attained and higher than the calculated rigid collapse load of 6000 lbs. The testing rig did not have much room for any appreciable amount of further side sway. A gradual unloading was done at this stage, to trace the path of unloading.

The first and the third hinges to form in the final mechanism, were at the foot of the right and left-hand columns respectively. These columns exhibited sufficient ductility to enable the final mechanism to form.

The deflections noticed at the end of the experiment, accompanied by a continual increase in the loads, more than adequately demonstrate the efficiency of the binders.

6.14 Presentation of results.

Loads V/s deflection.

The most convenient way of presenting the overall ductility of a structure, is to plot deflections against the applied loads. Graphs 6.1 to 6.3 show horizontal and vertical deflections plotted against W_V and W_H in respect of frames 1 to 3.

Hinge moments V/S applied load and distribution of moments at collapse.

The growth of bending moments in the frames at the critical sections is shown in Graphs 6.4

to 6.6. Comparison has been made with the theoretical development that would have taken place, had the frames been ideally elasto-plastic with a constant flexural rigidity in between the hinges throughout the frames, and also if the ratio of the vertical and the horizontal load had not changed during the experiment.

It will be seen that secondary moments existed in the frames before the commencement of the test. The author is of the opinion that this was due to the lack of fit introduced at the time of casting. Table 6.4 gives the relation between stress resultants and lack of fit at the foot of the right-hand column. It may be seen that considerable stresses can be caused by a small angular difference between the pedestals of the two columns.

The distribution of moments in the frames at the time of collapse is shown in Figs. 6.10

Moments VS rotation.

The moment rotation curves in respect of hinges at the top and bottom of the right-hand column, are shown in Graphs 6.7 to 6.9.

Distribution of curvature at critical sections.

The distribution of curvature at critical sections at the time of collapse, have been shown in FIG 6.11 & 6.12 in respect of FRAMES 1&2.

6.15 Discussion of Results.

Frames 1 and 2.

The brittle failure in Frame 1 due to the insufficient rotational capacity of the transom hinge, shows that Baker's theory over-estimates plastic rotations in over-reinforced I-sections.

The following questions, however, do arise when Table 6.1 is examined. Why did not failure occur at the foot of the right-hand column where the available rotation predicted by Baker was too small, or why did not the hinge at the top of the right-hand column have a brittle failure, inspite of the fact that the rotation needed at this hinge for full redistribution, was twice that needed at the other two hinges?

A solution is that rectangular sections have a greater capacity of rotation than predicted by Baker, even if such sections are over-reinforced. The author is of the opinion that the opposite is the case in I-sections. Unbound concrete in the flange of an over-reinforced I-section has less confinement in space than the corresponding areas under compression in rectangular beams. They have an additional degree of freedom of movement under compression forces, due to the presence of the exposed surface underneath the flange.

Baker's predictions of rotations in over-reinforced I-sections are therefore on the unsafe side and a suggested reduction factor is .5. This is also borne out from the moment rotation characteristics of simply supported I-sections obtained by the author.

Lateral binders, however, provide considerable ductility and permit the calculation of collapse loads by the rigid plastic theory. The load deflection and moment V/S load curves pertaining to Frame 2, amply prove this point.

The failure of Frame 2, which took place by the formation of a 5^{th} hinge is, however, a warning that lateral binders have to be used with caution after considering all possible combinations of loads that may occur in the structure.

Frame 3.

The experimental failure load (if failure be defined to be the point of maximum load) and a study of the development of moments at hinges, amply justify the assumption of a full redistribution of moments in this case.

The rigid plastic collapse load shown in Graph 6.6 has been calculated, using the formula proposed by Baker at Ankara, to take into account the effect of binders. It can be seen that each of the critical sections exceeds the predicted value.

An abnormal enhancement of about 30% in the plastic moment was also noticed in the pilot tests on columns described in Chapter 4. (Compare actual moments with Baker's predictions in Grphs 4.1 and 4.2.) The recent work done by Soliman(47) does not indicate the possibility of this tremendous increase. The author thinks that the ½" duct tubes in conjunction with closely spaced binders was responsible for this increase. Chan[17] observed a considerable increase in strength when compression reinforcement was used in conjunction with binders.

An attempt has not been made to compare the behaviour of the frame with Baker's predictions which are far too inaccurate in this case. The object of the test was to show the efficiency of the binders, compared with results obtained by Pietrzykowski.

6.16 Summary.

Results of tests on three portal frames have been described in this chapter. It has been concluded that checking of rotations cannot be dispensed with, at least in cases of I-sections in which Baker's predictions are on the unsafe side.

In the next chapter a theoretical discussion has been entered into, regarding the design of multi-storeyed frame. A method has been suggested to deal with adjustment of rotations.

TABLE 6.1

MOMENTS AND ROTATIONS AT L_1 AND L_2 IN FRAMES 1 & 2.

(Neglecting thrust).

HINGE NO.	d	e_{c1}	n_1d	M_1	e_{c2}	n_2d	M_2	
1	4.115	.002	1.76	79000	.004	1.6	88200	F1
					.0085	1.45	88500	F2
2	4.075	.002	1.75	78000	.004	1.6	87250	F1
					.0085	1.45	87500	F2
3	4.04	.002	1.85	75500	.004	1.65	86000	F1
					.0085	1.50	87200	F2

HINGE NO.	permissible rotation in Radians.	EI value $= \frac{M_1 n_1 d}{e_{c1}}$	Required θ_p for full redistribution in Radians.	Remarks
1	.00525	69.5×10^6	.01135	----Frame 1, p" = 0
	.0171			----Frame 2, p" = 2.5
2	.0106	68.2×10^6	.0227	----Frame 1, p" = 0
	.0344			----Frame 2, p" = 2.5
3	.016*	70×10^6	.01135	----Frame 1, p" = 0
	.052			----Frame 2, p" = 2.5

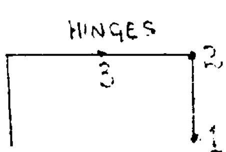

*these figs are slightly higher due to a higher value of $\overline{Z}/d$ when compared with hinges 1 and 2.

Note: These figs. are based on an average EI value of 69.2×10^6.

TABLE 6.2.

PROPERTIES OF X-SECTION OF AUTHOR'S FRAME 3, COMPARED TO THE PROPERTIES OF X-SECTION OF PIETRZYKOWSKI'S FRAME GK.

FRAME NO.	SIZE	CONCRETE STRENGTH.	REINFORCEMENT.	AXIAL LOADS	DEPTH OF NEUTRAL AXIS AT ULTIMATE LOAD.
Author's Frame 3.	6" x 4"	6000 lbs/sq"	2 Nos. .2" Ø tendons at a distance of 1½" and 2 Nos .2" Ø tendons at a distance of 4½" from fibre 2.	Required load on LHC = 56500 lbs. Required load on RHC = 62500 lbs Actual load = 60000 ± 1500 on both columns.	nd=4.5 ie n=1
Pietrzykowski's Frame GK	6½" x 3"	4" cube strength =8000 lb/sq" which may be taken as equivalent to a 6" cube strength of 7700 lbs/sq"	2 Nos. .2" Ø at a distance of 1¾" on either side of Centre line	4 X P, where P $=\frac{15(m_c+m_b)}{3}$ =12750 lbs ∴ Desired axial load = 51000 lbs. m_c=8.72 x 10 in lbs. m_b=12.75x 10 in.lbs.	nd=5" ie, n=1

Table 6.3

Frame No	Date of casting	Date of application of full pre-stress	Date of testing	Average cube strength
1	17.12.65	22.9.67 23	9.10.67	7000 lbs per sq"
2	21.1.66	19.10.67	30.10.67	7500 lbs per sq"
3	25.3.66	15.11.67	14.12.67	7000 lbs per sq"

TABLE 6.4.

SHOWING STRESS RESULTANTS UNDER UNIT VERTICAL, HORIZONTAL AND ROTATIONAL MOVEMENT AT THE FOOT OF THE RIGHT-HAND COLUMN.

Stress Resultants	Unit Vertical Movement (down)	Unit Horizontal Movement (Towards the right)	Unit Rotation (clockwise)
X_1 Vertical Reaction (upwards)	$-\frac{3}{8}\ \frac{EI}{h^3}$	0	$\frac{3}{8}\ \frac{EI}{h^2}$
X_2 horizontal thrust (towards left.)	0	$-\frac{12}{5}\ \frac{EI}{h^3}$	$-\frac{9}{5}\ \frac{RI}{h^2}$
X_3 moment anti-clockwise	$\frac{3}{8}\ \frac{EI}{h^2}$	$-\frac{9}{5}\ \frac{EI}{h^2}$	$-\frac{79}{40}\ \frac{EI}{h}$

Note: The above has been obtained from the following release system:

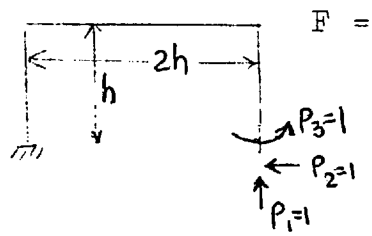

$$F = \frac{1}{EI}\begin{pmatrix} \frac{20}{3}h^3 & -3h^3 & 4h^2 \\ -3h^3 & \frac{8}{3}h^3 & -3h^2 \\ 4h^2 & -3h^2 & 4h \end{pmatrix}$$

$$F^{-1} = \frac{9EI}{40}\begin{pmatrix} \frac{5}{3h^3} & 0 & -\frac{5}{3h^2} \\ 0 & \frac{32}{3h^3} & \frac{8}{h^2} \\ \frac{-5}{3h^2} & \frac{8}{h^2} & \frac{79}{9h} \end{pmatrix}$$

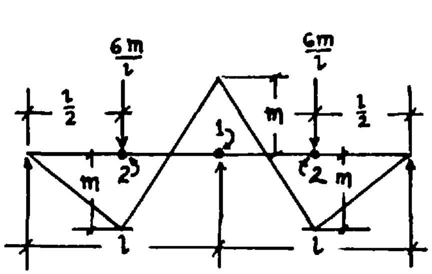

A

BENDING MOMENT DISTRIBUTION AT COLLAPSE

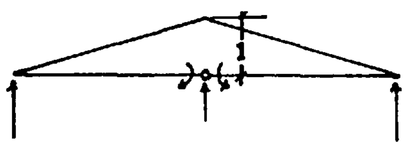

B

UNIT RESTRAINT AT HINGE 1

PLASTIC ROTATION AT HINGE 1, IS THE PRODUCT INTEGRAL OF A & B $= -\frac{ml}{12EI}$

2 SPAN CONTINUOUS BEAM, LENGTH OF SPAN = l

LEGEND

PLASTIC HINGES ⟶ ●

RELEASE " ⟶ ○

NOTE - 1. HINGES HAVE BEEN NUMBERED IN THE SAME SEQUENCE AS THEY OCCUR

2. PLASTIC MOMENT OF RESISTANCE IS EQUAL TO 'm' AT ALL CRITICAL SECTIONS

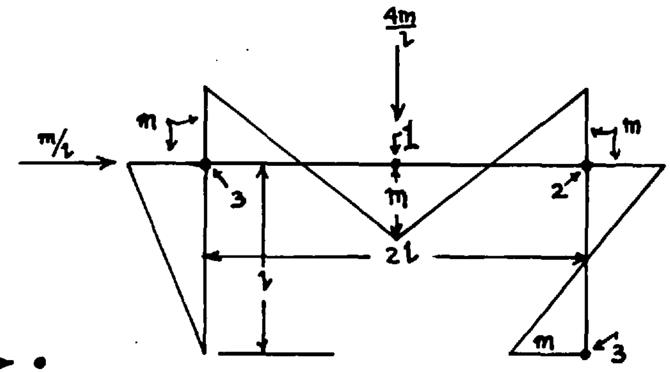

A

BENDING MOMENT DISTRIBUTION AT COLLAPSE

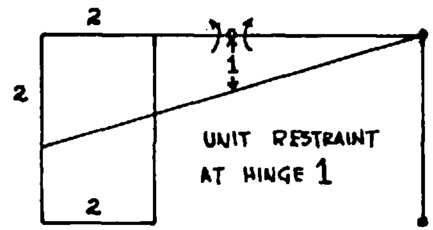

B

PLASTIC ROTATION AT HINGE 1, IS THE PRODUCT INTEGRAL OF A & B $= -\frac{ml}{EI}$

FIXED FOOTED PORTAL FRAME, SPAN = $2l$ & HEIGHT = l

FIG 6.1

SHOWING PLASTIC ROTATIONS NEEDED IN A CONTINUOUS BEAM COMPARED TO ROTATIONS NEEDED IN A PORTAL FRAME FOR FULL REDISTRIBUTION OF MOMENTS

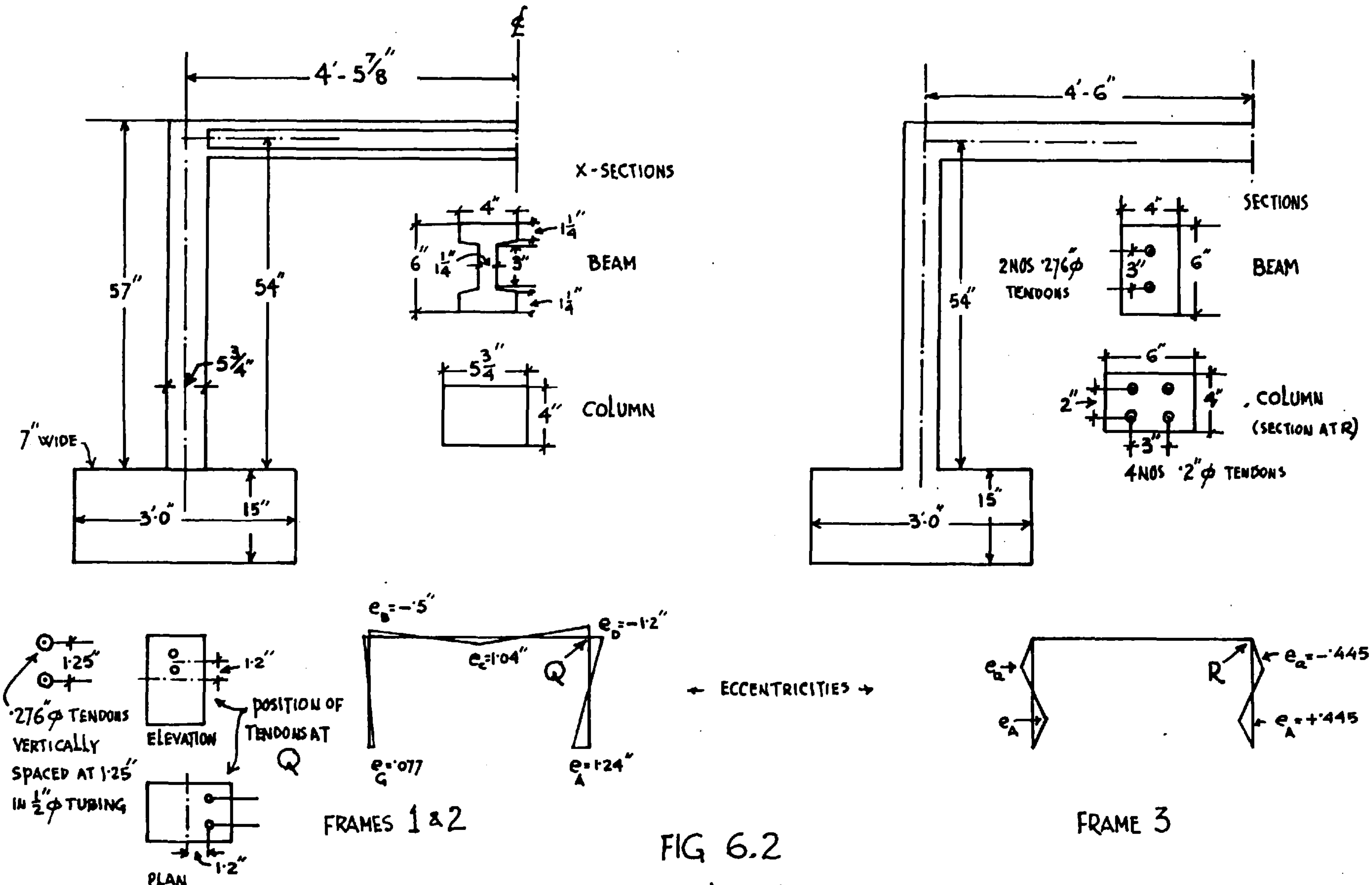

FIG 6.2

SHOWING GENERAL DETAILS OF FRAMES

FOR SHEAR REINFORCEMENT & M.S. BARS SEE FIG 6.5

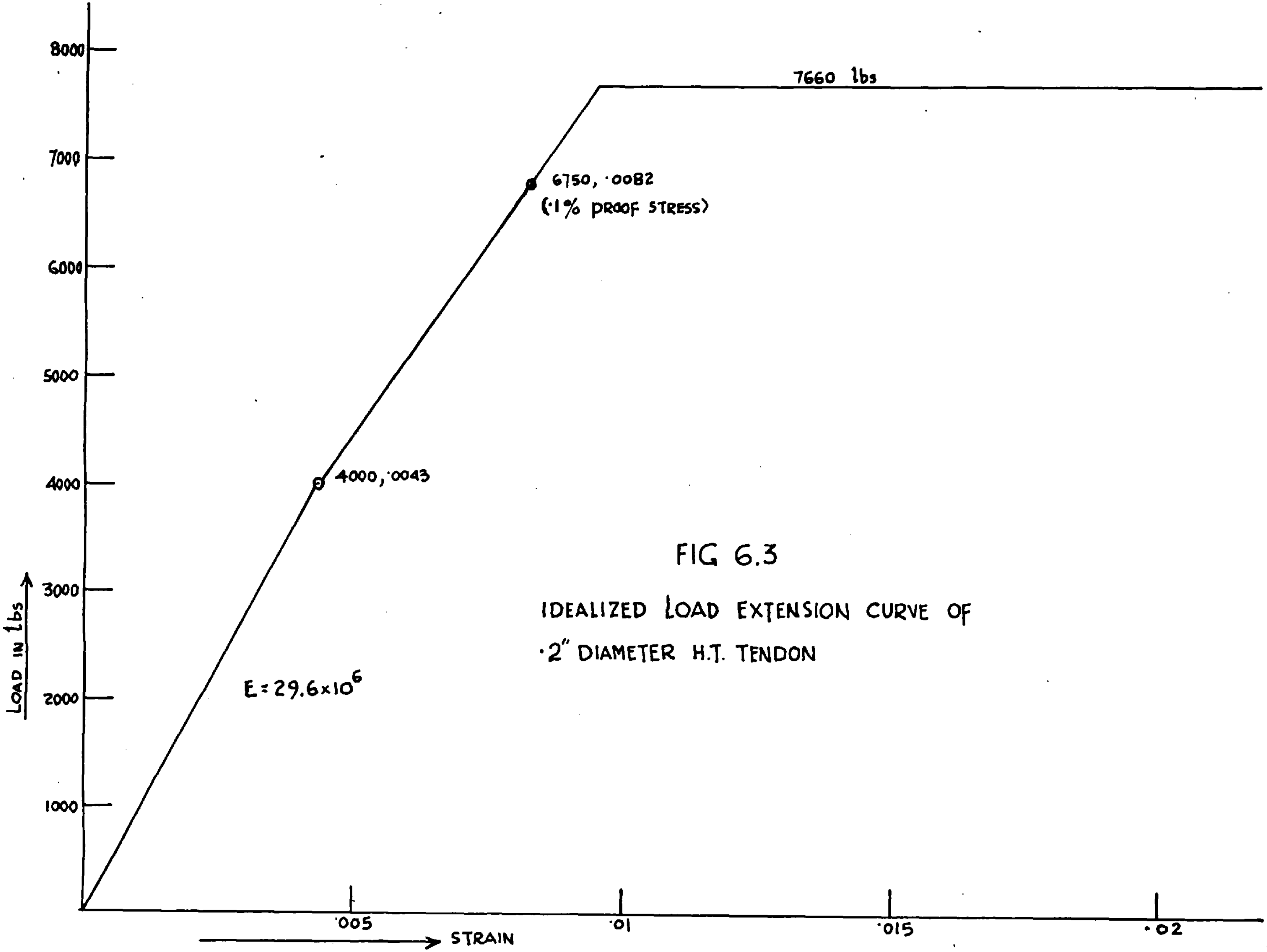

FIG 6.3

IDEALIZED LOAD EXTENSION CURVE OF ·2" DIAMETER H.T. TENDON

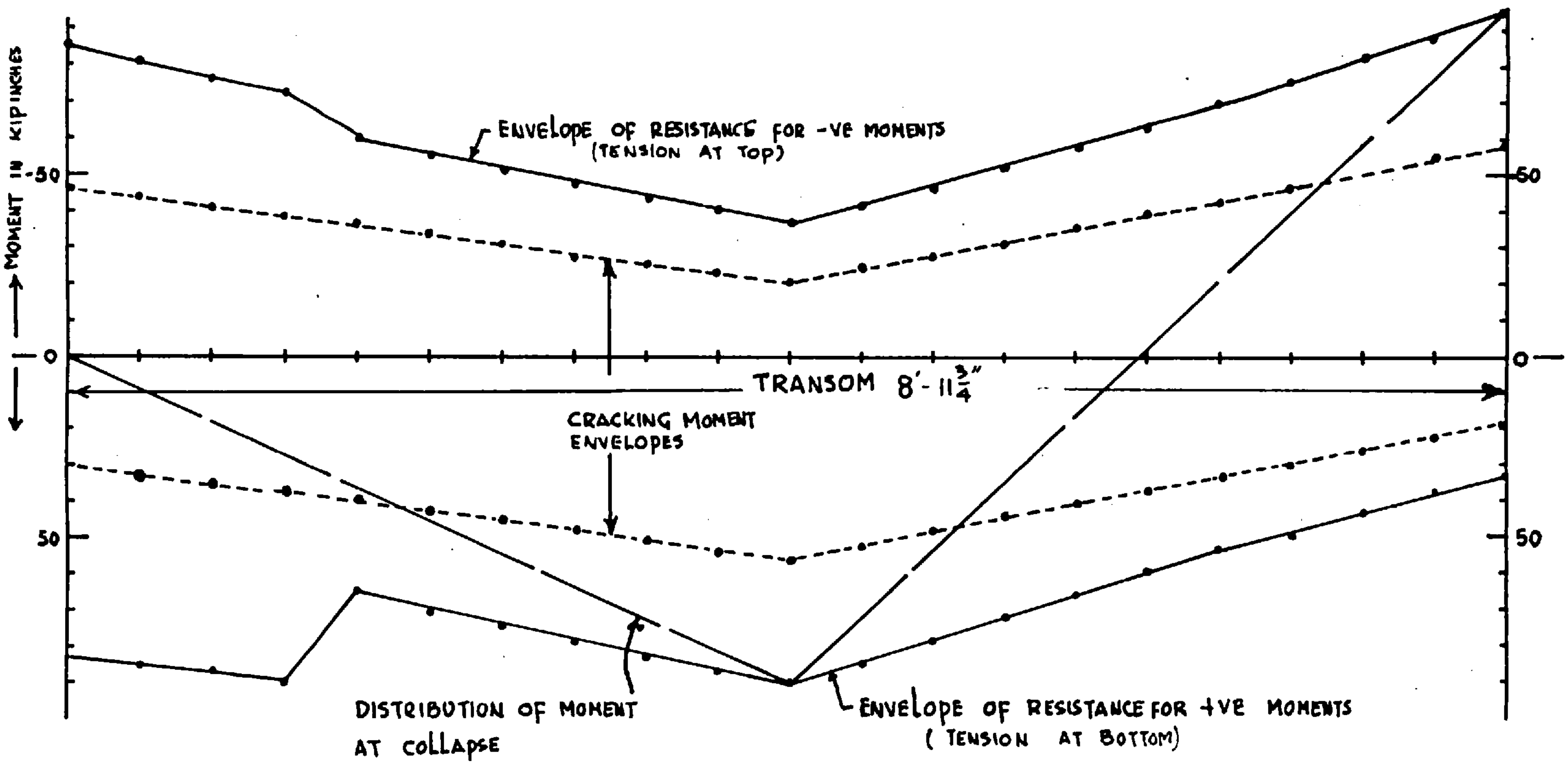

FIG 6.4 a

MAXIMUM MOMENT & CRACKING MOMENT ENVELOPES
IN TRANSOM
OF FRAME NO 2.

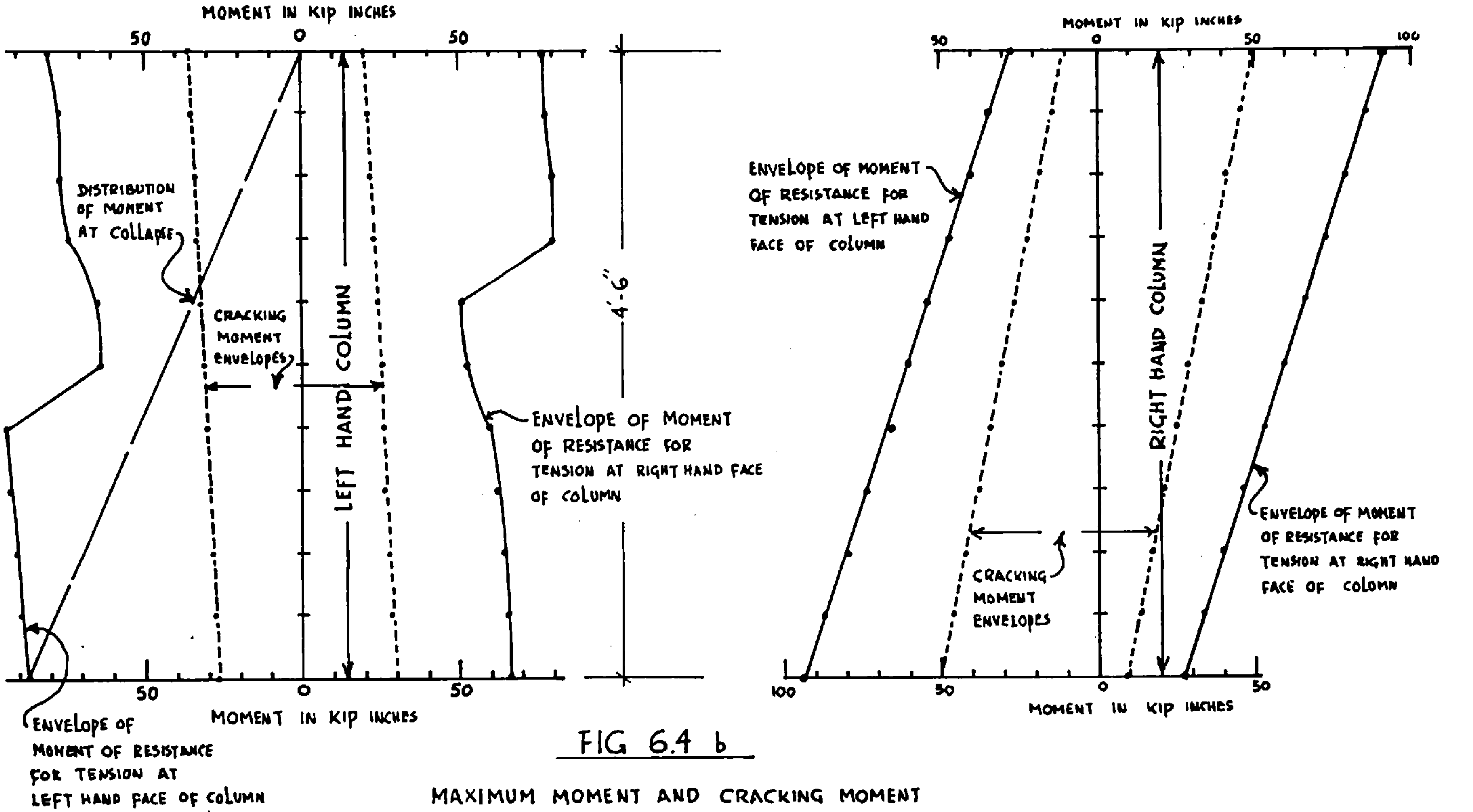

FIG 6.4 b

MAXIMUM MOMENT AND CRACKING MOMENT ENVELOPES IN COLUMNS, FRAME 2

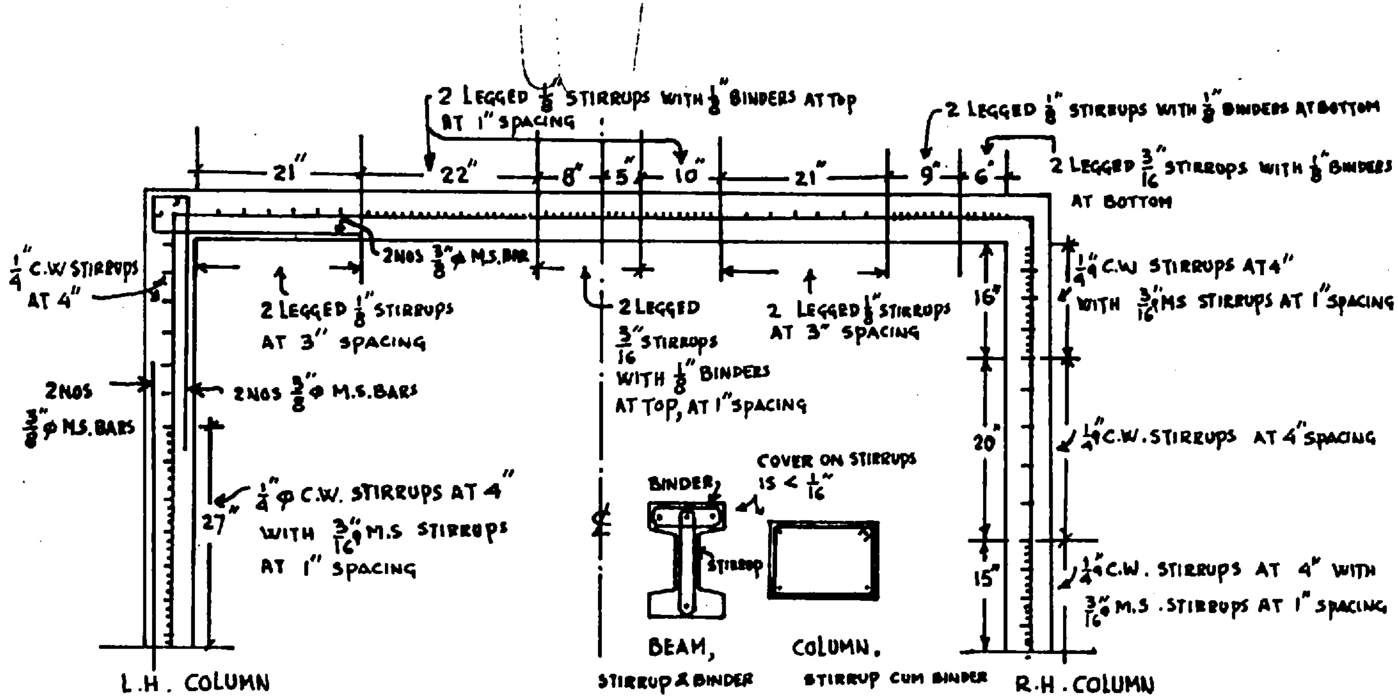

FRAME 2

DETAILS OF STIRRUPS, BINDERS & M.S. BARS.

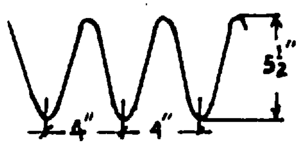

SHEAR REINFORCEMENT IN FRAME 1

2 LAYERS OF 1/8" φ MS BARS IN TRANSOM (ONE ON EACH SIDE OF DUCT TUBE) AND 1 LAYER OF 1/4" φ COLD WORKED BAR IN THE COLUMNS, BENT IN THE ABOVE SHAPE

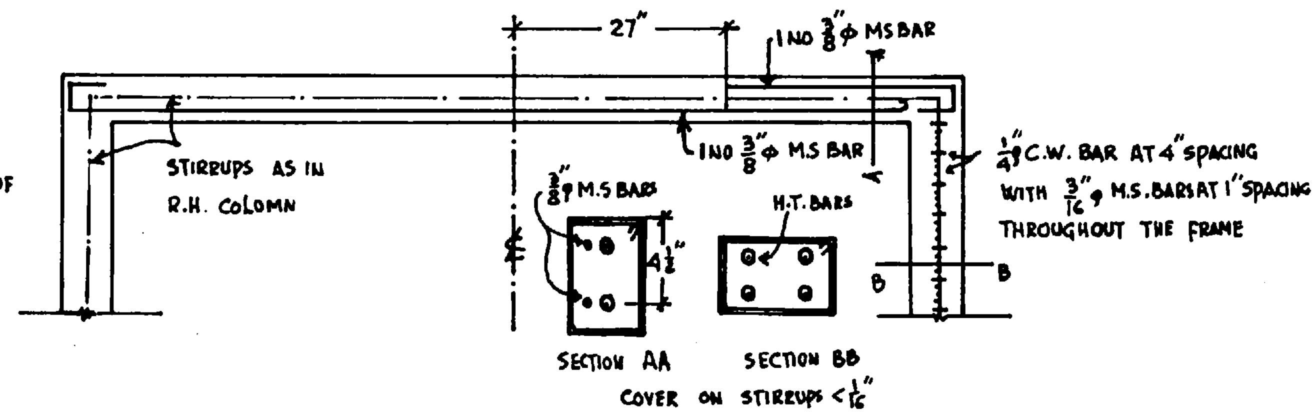

FRAME 3

DETAILS OF STIRRUPS & M.S. BARS

FIG 6.5

SHOWING BINDERS, STIRRUPS & M.S BARS IN FRAMES

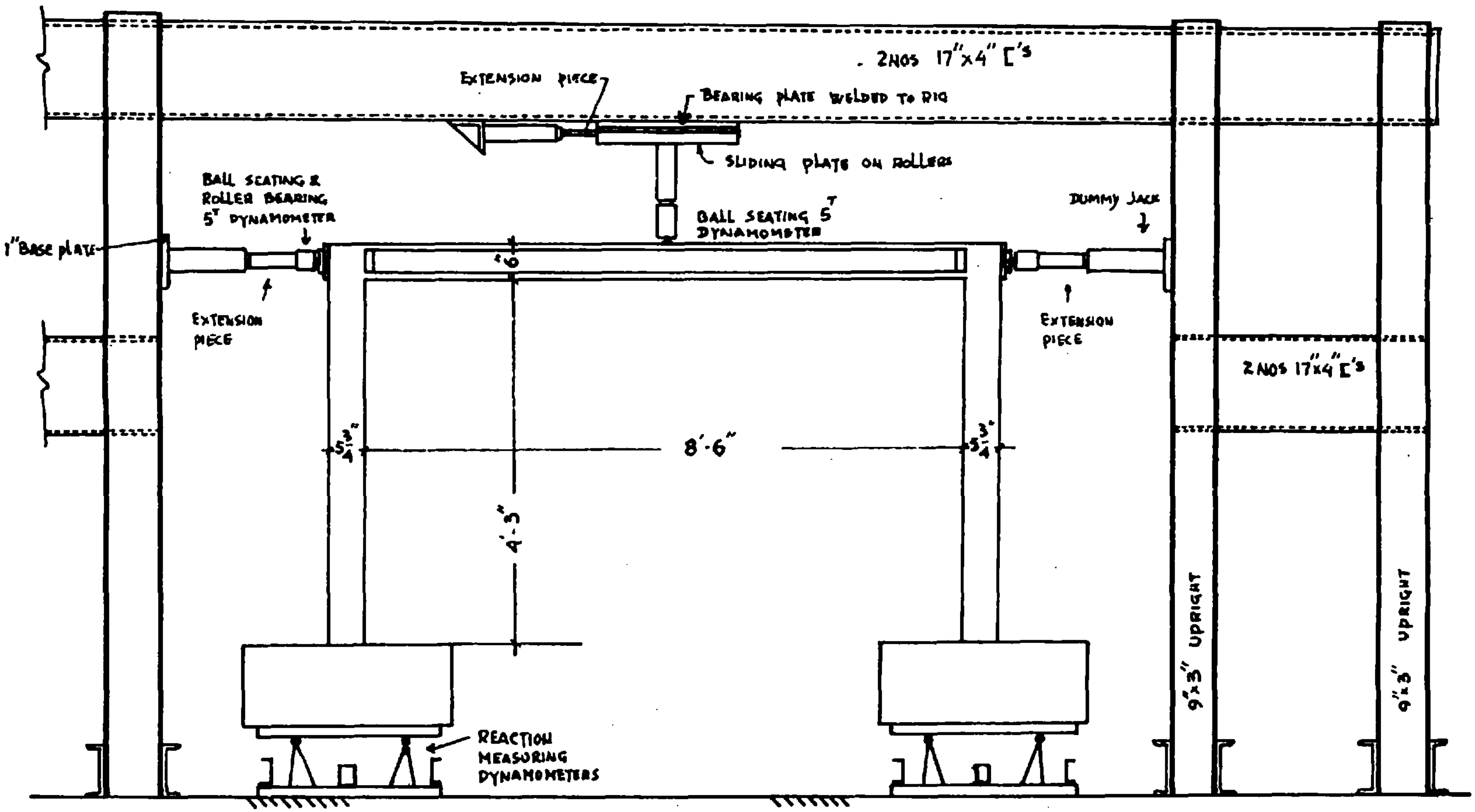

FIG 6.6

SHOWING TEST RIG - GENERAL DETAILS

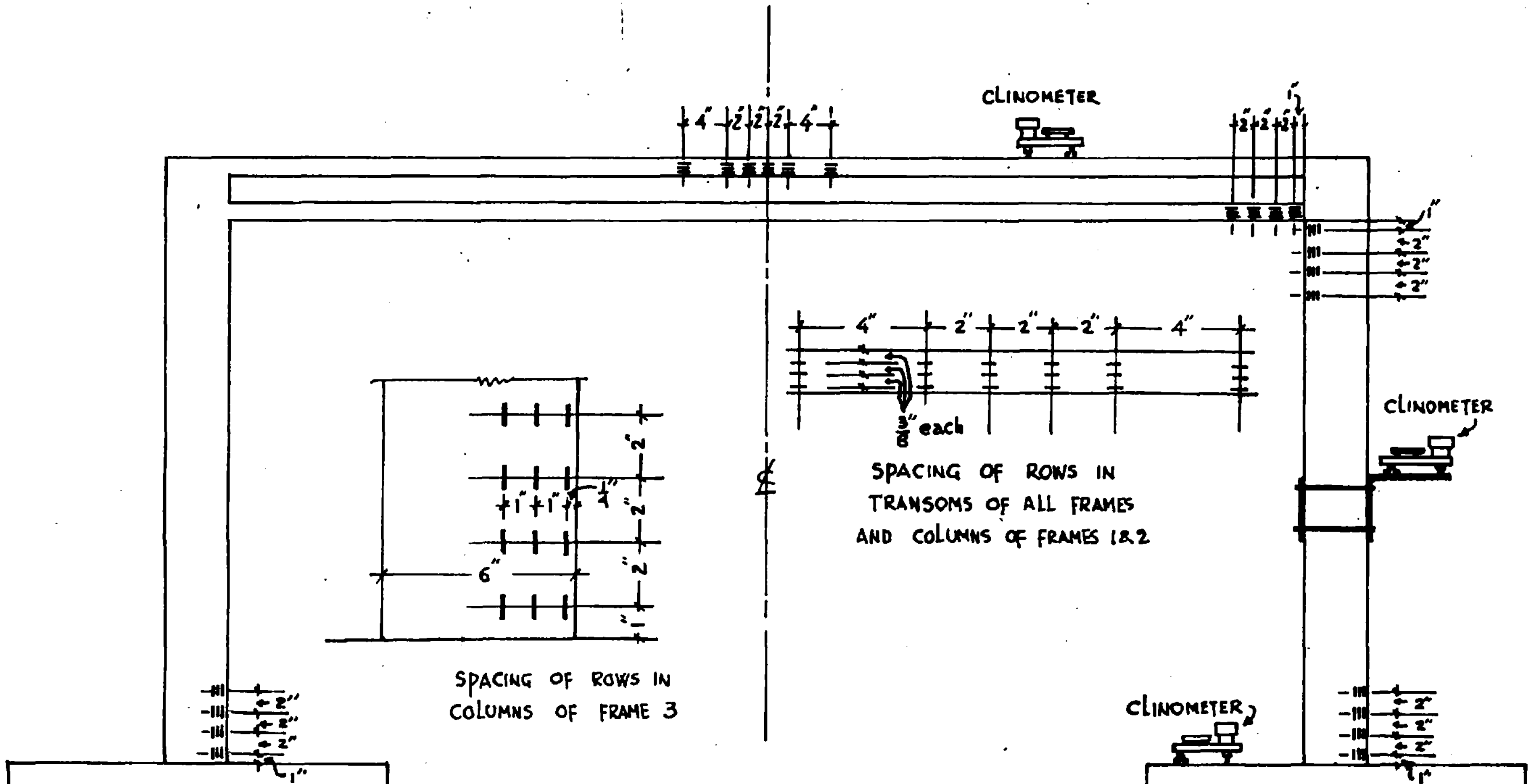

FIG 6.7

SHOWING POSITIONS OF STRAIN GAUGES (ELECTRICAL) CLINOMETERS & LAYOUT OF REACTION DYNAMOMETERS.

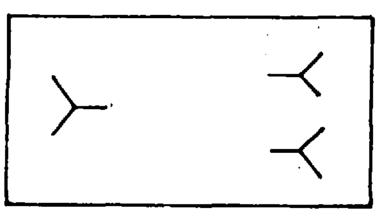

LAYOUT OF TRIPODS IN THE REACTION MEASURING DYNAMOMETER UNDER EACH PEDESTAL

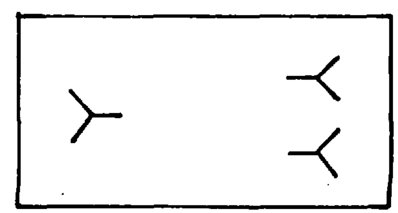

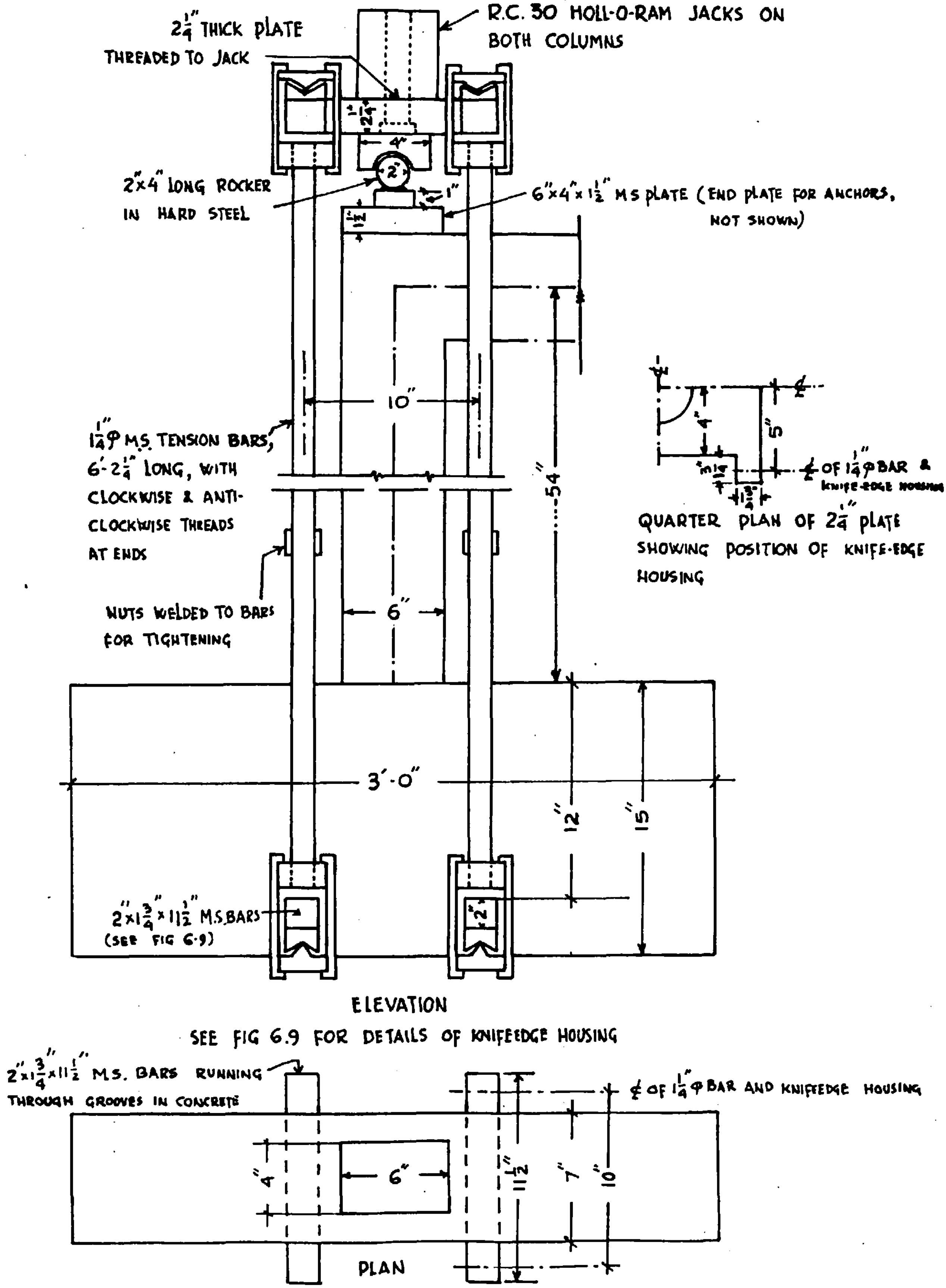

FIG 6.8

SHOWING DEVICE FOR APPLYING AXIAL LOAD

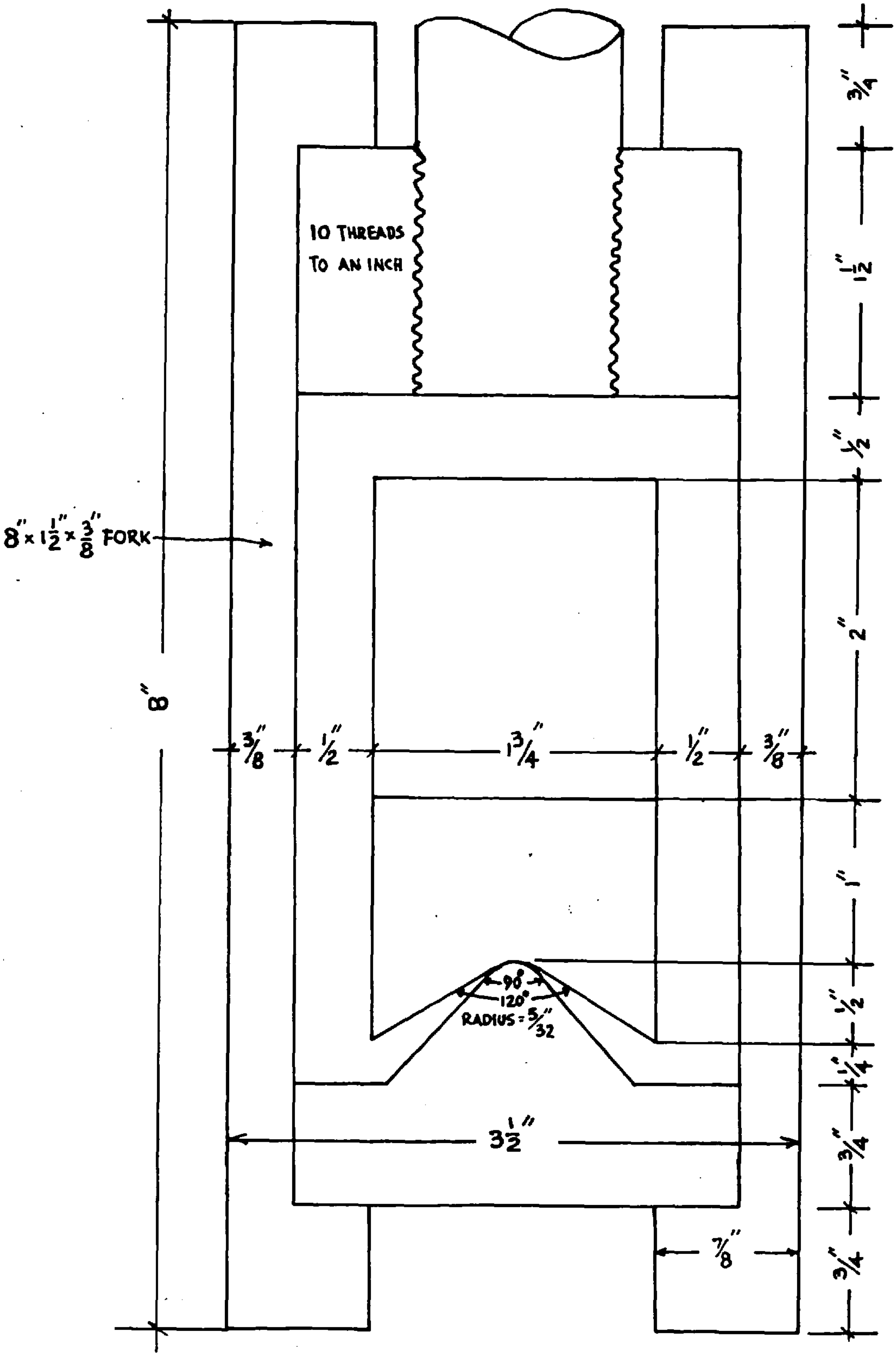

NOTE - KNIFE EDGES ARE IN KE 672 ALLOY

FIG 6.9

SHOWING DETAILS OF KNIFEEDGE HOUSING

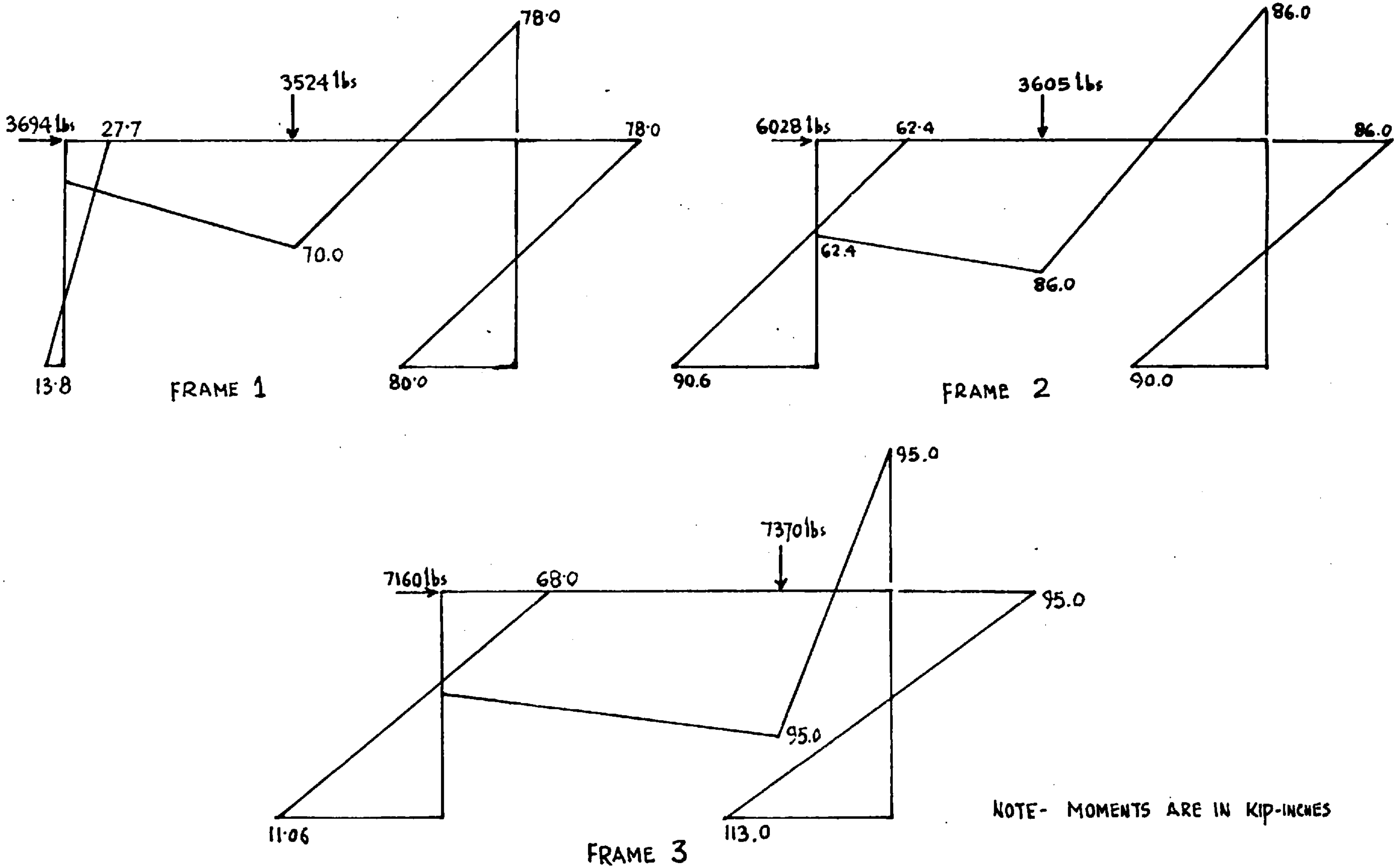

FIG 6.10

DISTRIBUTION OF MOMENTS AT FAILURE

NOTE- IN FRAME 3 THE DISTRIBUTION IS WHEN W_V & W_H ARE MAX.

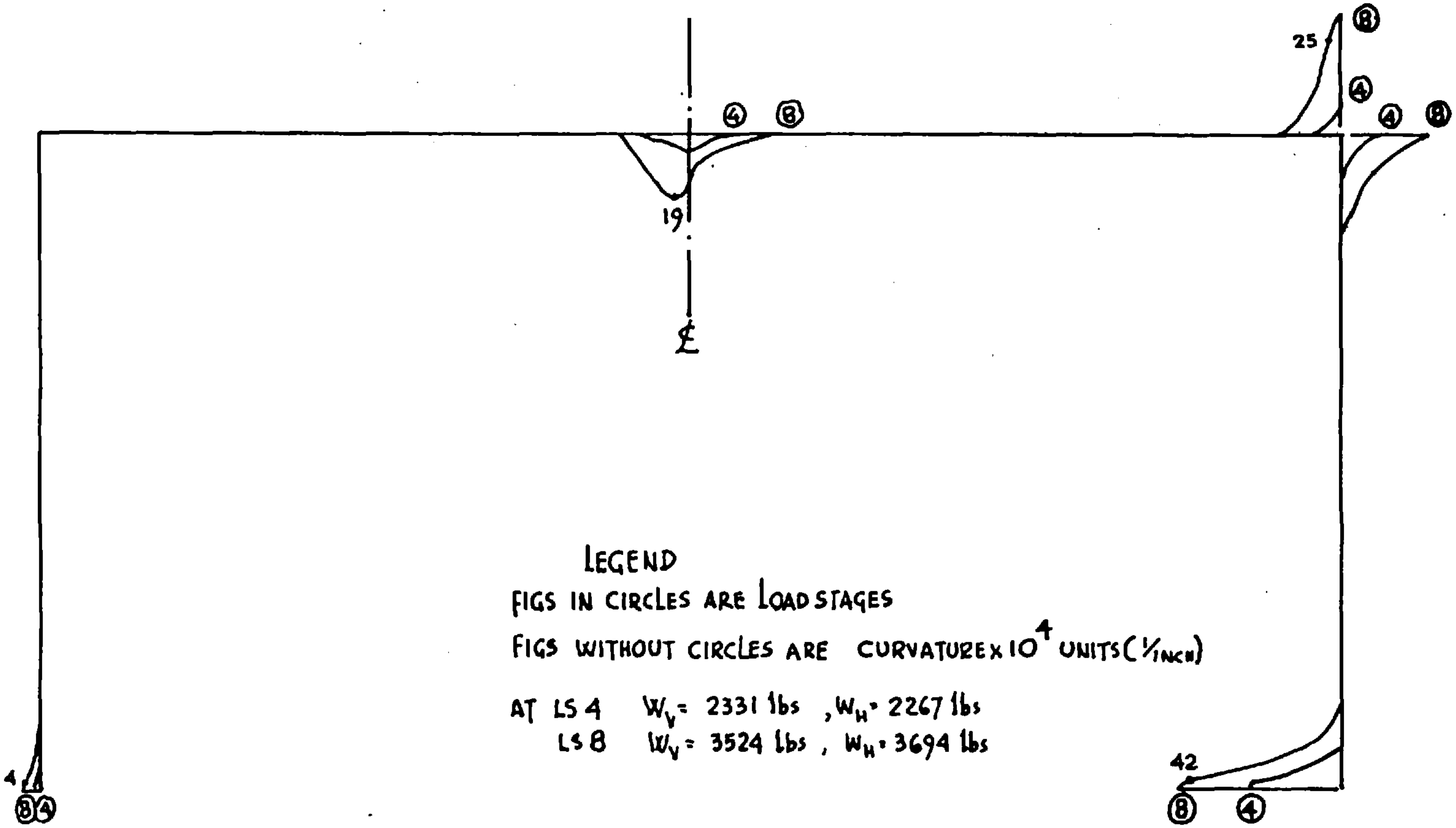

FIG 6.11.

DISTRIBUTION OF CURVATURE IN FRAME 1

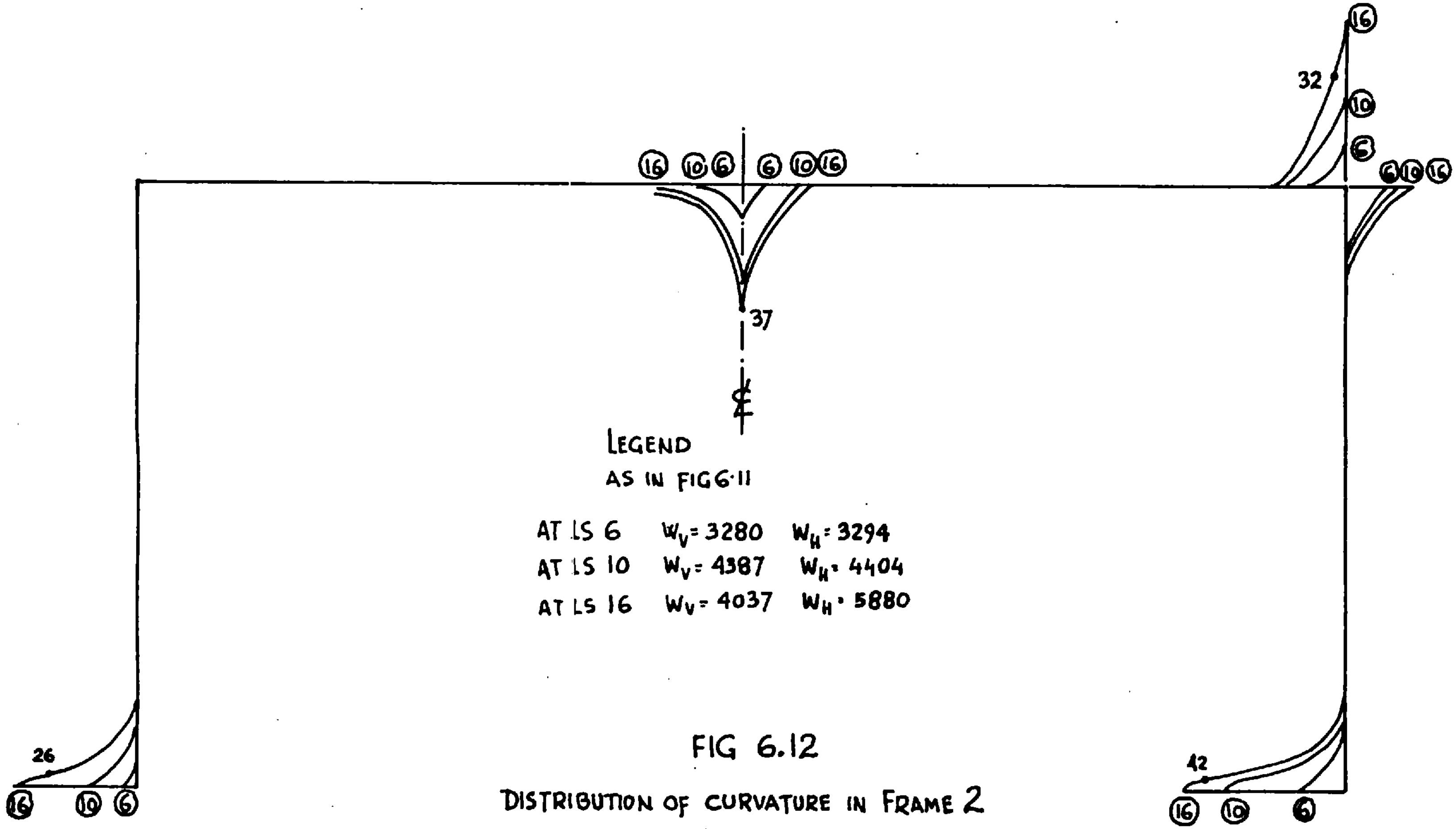

LEGEND
AS IN FIG 6·11

AT LS 6 W_V = 3280 W_H = 3294
AT LS 10 W_V = 4387 W_H = 4404
AT LS 16 W_V = 4037 W_H = 5880

FIG 6.12

DISTRIBUTION OF CURVATURE IN FRAME 2

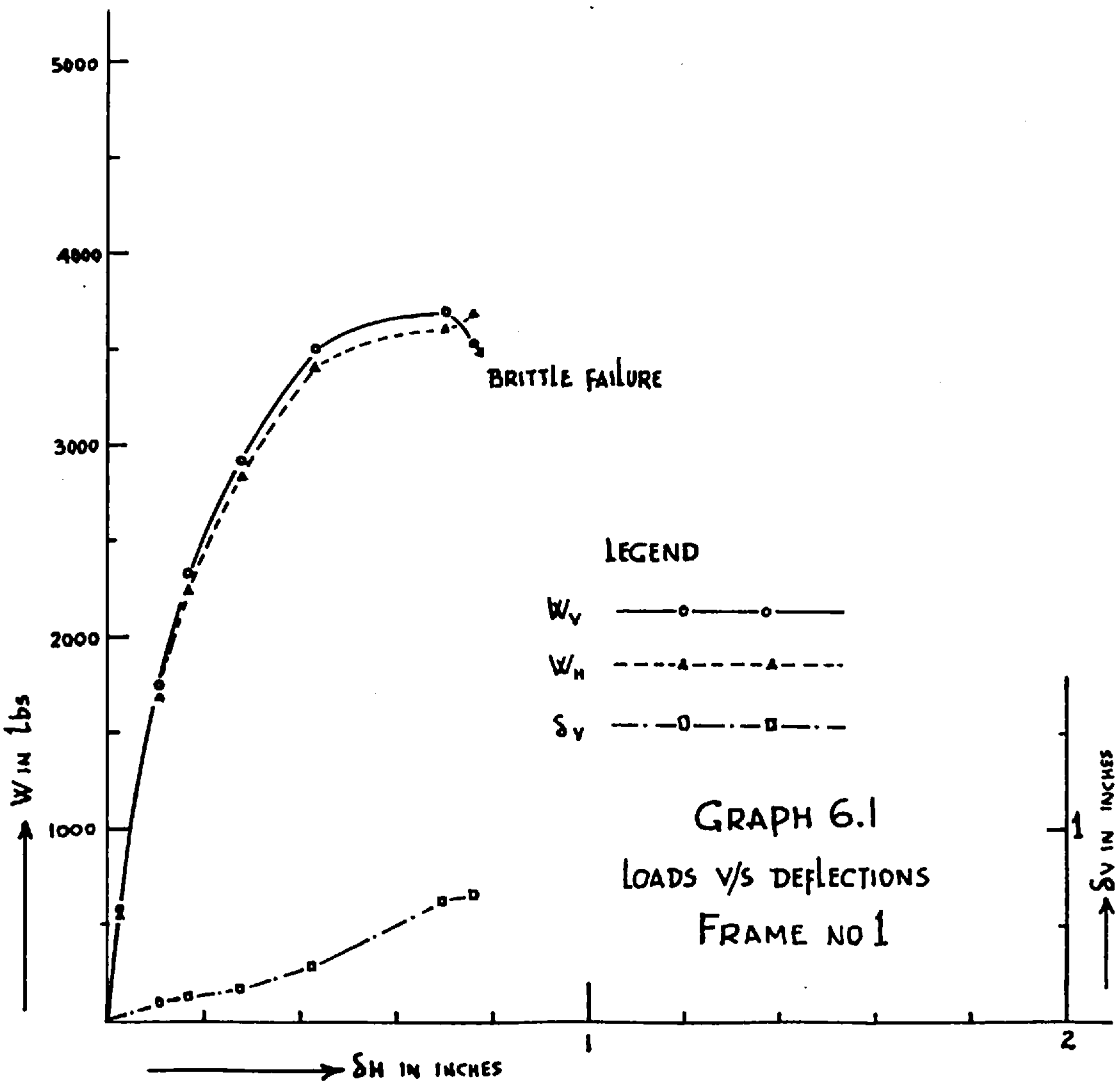

GRAPH 6.1
LOADS V/S DEFLECTIONS
FRAME NO 1

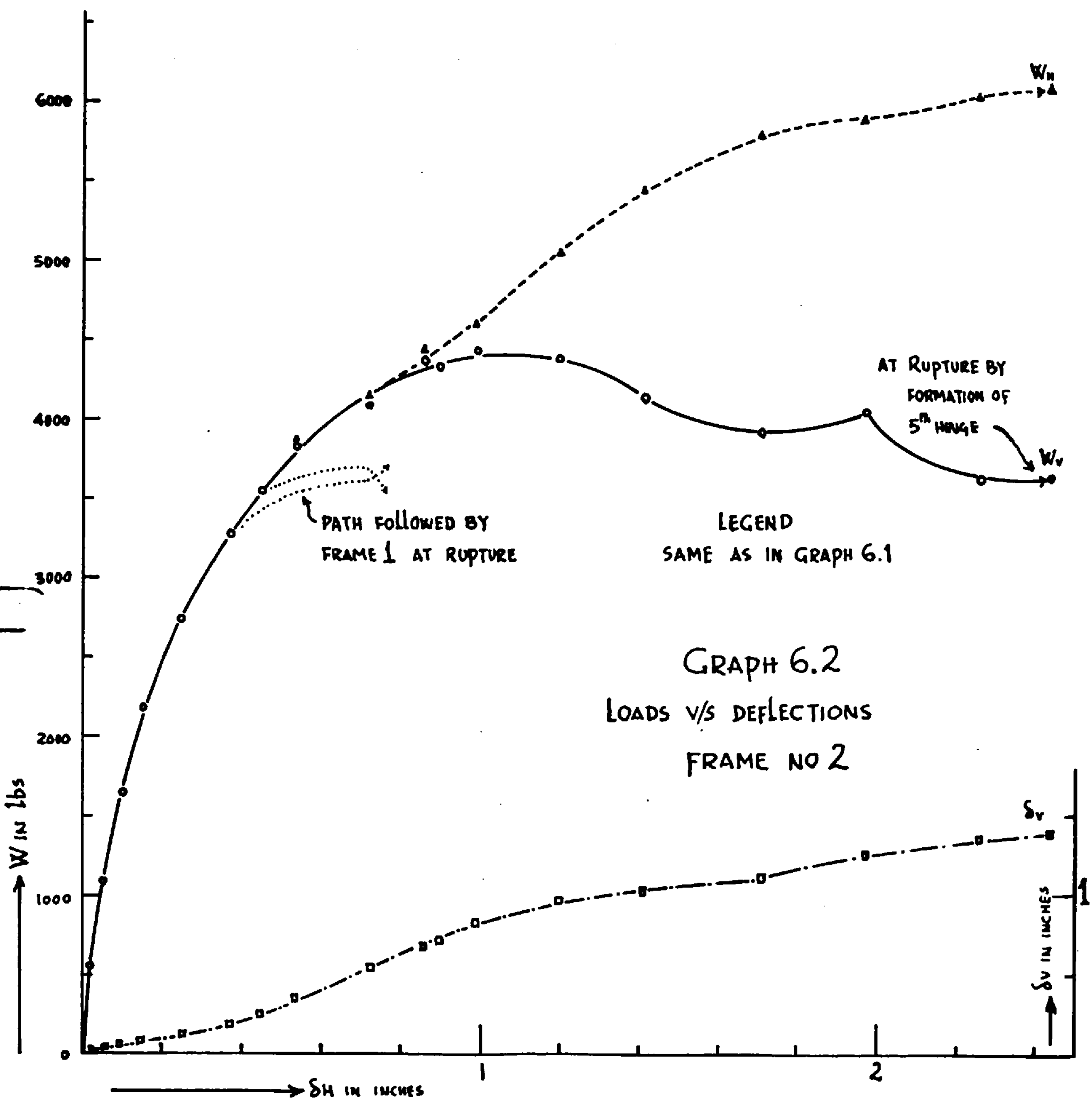

GRAPH 6.2
LOADS V/S DEFLECTIONS
FRAME NO 2

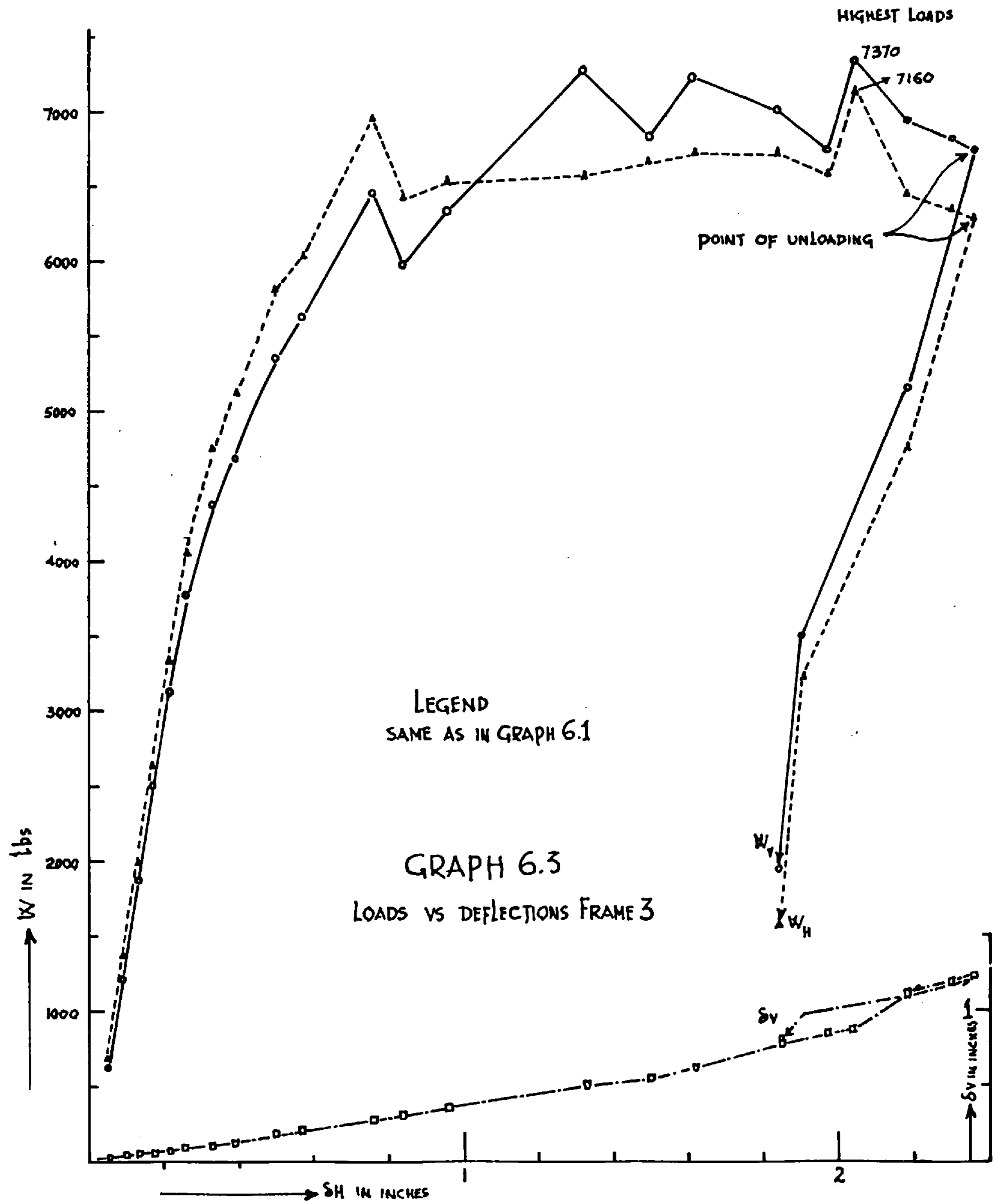

GRAPH 6.3
LOADS VS DEFLECTIONS FRAME 3

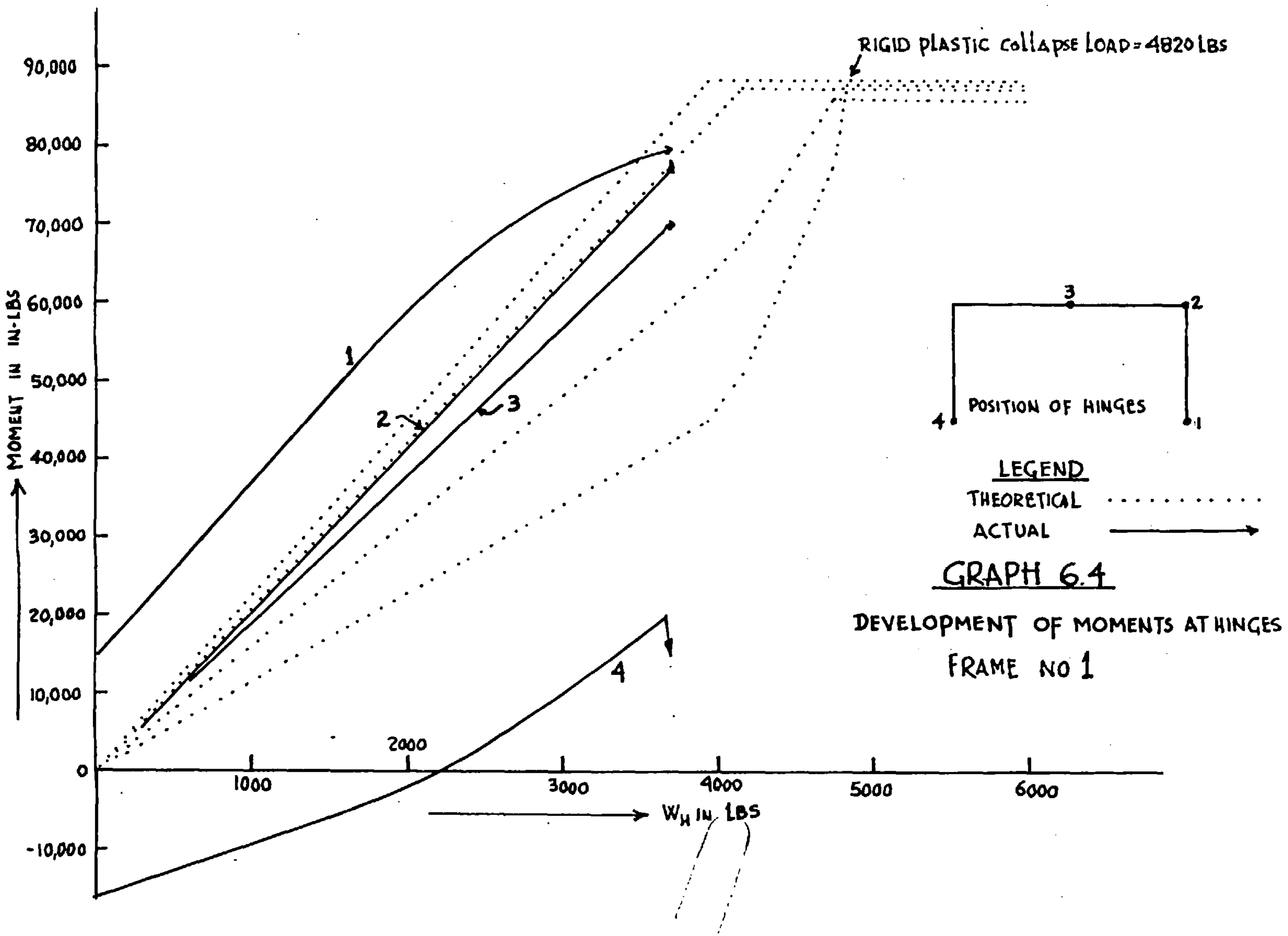

GRAPH 6.4

DEVELOPMENT OF MOMENTS AT HINGES

FRAME NO 1

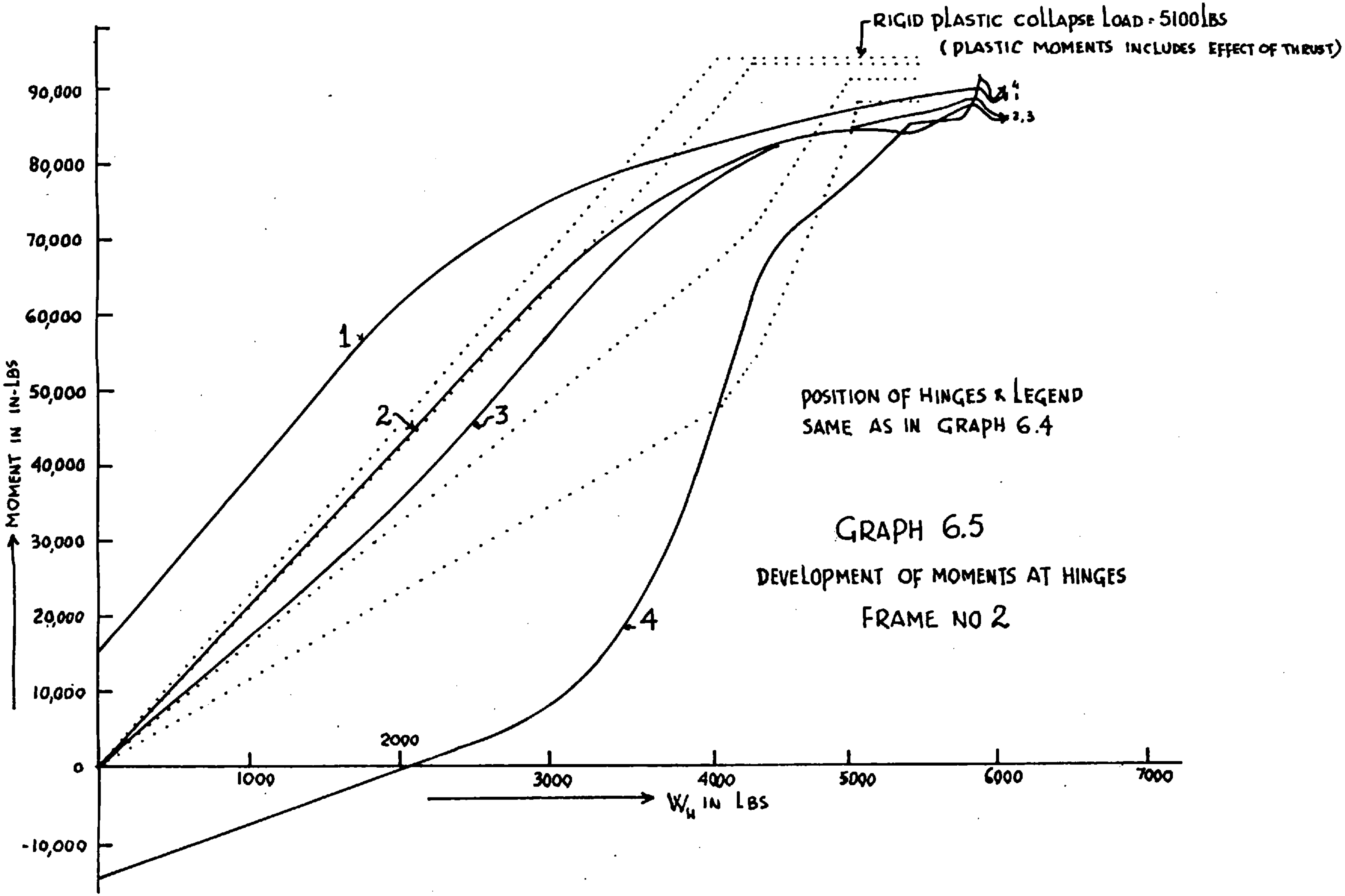

GRAPH 6.5

DEVELOPMENT OF MOMENTS AT HINGES

FRAME NO 2

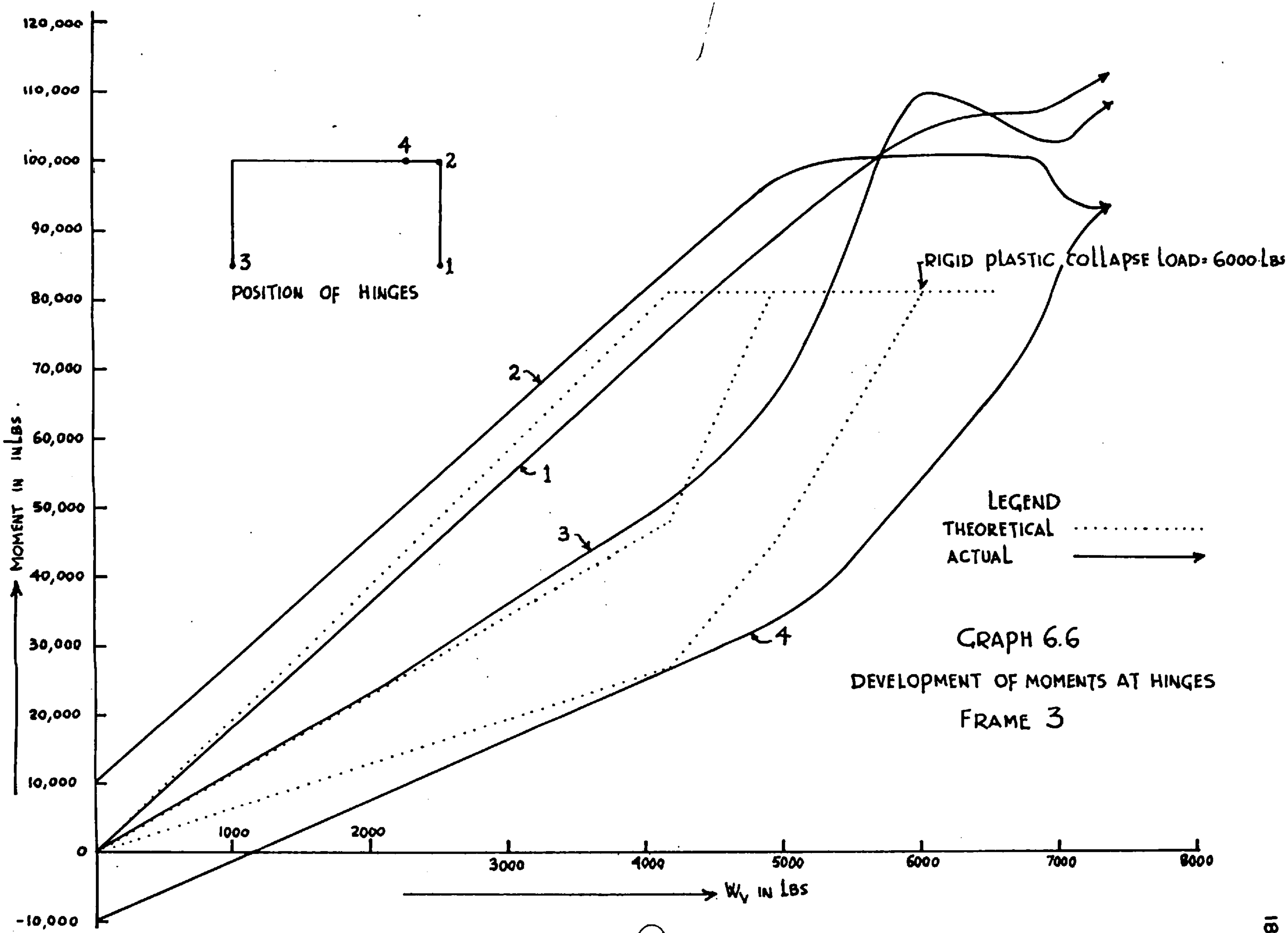

GRAPH 6.6
DEVELOPMENT OF MOMENTS AT HINGES
FRAME 3

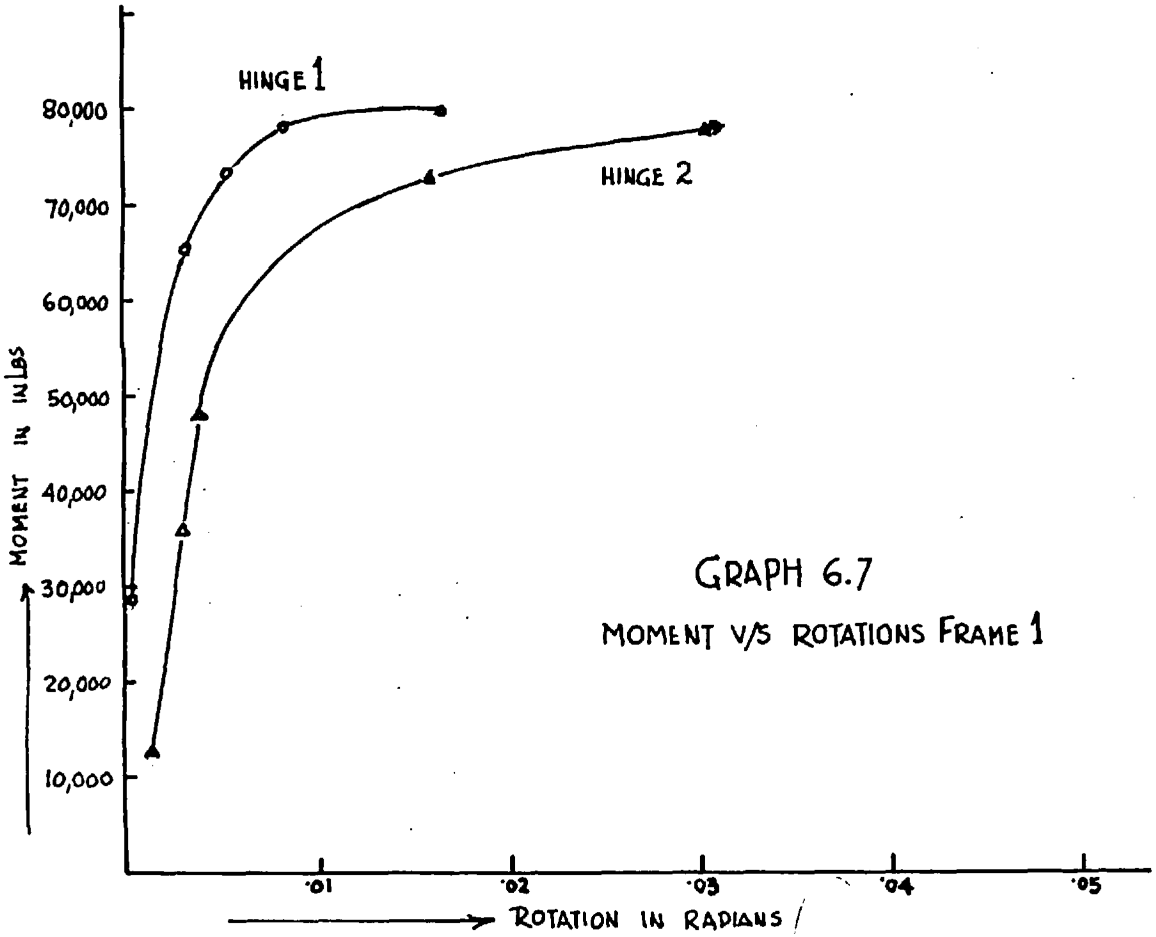

GRAPH 6.7

MOMENT V/S ROTATIONS FRAME 1

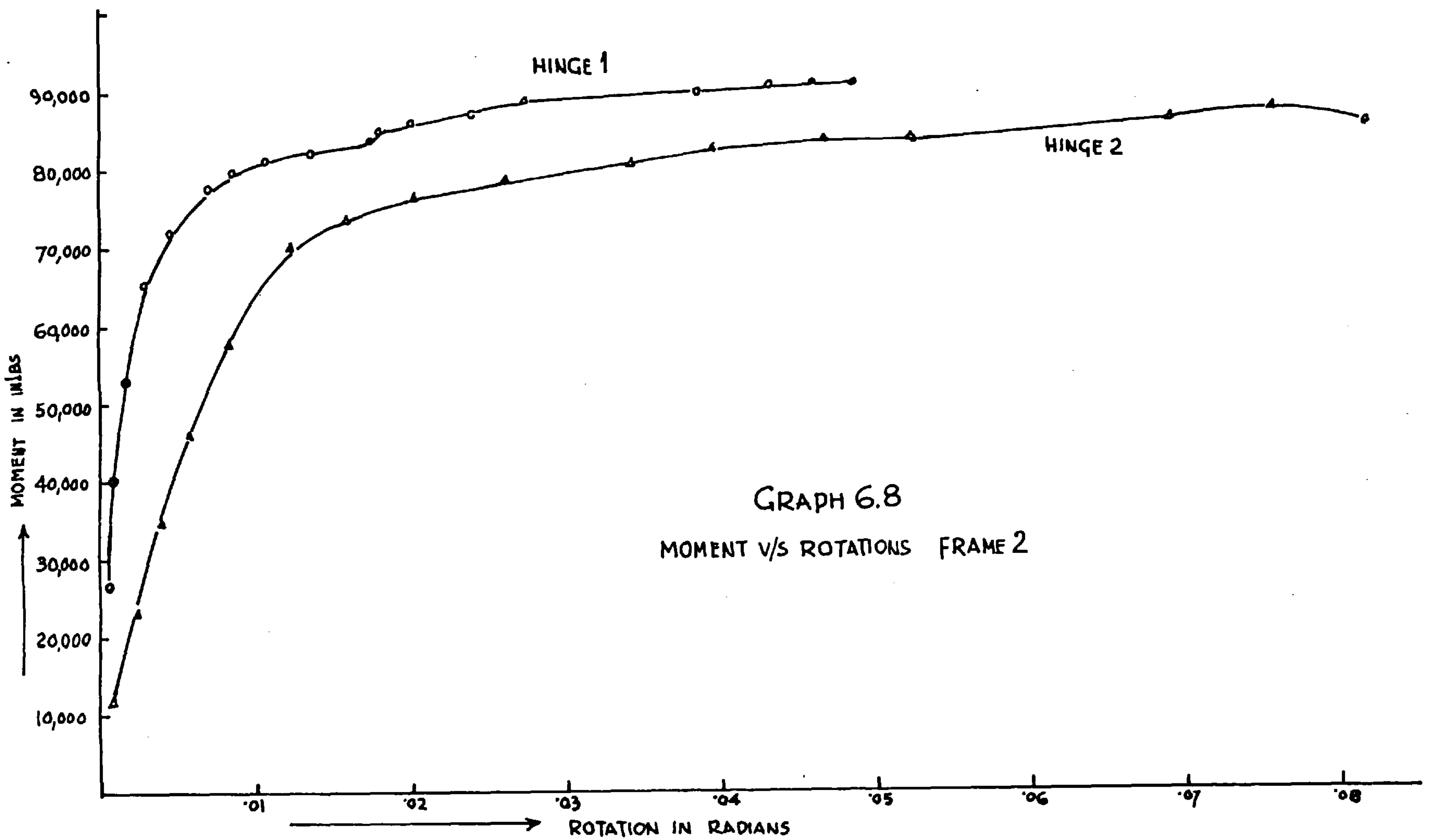

HINGE 1
HINGE 2
90,000
80,000
70,000
60,000
50,000
40,000
30,000
20,000
10,000
MOMENT IN IN.LBS
·01
·02
·03
·04
·05
·06
·07
·08
ROTATION IN RADIANS
GRAPH 6.8
MOMENT V/S ROTATIONS FRAME 2

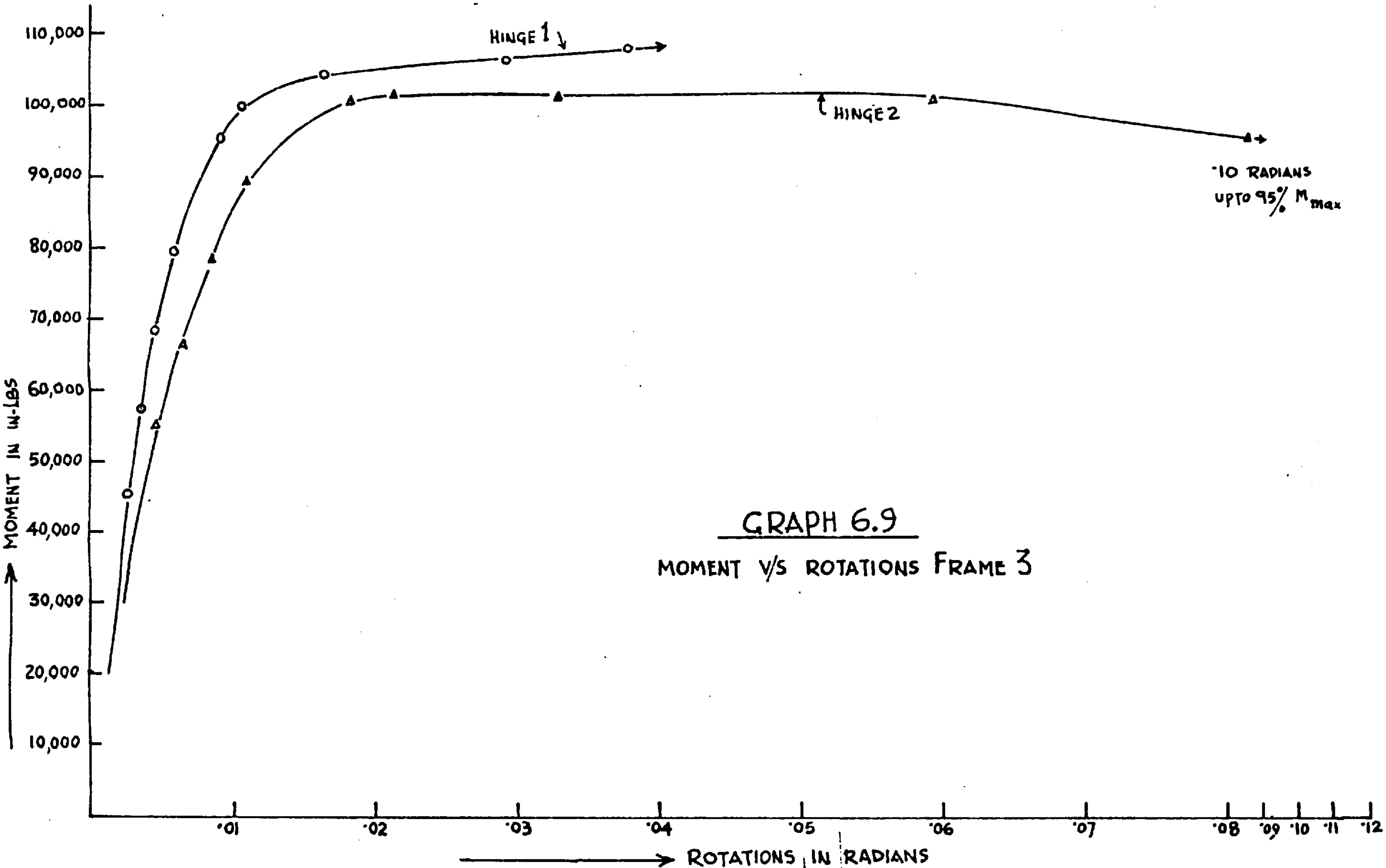

GRAPH 6.9

MOMENT V/S ROTATIONS FRAME 3

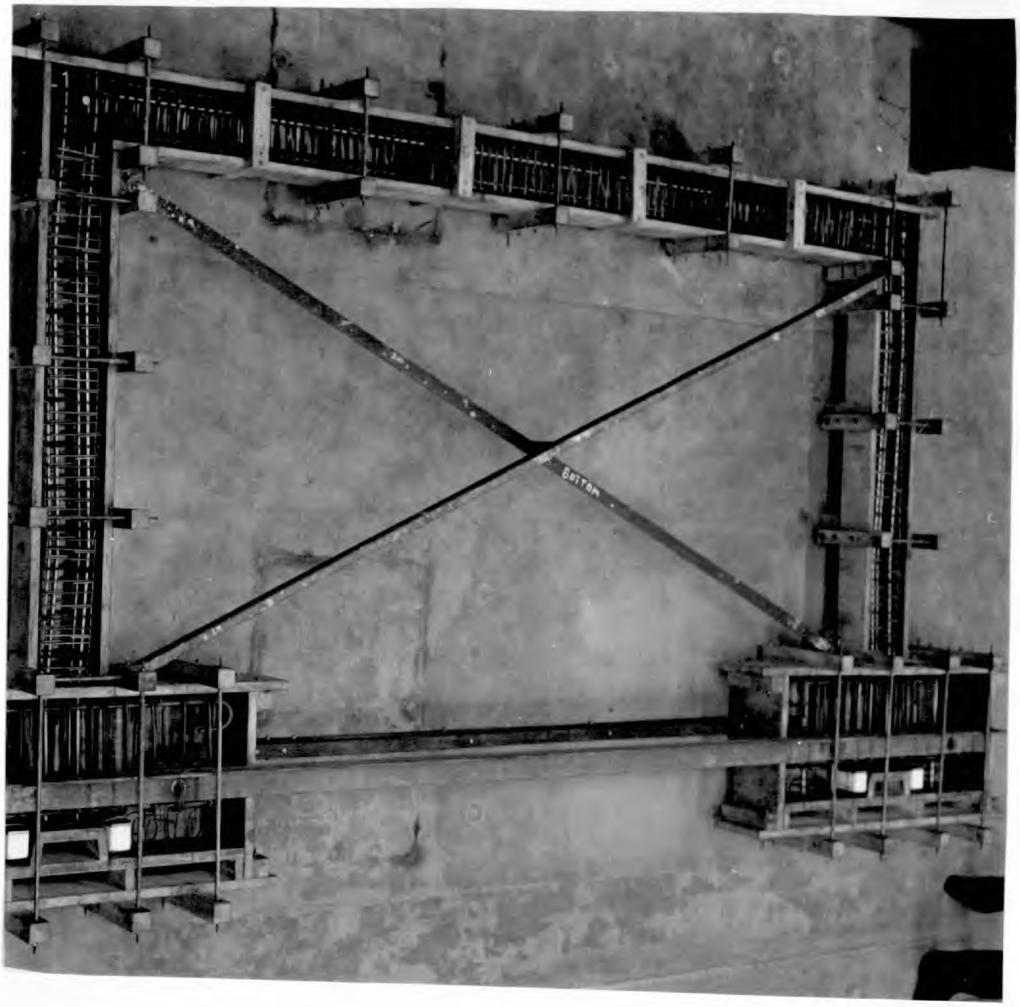

Plate 6.1 Formwork for Frame no 3

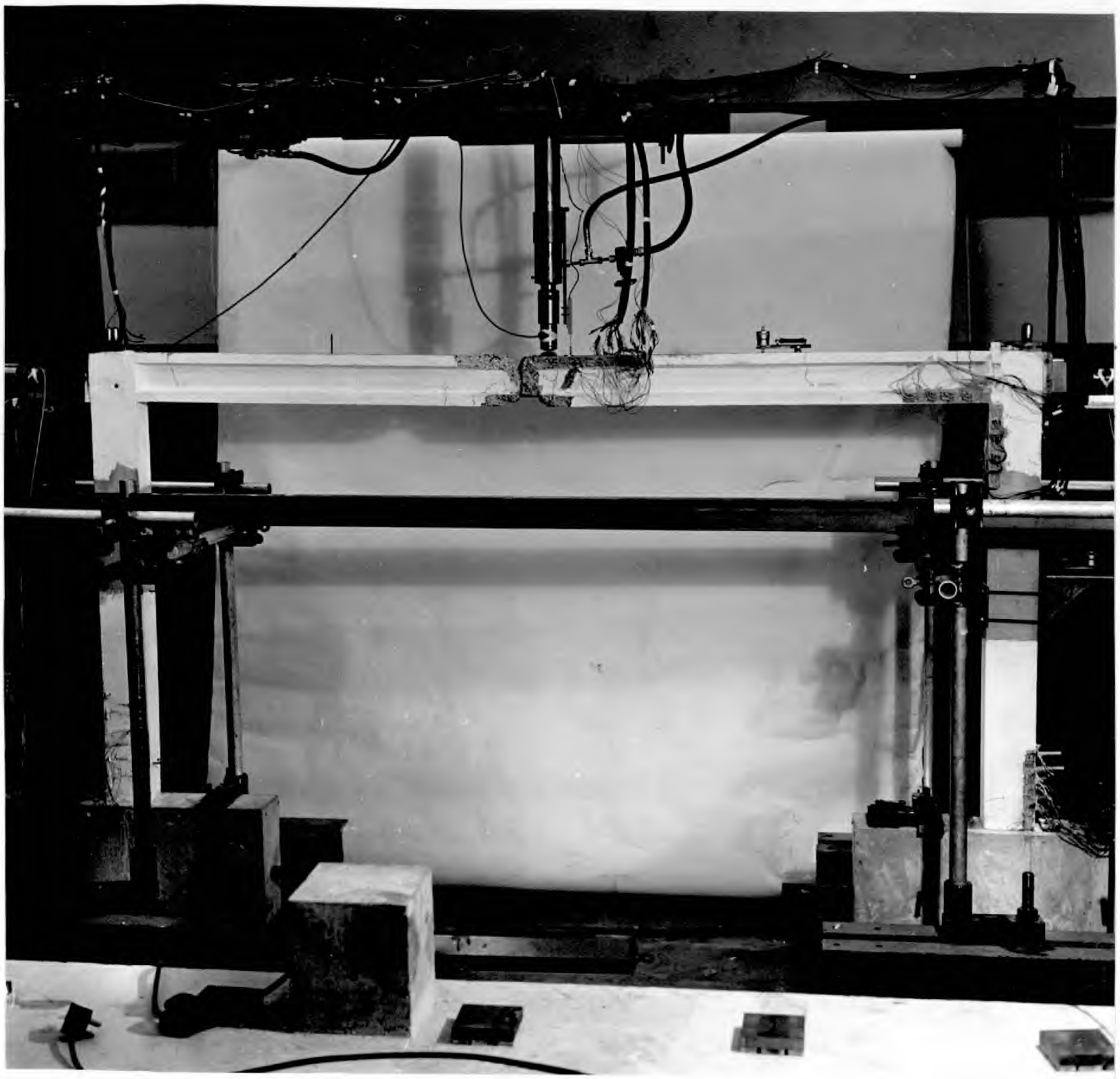

Plate 6.2 General veiw of Frame no. 1 after test

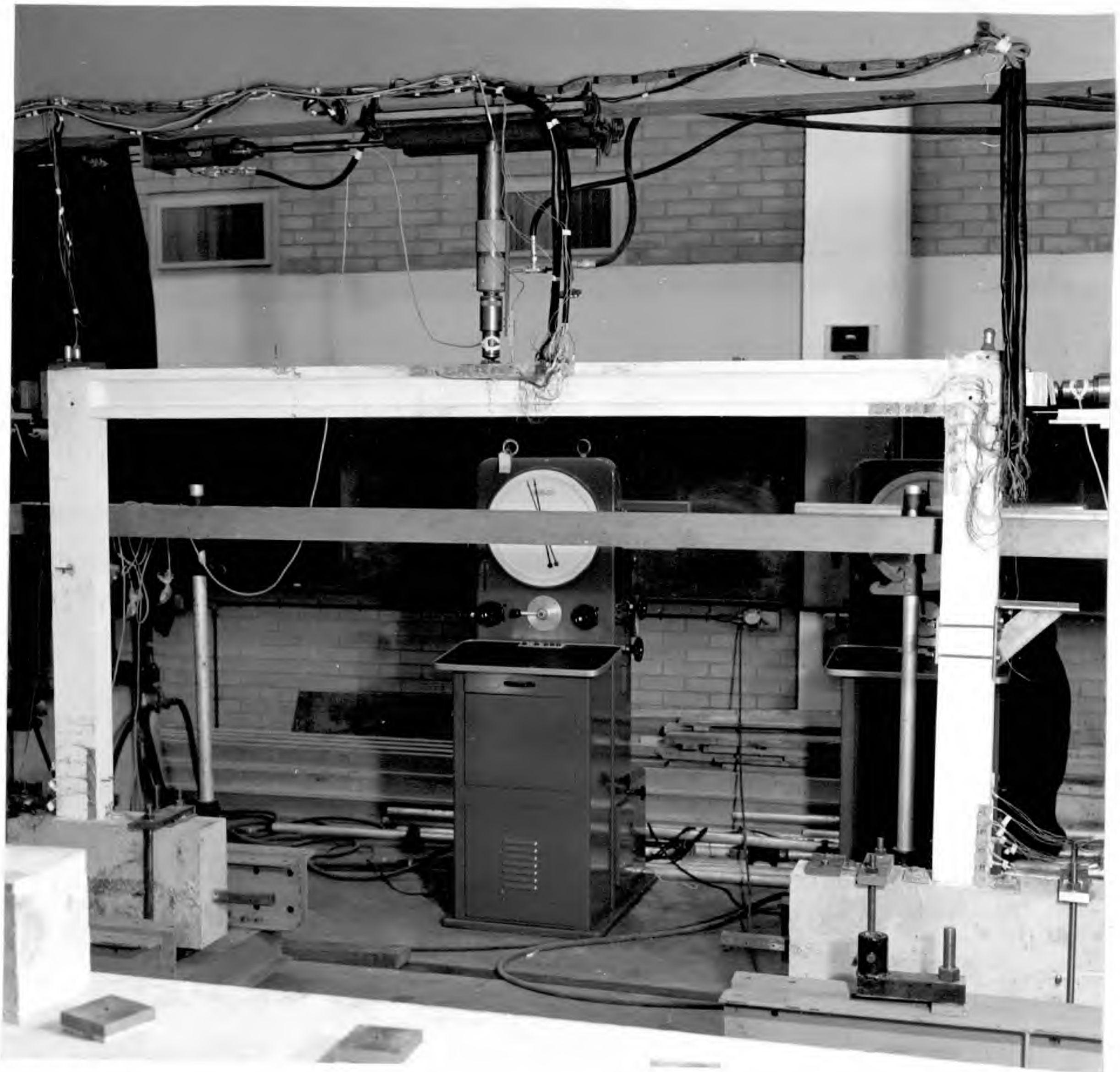

Plate 6.3 General veiw of Frame no. 2 after test

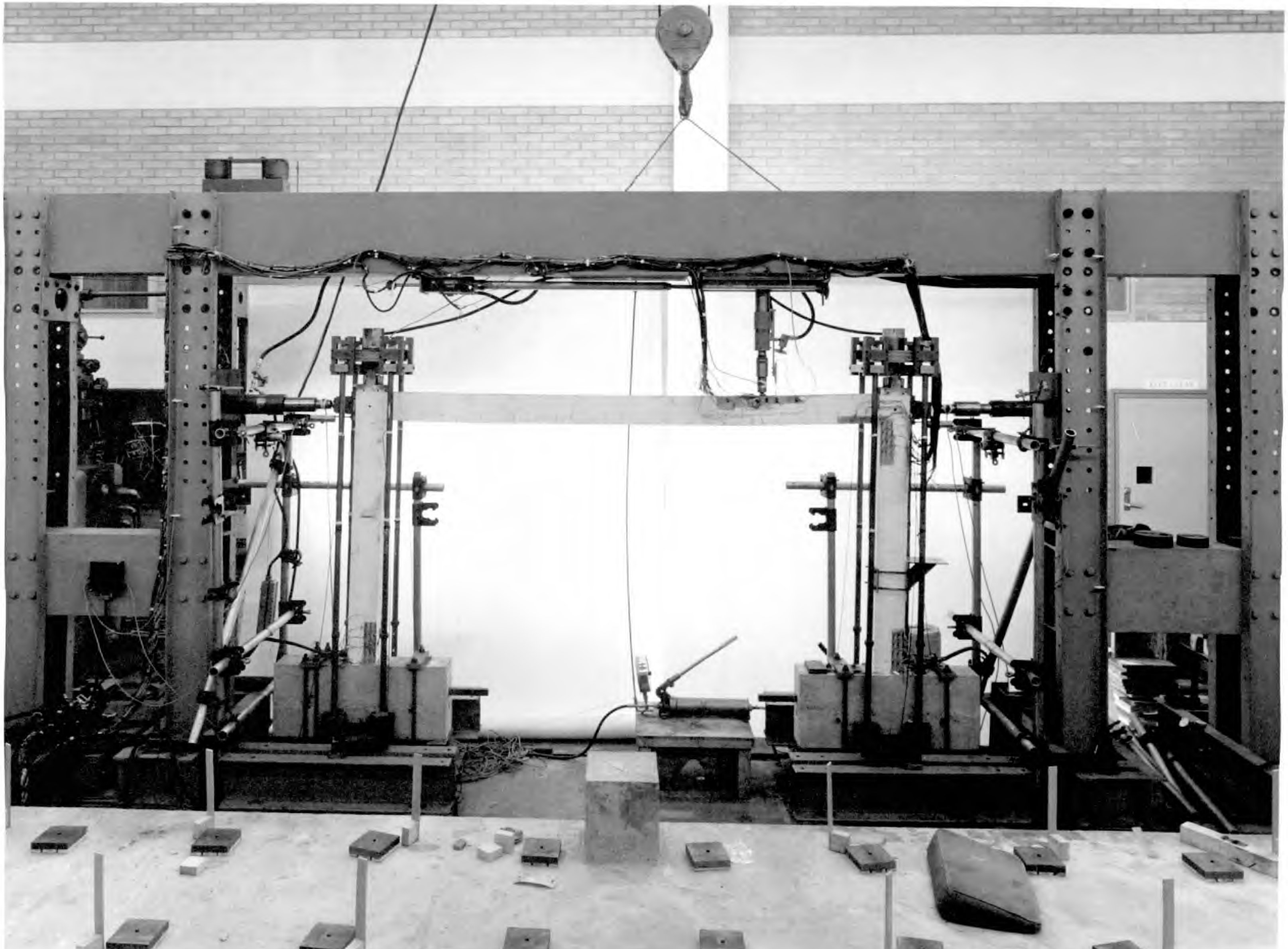

Plate 6.4 General veiw of Frame no. 3 after test

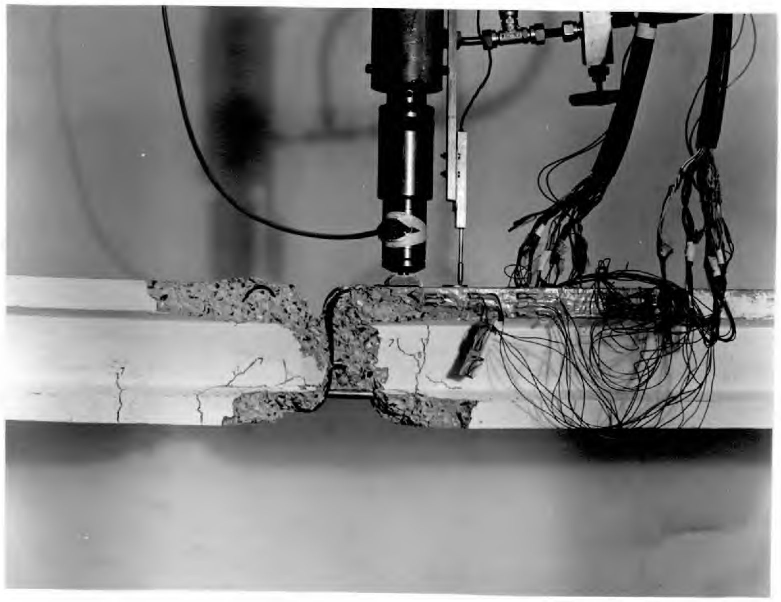

Transom hinge after collapse in Frame no. 1

Plate 6.5

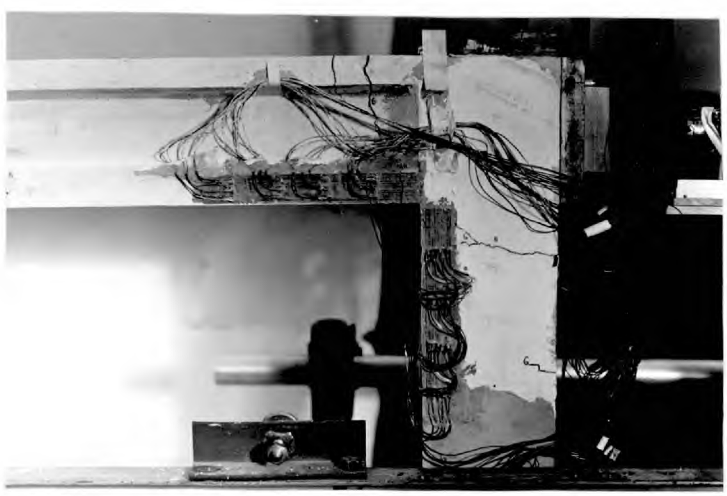

Hinge at the right hand corner of Frame no. 1

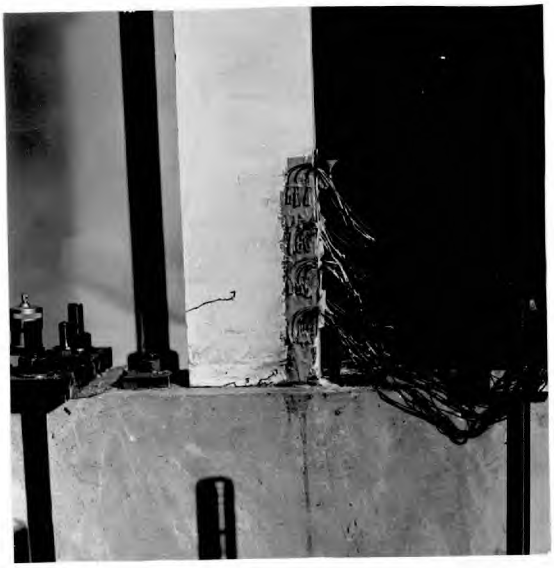

Hinge at the bottom of right hand column of Frame 1

Plate 6.6

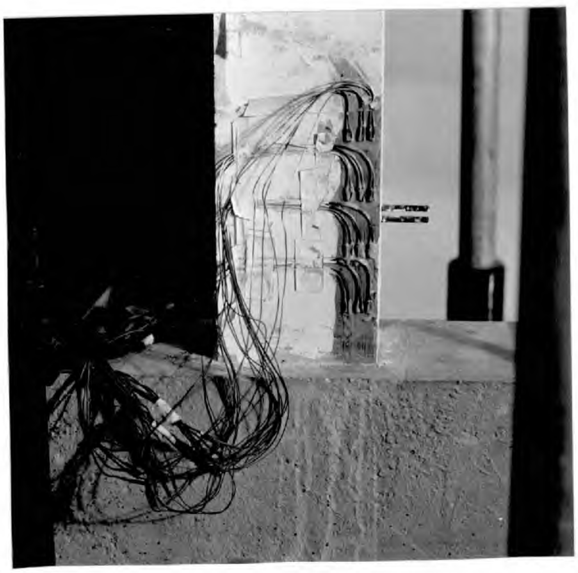

Showing foot of the left hand column of Frame 1

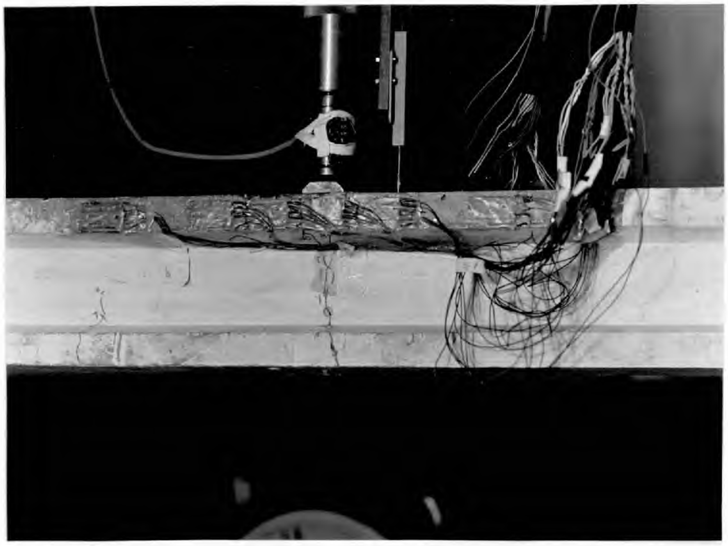

Transom hinge in Frame no. 2

Plate 6.7

Hinge at the right hand corner of Frame 2

Hinge at the bottom of right hand column of Frame 2

Plate 6.8

Hinge at the bottom of left hand column of Frame 2

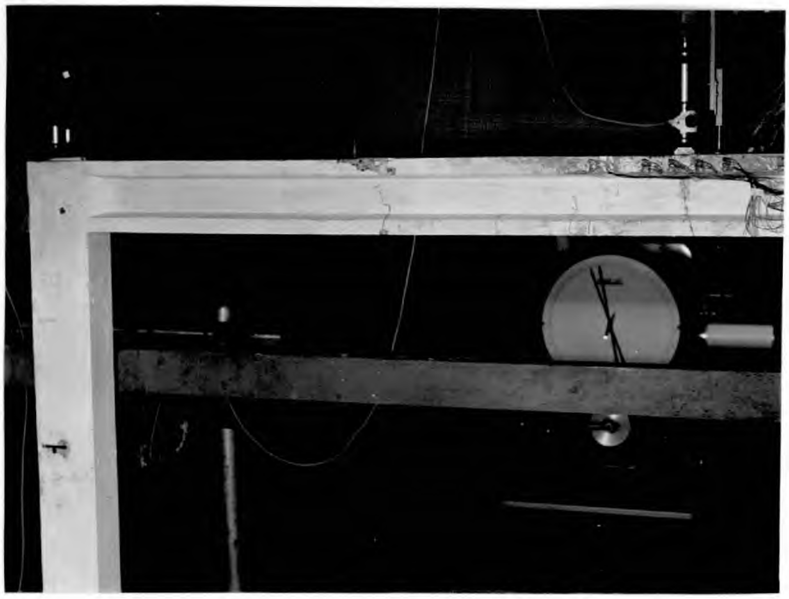

Fifth hinge in the transom of Frame 2

Plate 6.9

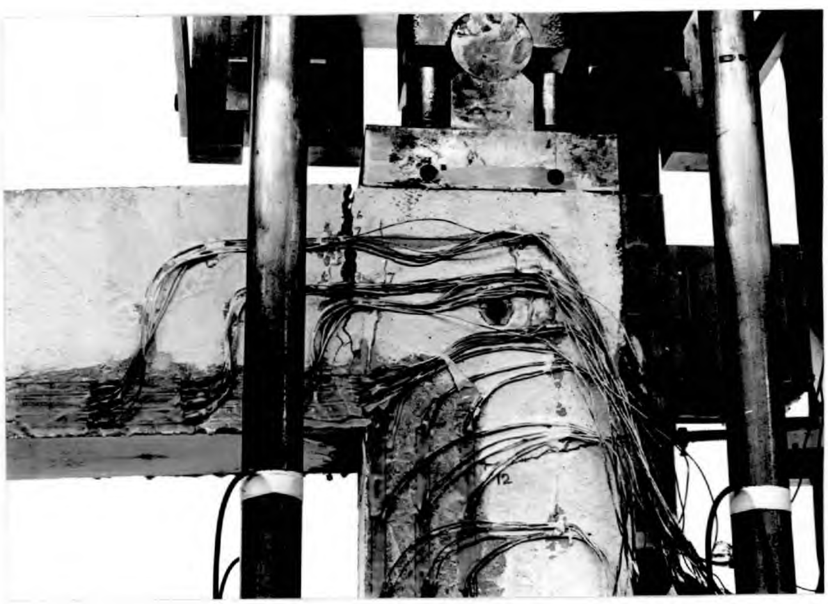

Hinge at the right hand corner of Frame 3

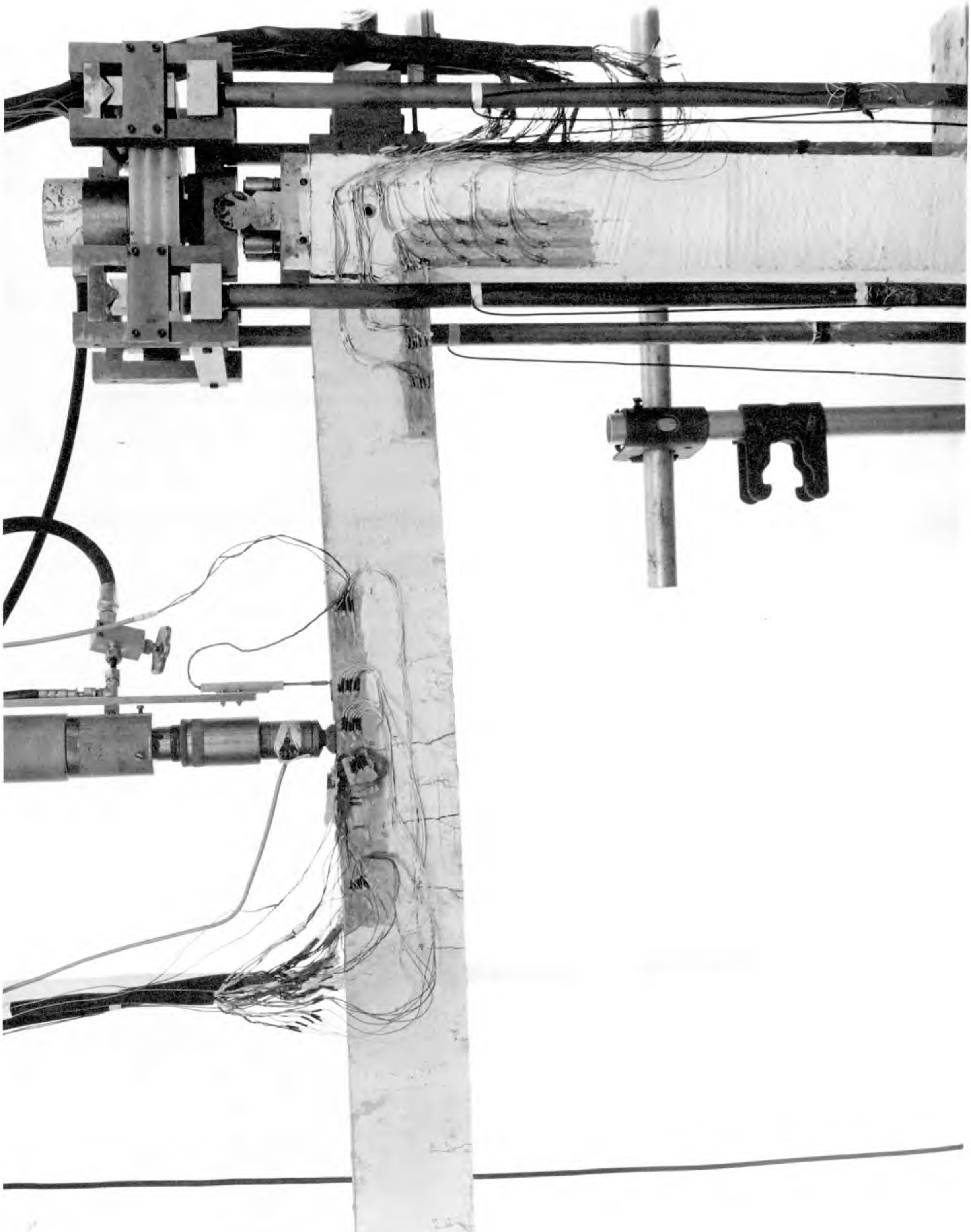

Plate 6.10 showing hinges in the transom of Frame 3 & details of axial loading device

Hinge at the bottom of left hand column of Frame 3

Plate 6.11

Hinge at the bottom of right hand column of Frame 3

CHAPTER 7.

THE COMPATIBILITY PROBLEM IN THE SIMPLIFIED LIMIT METHOD OF DESIGN - A METHOD SUGGESTED TO ADJUST ROTATIONS.

7.1 Baker's approach.

Baker's approach to the compatibility problem in a multistoreyed concrete frame, is summarized below. The design procedure is carried out on an idealised frame, the members of which are assumed to be elastic between the hinges. Inelastic rotations are assumed to be concentrated at hinges.(5) The steps of the procedure are as under.

1) A release system is chosen with n hinges, to make the structure statically determinate.

2) Plastic moment values are then chosen according to rules recommended in the concrete series design booklet by Tokarski and Poologasundranayagam,(42) to obtain an economic distribution of bending moment. It is ensured that the chosen bending moment distribution is in equilibrium with the factorised loads.

3) The rotations at the n hinges are then calculated with the help of graphs published in the above booklet. It may be remembered that these grphs can be used only for the particular recommended bending moment distribution. Designers have to draw their own curves, if they wish to improve on the distributions assumed in the published curves.

4) The plastic rotations given by 'θ_{pi}' in equation 1.3, are then adjusted by trial and error to positive values, which are within permissible limits.

5) Finally, an approximate elastic solution is obtained by adjusting the rotations to zero, to check on the serviceability condition. The bending moment at any critical section under the working load (load factor = 1), under the approximate elastic distribution as found above, must not exceed the yield moment (moment at L_1) of the section, giving rise to a large crack or an excessive deflection.

7.2 Modification suggested by author.

Adjustment of rotations is a tedious step in the above procedure. The author suggests that the inverse of the flexibility matrix of the structure be used, for adjusting rotations and obtaining an approximate elastic solution. The designer will not be required to invert the matrix himself, because the flexibility matrix as well as its inverse, in the case of multi-storeyed buildings, belong to a family of standard patterns. Tables pertaining to different types of buildings likely to be met in a design office, can be kept ready for use. The potentialities of these tables are discussed below.

7.3 Use of tables made from the inverse of the Flexibility matrix.

The following are the possible use of the above tables:-

1) The designer may use these tables as a powerful tool by means of which he can choose and adjust the rotation at any hinge, without affecting the rotations at other hinges. In fact all the objectionable rotations can be adjusted to permissible values in one single step.

2) The approximate elastic solution may be found in one single step by adjusting all hinge rotations to zero.

7.4 Details of the method suggested by the author.

The proposed method is based on the following equation:-

$$FX = -U^{(36)} \quad \ldots\ldots\ldots\ldots\ldots\ldots \quad 7.1$$

which when expanded, gives

$$\begin{pmatrix} f_{11} & f_{12} & f_{13} & \ldots f_{1n} \\ f_{21} & f_{22} & f_{23} & \ldots f_{2n} \\ \cdot & & & \\ \cdot & & & \\ \cdot & & & \\ \cdot & & & \\ f_{n1} & f_{n2} & f_{n3} & \ldots f_{nn} \end{pmatrix} \begin{pmatrix} X_1 \\ X_2 \\ \cdot \\ \cdot \\ \cdot \\ \cdot \\ X_n \end{pmatrix} = - \begin{pmatrix} U_1 \\ U_2 \\ \cdot \\ \cdot \\ \cdot \\ \cdot \\ U_n \end{pmatrix}$$

where F is the flexibility matrix of the structure (made determinate by introducing "n" hinge releases.)

X is the vector representing the unknown moments at the hinge releases.

U is the vector representing discontinuous rotations at the hinges due to external load.

FROM ABOVE

$$\begin{bmatrix} X_1 \\ X_2 \\ \cdot \\ \cdot \\ \cdot \\ X_n \end{bmatrix} = - \begin{bmatrix} p_{11} & p_{12} & \cdots & p_{1n} \\ p_{21} & p_{22} & \cdots & p_{2n} \\ \cdot & & & \\ \cdot & & & \\ \cdot & & & \\ p_{n1} & p_{n2} & \cdots & p_{nn} \end{bmatrix} \begin{Bmatrix} U_1 \\ U_2 \\ \\ \\ \\ U_n \end{Bmatrix}$$

$$\text{or} \quad X = -PU \quad \ldots\ldots\ldots\ldots\ldots\ldots 7.2$$

where $P = F^{-1}$

The above equation gives a set of values of 'X', (in this particular case a set of moments at hinge releases), which nullify the discontinuities at the releases given by the vector $\left\{ U_1 \ldots\ldots U_n \right\}$. In other words the values of 'X' thus obtained is the elastic distribution of moments.

Baker's method allows certain discontinuities at the release hinges which have to be adjusted within permissible values. A knowledge of 'X' values which nullify a unit rotation at each release by turn, will be extremely useful in following his method.

It is immediately seen that if in the vector U, U_1, equals -1, and all the other elements are zero, then the first column of P i.e., $\left\{ p_{11} \; p_{21} \ldots p_{n1} \right\}$ represents a set of 'X' values which cause a unit rotation of positive sign at Release No. 1, in order that U_1 is nullified and continuity is maintained at this release. It follows that the bending moment distribution which will cancel out a rotation of $-\alpha_1$ at release No. 1, is given by the vector:

$$\alpha_1 \left\{ p_{11} \quad p_{21} \ldots\ldots p_{n1} \right\}$$

The redistribution of moments which takes place by nullifying $-\alpha_1$, will not alter rotations at other hinges.

Similarly, the second column of P, represents a set of 'X' values which causes a positive unit rotation at Release No. 2 and so on. The reader can now identify the columns of P, with Macchi's imposed rotation co-efficients[34].

The pattern of the matrix P has been studied by the author by altering the following parameters in a series of multi-storeyed frames. All bays have been assumed to be of equal length, and each of the bays is complete.

1) The stiffness of columns and beams, as explained under

Let l_r = length of each bay in r^{th} storey

h_r = height of r^{th} storey

I_r = moment of inertia of beams in r^{th} storey

J_r = - ditto - of columns in r^{th} storey

$$y = \frac{h_r}{J_r} \Big/ \frac{l_r}{I_r} = \frac{h_{r+1}}{J_{r+1}} \Big/ \frac{l_{r+1}}{I_{r+1}} = \frac{Ih}{Jl}$$ (in general in all the storeys.)

$$s = \frac{h_r}{J_r} \Big/ \frac{h_{r+1}}{J_{r+1}} = \frac{l_r}{I_r} \Big/ \frac{l_{r+1}}{I_{r+1}}$$

Values of I and J are the same in all beams and columns in the same storey. Y has the same value in all the storeys. The value of s has been varied between the limits .66 and 1 and the value of y has been varied from 4 to 12

2) The number of bays has been varied from 3 to 5, for a constant number of storeys equal to 3.

3) The number of storeys has been varied from 3 to 5, for a constant number of bays equal to 3.

The results are presented in tables 7.1 to 7.29

The elements of the flexibility matrix were taken from Poolagasoundranayagam's thesis[41].

7.5 The design steps by the modified method.

1) Choose the same release system as in Baker's approach to make the structure statically determinate.

2) Calculate the discontinuous rotations at all hinges due to the applied loads only, acting on the reduced structure, and adjust them to zero with the help of co-efficients in the nearest table appropriate to the particular building under design. The approximate elastic bending moment distribution is thus known.

3) Choose plastic moment values and calculate rotations at the releases as in Baker's approach.

4) Adjust all objectionable rotations in one single step to positive values within permissible limits by using the appropriate table.

7.6. Bilinear idealization of prestressed concrete beams continuous over two spans.

Baker's assumption that the modulus of flexural rigidity, in the cracked stage, is constant between the hinge releases, no longer holds good in case of prestressed concrete members. Linear transformation may cause considerable variation in the effective depth of cables at different critical sections.

The cracked 'EI' value at the state L1, depends to a large extent on the effective depth and consequently varies considerably from one critical section to another. In the next paragraph, the author has suggested that a modified application of Macchi's method of imposed rotations, may be used to analyse a two span prestressed concrete continuous beam.

The distribution of bending moments corresponding to the first phase of a bilinear idealization, when the structure has different 'EI' values at the critical section, has to be found. A method has been suggested in 7.7. The redistributing effect of permissible rotations at the hinges may then be found out by the normal method suggested by Macchi, provided the imposed rotation co-efficients are also calculated for the idealized structure.

7.7. Use of the theory of imposed rotation in calculating the effect of a change in the 'EI' value in a part of a continuous beam.

Consider the elastic solution of a two span continuous beam of constant X-section with two equal point loads at the centre of each span (Fig. 7.1).

Let the EI value increase from EI to E_1I_1 in the length BD, such that $EI = KE_1I_1$ where $K < 1$.

Fig. 7.2 shows the bending moment diagram when a unit rotation is imposed in the indicated direction at C on the beam having a constant EI throughout its length. This diagram is also the influence line of the bending moment at the support, due to a unit rotation traversing the structure [34].

The bending moment at support caused by a unit rotation at the element 'dx', is therefore given by the ordinate 'y'.

As a first approximation, let us assume that this bending moment diagram for a unit rotation imposed at the support, also holds good for the changed structure with different 'EI' values.

The change in the EI value in a small length 'dx' causes a rotation of the magnitude

$$\left(\frac{m}{EI} - \frac{m}{E_1 I_1}\right) dx = \frac{m}{EI}(1-k)\, dx$$

where 'm' is the ordinate corresponding to the length 'dx' in Fig. 7.1.

The corresponding change in the BM at the support

$$= \frac{m}{EI}(1-k) y\, dx$$

The total change in the support moment

$$= \frac{(1-k)}{EI} \int my\, dx$$

in the length 2 BC

$$= \frac{2(1-k)}{EI}$$ (sum of the product of ordinates of diagram BOC and BB'OC in Figs 7.1 and 7.2)

$$= \frac{2(1-k)}{EI} \times \frac{3L}{66} \left(\frac{6}{32}\left(3 + \frac{12}{11}\right)\right) \frac{EI}{L} \cdot wL.$$

$$= .07\,(1-k)wL \quad \ldots\ldots\ldots\ldots\ldots\ldots\ldots\ldots 7.3$$

The change in the support moment found by equation 7.3, is however, approximate, as it neglects the change in the position of the point of contra-flexure. This would have been more correctly evaluated if the correct imposed rotation co-efficients were employed in the above diagram integration.

It is also observed that Fig. 7.2 is a bending moment diagram and it can be corrected to a first degree of approximation by integrating BB'OC with itself. The correction in the imposed rotation co-efficient at the support is therefore:

$$2 \times \frac{(1-k)}{EI} \times \frac{3}{66} L \left[\frac{12}{11}\left(\frac{24}{11}+\frac{3}{2}\right) + \frac{3}{2}\left(3+\frac{12}{11}\right)\right]\left(\frac{EI}{L}\right)^2$$

$$= (1-k)\frac{3}{2} \times .615 \frac{EI}{L} = \frac{3}{2} p \frac{EI}{L} \text{ where } p = .615(1-k)$$

The ordinate of the Fig.7.2 at the support is therefore $\frac{3}{2}(1+p)\frac{EI}{L}$. If this process is repeated, the ordinate is given by the expression

$$\frac{3}{2}\frac{EI}{L}(1 + p + p^2 + p^3 + \ldots\ldots)$$

using this in equation 7.3, we get the change in bending moment as

$$.07\ (1-k)(1 + p + p^2 + p^3 \ldots\ldots)WL \ldots\ldots 7.4$$

$$= \ .07\left[(1-k)/(1-p)\right]WL \text{ as } p < 1$$

If the EI value increases in the region AB from EI to E_1I_1, instead of in the region BC, the change in the moment at support, is given by

$$-\ .07(1-k)(1+p_1+p_1^2+p_1^3+\ldots)WL \text{ when } k = \frac{EI}{E_1I_1} \text{ as before.}$$

$$= -\ .07\left[(1-k)/(1-p_1)\right]WL \ldots\ldots\ 7.5 \text{ and } p_1 = (1-k) \times .385.$$

The necessity of forming a new flexibility matrix and inverting the same is avoided by this iterative process.

7.8 Ultimate strength of 2 span continuous prestressed beams.

The following steps are suggested in checking the ultimate strength of 2 span continuous prestressed beams.

1) Calculate moments at L_1 and L_2 at all critical sections, by using graphs. (Those in chapter 2 cover a wide range.) Also find n_1 and e_{c1} at these sections.

2) Calculate the cracked modulus of flexural rigidity at L_1 at all the hinges from the formula

$$EI = \frac{M_1 n_1 d}{e_{c1}}$$

3) Assume in the first trial, that the calculated moments at L_2 are attained by the beam at all the critical sections i.e., in other words there is complete redistribution of moments. The points of contraflexure, according to this bending moment diagram, may be established.

4) The beam may then be assumed to have different 'EI' values in the different zones between points of contraflexure. The 'EI' value in each zone is assumed to remain constant and is equal to the cracked 'EI' value at L_1 as found for the critical section contained in that zone.

   Calculate the new distribution of elastic moments due to these alterations in 'EI' values as suggested in 7.7.

5) From 4), the ratio of the support to span moments for the elastic distribution of bending moments in the idealized structure is known. The ratio of the moment M_2 at the support to M_2 at the span is also known. The first hinge to form can therefore be established as well as the bending moment distribution which occurs at this stage.

6) The solution of the problem now lies in finding out the maximum possible redistribution of moments that can be obtained by imposing rotations at the critical sections up to the maximum permissible values.

Three beams tested by Morice and Lewis in the Cement and Concrete Association , have been analysed by the author in 7.9 and 7.10 by the above procedure, using the method suggested in 7.7 to calculate the distribution of elastic moments in the structure, having modified values of EI. Results have been compared with those found by Guyon.

7.9. Analysis of C and C.A. beams.

Morice and Lewis tested 28 two span beams to failure load in the Cement and Concrete Association(29). The spans were 7'6" long and the beams had a constant rectangular section of 6" depth by 4" width. The cables were of the Freyssinet type, each having eight wires of 0.2" diameter. The nominal prestressing force was 30,000 lbs. The high tensile steel had a tensile strength of 105.5 tons/ins^2, the ultimate force in the cable being about 59,000 lbs.

Beam Nos. 12, 13 and 14 were chosen for analysis and dicussion, because they fell within the range of the values of ω and n_2, for which calculations of moments at L_1 and L_2 were done by the author, as described in chapter 2 of this thesis. Further, reactions were measured in these beams and the analyzed results could be compared with the experimental.

7.10 The properties of the C & CA beams are summarized below.

MIDSPAN

Beam No.	max. flex. strength f''_c.	depth of cable.	$\omega = \frac{A_t}{bd} \cdot \frac{f_{s_2}}{f''_c}$	n_1	m_1	$EI = \frac{M_1 n_1 d}{e_{c1}}$, $e_{c1} = .002$	m_2
12	4830	3.6	.85	.78	$.367 \frac{M_1}{}$; $M_1 = 92200$	13×10^7	$.38 \frac{M_2}{}$; $M_2 = 95500$
13	4780	3.5	.885	.80	$.374 \frac{M_1}{}$; $M_1 = 88000$	12.35×10^7	$.383 \frac{M_2}{}$; $M_2 = 90000$
14	4690	3.4	.93	.83	$.381 \frac{M_1}{}$; $M_1 = 82750$	11.7×10^7	$.387 \frac{M_2}{}$; $M_2 = 84000$

cont....

cont....

SUPPORT

Beam No.	d	ω	n_1	m_1	$EI = \frac{M_1 n_1 d}{e_{c1}}$	m_2
12	4.2	.73	.7	.344 [illegible] M_1 = 117500	17.3 x10^7	.366 [illegible] M_2 = 125000
13	5.1	.605	.615	.315 [illegible] M_1 = 157000	24.7 x10^7	.35 [illegible] M_2 = 174000
14	5.1	.62	.625	.319 [illegible] M_1 = 156000	24.8 x10^7	.352 [illegible] M_2 = 172000

NOTE - 1) All the above beams are highly over-reinforced (limiting value of e_{c1} = .002, has been assumed at L_1).

2) The computed values of , m_1, m_2, etc. are given in Table 7.30. (These results are not shown in the graphs plotted in Chapter 2.)

Beam No.12.

Fig. 7.3 shows the distribution of moments in beam 12 if full redistribution takes place. It will be observed that the change in the length BC is small. The point of contraflexure dividing the regions of different EI values have therefore been assumed to be the same as in the elastic case. The correction in the bending moment distribution is obtained from equation 7.4.

k = ratio of flexural regidities = $^{13}/_{17.3}$ = .75

$p = (1-k)\ .615 = .154$

The correction in the bending moment

$$= \frac{.07(1-.75)}{(1-.154)}\ WL = .02\ WL$$

The BM at support is (.1875 + .02) WL = .2075 WL
and the mid span moment = (.25 - .1037)WL = .1463 WL

Calculation of cracking moments.

If e_1 is the eccentricity at midspan and e_2 is the eccentricity at the support, the condition for concordancy is given by

$$3\ e_1 = 2.5\ e_2$$

If the cable is not concordant, the secondary moments are as under:-

i) At support = $\frac{P}{4}\ (2.5\ e_2 - 3\ e_1)$ where P = prestressing force.

ii) At midspan = $\frac{P}{8}\ (2.5\ e_2 - 3e_1)$.

The tensile strength in flexure has been assumed to be 12% of the permissible compressive stress, (same as assumed by Guyon). The cracking moments on the basis of the above data, after accounting for the secondary moments, but neglecting the increase in prestress, are

i) At support = 70900 in lbs.

ii) At mid span = 66900 in lbs.

The ratio of the moments at support and midspan, under the elastic distribution is 6:5.
Obviously the support is the critical section to crack first.

Distribution of moments at ultimate.

If it is assumed that the moment M_2(125000 in lbs.) is first attained by the support, then the corresponding mid span moment $= \frac{125000 \times .1463}{.2075} = 88000$ in lbs.

The increase of further moment at the mid span due to the plastic rotation at the support, is calculated as follows.

$e_{c2} = .0030$ (for $\omega = .73$ from the table).

The permissible rotation according to equation 2.16

$$= 2 \times .4\ (.0030 - .0020) \times \frac{51}{4.2} = .0097$$

Subtract from this the elastic rotation between L_1 and L_2, because the initial phase of the bilinear relation is assumed to hold good until the moment M_2 is reached.

$$\therefore \text{ The plastic rotation} = .0097 - \frac{125000 - 117500}{17.3 \times 10^7} \times 25.5$$

$$= .0086$$

The possible redistribution of moment at the support due to this rotation

$$= .0086 \times \frac{13 \times 10^7}{90} \times \frac{3}{2} \times \frac{1}{(1-.154)}$$

$$= 22000 \text{ in lbs.}$$

At mid span, the corresponding redistribution is 11000 in lbs.

If the elastic distribution before the plastic rotation takes place, is as follows:-

1) At support = - 147000
2) At mid span = $147000 \times \frac{.1463}{.2075} = 10360$

Then after redistribution the moments will be

1) At support = - 125000 (-147000 + 22000)
2) At mid span = 114600 (103600 + 11000)

Since the moment at mid span cannot exceed the value M_2, we observe that after full redistribution, the moment at mid span at failure is expected to be 95500 in lbs. only.

Beam No.13.

Fig. 7.4 shows the BM distribution in Beam 13 if ultimate moments are attained both at the support and mid point. The ratio of the support and the mid span moment is approx. 2:1. Fig.7.5 shows the elastic distribution of bending moments under a constant modulus of flexural rigidity. It also shows the two regions in which different EI values are applicable after cracking. A significant change takes place in the point of contraflexure, the effect of which has been taken into account. The EI values are in the ratio 2:1.

The correction to a first order of degree in the imposed rotation coefficient for the support, is obtained by integrating the diagram (Fig.7.6) with itself in the length RS.
If the value of this correction is $\frac{3}{2}\frac{EI}{L}.p$, then the correct unposed moment at support is

$\frac{3}{2}\frac{EI}{L(1-p)}$ (see equation 7.4).

In this case the value of p is

$$\frac{2}{3} \times 2 \times (1-k) \times \frac{1}{6x3}\left[1(2+\frac{3}{2}) + \frac{3}{2}(3+1)\right] = .35 \quad \begin{matrix}\text{(putting}\\ k = .5)\end{matrix}$$

Hence the correct imposed moment

$$= \frac{3}{2 \times .65} \times \frac{El}{L} = \frac{3}{2}\frac{El}{L} \times 1.54 \; .... \; 7.8$$

The correction in the elastic bending moment distribution is obtained by integrating the portion PQ of Fig 7.5 with the portion RS of Fig 7.6 and then multiplying by the factor 1.54. The value of this change

$$2(1-k) \quad \times \quad \left[\frac{.27}{6}\left\{.1875(3+\frac{12}{11})\right\} - \frac{.06}{6}\left\{.0417(2+\frac{12}{11})\right\}\right] \times 1.54\ WL$$

$= (1-k)\ (.07-.0023) \times 1.54\,xWL = 0.05\,xWL$ say.

The support moment is therefore $(.1875 + .05)WL = .2375\,WL$
and the mid span moment $= (.25 - .1187)WL = .131\,xWL$ say.

Cracking moments.

Similar calculations as in Beam No. 12, reveal that the cracking moments are as follows:-

At support = 741,000 in lbs.

At mid point = 708000 in lbs.

(Ratio is 1.04 against elastic moment ratio of 1.2). Cracking has therefore to commence at the support.

Distribution of bending moments at the ultimate.

Assuming that the moment M_2 is reached at the support, the corresponding point at the mid span is $\frac{.131}{.2375} \times 174000 = 96000$

Since this is more than the moment at L_2 at the mid span, we will therefore assume that the moment M_2 is first reached at the mid span and the moment at the support will depend on the amount of redistribution available from rotation at mid span.

Let the elastic moment at mid span before redistribution = 90000 lbs.

The corresponding elastic moment at support before redistribution $= \frac{90000 \times .2375}{.131}$

$= 163500$ in lbs.

e_{c2} at mid span = .0028

The permissible rotation at mid span hinge

$= 2 \times .4\ (.0028 - .002) \times \frac{60}{3.5} = .0100$

Subtract the elastic rotation between L_1 and L_2

which is $\left(\frac{90000-88000}{12.35 \times 10^7}\right) \times \frac{60}{2} = .0005$

The permissible rotation is therefore = .0095

The redistribution moment at support due to this rotation $= \frac{1}{2} \times .0095 \times \frac{12.35 \times 10^7}{90} \times \frac{3}{2} \times 1.54$

$= 15000$ in lbs.

Since there are two spans, the total redistribution moment at support $= 30000$ in lbs

and consequently the corresponding redistribution at the mid span shall be 15000 in lbs.

If the moment at mid span before redistribution is increased to 105000, the corresponding moment at support $= 105000 \times \frac{.2375}{.131} = 190000.$

The moments after redistribution are:

At mid span $105000 - 15000 = 90000$ in lbs.

at support $190000 + 30000 = 220000$ in lbs., but its maximum value is 174000

In Beam 13 again we get a condition of full redistribution and the maximum values of moments are reached both at support and mid span.

Beam 14.

In this case, the bending moment distribution and the rate of EI values at the ultimate, are similar to those for Beam No. 13. The condition of full redistribution applies to this beam also.

The results of the analysis are summarised below.

PROPERTIES OF SECTION.			PROPERTIES OF STRUCTURE.				
(1) BEAM NO.	(2) Ultimate Moment Analyzed by computer.	(3) Ultimate moment calculated by Guyon.	(4) Moment at failure calculated by author's suggestion in Baker's analysis for compatibility.	fract. of actual.	(5) Moment at failure calculated by Guyon with his adoption coefficients.	fract. of actual.	(6) Actual moment at failure.
	MID SPAN						
12	95500	108700	95500	.845	102500	.906	113000
13	90000	101300	90000	1.03	98500	1.13	87000
14	84000	96000	84000	.91	93250	1.01	92500
	SUPPORT						
12	125000	137200	125000	1.0	137200	1.1	125000
13	174000	182000	174000	1.01	182000	1.05	173000
14	172000	184000	172000	1.13	184000	1.21	157000

Table 7.1

3 Storeys & 3 Bays- Unit Rotation at Hinge 13b

Hinge Moments	Case 1 $X=\frac{2}{3}$, $Y=4$	Case 2 $X=\frac{5}{6}$, $Y=4$	Case 3 $X=1$, $Y=4$	Case 4 $X=\frac{2}{3}$, $Y=8$	Case 5 $X=\frac{2}{3}$, $Y=12$
X13b	1.7975	1.7967	1.7960	1.7056	1.6721
X23b	-.4671	-.4670	-.4668	-.4377	-.4262
X33b	-.0582	-.0579	-.0577	-.0296	-.0197
X23a	.2949	.2935	.2922	.1579	.1079
X33a	-.2120	-.2113	-.2107	-.1163	-.0802
X23c	.0788	.0764	.0740	.0457	.0322
X33c	-.1584	-.1562	-.1541	-.0864	-.0595
X43c	-.0857	-.0846	-.0836	-.0445	-.0300
X12b	.0449	.0438	.0427	.0282	.0204
X22b	-.0479	-.0474	-.0469	-.0272	-.0190
X32b	-.0791	-.0781	-.0772	-.0430	-.0293
X22a	-.0170	-.0166	-.0161	--	--
X32a	.0146	.0143	.0140	--	--

Table 7.2

3 Storeys & 3 Bays- Unit Rotation at Hinge 23b

Hinge Moments	Case 1 $X=\frac{2}{3}, Y=4$:	Case 2 $X=\frac{5}{6}, Y=4$:	Case 3 $X=1, Y=4$:	Case 4 $X=\frac{2}{3}, Y=8$:	Case 5 $X=\frac{2}{3}, Y=12$
X13b	-.4671	-.4670	-.4669	-.4377	-.4262
X23b	1.8795	1.8778	1.8763	1.7562	1.7085
X33b	-.2358	-.2345	-.2333	-.1373	-.0968
X23a	.0613	.0606	.0600	.0328	.0224
X33a	.3769	.3746	.3725	.2484	.1443
X13c	-.0856	-.0839	-.0823	-.0454	-.0308
X33c	.1381	.1339	.1301	.0825	.0588
X43c	-.1370	-.1327	-.1287	-.0800	-.0567
X12b	-.0460	-.0452	-.0444	-.0266	-.0187
X22b	.0899	.0873	.0847	.0600	.0444
X32b	-.1060	-.1028	-.0999	-.0695	-.0515
X32a	-.0294	-.0284	-.0275	--	--
X32c	-.0166	-.0158	-.0151	---	--

Table 7.3

3 Storeys & 3 Bays-- Unit Rotation at Hinge 33b

Hinge Moments	Case 1 $X=\frac{2}{3}, Y=4$:	Case 2 $X=\frac{5}{6}, Y=4$:	Case 3 $X=1, Y=4$:	Case 4 $X=\frac{2}{3}, Y=8$:	Case5 $X=\frac{2}{3}, Y=12$
X13b	-.0582	-.0579	-.0577	-.0296	-.0197
X23b	-.2358	-.2345	-.2333	-.1373	-.0968
X33b	.6264	.6234	.6207	.3524	.2455
X23a	-.1698	-.1693	-.1688	-.0898	-.0609
X33a	-.1025	-.1016	-.1007	-.0683	-.0504
X13c	-.1372	-.1341	-.1312	-.0783	-.0551
X23c	-.1661	-.1649	-.1637	-.0886	-.0603
X33c	-.1247	-.1219	-.1192	-.0745	-.0532
X43c	.2030	.1961	.1896	.1231	.0883
X12b	-.0809	-.0803	-.0797	-.0436	-.0297
X22b	-.0196	-.0172	-.1050	-.0707	-.0521
X32b	.1534	.1483	.1435	.1060	.0797
X22a	.0068	.0068	.0069	--	--
X32a	.0213	.0204	.0195	.0079	.0040
X12c	.0096	.0089	.0083	.0036	.0019
X32c	.0088	.0081	.0075	.0036	.0019
X42c	-.0227	-.0214	-.0202	-.0080	-.0041
X21b	.0079	.0074	.0069	.0034	.0018
X31b	-.0175	-.0165	-.0156	-.0069	-.0037

Table 7.4

3 Storeys & 3 Bays--- Unit Rotation at Hinge 23a

Hinge Moments	Case 1 $X=\frac{2}{3}, Y=4$:	Case 2 $X=\frac{5}{6}, Y=4$:	Case 3 $X=1, Y=4$:	Case 4 $X=\frac{2}{3}, Y=8$:	Case 5 $X=\frac{2}{3}, Y=12$
X13b	.2949	.2935	.2922	.1579	.1079
X23b	.0613	.0606	.0599	.0328	.0224
X33b	-.1698	-.1693	-.1688	-.0898	-.0609
X23a	.6718	.6682	.6647	.3663	.2522
X33a	-.1507	-.1507	-.1507	-.0835	-.0609
X13c	-.1298	-.1255	-.1214	-.0758	-.0538
X23c	.2170	.2104	.2041	.1283	.0910
X33c	-.1647	-.1630	-.1613	-.0873	-.0595
X43c	-.1712	-.1685	-.1659	-.0899	-.0609
X12b	.0636	.0620	.0605	.0411	.0299
X22b	-.0116	-.0123	-.0129	--	--
X32b	-.1539	-.1515	-.1492	-.0854	-.0589
X22a	-.0465	-.0450	-.0436	-.0150	-.0073
X32a	.0112	.0110	.0108	.0034	--
X12c	.0091	.0083	.0076	.0036	--
X22c	-.0264	-.0252	-.0241	-.0086	-.0042
X11b	-.0086	-.0083	-.0080	--	--

Table 7.5

3 Storeyes & 3 Bays-- Unit Rotation at Hinge33a

Hinge Moments	Case 1 $X=\frac{2}{3}, Y=4$:	Case 2 $X=\frac{5}{6}, Y=4$:	Case 3 $X=1, Y=4$:	Case 4 $X=\frac{2}{3}, Y=8$:	Case5 $X=\frac{2}{3}, Y=12$
X13b	-.2120	-.2113	-.2107	-.1163	-.0802
X23b	.3769	.3746	.3725	.2084	.1443
X33b	-.1025	-.1016	-.1007	-.0683	-.0503
X23a	-.1507	-.1507	-.1507	-.0835	-.0578
X33a	.6718	.6682	.6646	.6647	.3663
X13c	-.1712	-.1685	-.1659	-.0899	-.0609
X23c	-.1647	-.1629	-.1613	-.0873	-.0595
X33c	.2170	.2104	.2041	.1283	.0910
X43c	-.1298	-.1255	-.1214	-.0758	-.0538
X12b	-.1419	-.1397	-.1375	-.0813	-.0571
X22b	.1068	.1033	.1000	.0722	.0537
X32b	-.0979	-.0948	-.0920	-.0648	-.0438
X22a	.0112	.0110	.0108	--	--
X32a	-.0465	-.0450	-.0436	-.0150	-.0073
X32c	-.0264	-.0252	-.0241	-.0086	-.0042
X42c	.0091	.0083	.0076	.0037	--
X21b	-.0138	-.0131	-.0125	-.0050	-.0026

Table 7.6

3 Storeys & 3 Bays---Unit Rotation at Hinge 13c

Hinge Moments	Case 1 $X=\frac{2}{3}, Y=4$:	Case 2 $X=\frac{5}{6}, Y=4$:	Case 3 $X=1, Y=4$:	Case 4 $X=\frac{2}{3}, Y=8$:	Case 5 $X=\frac{2}{3}, Y=12$
X13b	.0072	.0073	.0073	.0042	.0029
X23b	-.0855	-.0839	-.0823	-.0454	-.0308
X33b	-.1372	-.1341	-.1312	-.0783	-.0551
X23a	-.1298	-.1255	-.1214	-.0758	-.0538
X33a	-.1712	-.1685	-.1659	-.0899	-.0609
X13c	.6829	.6634	.6451	.3670	.2521
X23c	-.1294	-.1213	-.1138	-.0753	-.0535
X33c	-.1737	-.1708	-.1680	-.0906	-.0612
X43c	-.1444	-.1392	-.1343	-.0801	-.0558
X12b	.1270	.1255	.1240	.0676	.0459
X22b	-.1008	-.09[illegible]6	-.0964	-.0573	-.0399
X32b	-.1049	-.1014	-.0982	-.0671	-.0494
X22a	.0614	.0587	.0562	.0198	.0097
X32a	.0170	.0170	.0170	.0039	--
X12c	-.0550	-.0516	-.0484	-.0179	-.0088
X22c	.0349	.0328	.0308	.0115	.0057
X32c	.0168	.0166	.0164	.0044	--
X42c	.0249	.0234	.0220	.0082	.0041
X21b	.0105	.0102	.0100	--	--
X31b	.0192	.0181	.0171	.0071	.0037
X21a	-.0076	-.0071	-.0066	--	--

Table 7.7

3 Storeyes & 3 Bays--- Unit Rotation at Hinge 23c

Hinge Moments	Case 1 $X=\frac{2}{3}, Y=4$:	Case 2 $X=\frac{5}{6}, Y=4$:	Case 3 $X=1, Y=4$:	Case 4 $X=\frac{2}{3}, Y=8$:	Case 5 $X=\frac{2}{3}, Y=12$
X13b	.0789	.0764	.0740	.0457	.0322
X33b	-.1661	-.1649	-.1637	-.0886	-.0603
X23a	.2170	.2104	.2041	.1283	.0910
X33a	-.1647	-.1629	-.1613	-.0873	-.0595
X13c	-.1294	-.1213	-.1138	-.0753	-.0535
X23c	.7066	.6919	.6778	.3753	.2562
X33c	-.1649	-.1603	-.1559	-.0872	-.0594
X43c	-.1737	-.1708	-.1680	-.0906	-.0612
X12b	.2708	.2665	.2624	.1506	.1044
X22b	.0559	.0552	.0546	.0312	.0217
X32b	-.1570	-.1540	-.1512	-.0867	-.0596
X22a	-.1030	-.0999	-.0969	-.0307	-.0146
X32a	.0317	.0309	.0301	.0093	.0044
X12c	.0244	.0226	.0209	.0084	.0042
X22c	-.0495	-.0471	-.0448	-.0154	-.0075
X32c	.0122	.0117	.0112	--	--
X11b	-.0154	-.0148	-.0142	-.0050	--
X21a	.0086	.0081	.0077	--	--

Table 7.8

3 Storeys & 3 Bays--- Unit Rotation at Hinge 33c

Hinge Moments	Case 1 $X=\frac{2}{3}, Y=4$:	Case 2 $X=\frac{5}{6}, Y=4$:	Case 3 $X=1, Y=4$:	Case 4 $X=\frac{2}{3}, Y=8$:	Case 5 $X=\frac{2}{3}, Y=12$
X13b	-.1584	-.1562	-.1541	-.0864	-.0595
X23b	.1381	.1340	.1300	.0825	.0588
X33b	-.1247	-.1219	-.1192	-.0745	-.0532
X23a	-.1647	-.1629	-.1613	-.0873	-.0595
X33a	.2170	.2104	.2040	.1283	.0909
X13c	-.1737	-.1708	-.1680	-.0906	-.0612
X23c	-.1649	-.1603	-.1558	-.0872	-.0594
X33c	.7066	.6919	.6778	.3753	.2562
X43c	-.1294	-.1213	-.1138	-.0753	-.0535
X12b	-.1890	-.1846	-.1803	-.1091	-.0767
X22b	.3328	.3255	.3185	.1939	.1371
X32b	-.0683	-.0628	-.0577	-.0555	-.0438
X22a	.0317	.0309	.0301	.0093	.0043
X32a	-.1030	-.0998	-.0969	-.0307	-.0146
X22c	.0123	.0117	.0112	.0036	--
X32c	-.0494	-.0471	-.0448	-.0154	-.0075
X42c	.0244	.0226	.0209	.0084	.0042
X11b	.0129	.0124	.0119	.0042	--
X21b	-.0255	-.0241	-.0228	-.0089	-.0045
X31b	.0169	.0156	.0144	.0069	.0037
X31a	.0086	.0081	.0077	--	--

Table 7.9

3 Storeys & 3 Bays--- Unit Rotation at Hinge 43c

Hinge Moments	Case 1 $X=\frac{2}{3}, Y=4$:	Case 2 $X=\frac{5}{6}, Y=4$;	Case 3 $X=1, Y=4$:	Case 4 $X=\frac{2}{3}, Y=8$:	Case 5 $X=\frac{2}{3}, Y=12$
X13b	-.0857	-.0846	-.0836	-.0445	-.0300
X23b	-.1370	-.1327	-.1287	-.0800	-.0567
X33b	.2030	.1961	.1896	.1831	.0883
X23a	-.1712	-.1685	-.1659	-.0899	-.0609
X33a	-.1292	-.1255	-.1214	-.0758	-.0538
X13c	-.1444	-.1392	-.1343	-.0801	-.0558
X23c	-.1737	-.1708	-.1680	-.0906	-.0612
X33c	-.1294	-.1213	-.1138	-.0753	-.0535
X43c	.6828	.6634	.6451	.3670	.2521
X12b	-.0558	-.0552	-.0546	-.0293	-.0197
X22b	-.1950	-.1881	-.1817	-.1231	-.0897
X32b	.5432	.5287	.5150	.3240	.2314
X22a	.0170	.0170	.0170	.0039	---
X32a	.0614	.0587	.0562	.0192	.0097
X12c	.0249	.0234	.0220	.0082	.0041
X22c	.0168	.0166	.0164	.0044	---
X32c	.0349	.0328	.0308	.0115	.0057
X42c	-.0550	-.0516	-.0484	-.0179	-.0088
X21b	.0267	.0251	.0237	.0096	.0049
X31b	-.0415	-.0389	-.0365	-.0154	-.0079
X31a	-.0076	-.0071	-.0066	---	---

Table 7.10

3 Storeys & 3 Bays --- Unit Rotation at Hinge 12b

Hinge Moments	Case 1 $X=\frac{2}{3}, Y=4$:	Case 2 $X=\frac{5}{6}, Y=4$:	Case 3 $X=1, Y=4$:	Case 4 $X=\frac{2}{3}, Y=8$:	Case 5 $X=\frac{2}{3}, Y=12$
X13b	.0449	.0438	.0427	.0282	.0204
X23b	-.0460	-.0452	-.0444	-.0266	-.0187
X33b	-.0809	-.0803	-.0797	-.0436	-.0297
X23a	.0637	.0620	.0605	.0411	.0299
X33a	-.1419	-.1397	-.1375	-.0813	-.0571
X13c	.1270	.1255	.1240	.0676	.0459
X23c	.2707	.2665	.2624	.1506	.1044
X33c	-.1890	-.1846	-.1803	-.1091	-.0767
X43c	-.0558	-.0552	-.0546	-.0293	-.0197
X12b	2.8577	2.3150	1.9525	2.6532	2.5751
X22b	-.7464	-.6047	-.5099	-.6872	-.6621
X32b	-.1403	-.1219	-.1094	-.0735	-.0494
X22a	.4126	.3231	.2637	.2276	.1574
X32a	-.2867	-.2231	-.1809	-.1646	-.1155
X22c	.1062	.0801	.0629	.0646	.0463
X32c	-.2213	-.1718	-.1390	-.1245	-.0867
X42c	-.1252	-.0982	-.0802	-.0662	.0448
X11b	.0599	.0454	.0358	.0398	.0293
X21b	-.0663	-.0516	-.0419	-.0388	-.0275
X31b	-.1150	-.0901	-.0735	-.0637	-.0438

Table 7.11

3 Storeys & 3 Bays---Unit Rotation at Hinge22b

Hinge Moments	Case 1 $X=\frac{2}{3}$, Y=4:	Case 2 $X=\frac{5}{6}$, Y=4:	Case 3 X=1;Y=4:	Case 4 $X=\frac{2}{3}$;Y=8;	Case 5 $X=\frac{2}{3}$,Y=12
X13b	-.0479	-.0474	-.0469	-.0272	--
X23b	.0899	.0872	.0847	.0600	.0444
X33b	-.1096	-.1072	-.1050	-.0707	-.0521
X33a	.1068	.1033	.1000	.0722	.0537
X13c	-.1008	-.0986	-.0964	-.0573	-.0399
X23c	.0558	.0552	.0545	.0312	.0217
X33c	.3328	.3255	.3185	.1939	.1371
X43c	-.1950	-.1881	-.1817	-.1231	-.0897
X12b	-.7464	-.6047	-.5099	-.6872	-.6621
X22b	3.0182	2.4479	2.0664	2.7633	2.6578
X32b	-.4959	-.4186	-.3658	-.3103	-.2255
X22a	.0871	.0680	.0554	.0477	.0329
X32a	.5109	.3970	.3215	.2944	.2073
X12c	-.1241	-.0966	-.0783	-.0671	-.0459
X32c	.1794	.1345	.1051	.1140	.0832
X42c	-.1851	-.1402	-.1109	-.1124	-.0811
X11b	-.0663	-.0516	-.0419	-.0388	-.0275
X21b	.1168	.0876	.0686	.0830	.0630
X31b	-.1430	-.1085	-.0859	-.0975	-.0735
X31a	-.0404	-.0306	-.0242	--	--

Table 7.12

3 Storeys & 3 Bays--- Unit Rotation at Hinge 32b

Hinge Moments	Case 1 $X=\frac{2}{3}, Y=4$	Case 2 $X=\frac{5}{6}, Y=4$	Case 3 $X=1, Y=4$	Case 4 $X=\frac{2}{3}, Y=8$	Case 5 $X=\frac{2}{3}, Y=12$
X13b	-.0791	-.0781	-.0772	-.0430	-.0292
X23b	-.1060	-.1028	-.1000	-.0695	-.0514
X33b	.1534	.1483	.1435	.1060	.0797
X23a	-.1539	-.1515	-.1492	-.0854	-.0589
X33a	-.0979	-.0948	-.0920	-.0648	-.0483
X13c	-.1049	-.1014	-.0982	-.0671	-.0494
X23c	-.1570	-.1540	-.1512	-.0867	-.0596
X33c	-.0683	-.0628	-.0577	-.0555	-.0438
X43c	.5432	.5288	.5150	.3241	.2314
X12b	-.1403	-.1219	-.1094	-.0735	-.0493
X22b	-.4958	-.4186	-.3658	-.3103	-.2255
X32b	1.3743	1.1721	1.0344	.8152	.5808
X22a	-.2367	-.1853	-.1511	-.1303	-.0895
X32a	-.1096	-.0796	-.0602	-.0857	-.0669
X12c	-.1873	-.1435	-.1147	-.1105	-.0790
X22c	-.2335	-.1825	-.1486	-.1286	-.0885
X32c	-.1613	-.1221	-.0965	-.1019	-.0747
X42c	.2623	.1958	.1525	.1691	.1244
X11b	-.1150	-.0905	-.0735	-.0635	-.0438
X21b	-.1430	-.1085	-.0859	-.0975	-.0735
X31b	.1963	.1463	.1138	.1453	.1122
X31a	.0276	.0203	.0157	.0108	.0057
X11c	.0144	.0107	—	—	—
X41c	-.0340	-.0256	-.0201	-.0120	-.0061

Table 7.13

3 Storeys & 3 Bays--- Unit Rotation at Hinge 22a

Hinge Moments	Case 1 $X=\frac{2}{3}, Y=4$:	Case 2 $X=\frac{5}{6}, Y=4$:	Case 3 $X=1, Y=4$:	Case 4 $X=\frac{2}{3}, Y=8$:	Case 5 $X=\frac{2}{3}, Y=12$
X13b	-.0171	-.0166	-.0161	--	--
X23a	-.0465	-.0450	-.0436	-.0150	-.0073
X33a	.0112	.0110	.0108	--	--
X13c	.0614	.0587	.0562	.0198	.0097
X23c	-.1030	-.0999	-.0969	-.0307	-.0146
X33c	.0317	.0309	.0301	.0093	.0044
X43c	.0170	.0170	.0170	--	--
X12b	.4126	.3231	.2637	.2276	.1574
X22b	.0871	.0680	.0554	.0477	.0329
X32b	-.2367	-.1853	-.1511	-.1303	-.0895
X22a	1.0265	.8199	.6822	.5527	.3794
X32a	-.2314	-.1860	-.1556	-.1262	-.0869
X12c	-.2015	-.1569	-.1274	-.1150	-.0812
X22c	.3352	.2616	.2128	.1941	.1370
X32c	-.2484	-.1969	-.1625	-.1312	-.0893
X42c	-.2556	-.2012	-.1650	-.1346	-.0912
X11b	.0976	.0764	.0624	.0620	.0450
X21b	-.0168	-.0142	-.0124	--	--
X31b	-.2301	-.1811	-.1486	-.1279	-.0883
X21a	-.0731	-.0572	-.0467	-.0230	-.0111
X31a	.0175	.0138	.0114	--	--
X11c	.0177	.0137	.0111	.0063	--
X21c	-.0443	-.0347	-.0283	-.0137	-.0066

Table 7.14

3 Storeys & 3 Bays— Unit Rotation at Hinge 32a

Hinge Moments	Case 1 $X=\frac{2}{3}, Y=4$:	Case 2 $X=\frac{5}{6}, Y=4$:	Case 3 $X=1, Y=4$:	Case 4 $X=\frac{2}{3}, Y=8$:	Case 5 $X=\frac{2}{3}, Y=12$
X13b	.0146	.0143	.0140	—	—
X23b	-.0294	-.0284	-.0274	-.0097	-.0048
X33b	.0213	.0204	.0195	.0079	.0040
X23a	.0112	.0109	.0180	—	—
X33a	-.0465	-.0450	-.0436	-.0149	-.0073
X13c	.0170	.0170	.0170	—	—
X23c	.0317	.0309	.0301	.0093	.0044
X33c	-.1030	-.0999	-.0969	-.0307	-.0146
X43c	.0614	.0587	.0562	.0199	.0097
X12b	-.2867	-.2231	-.1809	-.1646	-.1155
X22b	.5109	.3969	.3215	.2944	.2073
X32b	-.1096	-.0796	-.0602	-.0857	-.0669
X22a	-.2314	-.1860	-.1556	-.1262	-.0869
X32a	1.0265	.8199	.6822	.5527	.3794
X12c	-.2556	-.2012	-.1650	-.1346	-.0912
X22c	-.2484	-.1968	-.1625	-.1312	-.0893
X32c	.3352	.2616	.2128	.1941	.1370
X42c	-.2015	-.1569	-.1274	-.1150	-.0812
X11b	-.2141	-.1688	-.1386	-.1222	-.0857
X21b	.1644	.1280	.1038	.1091	.0808
X31b	-.1506	-.1173	-.0952	-.0980	-.0727
X21a	.0175	.0138	.0114	—	—
X31a	-.0732	-.0347	-.0283	-.0137	-.0066
X31c	-.0443	-.0347	-.0283	-.0137	-.0066
X41c	.0177	.0137	.0110	.0063	—

Table 7.15

3 Storeys & 3 Bays---- Unit Rotation at Hinge 12c

Hinge Moments	Case 1 $X=\frac{2}{3}, Y=4$:	Case 2 $X=\frac{5}{6}, Y=4$:	Case 3 $X=1, Y=4$:	Case 4 $X=\frac{2}{3}, Y=8$:	Case 5 $X=\frac{2}{3}, Y=12$
X13c	-.0550	-.0516	-.0484	-.0179	-.0088
X23c	.0244	.0226	.0209	.0084	.0042
X43c	.0249	.0234	.0220	.0082	.0041
X12b	—	—	—	.0057	.0041
X22b	-.1241	-.0965	-.0783	-.0671	-.0459
X32b	-.1873	-.1435	-.1147	-.1105	-.0789
X22a	-.2015	-.1569	-.1274	-.1150	-.0812
X32a	-.2556	-.2012	-.1650	-.1346	-.0912
X12c	1.0304	.8019	.6505	.5517	.3785
X22c	-.1980	-.1491	-.1171	-.1137	-.0805
X32c	-.2603	-.2048	-.1679	-.1359	-.0918
X42c	-.2201	-.1703	-.1373	-.1208	-.0840
X11b	.1905	.1506	.1240	.1014	.0688
X21b	-.1511	-.1181	-.0962	-.0859	-.0598
X31b	-.1577	-.1220	-.0985	-.1008	-.0741
X21a	.0961	.0741	.0597	.0305	.0148
X31a	.0255	.0204	.0170	.0058	—
X11c	-.0960	-.0745	-.0603	-.0294	-.0141
X21c	.0599	.0464	.0374	.0187	.0091
X31c	.0246	.0195	.0161	.0064	—
X41c	.0432	.0334	.0270	.0135	.0065

Table 7.16

3 Storeys & 3 Bays--- Unit Rotation at Hinge 22c

Hinge Moments	Case 1 $X=\frac{2}{3}, Y=4$:	Case 2 $X=\frac{5}{6}, Y=4$:	Case 3 $X=1, Y=4$:	Case 4 $X=\frac{2}{3}, Y=8$:	Case 5 $X=\frac{2}{3}, Y=12$
X13b	--	-.0094	-.0090		
X23a	-.0264	-.0252	-.0241	--	--
X13c	.0349	.0328	.0308	-.0086	-.0042
X23c	-.0495	-.0471	-.0448	.0115	.0057
X33c	.0123	.0117	.0112	-.0154	-.0075
X43c	.0168	.0166	.0164	--	--
X12b	.1062	.0801	.0629	--	--
X22b	-.0148	-.0133	-.0122	.0646	.0463
X32b	-.2334	-.1825	-.1485	--	--
X22a	.3352	.2616	.2128	-.1286	-.0885
X32a	-.2484	-.1968	-.1625	.1941	.1370
X12c	-.1978	-.1491	-.1171	-.1312	-.0893
X22c	1.0655	.8355	.6828	-.1137	-.0805
X32c	-.2474	-.1924	-.1559	.5639	.3846
X42c	-.2603	-.2048	-.1679	-.1308	-.0891
X11b	.4063	.3200	.2625	-.1358	-.0918
X21b	.0844	.0668	.0551	.2258	.1566
X31b	-.2357	-.1851	-.1514	.0469	.0326
X21a	-.1593	-.1243	-.1011	-.1301	-.0894
X31a	.0484	.0379	.0308	-.0469	-.0222
X11c	.0442	.0342	.0275	.0140	.0066
X21c	-.0830	-.0646	-.0525	.0140	.0068
X31c	.0208	.0164	.0134	-.0246	-.0117
				.0058	--

Table 7.17

3 Storeys & 3 Bays---- Unit Rotation at Hinge 32c

Hinge Moments	Case 1 $X=\frac{2}{3}, Y=4$:	Case 2 $X=\frac{5}{6}, Y=4$:	Case 3 $X=1, Y=4$:	Case 4 $X=\frac{2}{3}, Y=8$:	Case 5 $X=\frac{2}{3}, Y=12$
X23b	-.0166	-.0158	-.0151	--	--
X33a	-.0264	-.0252	-.0241	--	--
X13c	.0168	.0166	.0164	-.0086	-.0042
X23c	.0123	.0117	.0112	--	--
X33c	-.0495	-.0471	-.0448	--	--
X43c	.0349	.0328	.0308	-.0154	-.0075
X12b	-.2213	-.1718	-.1390	.0115	.0057
X22b	.1794	.1345	.1051	-.1245	-.0867
X32b	-.1613	-.1221	-.0965	.1140	.0832
X22a	-.2484	-.1969	-.1625	-.1019	-.0747
X32a	.3352	.2616	.2128	-.1312	-.0893
X12c	-.2603	-.2048	-.1679	.1941	.1370
X22c	-.2474	-.1924	-.1559	-.1358	-.0918
X32c	1.0655	.8355	.6828	-.1308	-.0891
X42c	-.1980	-.1491	-.1171	.5639	.3846
X11b	-.2834	-.2213	-.1801	-.1137	-.0805
X21b	.4999	.3911	.3190	-.1636	-.1150
X31b	-.1027	-.0756	-.0580	.2910	.2058
X21a	.0484	.0378	.0308	-.0834	-.0657
X31a	-.1593	-.1243	-.1011	.0141	.0066
X21c	.0208	.0164	.0134	-.0470	-.0222
X31c	-.0830	-.0647	-.0525	.0058	--
X41c	.0442	.0342	.0275	-.0246	-.0117
				.0140	.0068

Table 7.18

3 Storeys & 3 Bays --- Unit Rotation at Hinge 42c

Hinge Moments	Case 1 $X=\frac{2}{3}, Y=4$:	Case 2 $X=\frac{5}{6}, Y=4$:	Case 3 $X=1, Y=4$:	Case 4 $X=\frac{2}{3}, Y=8$:	Case 5 $X=\frac{2}{3}, Y=12$
X23b	.0107	.0099	.0093	---	---
X33b	-.0227	-.0214	-.0202	-.0080	-.0041
X13c	.0249	.0234	.0220	.0082	.0041
X33c	.0244	.0226	.0209	.0084	.0042
X43c	-.0550	-.0516	-.0484	-.0179	-.0088
X12b	-.1252	-.0981	-.0802	-.0662	-.0449
X22b	-.1851	-.1402	-.1109	-.1124	-.0811
X32b	.2623	.1958	.1525	.1691	.1244
X22a	-.2556	-.2012	-.1650	-.1346	-.0912
X32a	-.2015	-.1569	-.1274	-.1150	-.0812
X12c	-.2201	-.1703	-.1374	-.1208	-.0840
X22c	-.2603	-.2048	-.1679	-.1358	-.0918
X32c	-.1980	-.1491	-.1171	-.1137	-.0805
X42c	1.0304	.8018	.6505	.5517	.3785
X11b	-.0837	-.0663	-.0547	-.0440	-.0296
X21b	-.2923	-.2256	-.1815	-.1846	-.1345
X31b	.8145	.6342	.5148	.4860	.3470
X21a	.0255	.0204	.0170	.0058	.0024
X31a	.0961	.0741	.0596	.0305	.0149
X11c	.0432	.0334	.0270	.0135	.0065
X21c	.0247	.0195	.0161	.0063	---
X31c	.0560	.0464	.0374	.0187	.0091
X41c	-.0960	-.0745	-.0602	-.0294	-.0141

Table 7.19

3 Storeys 3 Bays----- Unit Rotation at Hinge 11b

Hinge Moments	Case 1 $X=\frac{2}{3}, Y=4$:	Case 2 $X=\frac{5}{6}, Y=4$:	Case 3 $X=1, Y=4$:	Case 4 $X=\frac{2}{3}, Y=8$:	Case 5 $X=\frac{2}{3}, Y=12$
X12b	.0600	.0454	.0358	.0399	.0293
X22b	-.0663	-.0516	-.0419	-.0388	-.0275
X32b	-.1150	-.0901	-.0735	-.0637	-.0438
X22a	.0976	.0764	.0624	.0620	.0450
X32a	-.2141	-.1688	-.1386	-.1222	-.0857
X12c	.1905	.1506	.1240	.1014	.0689
X22c	.4063	.3200	.2625	.2259	.1566
X32c	-.2834	-.2213	-.1801	-.1636	-.1150
X42c	-.0837	-.0663	-.0547	-.0440	-.0296
X11b	4.2940	2.7837	1.9571	3.9821	3.8639
X21b	-1.1205	-.7262	-.5102	-1.0313	-.9934
X31b	-.2128	-.1481	-.1109	-.1108	-.0742
X21a	.6317	.3977	.2718	.3457	.2382
X31a	-.4360	-.2722	-.1845	-.2491	-.1744
X21c	.1825	.1138	.0771	.1044	.0731
X31c	-.3514	-.2211	-.1510	-.1929	-.1332
X41c	-.1979	-.1259	-.0868	-.1018	-.0683

Table 7.20

3 Storeys & 3 Bays--- Unit Rotation at Hinge21b

Hinge Moments	Case 1 $X=\frac{2}{3}, Y=4$:	Case 2 $X=\frac{5}{6}, Y=4$:	Case 3 $X=1, Y=4$:	Case 4 $X=\frac{2}{3}, Y=8$:	Case 5 $X=\frac{2}{3}, Y=12$
X43c	--	--	.0237	--	--
X12b	-.0663	-.0516	-.0419	--	--
X22b	.1168	.0876	.0686	.0830	.0630
X32b	-.1430	-.1085	-.0859	-.0975	-.0735
X32a	.1644	.1279	.1038	.1091	.0808
X12c	-.1511	-.1181	-.0962	-.0859	-.0598
X22c	.0844	.0668	.0551	.0469	.0326
X32c	.4999	.3912	.3191	.2910	.2058
X42c	-.2923	-.2256	-.1815	-.1846	-.1345
X11b	-1.1205	-.7263	-.5103	-1.0313	-.9934
X21b	4.5429	2.9493	2.0759	4.1507	3.9896
X31b	-.7555	-.5110	-.3725	-.4705	-.3409
X21a	.1374	.0868	.0595	.0737	.0504
X31a	.7871	.4921	.3340	.4491	.3149
X11c	-.2019	-.1281	-.0882	-.1051	-.0708
X31c	.3074	.1903	.1280	.1845	.1316
X41c	-.3177	-.1984	-.1346	-.1830	-.1290

Table 7.21

3 Storeys & 3 Bays--- Unit Rotation At Hinge 31b

Hinge Moments	Case 1 $X=\frac{2}{3}, Y=4$:	Case 2 $X=\frac{5}{6}, Y=4$:	Case 3 $X=1, Y=4$:	Case 4 $X=\frac{2}{3}, Y=8$:	Case 5 $X=\frac{2}{3}, Y=12$
X33b	--	--	-.0165	-.0156	--
X13c	--	.0181	.0171	--	--
X33c	--	.0156	.0143	--	--
X43c	-.0415	-.0389	-.0366	-.0154	--
X12b	-.1150	-.0901	-.0735	-.0637	-.0438
X22b	-.1430	-.1085	-.0859	-.0975	-.0735
X32b	.1963	.1463	.1138	.1453	.1122
X22a	-.2301	-.1811	-.1486	-.1279	-.0883
X32a	-.1506	-.1173	-.0952	-.0980	-.0727
X12c	-.1577	-.1220	-.0985	-.1008	-.0741
X22c	-.2357	-.1851	-.1514	-.1301	-.0894
X32c	-.1027	-.0756	-.0580	-.0834	-.0657
X42c	.8145	.6342	.5142	.4861	.3470
X11b	-.2128	-.1481	-.1109	-.1108	-.0742
X21b	-.7555	-.5110	-.3725	-.4705	-.3410
X31b	2.0873	1.4260	1.0497	1.2332	.8767
X21a	-.3597	-.2260	-.1540	-.1967	-.1347
X31a	-.1732	-.1019	-.0650	-.1331	-.1029
X11c	-.3097	-.1939	-.1318	-.1764	-.1240
X21c	-.3605	-.2272	-.1554	-.1951	-.1336
X31c	-.2672	-.1652	-.1109	-.1633	-.1177
X41c	.4557	.2817	.1891	.2768	.1986

Table 7.22

3 Storeys & 3 Bays--- Unit Rotation at Hinge 21a

Hinge Moments	Case 1 $X=\frac{2}{3}$, Y=4:	Case 2 $X=\frac{5}{6}$, Y=4:	Case 3 X=1, Y=4:	Case 4 $X=\frac{2}{3}$, Y=8:	Case 5 $X=\frac{2}{3}$, Y=12
X23c	--	--	.0077	--	--
X12b	-.0241	-.0185	-.0148	--	--
X22a	-.0732	-.0572	-.0467	-.0239	-.0111
X32a	.0175	.0138	.0114	--	--
X12c	.0961	.0741	.0596	.0305	.0149
X22c	-.1593	-.1243	-.1011	-.0470	-.0222
X32c	.0484	.0379	.0308	.0141	.0066
X42c	.0255	.0204	.0170	--	--
X11b	.6317	.3977	.2717	.3457	.2382
X21b	.1374	.0868	.0596	.0737	.0504
X31b	-.3597	-.2260	-.1540	-.1967	-.1347
X21a	1.5781	1.0141	.7069	.8417	.5754
X31a	-.3470	-.2232	-.1558	-.1894	-.1305
X11c	-.3509	-.2262	-.1581	-.1891	-.1301
X21c	.5728	.3689	.2577	.3136	.2165
X31c	-.3897	-.2498	-.1737	-.2020	-.1365
X41c	-.4088	-.2613	-.1813	-.2085	-.1398

Table 7.23

3 Storeys & 3 Bays --- Unit Rotation at Hinge 31a

Hinge Moments	Case 1 $X=\frac{2}{3}, Y=4$:	Case 2 $X=\frac{5}{6}, Y=4$:	Case 3 $X=1, Y=4$:	Case 4 $X=\frac{2}{3}, Y=8$:	Case 5 $X=\frac{2}{3}, Y=12$
X33c	--	--	.0077	--	--
X12b	.0201	.0154	.0123	--	--
X22b	-.0404	-.0306	-.0242	--	--
X32b	.0276	.0203	.0157	-.0138	-.0069
X22a	.0175	.0138	.0114	.0108	--
X32a	-.0732	-.0572	-.0466	--	--
X12c	.0255	.0204	.0170	-.0230	-.0111
X22c	.0484	.0379	.0308	--	--
X32c	-.1593	-.1243	-.1011	.0141	.0066
X42c	.0961	.0741	.0596	-.0469	-.0222
X11b	-.4360	-.2722	-.1845	.0305	.0149
X21b	.7871	.4921	.3340	-.2491	-.1744
X31b	-.1732	-.1019	-.0650	.4491	.3149
X21a	-.3470	-.2232	-.1558	-.1331	-.1029
X31a	1.5781	1.0141	.7069	-.1894	-.1305
X11c	-.4088	-.2613	-.1813	.8417	.5754
X21c	-.3898	-.2498	-.1737	-.2086	-.1398
X31c	.5728	.3689	.2577	-.2020	-.1365
X41c	-.3509	-.2262	-.1581	.3135	.2165
				-.1891	-.1301

Table 7.24

3 Storeys & 3 Bays--- Unit Rotation 11c

Hinge Moments	Case 1 $X=\frac{2}{3}, Y=4$:	Case 2 $X=\frac{5}{6}, Y=4$:	Case 3 $X=1, Y=4$:	Case 4 $X=\frac{2}{3}, Y=8$:	Case 5 $X=\frac{2}{3}, Y=12$
X32b	.0144	.0107	.0083	--	--
X22a	.0177	.0137	.0111	--	--
X12c	-.0960	-.0745	-.0603	-.0294	-.0141
X22c	.0442	.0342	.0276	.0140	.0068
X42c	.0432	.0334	.0270	.0135	.0065
X21b	-.2019	-.1281	-.0882	-.1051	-.0708
X31b	-.3097	-.1939	-.1318	-.1764	-.1240
X21a	-.3509	-.2262	-.1581	-.1891	-.1301
X31a	-.4088	-.2613	-.1813	-.2086	-.1398
X11c	1.7518	1.1226	.7805	.8914	.5986
X21c	-.3870	-.2486	-.1732	-.2000	-.1353
X31c	-.4160	-.2662	-.1848	-.2097	-.1401
X41c	-.3880	-.2492	-.1736	-.2004	-.1355

Table 7.25

3 Storeys & 3 Bays--- Unit Rotation at Hinge 21c

Hinge Moments	Case 1 $X=\frac{2}{3}, Y=4$:	Case 2 $X=\frac{5}{6}, Y=4$:	Case 3 $X=1, Y=4$:	Case 4 $X=\frac{2}{3}, Y=8$:	Case 5 $X=\frac{2}{3}, Y=12$
X12b	--	--	-.0092	--	--
X22a	-.0443	-.0347	-.0283	-.0137	-.0066
X12c	.0599	.0464	.0374	.0187	.0091
X22c	-.0830	-.0647	-.0525	-.0247	-.0117
X32c	.0208	.0164	.0134	--	--
X42c	.0247	.0195	.0161	--	--
X11b	.1825	.1139	.0771	.1044	.0731
X21b	-.0175	-.0123	-.0093	--	--
X31b	-.3605	-.2272	-.1554	-.1951	-.1336
X21a	.5728	.3689	.2577	.3136	.2165
X31a	-.3897	-.2498	-.1737	-.2020	-.1365
X11c	-.3870	-.2486	-.1732	-.2000	-.1353
X21c	1.7505	1.1216	.7798	.8916	.5988
X31c	-.4182	-.2677	-.1859	-.2100	-.1402
X41c	-.4160	-.2661	-.1848	-.2097	-.1401

Table 7.26

3 Storeys & 3 Bays--- Unit Rotation at Hinge 31c

Hinge Moments	Case 1 $X=\frac{2}{3},Y=4$:	Case 2 $X=\frac{5}{6},Y=4$:	Case 3 $X=1,Y=4$:	Case 4 $X=\frac{2}{3},Y=8$:	Case 5 $X=\frac{2}{3},Y=12$
X22b	-.0248	-.0188	-.0149	--	--
X32a	-.0443	-.0347	-.0283	-.0137	-.0066
X12c	.0247	.0195	.0161	--	--
X22c	.0208	.0164	.0134	--	--
X32c	-.0830	-.0647	-.0526	-.0247	-.0117
X42c	.0600	.0464	.0374	.0187	.0091
X11b	-.3514	-.2211	-.1510	-.1930	-.1332
X21b	.3074	.1903	.1279	.1845	.1316
X31b	-.2673	-.1652	-.1109	-.1633	-.1177
X21a	-.3898	-.2498	-.1737	-.2020	-.1365
X31a	.5728	.3689	.2577	.3136	.2165
X11c	-.4160	-.2662	-.1848	-.2097	-.1401
X21c	-.4182	-.2677	-.1859	-.2100	-.1402
X31c	1.7505	1.1216	.7798	.8916	.5988
X41c	-.3870	-.2486	-.1732	-.2000	-.1353

Table 7.27

3 Storeys & 3 Bays --- Unit Rotation at Hinge 41c

Hinge Moments	Case 1 $X=\frac{2}{3}, Y=4$:	Case 2 $X=\frac{5}{6}, Y=4$:	Case 3 $X=1, Y=4$:	Case 4 $X=\frac{2}{3}, Y=8$:	Case 5 $X=\frac{2}{3}, Y=12$
X22b	--	.0123	.0096	--	--
X32b	-.0340	-.0256	-.0201	-.0120	-.0061
X32a	.0177	.0137	.0111	--	--
X12c	.0432	.0334	.0270	.0135	.0065
X32c	.0442	.0342	.0276	.0140	.0068
X42c	-.0960	-.0745	-.0603	-.0294	-.0141
X11b	-.1979	-.1259	-.0868	-.1018	-.0683
X21b	-.3177	-.1984	-.1346	-.1830	-.1290
X31b	.4558	.2817	.1891	.2768	.1986
X21a	-.4088	-.2613	-.1813	-.2086	-.1398
X31a	-.3509	-.2262	-.1581	-.1891	-.1301
X11c	-.3880	-.2492	-.1736	-.2004	-.1355
X21c	-.4160	-.2662	-.1848	-.2097	-.1401
X31c	-.3870	-.2486	-.1732	-.2000	-.1353
X41c	1.7518	1.1226	.7805	.8914	.5986

Table 7.28

Unit Rotation at Hinge 22b

Effect of increasing No. of Storeys

Hinge Moments	3 Storeys 3 Bays	4 Storeys 3 Bays	5 Storeys 3 Bays
X13b	-.0479	-.0479	-.0479
X23b	.0899	.0899	.0899
X33b	-.1096	-.1096	-.1096
X33a	.1068	.1068	.1068
X13c	-.1008	-.1008	-.1008
X23c	.0558	.0558	.0558
X33c	.3328	.3328	.3328
X43c	-.1950	-.1950	-.1950
X12b	-.7464	-.7464	-.7464
X22b	3.0182	3.0181	3.0181
X32b	-.4959	-.4958	-.4958
X22a	.0871	.0871	.0871
X32a	.5109	.5108	.5108
X12c	-.1241	-.1241	-.1241
X32c	.1794	.1793	.1793
X42c	-.1851	-.1850	-.1850
X11b	-.0663	-.0664	-.0664
X21b	.1168	.1175	.1175
X31b	-.1430	-.1438	-.1438
X31a	-.0404	-.0394	-.0394

Note that the effect of increasing the no. of storeys is not significant

Table 7.29

Unit Rotation at Hinge 22b

Effect of increasing No. of Bays

Hinge Moments	3 Storeys 3 Bays	3 Storeys 4 Bays	3 Storeys 5 Bays
X13b	-.0479	-.0379	-.0315
X23b	.0899	.0720	.0785
X33b	-.1096	—	—
X43b	—	-.0477	—
X53b	—	—	.0462
X23a	—	—	—
X33a	.1068	.1126	.1254
X43a	—	-.1032	-.0866
X53a	—	—	-.0497
X13c	-.1008	-.0971	-.0867
X23c	.0558	.0629	.0768
X33c	.3328	.3303	.3421
X43c	-.1950	-.1539	-.1353
X53c	—	—	-.0364
X63c	—	—	-.0483
X12b	-.7464	-.7522	-.7335
X22b	3.0182	3.0795	3.1013
X32b	-.4959	-.7412	-.7526
X42b	—	-.0577	.0892
X52b	—	—	-.1228
X22a	.0871	.0958	.1168
X32a	.5109	.5026	.5206
X42a	—	-.2341	-.2061
X52a	—	—	-.0523
X12c	-.1241	-.1198	-.1016
X22c	—	—	—
X32c	.1794	.1816	.2014
X42c	-.1851	-.1628	-.1377
X52c	—	-.0713	-.0716
X62c	—	—	-.0749
X11b	-.0663	-.0549	-.0432
X21b	.1168	.0972	.1066
X31b	-.1430	-.0411	-.0331
X41b	—	-.0697	-.0437
X51b	—	—	-.0632
X21a	—	—	—
X31a	-.0404	—	—
X41a	—	—	—
X51a	—	—	—

Table 7.30
Properties of over-reinforced rectangular beams

At L_1			At L_2			
n_1	ω	m_1	n_2	ω	m_2	e_{c_2}
.75	.8074	.3594	.74	.806	.375	.00292
.76	.8226	.3623	.75	.822	.376	.00290
.77	.8377	.3651	.76	.837	.378	.00288
.78	.8529	.3679	.77	.852	.380	.00286
.79	.8682	.3706	.78	.867	.381	.00285
.80	.8834	.3733	.79	.883	.383	.00283
.81	.8986	.3760	.80	.898	.384	.00281
.82	.9138	.3786	.81	.913	.385	.00280
.83	.9291	.3811	.82	.928	.387	.00278
.84	.9443	.3836	.83	.942	.388	.00277
.85	.9595	.3860	.84	.957	.389	.00275
.61	.5977	.3136	.60	.595	.347	.00325
.62	.6124	.3172	.61	.608	.350	.00322
.63	.6272	.3208	.62	.622	.352	.00319
.64	.6420	.3243	.63	.637	.354	.00317
.65	.6569	.3277	.64	.651	.356	.00314
.66	.6718	.3311	.65	.666	.358	.00312
.67	.6868	.3344	.66	.681	.360	.00309
.68	.7017	.3377	.67	.697	.362	.00307
.69	.7168	.3410	.68	.712	.364	.00304
.70	.7318	.3442	.69	.728	.366	.00302
.71	.7469	.3473	.70	.744	.368	.00300
.72	.7620	.3504	.71	.760	.370	.00298
.73	.7771	.3534	.72	.775	.371	.00296
.74	.7922	.3564	.73	.791	.373	.00294

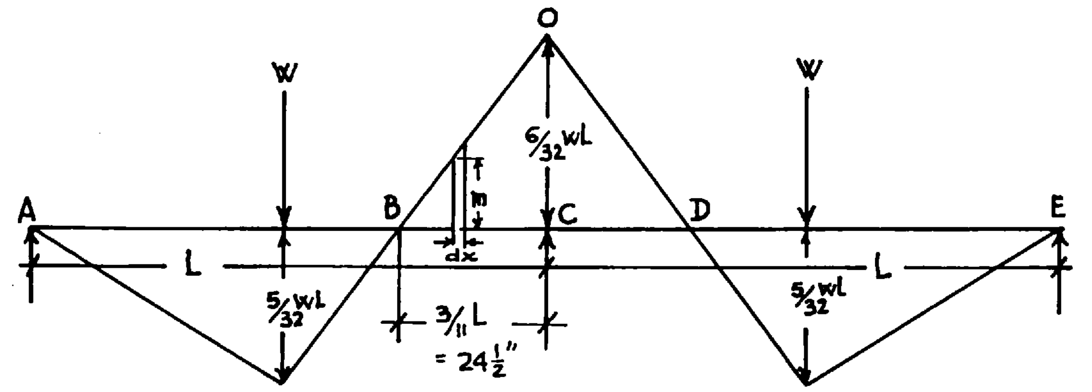

FIG 7.1

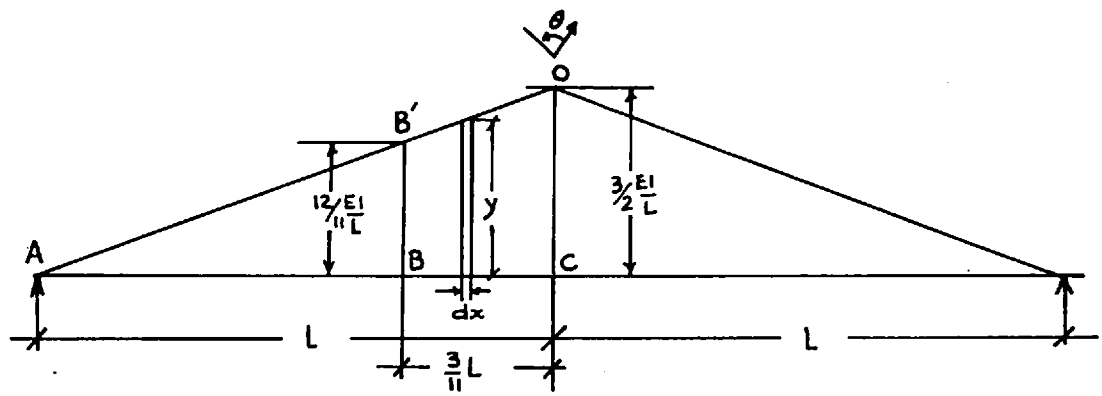

FIG 7.2

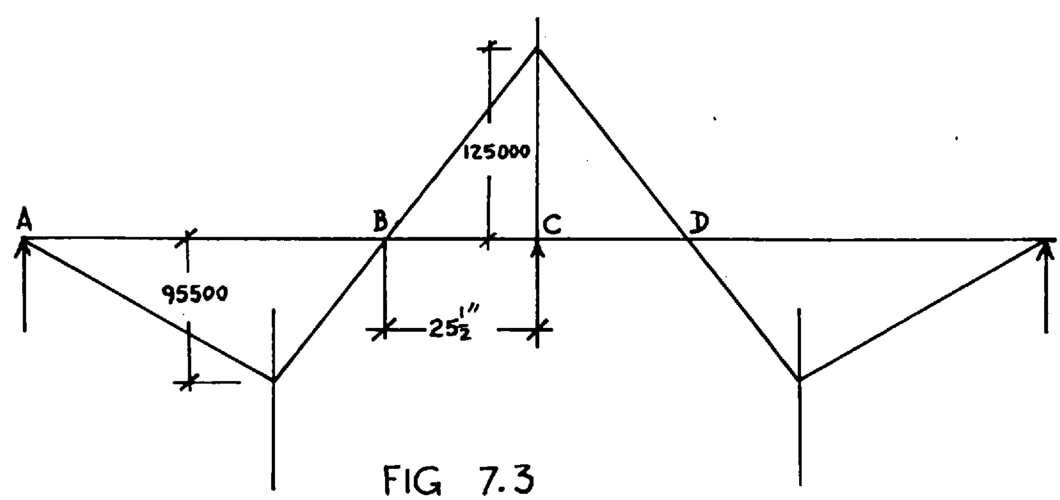

FIG 7.3

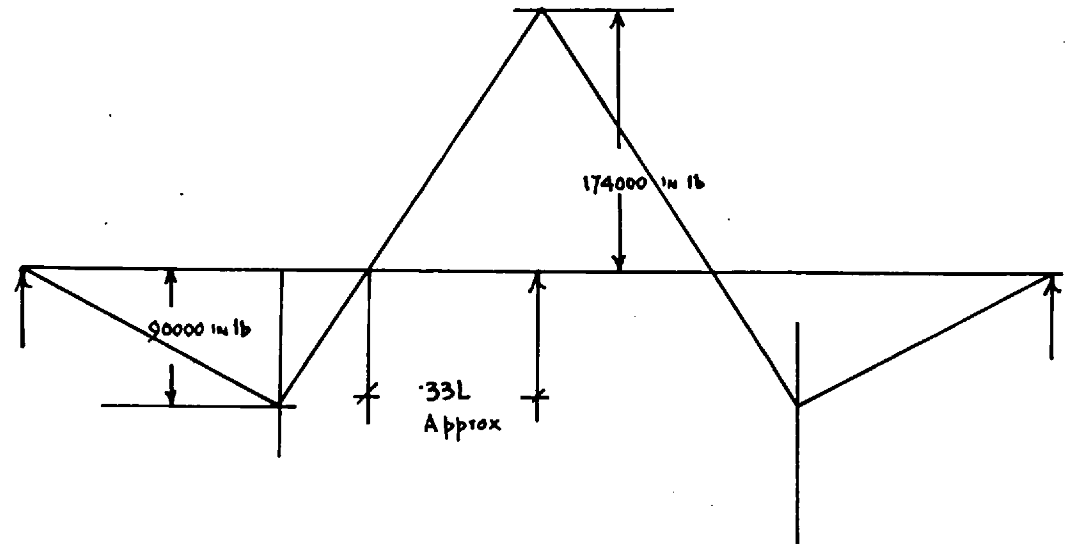

FIG 7.4

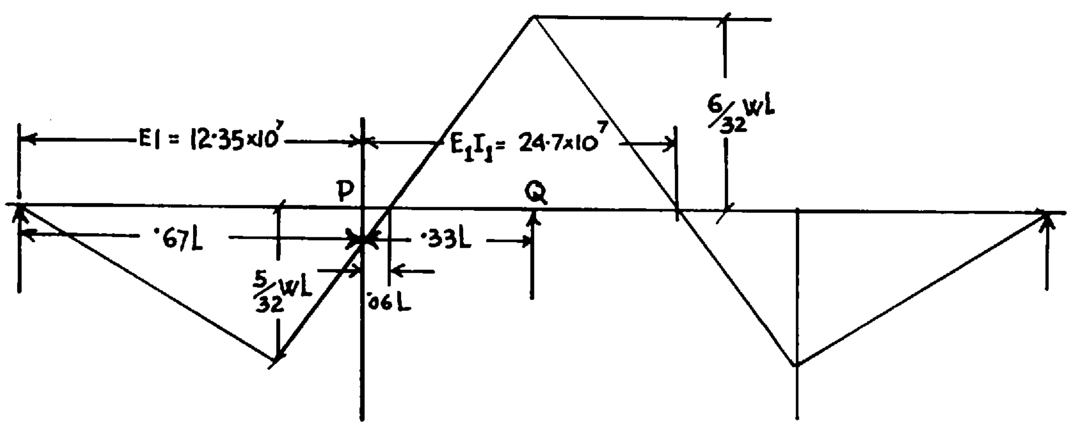

FIG 7.5

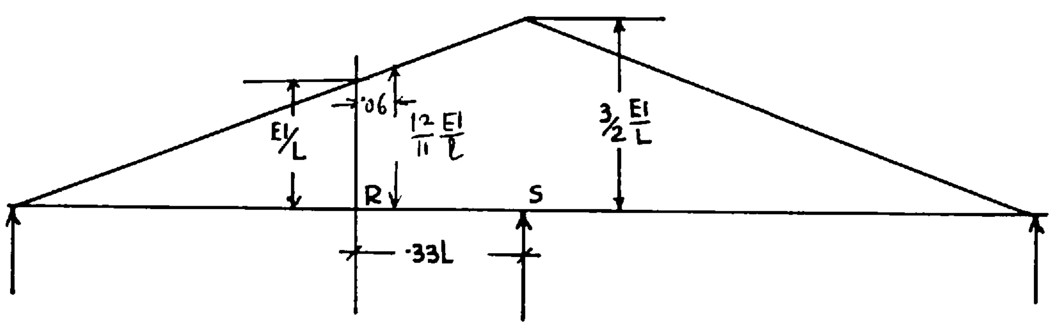

FIG 7.6

CHAPTER 8.

CONCLUSION AND SUGGESTION FOR FURTHER WORK.

8.1 It is concluded from the behaviour of Frame 1 (Chapter 6), that over-reinforced I-sections, in a prestressed concrete frame can have a brittle type failure and such a failure may occur without significant warning and before sufficient hinges are developed to form a mechanism.

It is also observed that an I-section is less ductile than a corresponding rectangular section. The author is of opinion that this is due to the buckling of the flange.

Pietrzykowski[40] observed that full re-distribution of moments did not necessarily take place in a frame in which the columns are heavily loaded.

The author has concluded from the test results of Frames 2 and 3, that adequate rotations to enable the frame to attain a state of full re-distribution of moments may be obtained in a prestressed concrete frame, irrespective of the fact that the critical sections be over-reinforced or may be subjected to high axial loads, provided the frame is reinforced with an adequate amount of binders.

An attempt has been made in appendix 16 to calculate the discontinuous rotations at hinges that would occur, if a Trilinear Idealization of moment curvature relationships is adopted at the critical sections of Frame 2. A significant difference is not noticed between the results obtained and those derived from a bilinear idealization.

This is due to the low cracking moment at the critical section at the foot of the left-hand column.

The presence of internal stresses in a frame can appreciably modify the hinge rotations. Calculations in respect of frame 2 are presented in appendix 17. Conclusions of this thesis are however, not affected. Not only are small secondary stresses unavoidable in an actual structure, but also it may be pointed out that a more severe demand on hinge rotations may arise in an actual structure as the sway load is decreased.

8.2 A suggestion for a future design method.

Let us assume that depending on further research and evidence a design method is found to be suitable for applicability to reinforced concrete or prestressed concrete framed skeletal structures when a complete collapse mechanism is about to form, i.e., in which n + 1 critical sections attain their moments of resistance under the factorized loads, but at all other critical sections, the moment is less than their respective moments of resistance.

Let us also assume that at the end of the above stage rotations have been calculated in the correct sense at the n + 1 hinges (including zero rotation at the last hinge). These rotations are unique, provided the problem of opening and closing of hinges has not arisen, and it is not possible to adjust their values.

The final problem is therefore to ensure that these rotations do take place by the adequate provision of binders where necessary. Suitable graphs showing the rotational capacities of hinges for different depths of neutral axis and different quantities of binders with more realistic values than presented in (11) will be useful for this purpose.

In an actual structure, if it is assumed that the moments of resistance m^* and the 'EI' value at the state of L_1 is the same at all critical sections, the rotation at a hinge will be found to be given by the expression

$$\frac{Km^*\ell}{EI}$$

where K is a parameter which determines the position of the hinge and ℓ is a constant depending on the dimensions of the frame.

$$\text{putting} \quad EI = \frac{M_1}{e_{c_1} / n_1 d}$$

$$\text{the rotation is} \quad \frac{Km^*\ell}{M_1} \cdot \frac{e_{c_1}}{n_1 d}$$

If the permissible rotation is obtained from equation 2.16 and provided the value of 'Z' is the same on both sides of the critical section, the following inequality must hold good.

$$2 \times .8\,(e_{c2} - e_{c1})\; K_1 K_2 \frac{Z}{d} > \frac{Km^* \ell}{M_1} \cdot \frac{e_{c1}}{n_1 d}$$

putting $Z = c\ell$

$$e_{c2} - e_{c1} > \frac{km^*}{M_1} \cdot \frac{1}{1.6\; K_1 K_2} \cdot \frac{e_{c1}}{n_1}$$

or $$\frac{e_{c2}}{e_{c1}} > 1 + K.\frac{m^*}{M_1} \cdot \frac{1}{1.6\; C\; K_1 K_2 n_1}$$

If the following values are assumed to hold good

$$m^* \simeq M_1$$

$$K = .2$$

$$C = .25$$

$$K_1 K_2 = .5$$

$$n_1 = .5$$

$$\frac{e_{c2}}{e_{c1}} > 1 + \frac{.2}{1.6 \times .25 \times .5 \times .5}$$

i.e., > 3

In simple cases, the problem reduces to a checking of the ratio $\frac{e_{c2}}{e_{c1}}$. Thereafter e_{c2} can be altered by providing the necessary quantity of binders.

8.3 Suggestions for future work.

The author has already pointed out that a state of full redistribution of moments may be achieved in a continuous beam without great difficulty, provided support moments are reduced with a corresponding increase in span moments.

However, if the overall economy of a continuous beam subjected to a uniformly distributed load plus live load, depends on a minimum volume of steel, it may be necessary to redistribute moments in the opposite direction i.e., a reduction of span moments may be necessary, accompanied by an increase in support moments.

It has been shown in appendix 18 that the hinge rotations needed at mid span hinges are comparatively higher. Thus Tests on 3 span continuous beams with over-reinforced I-sections should be carried out.

The author has discussed in Chapter 5, the behaviour of a cracked prestressed section. A computer programme for a non-linear analysis of frames, using the flexibility matrix and the equivalent 'EI' method proposed by the author, which takes into account the rib shortening effect by using the appropriate 'EA' value, and the change in the internal geometry by the 'effective' centroid method, also suggested by the author, and which also includes the effect of the change in the external geometry, will be extremely useful for further studies of frame behaviour.

APPENDIX - 1

FLOW DIAGRAM FOR CALCULATING (i) m_2 vs ω
(ii) n_2 vs ω

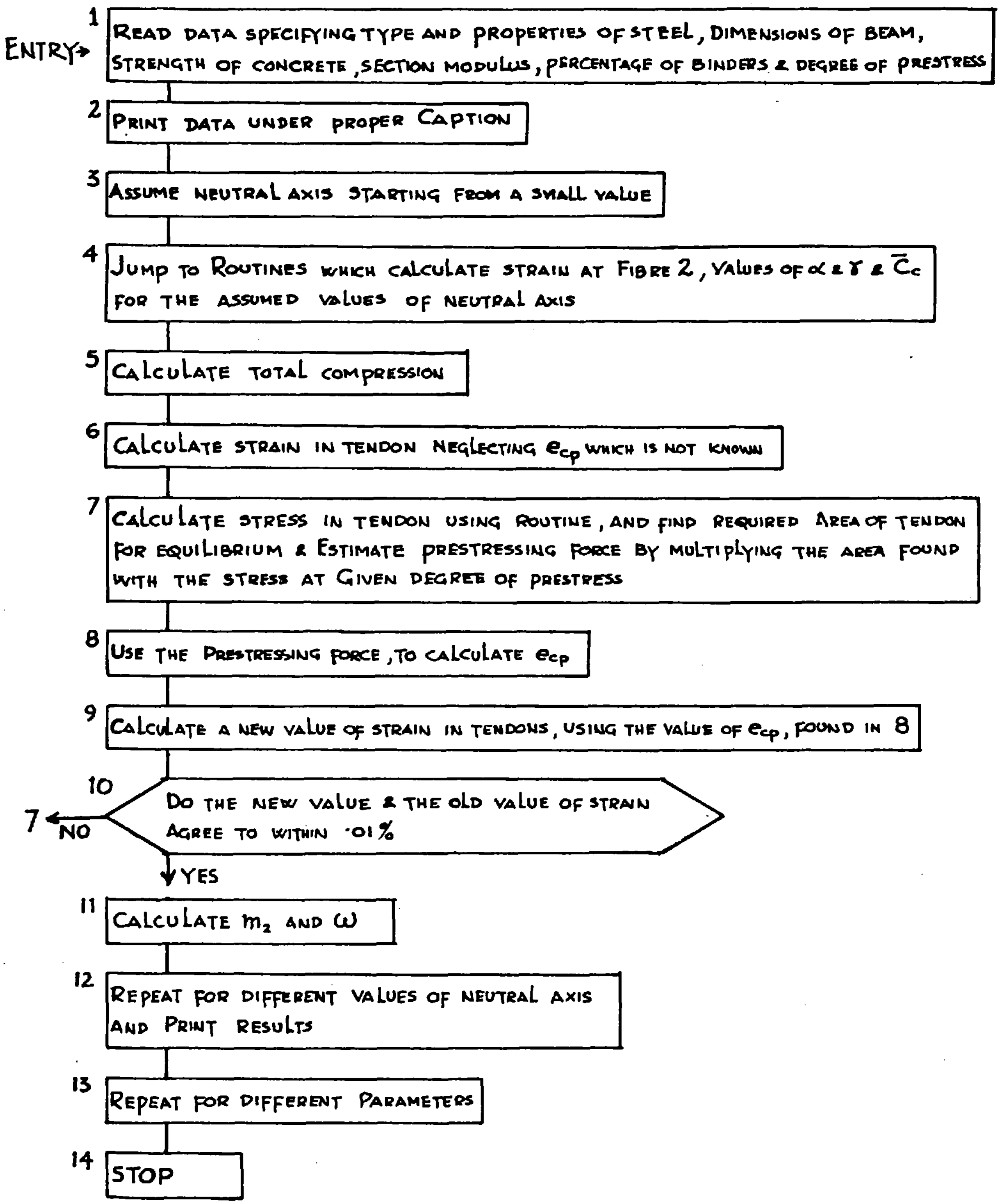

APPENDIX - 2

SUMMARY OF MIX DESIGN

1) Required strength of 6" cubes = $\frac{6000}{1.35}$ = 4450 p.s.i.
corresponding strength of 4" cubes = 4450 x 1.04
= 4620 p.s.i.
(Road note No.4, is based on 4" cube strength).

2) The water cement ratio for the above strength is .55.

3) For irregular aggregate ¾" down and low workability, the Aggregate cement ratio using curve No.3 is 6.00:1.

4) The proportioning by weight of all the constituents for each cft. of concrete is carried out as follows.

The volume of one beam & control specimens = 4 cft.

	1	2	3	4
	weight in lbs	sp.gr.	volume	weight of material per cft. in lbs.
F.a.	240	2.65	1.45	48
cement	100	3.12	.51	20
C.A.	360	2.65	2.17	72
water	55	1.00	.88	11
			5.01	

Say 5.00 cft.

An addition of 5% was made in col. 4, to make up for wastage.

The above mix was found to be too wet and the aggregate cement ratio actually used was 6.10:1.

APPENDIX - 3

CALCULATION OF CRACKING MOMENT IN BEAM NO. 5

Section Properties

	A	I	Z_1	Z_2	e_1	e_2
Grouted condition	35.93	250.67	63.8	61.2	3.92	4.08
Ungrouted condition	32.66	234.47	57.0	60.0	4.10	3.90

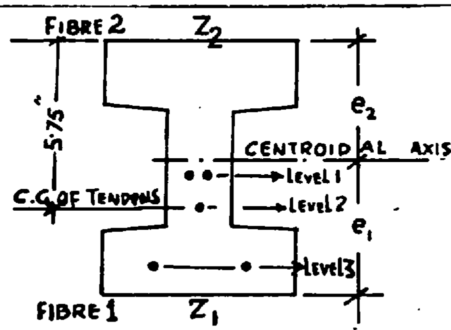

Average prestressing force (after losses) in each wire = 7560 lbs.

The stresses due to prestress and dead load, in ungrouted condition are as under.

f_{max} at fibre 1 =

$$\underset{(a)}{\frac{5 \times 7560}{32.66}} + \underset{(b)}{\frac{5 \times 7560 \times (5.75-3.90)}{57}} - \underset{(c)}{\frac{2400}{57}} = 2350$$

f_{min} at fibre 2 = a - b + c = 30

As a first approximation assume that the combined stresses due to prestress, dead load and live load are as follows.

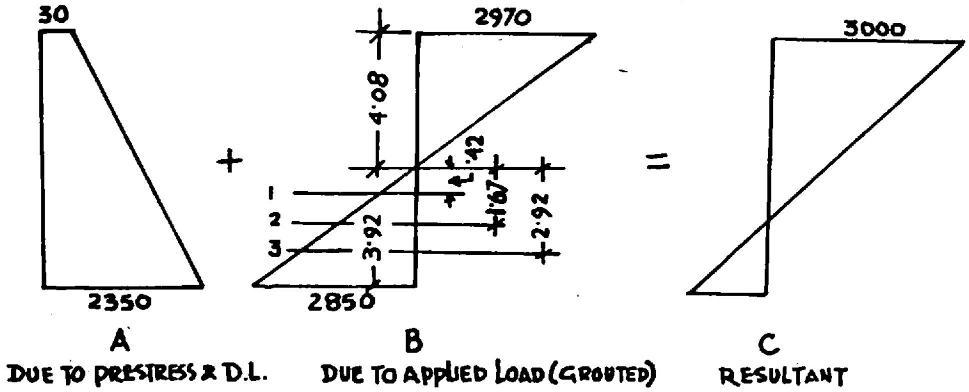

Due to the applied load, the prestressing force will increase, the assessment of which has been made as under.

	Level 1	Level 2	Level 3
change in stress	305	1213	2120
change in strain	.000061	.000242	.000424

(Assume E= $5x10^6$ in lb units)

The resultant force in each tendon is given in the following table

Tendon No.	Level	Initial strain	New strain	New force
1 & 2	1	.00435	.00441	2x7700
3	2	.00435	.00459	8000
4	3	.00430	.00472	8300
5	3	.004275	.00470	8300

The revised stresses due to prestress, dead load & those due to applied load to cause cracking by inducing a resultant tension of 500 lbs./sq. in. at fibre 1, are shown in the following diagram.

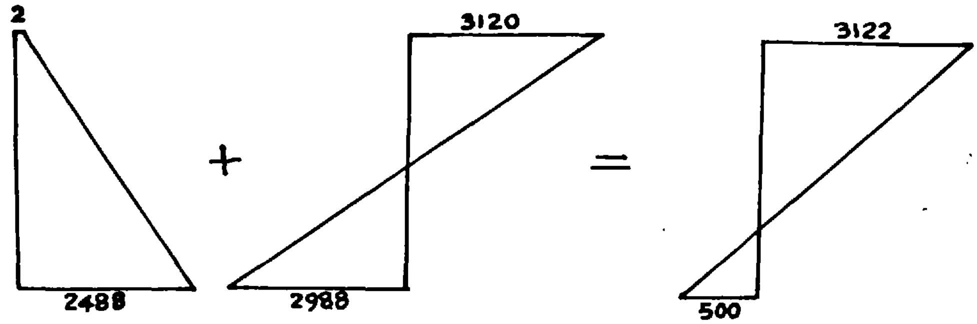

An improved value of cracking moment is therefore
= 2988 x 63.8 + 2400 (dead load moment)
=193400 in lbs.

The cracking moment according to Illinois bulletin No. 452, is given by the expression

$$f_t bd^2 \sqrt[2]{\frac{b'}{b}} \left(1 + \frac{F_{st}}{A_c f_t} \right)$$

Where f_t= 500 lbs./sq. in.

F_{se} = 37800 lbs.

b' = 2.25"

b = 6"

A_c = 34 sq. in. (approx)

On substuting the above values, the cracking moment will be found to be 195000 in lbs., which is close to the value obtained above.

APPENDIX - 4

CALCULATION OF STRESSES IN ANCHORAGE ZONE.

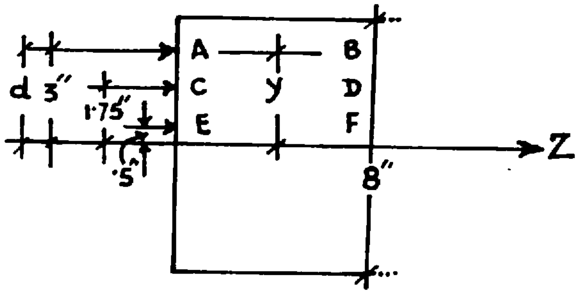

ELEVATION

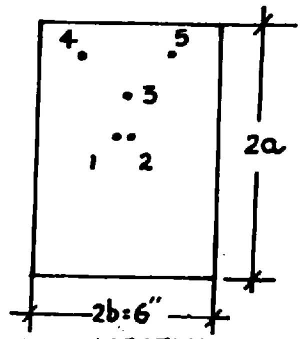

X-SECTION

Calculation of stresses along AB

Average stress in the X-section due to each tendon

$= \frac{7560}{48} = 157$ lbs./sq.in.

The coefficients for calculating stresses at various levels of z, for y = ¾a, as taken from Table 1 on page 516 of Guyon's 'Prestressed concrete' Vol. 1, are as under.

Tendon No.	Value of d	at z=0	at z=a/6	at z=a/3	at z=a/2
4 & 5	¾a	-2,079	-1.389	-.737	-.262
3	½a(approx)	-1.258	.580	-.227	-.425
1 & 2	¼a(approx)	- .865	-.387	-.486	-.364

The worst case is at z=0, where the net tensile stress = -2,079 x 314 - 1.258 x 157 - .865 x 314

= -1120 lbs./sq.in. (Negative sign stands for tension.)

Similarly tensile stresses were calculated along CD and EF.

An average value of 400 lbs./sq.in. was assumed. Total tensile force in a length of 4" along z is then = 400 x 6 x 4 = 9600 lbs.

Required area of mild steel = $\frac{9600}{20000}$ = .48 sq. in.

Area actually provided = .392 sq. in. (8 No.¼" Ø M.S. Bars)

APPENDIX - 5.

CALCULATION OF LOSSES IN PRESTRESS

(a) Losses due to elasticity of concrete (as applicable to post-tensioned beams, with straight cable which are consecutively tensioned).

If the beam has a total proportion of steel = 'p' in 'n' cables, area of each cable = $\frac{pA}{n}$ where A = total area.of concrete.

Let e_{s1}, e_{s2}, ... e_{sn}, be the respective eccentricities.

Stress in concrete at the level of x^{th} cable due to stress P_i in y^{th} cable = $p_i . \frac{p}{n}(1 + \frac{e_{sx}.e_{sy}}{r^2})$, where r = radius of gyration about x axis. The corresponding loss in prestress in x^{th} cable = $p_i \frac{pm}{n}(1 + \frac{e_{sx}.e_{sy}}{r^2})$ where m = modular ratio.

The total loss of stress when all the cables have been tensioned, where both vertical and horizontal eccentricities are present

$$= p_i \frac{mp}{n}\left[n - x + \frac{e_{sx}\{e_{s(x+1)} + e_{s(x+2)} + \cdots e_{sn}\}}{r^2} + \frac{e''_{sx}\{e''_{s(x+1)} + e''_{s(x+2)} + e''_{sn}\}}{r''^2}\right]$$

(where r" is the radius of gyration about y axis)

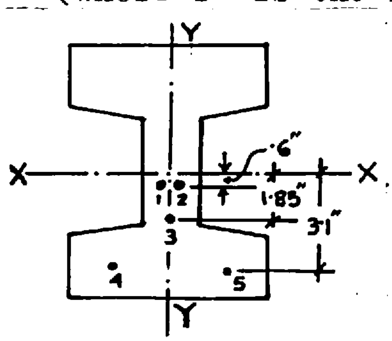

$m = \frac{30}{5} = 6$ say, Area of each tendon = .0596

Net effective area = 32.659 sq"

moment of inertia about yy = 76.67 in^4

$r''^2 = 2.35.$

moment of inertia about xx = 234.47 in^4

$r^2 = 7.17.$

Let tendons 1 to 5 be consecutively tensioned and let the desired force in each tendon after transfer from jack be 8000 lbs.

Loss in 1st wire.

$$= \frac{8000 \times 6 \times .0596}{32.659} \left\{ 4 + \frac{.6(.6 + 1.85 + 3.1 + 3.1)}{7.17} \right\}$$

= 415 lbs.

(b) Losses due to shrinkage.

After post tensioning, the beams were soon grouted. The effect of shrinkage after this stage in the beam, is as if they were pretensioned.

The total shrinkage strain does not cause an equal amount of loss of strain in steel because of elastic recovery in concrete.

Loss of strain in steel = shrinkage strain - elastic recovery of concrete.

If loss of steel stress is denoted by L_{psh} and σ denotes the shrinkage strain, then

$$L_{psh} = \sigma E_s - m\,\delta_f$$

where δ_f is change in concrete stress at the level of wire.

Compare this with the following equation which is applicable in case of a pre-tensioned beam, to find the loss of stress in steel after transfer.

$$p_t = p_i - m.f \text{ ....} \quad (B)$$

where p_t is the final stress in a wire

p_i " " initial " before transfer.

f is the concrete stress at the level of wire after transfer

Also $$p_t = p_i \left\{ \frac{r^2 + mp(r_s^2 - e.e_s)}{r^2 + mp(r^2 + r_s^2) + m^2p^2(r_s^2 - e_s^2)} \right\} \quad \text{---} (C)$$

where e_s = distance of C.G. of wires from centroid.

r_s = radius of gyration of wires only.

Loss of steel stress is found by substituting σ Es in the above formula in place of p_i.

Take the case of Beam No. 5

A = 35.93 (grouted condition), $mp = \frac{6x5x.0596}{35.93} = .0498$ = say .05

I = 250.67

$r^2 = 7.15$ $\qquad m^2p^2 = .0025$

$r_s^2 = \frac{(2x.42^2+2x.92^2+1.67^2)}{5} = 4.05$ $\qquad e_s = 1.67,\ e_s^2 = 2.78$

$e = .42$

$\therefore$ Loss in 1st and 2nd wire

$$= \sigma \times 30.4 \times 10^6 \frac{\{7.15 + 0.5(4.05 - .42 \times 1.67)\}}{7.15 + .05 \times 11.2 + .0025(4.05 - 2.78)}$$

$$= 28.8 \times \sigma \times 10^6$$

The value of σ has been taken as 15×10^{-6} (44)

$\therefore$ loss of stress = 430 lbs/sq.in. (Difference between the 26th and 36th day).

Loss of force = 430 x .0596
= say 25 lbs.

(c) <u>Loss due to creep of concrete</u>

Creep is proportional to the final stress in the concrete. The stress in each tendon immediately after post tensioning is not the same. An approximate expression for calculating the loss due to creep is however, obtained as follows, by neglecting this difference.

If p'_{t1} is the stress after creep loss has taken place in wire no. 1 and p_t is the stress in each wire immediately after transfer

then $p'_{t1} = p_t - E_s \gamma f_1 + m \delta f_1$ (neglect the last item, which represents elastic recovery.)

where f_1 is the final concrete stress adjacent to wire No.1

and γ is the creep strain per lb per sq. inch.

or $p'_{t1} = p_t - m E_c \gamma f_1$

Compare this with equation (B) for pretensioned beams.

Also loss of stress 'δt' in a wire is given by the expression

$$\delta t = \frac{p_i m p \left\{ r^2 + mp(r_s^2 - e_s^2) + e.e_s \right\}}{r^2 + mp(r^2 + r_s^2) + m^2p^2(r_s^2 - e_s^2)} \quad \ldots\ldots\ldots(D)$$

$\therefore$ Loss due to creep 'L_{pc} is obtained by substituting $mE_c\gamma$ in place of m and p_t in place of p_i

$$\therefore L_{pc} = \frac{P_t m p \gamma E_c \left\{ r^2 + mp\gamma E_c(r_s^2 - e_s^2) + e.e_s \right\}}{r^2 + mp\gamma E_c(r^2 + r_s^2) + m^2p^2\gamma^2E_c^2(r_s^2 - e_s^2)}$$

<u>Take the case of Beam 5</u>

The specific creep factor (at the end of 10 days) has been taken as 110 x 10^{-9}, from graphs published for similar type of concrete in magazine of Concrete Research Vo. 14, No. 40[44]

$mp = .05 \qquad m^2p^2 = .0025$

$\gamma E_c = 110 \times 10^{-9} \times 5 \times 10^6 = .55$

$r_s^2 = 4.05 \quad , \quad r^2 = 7.15$

$e_s = 1.67 \quad , \quad e_s^2 = 2.78$

$e = .42$

L_{pc} in 1st and 2nd wire.

$$= P_t \frac{.05 \times .55 \left\{ 7.15 + .0275(4.05 - 2.78) + .42 \times 1.67 \right\}}{7.15 + .0275(7.15 + 4.05) + .00075(4.05 - 2.78)}$$

$$= P_t \times \frac{.217}{7.46}$$

$= .029\ P_t$ say $.03\ P_t$

$= 255$ lbs. ($P_t = 8500$).

APPENDIX - 6.

CALCULATIONS OF MOMENTS AND ROTATIONS AT L_1 and L_2 in BEAM NO. 4.

Calculations at L_1

(a) $\bar{C}_c$ = .8 C_u = .8 x 6300 = 5040 lbs/sq"

(b) Value of e_p in Wire No. 1.

Strain attained by wire before locking off = 5860 micro strains..........................(A)

The corresponding force from stress-strain curve = 10250 (Fig 3.2). Note that the attained force is beyond the initial straight portion of the s-s curve.

Strain attained by wire after release of jack = 4900

The corresponding force as read on a st. line which is parallel to the initial slope of the s-s curve and passes through the point on the s-s curve corresponding to the strain at 'A' = 8500 lbs

Losses due to

1) elasticity - 320 lbs
2) shrinkage = 25 lbs
3) creep of concrete = 220 lbs
4) creep in steel = .04 (8500 - 320) = 328 lbs

Total = 893 say 900, lbs

Net force at the time of testing the beam = 7600

corresponding strain i.e., e_p = .0044

(c) Values of e_p and e_{cp} at different levels.

These values are tabulated below. Values of e_{cp} have been calculated from an average prestressing force after losses and taking the value of E_c as 5×10^6.

e_p and e_{cp} at various levels.

WIRE NO.	LEVEL	e_p	e_{cp}	total of av. e_p + e_{cp}
1	1	.0044	.00022	.00462
2	1	.00435	.00022	.00462
3	2	.0044	.00034	.00474
4	2	.0045	.00034	.00474
AT CG of tendons		Av. e_p = .0044	.00028	.00468

Av. = .00440

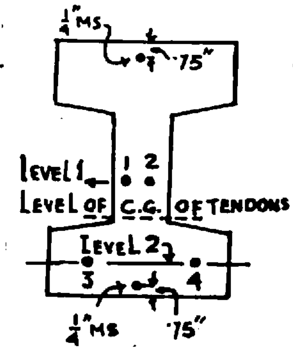

(d) Calculation of Strains.

The beam is under-reinforced and the state of L_1 will be attained when a tensile strain of .00735 - (value of $e_p + e_{cp}$ at C.G. of tendons) (Say .00267) is attained by the concrete at the level of C.G. of the tendons. (The strain of .00735 corresponds to 1% proof stress in steel.)

Assume $n_1 = .41$

$n_1 d = 2.36$

$d - n_1 d = 3.39$

Values of strain.

1) At top flange $= \dfrac{.00267}{3.39} \times 2.36 = .00186$

corresponding values of α and γ are, .645 and .371.

2) At the level of M.S. Bar in compression

$= \dfrac{.00267}{3.39} \times 1.61 = .00127$

3) At bottom of flange $= \dfrac{.00267}{3.39} \times .36 = .000284$,

α and γ at this level are .132 and .336.

The stress in concrete at this level

$$= 5040 \left\{1 - \left(1 - \frac{.000284}{.0020}\right)^2\right\} = 1310$$

4) At mid height of fillet = $\frac{.00267}{3.39} \times .235 = .000185$

The stress in concrete at this level = 850

5) At the level of tendons 1 and 2

$= \frac{.00267}{3.39} \times 2.14 = .00168.$

Total strain = .00630, total force using the idealized curve Fig. 3.4 = 2 x 10050 lbs.

6) At the level of tendons 3 and 4

$= \frac{.00267}{3.39} \times 4.64 = .00366.$

Total strain = .00840, total force using the idealized curve = 2 x 12500 lbs.

7) At the level of M.S. Bar at bottom

$= \frac{.00267}{3.39} \times 4.89 = .00385$

The strain exceeds the yield point,

$\therefore$ force .049 x 47000 = 2300 lbs.

(e) Total Tension = 20100 + 25000 + 2300 = 47400 lbs

(f) Total Compression = .645 x 6 x 2.36 x 5040 = 46000

Deduct for reduced width below flange

$(-)\ .132 \times 3.75 \times .36 \times 5040 = -900$

by Simpson's rule, force in fillet

$= \frac{1}{6 \times 4}\left(3.75 \times 1310 + 4 \times \frac{3.75}{2} \times 850\right) = +470$

Force in M.S.Bar = $.049 \times 30 \times 10^5 \times .00127 = 1900$

Total = 47470 lbs

(g) Moment at L_1 (Take moments about the C.G. of tendons.)

Due to concrete under compression

46000 (5.75 - .371 x 2.36)	=	2240000	
(-) 900 (3.75 - .336 x .36)	=	(-) 3270	
470 (5.75 - 2.08)	=	1725	(assume C.G. of fillet force at 2.08" below top of beam.)
due to M.S. Bar in compression			
1900 x 5	=	9500	
due to M.S. Bar in tension			
2300 x 1.5	=	3450	
due to difference of tensions in H.T. bars			
4900 x 1.25	=	6100	
∴ M_1	=	241505	

$$\frac{M_1}{M_{max}} = \frac{241500}{262300} = .92$$

(h) Rotation at L_1

$$= \frac{41 \times .00186}{2.36} = .0323$$

CALCULATIONS AT L_2

STRESS - BLOCK USED IS THAT PRESENTED BY 'BAKER' AT ANKARA, FOR DETAILS REFER TO CHAPTER 2.

Anticipated $n_2 = .35$.

Ultimate strain at top fibre $= .0015(1.0 + \frac{0.7}{.35}) = .0045$

$k = .443$, $\alpha = .852$

$k^2 = .197$

$$\gamma = \frac{6.197 - 4 \times .443}{12 - 4 \times .443} = .442$$

(a) <u>Values of strain</u> at trial value of n_2 = .335

n_2d = 1.93, $d - n_2d$ = 3.82

1) at level of M.S.Bar in compression

$= \frac{1.18}{1.93} \times .0045 = .00275$ (above yield point)

force in M.S. Bar = 2300

2) At the level of tendons 1 and 2

$= \frac{2.57}{1.93} \times .0045 = .0060$

Total strain = .01062, the force in the two tendons, using the idealized s-s curve = 25000

3) Similarly force in tendons 3 and 4 = 25000

4) Force in M.S. Bar in tension = 2300

(b) Total tension = 52300 lbs.

(c) <u>Total compression</u>

Due to concrete under compression

= .852 x 6 x 1.93 x 5040 = 497000

Due to M.S. Bar under compression

= = 2300

Total 52000 lbs.

neglect the small difference between tension and compression.

Also neglect the difference between anticipated n_2 and calculated value of n_2.

A revision of calculation by changing the stress block is not necessary.

The revised value of e_{c2} will be found to be .0046.

(d) <u>Moment at L_2</u>

Due to Concrete area, 497000 (5.75 - .442 x 1.93) = 245000

Due to M.S.Bar in compression 2300x5 = 11500

Due to M.S. " " tension 2300x1.5 = 3450

259950

$\frac{M_2}{M_{max}} = \frac{260000}{262300} = 1$ say. say 260000

(e) Rotation at L_2

$$= .0323 + 2 \times .8\,(.0046 - .00186) \times .5 \times \frac{41}{5.75}$$

(where .0046 is the value of e_{c2} recalculated for finding the rotation only.)

$$= .0479 \text{ RADIANS}$$

APPENDIX - 7.

MOMENT CURVATURE RELATIONS FROM CURVATURE DISTRIBUTION DIAGRAMS.

Moment curvature relations at the centres of 6 gauges near the critical section, has been plotted in case of Beams 3, 4 and 5 (vide graph 3.11).

The dimensionless parameters M/M_{max} and K/K_{max} have been graphically connected in the following way.

Take the example of Beam No.3.

The ordinate OY represents half the length of the beam between the support and the critical section at centre. The dotted curves represent the curvature distribution at various stages of loading.

The ordinate OY has been divided into 10 equal parts and it also represents the various fractions of the parameter M/M_{max}.

The line YZ shows the fractions of the parameter $\frac{K}{K_{max}}$, which have been used for plotting the curvature distribution as well as the relation between $\frac{M}{M_{max}}$ and $\frac{K}{K_{max}}$.

XO shows the various load stages as a fraction of the final load stage (which is L.S.14). OX is of the same length as OY and YZ.

The centres of gauges 1 to 6 are plotted at their respective position on OY and connected with X by straight lines which are partly shown terminated by letters G_1, G_2 - G_6 etc.

Let it be required to plot the relevant point on the M/M_{max} v_s K/K_{max} curve for gauge No. 3 at L.S.10.

Let the horizontal through the point corresponding to gauge No. 3, on OY, meet the curvature distribution curve for L.S.10 at the point P. The vertical PQ through P must pass through the desired point.

Let a vertical line be drawn through the point representing L.S.No.10 on XO and let it cut the sloped line joining gauge No. 3 at S. The horizontal RS through S then gives the required fraction on the ordinate oy representing M/M_{max}.

The required point is the intersection of PQ and RS, and is shown by a triangle. All points relating to the curve for gauge No. 3, for different load stages are shown by small triangles.

Appendix 8

Elastic analysis of Frames 1 2 & 3

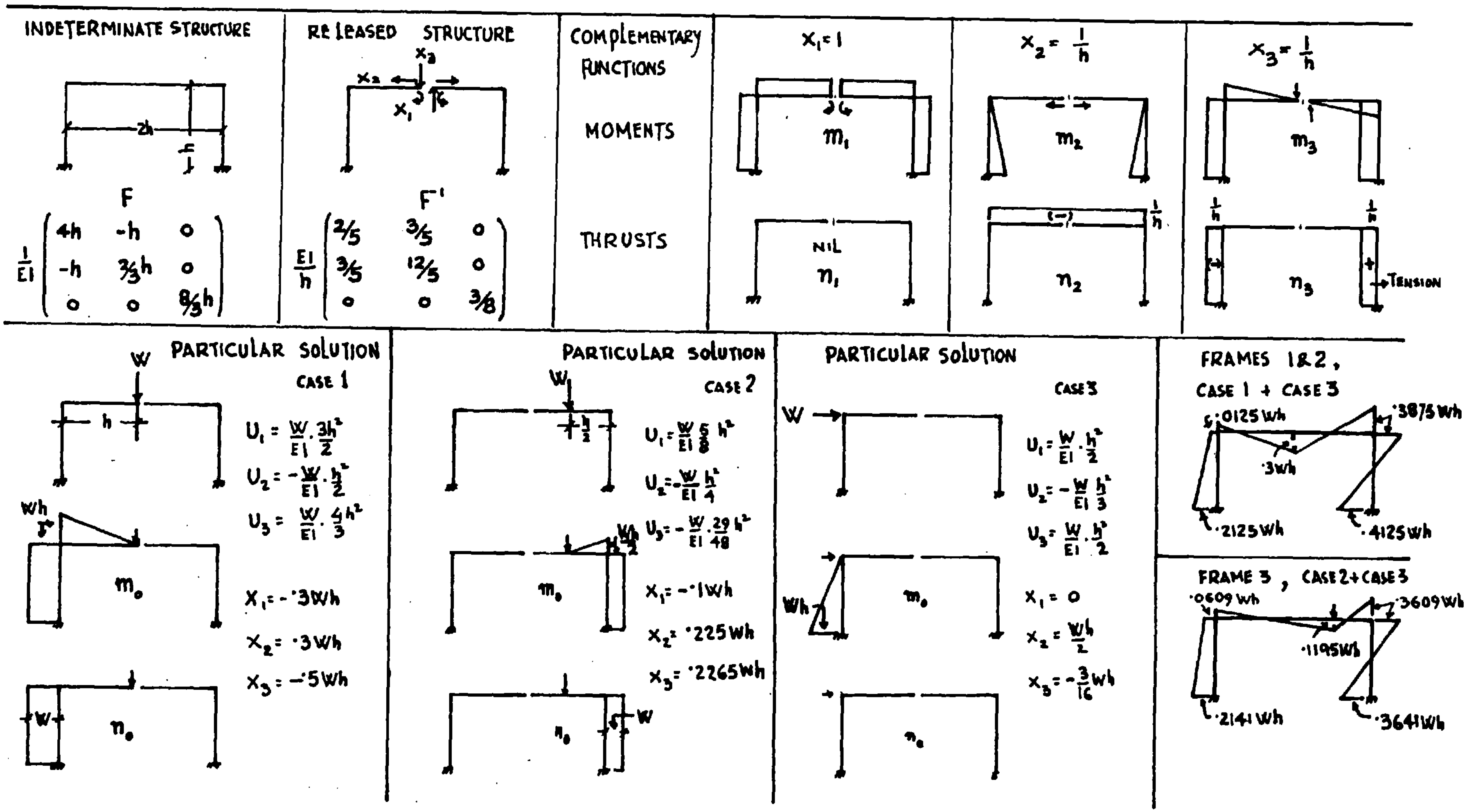

APPENDIX 9

CALCULATIONS FOR CONCORDANCY

	FRAMES 1&2	FRAME 3
LET THE +VE DIRECTION OF ECCENTRICITIES BE AS →	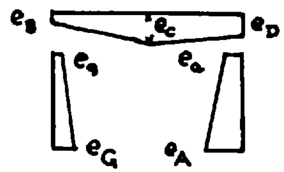	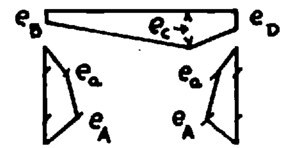 NOTE– ECCENTRICITIES IN COLUMNS ARE AT QUARTER LENGTHS
THE CONDITION $U^{P}_{123} = 0$, GIVES	$\int \frac{m_p m_1 ds}{EI} = 0$, OR $e_B + 2e_c + e_D + e_a + e_A + e_g + e_G = 0$ — ① $\int \frac{m_p m_2 ds}{EI} + \int \frac{n_p n_2 ds}{EA} = 0$, OR $e_a + e_g + 2(e_A + e_G) = \frac{P_B}{EA_B} \cdot \frac{2h}{h} \cdot \frac{6EI_c}{P_c h}$ where P_B = THRUST IN BEAM, P_c = THRUST IN COLUMN A_B = AREA OF X-SECTION IN BEAM, I_c = MOMENT OF INERTIA OF COLUMN. ASSUMING $P_B = P_c$ & SUBSTITUTING THE VALUES OF A_B, I_c & h, WE GET $e_a + e_g + 2(e_A + e_G) = {\cdot}94$ — ② $\int \frac{m_p \cdot m_3 ds}{EI} = 0$, OR $2e_B - 2e_D + 3(e_g - e_a + e_G - e_A) = 0$ — ③	$\int \frac{m_p m_1 ds}{EI} = 0$, OR $3e_B + 4e_c + e_D + 3e_a + 3e_A = 0$ $\int \frac{m_p m_2 ds}{EI} + \int \frac{n_p n_2}{EA} = 0$, OR $\frac{2h}{8I}(e_a + 2e_A) = \frac{2}{A}$ where A = AREA OF X-SECTION OF BEAM OR COLUMN I = MOMENT OF INERTIA OF BEAM OR COLUMN SUBSTITUTING THE VALUES OF h, I & A, WE GET $e_a + 2e_A = {\cdot}444$ — ② $\int \frac{m_p m_3 ds}{EI} = 0$, OR $9e_B - 4e_c - 5e_D = 0$ — ③
PROPOSED ECCENTRICITIES →	$e_a = e_D = -1{\cdot}2$, $e_g = e_B = -{\cdot}5$ $e_c = 1{\cdot}04$, $e_A = 1{\cdot}243$, $e_G = {\cdot}077$	$e_a = -{\cdot}445$, $e_A = {\cdot}445$ $e_B = e_c = e_D = 0$

APPENDIX 10

STEP BY STEP ANALYSIS OF FRAMES

	FRAMES 1 & 2				FRAME 3			
STAGE	SRUCTURE & RELEASES	F	X_{123}	B.M. DISTRIBUTION	STRUCTURE & RELEASES	F	X_{123}	BM DISTRIBUTION
1	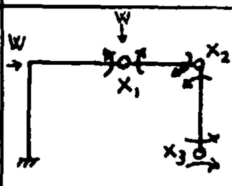 1ST HINGE AT X_3	$\frac{h}{EI}\begin{pmatrix} \frac{20}{3} & \frac{11}{3} & 1 \\ \frac{11}{3} & \frac{10}{3} & \frac{2}{3} \\ 1 & \frac{2}{3} & \frac{2}{3} \end{pmatrix}$	$X_1 = \cdot 3wh$ $X_2 = \cdot 3875wh$ $X_3 = \cdot 4125wh = m$	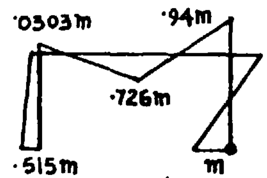 $W_1 = 2{\cdot}425\frac{m}{h}$	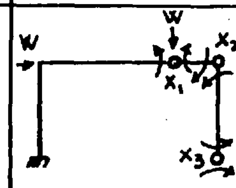 1st HINGE AT X_3 & 2nd " " " X_2	$\frac{h}{EI}\begin{pmatrix} \frac{80}{3} & \frac{62}{3} & 2 \\ \frac{62}{3} & \frac{52}{3} & \frac{5}{3} \\ 2 & \frac{5}{3} & \frac{2}{3} \end{pmatrix}$	$X_1 = \cdot 1195Wh$ $X_2 = \cdot 3609Wh$ $X_3 = \cdot 3641Wh = m$	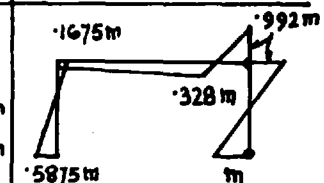 $W_1 = 2{\cdot}75\frac{m}{h}$
2	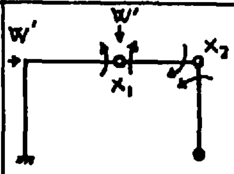 2nd HINGE AT X_2	$\frac{h}{EI}\begin{pmatrix} \frac{20}{3} & \frac{11}{3} \\ \frac{11}{3} & \frac{10}{3} \end{pmatrix}$	$X_1 = \cdot 342W'h$ $X_2 = \cdot 424W'h$ $\cdot 424W'h = \cdot 06m$ $W' = \cdot 142\frac{m}{h}$	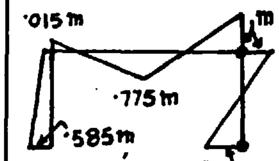 $W_2 = W_1 + W' = 2{\cdot}567\frac{m}{h}$	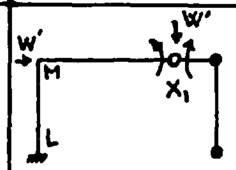 3rd HINGE AT L	$\frac{h}{EI} \cdot \frac{80}{3}$	$X_1 = \cdot 426W'h$ MOMENT AT L $= \cdot 792W'h$ $\cdot 792W'h = \cdot 4125m$ $W' = \cdot 52m/h$	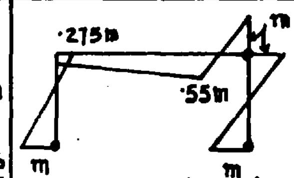 $W_2 = W_1 + W' = 3{\cdot}27\frac{m}{h}$
3	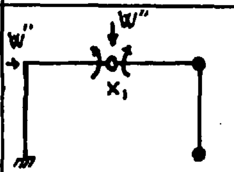 3rd HINGE AT X_1	$\frac{h}{EI} \cdot \frac{20}{3}$	$X_1 = \cdot 575W''h$ $\cdot 575W''h = \cdot 225m$ $W'' = \cdot 39\frac{m}{h}$	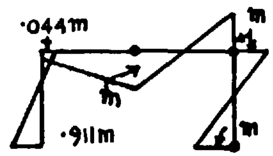 $W_3 = W_2 + W'' = 2{\cdot}957\frac{m}{h}$	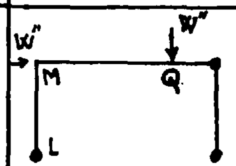 4th & 5th HINGE AT Q & M	MOMENT AT Q $= \cdot 625W''h$	$\cdot 625W''h = \cdot 45m$ $W'' = \cdot 72\frac{m}{h}$	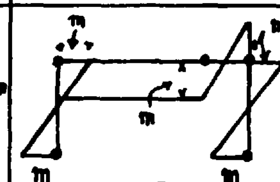 $W_3 = W_2 + W'' = 3{\cdot}99\,m/h$ COLLAPSE LOAD BY VIRTUAL WORK = 4m/h
4	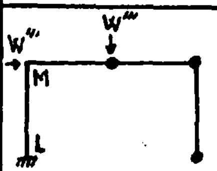 4th HINGE AT L	MOMENT AT L $= 2W'''h$	$2W'''h = \cdot 089m$ $W''' = \cdot 0445\frac{m}{h}$	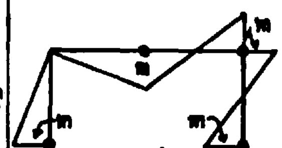 $W_4 = W_3 + W''' = 3{\cdot}0015\frac{m}{h}$				

COLLAPSE LOAD BY VIRTUAL WORK = $\frac{3m}{h}$

LEGEND

RELEASE HINGES → o

PLASTIC HINGES → •

PLASTIC MOMENT OF RESISTANT IN BEAM & COLUMNS → m

TOTAL LOAD $W_{1,2}$ etc

ADDITIONAL LOAD W', W'' etc

APPENDIX 11

COLLAPSE LOAD UNDER DIFFERENT MECHANISMS

FRAMES 1 & 2

VIRTUAL WORK EQUATION

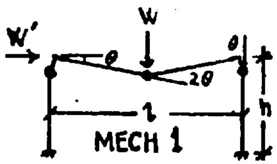

$$\frac{Wl}{2}\times\theta = m(\theta+\theta+2\theta)$$

$$W = \frac{8m}{l}$$

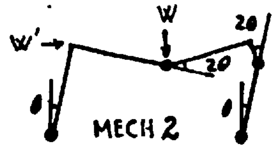

$$\frac{Wl}{2}\times\theta + W'h\theta = m(\theta+\theta+2\theta+2\theta)$$

$h = \frac{l}{2}$ $\therefore$ $W = \frac{6m}{\frac{l}{2}(1+T)}$, $T = \frac{W'}{W}$

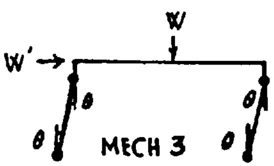

$W'h\theta = 4m\theta$, $W' = TW$

$$\therefore W = \frac{8m}{Tl}$$

PUTTING $T=1$ $W = \frac{8m}{l}$ FOR MECH 1 & 3

& $W = \frac{6m}{l}$ FOR MECH 2

IF $W = W'$, FAILURE WILL OCCUR UNDER MECH 2

FRAME 3

VIRTUAL WORK EQUATION

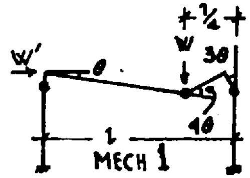

$$\frac{W3l}{4}\theta = m(\theta+3\theta+4\theta)$$

$$W = 10\tfrac{2}{3}\frac{m}{l}$$

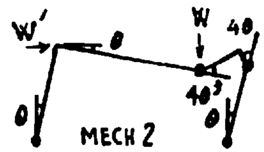

$$\frac{W.3l}{4}\theta + W'h\theta = m(\theta+\theta+4\theta+4\theta)$$

$$W = \frac{10m}{\frac{3l}{4}+\frac{Tl}{2}}$$

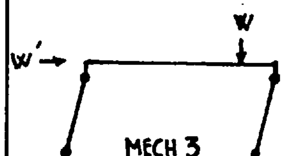

$$W'h\theta = 4m\theta$$

$$W = \frac{8m}{Tl}$$

PUTTING $T=1$ $W = \frac{10{\cdot}67m}{l}$ FOR MECH 1

$W = \frac{8m}{l}$ FOR BOTH MECH 2 & 3

IF $W = W'$, FAILURE WILL OCCUR UNDER A COMBINATION OF MECH 2 & 3 (OVERCOMPLETE MECH)

PIETRZYKOWSKI'S FRAME

VIRTUAL WORK EQUATION

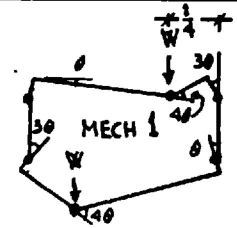

$$W.\frac{3l}{4}.\theta = m_c(\theta+3\theta) + m_b.4\theta$$

$$W = \frac{16(m_c+m_b)}{3l}$$

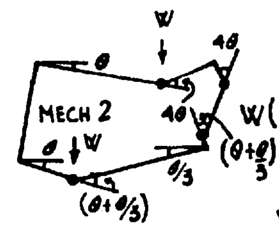

$$W\left(\frac{3l\theta}{4}+\frac{l\theta}{4}\right) = m_c\left(4\theta+\theta+\frac{\theta}{3}\right) + m_b(4\theta+\theta+\theta/3)$$

$$W = \frac{16(m_c+m_b)}{3l}$$

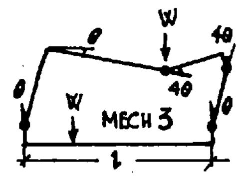

$$W.\frac{3l}{4}\theta = m_c.6\theta + m_b.4\theta$$

$$W = \frac{24(m_c+m_b)}{3l}$$

FAILURE WILL OCCUR UNDER A COMBINATION OF MECH 1 & 2 i.e, ALL 6 HINGES WILL FORM

APPENDIX 12

CALCULATION OF ROTATIONS AT COLLAPSE

	FRAMES 1&2	FRAME 3
CHOSEN RELEASE SYSTEM & COMPLEMENTARY FUNCTION MOMENT DIAGRAMS	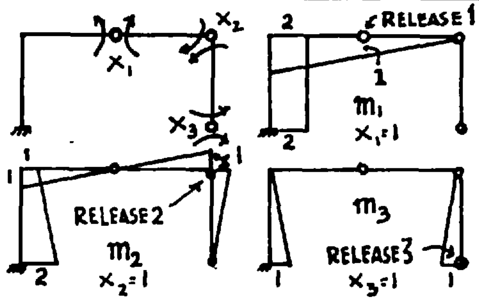	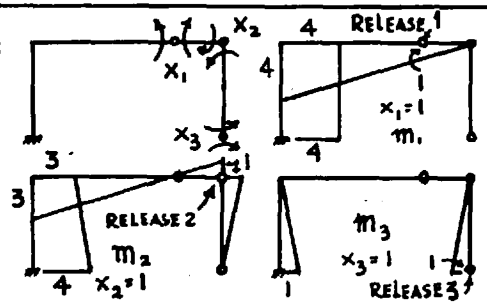
DISTRIBUTION OF BENDING MOMENT AT COLLAPSE	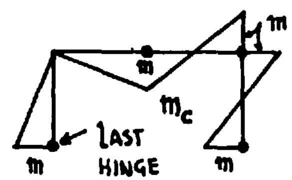	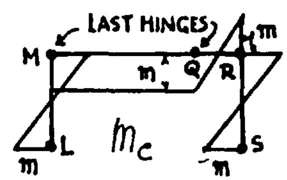
ROTATIONS AT HINGES OBTAINED BY INTEGRATING m_c DIAGRAM WITH m_{123} DIAGRAMS	ROTATION OF PLASTIC HINGE AT RELEASE NO 1 $= -\frac{mh}{6EI}$ DO AT RELEASE 2 $= -\frac{mh}{3EI}$ DO AT RELEASE 3 $= -\frac{mh}{6EI}$	ROTATION OF PLASTIC HINGES AT RELEASE NO 1 $= \frac{23}{6}\frac{mh}{EI}$ AT RELEASE NO 2 $= \frac{7}{3}\frac{mh}{EI}$ AT RELEASE NO 3 $= 0$ NOTE - THE CHOSEN RELEASE SYSTEM INCLUDES ONE LAST HINGE, (RELEASE 1) AND HINGE ROTATIONS AT RELEASES 1 & 2 ARE NOT OF CORRECT SIGN

CORRECT ROTATIONS IN FRAME 3

ROTATION AT RELEASE 1 MUST BE O. THE TRANSFORMATION MATRIX TO CONVERT A ROTATION OF $\frac{23}{6}\frac{mh}{EI}$ AT Q, TO O IS GIVEN BY

$$dv = K\,du$$

$$\begin{vmatrix} dv_1 \\ dv_2 \\ dv_3 \end{vmatrix} = \begin{vmatrix} K_1 \\ K_2 \\ K_3 \end{vmatrix} du \qquad \text{WHERE } du = -\frac{23}{6}\frac{mh}{EI}$$

K_1, K_2, K_3 ARE THE ORDINATES OF BENDING MOMENT DIAGRAMS AT Q, FOR UNIT MOMENT ACTING AT L, R & S (I.E., THE POINTS WHERE HINGES DO FORM PRIOR TO COLLAPSE)

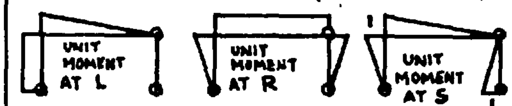

FROM ABOVE DIAGRAMS

$K_1 = \frac{1}{4}$, $K_2 = 1$, $K_3 = \frac{1}{4}$

$\therefore$ CORRECT ROTATIONS PRIOR TO COLLAPSE ARE

AT L, $\left(0 - \frac{23}{6}\times\frac{1}{4}\right)\frac{mh}{EI} = -\frac{23}{24}\frac{mh}{EI}$

AT R, $\left(\frac{7}{3} - \frac{23}{6}\right)\frac{mh}{EI} = -\frac{3}{2}\frac{mh}{EI}$

AT S, $\left(0 - \frac{23}{6}\times\frac{1}{4}\right)\frac{mh}{EI} = -\frac{23}{24}\frac{mh}{EI}$

AT Q, $\left(\frac{23}{6} - \frac{23}{6}\right)\frac{mh}{EI} = 0$

APPENDIX 13.

EFFECTIVE CENTROID OF A SECTION SUBJECTED TO PLASTICITY.

DATA:- Concrete cube strength = 5000 lbs/sq.".
Assumed cylinder " = 4000 lbs/sq.".
Yield stress of M.S.Bars= 47000 lbs/sq.".
E for M.S. Bars = 30.5×10^6 lbs/sq.".

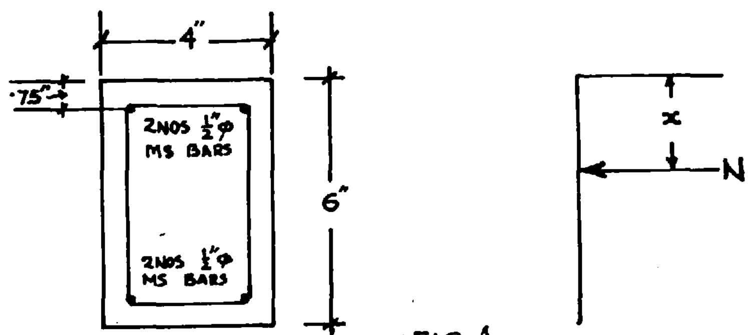

FIG 1

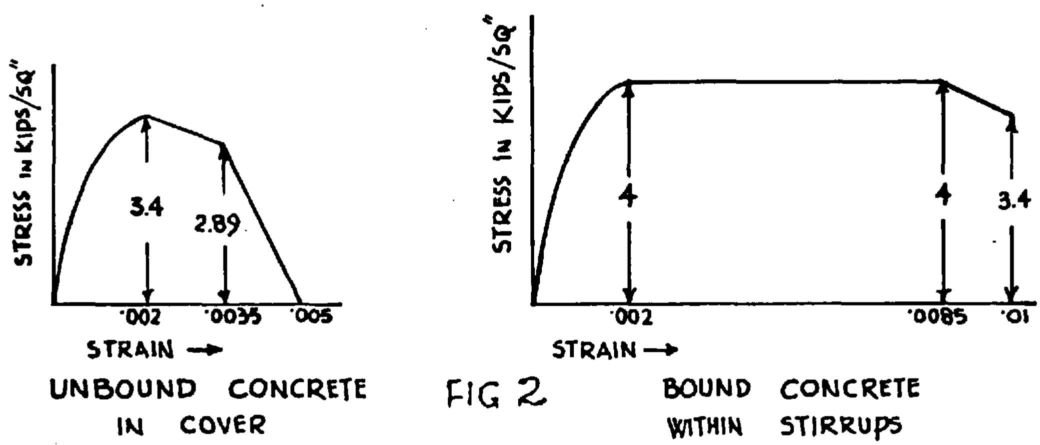

FIG 2

The section shown in Fig.1, was analyzed by the author, with the aid of the computer of the Cement and Concrete Association, using Cranston's M-P-Ø-θ programme. Concrete which was outside the zone bound by stirrups was treated as unbound and was assumed to have a different stress-strain characteristic, as shown in Fig.2.

Three cases were investigated in which the values of N varied from 0 to 40 and the values of x were .75", 1.5" and 3". The M-K curves are presented in Figs 3 to 5. It can be noticed that in Fig 3, the M-K curve for N=0 is at the top and the curve for N=40 is at the bottom. The opposite is true in Fig 5. In Fig 4, when x = 1.5", a crowding of the curves is noticeable in the inelastic zone. In fact a crossing over of the curves can be seen, the curve for N = 30 being within the envelopes for N = 10 and N = 20.

If N is plotted against K as shown in Figs 6, 7 and 8, it may be seen that when x = 1.5" (Fig 7), there is a minimum value of curvature, i.e. $\frac{dK}{dN} = 0$, for at least one case in the neighbourhood of the ultimate.

The value of 'x' found above (which is 1.5") satisfies the condition of being the effective centroid for N = 22, and M = 90.

We observe from Fig 4, that , for a wide range of axial loads, the values of moments are within a close range, for the same value of K.

The author thinks that in a practical case, the value of 'x' if assessed by calculating the position of the neutral axis at the ultimate moment, when N = 0, is sufficiently accurate. Further verification is however necessary. In the particular case investigated, it is true that the depth of the neutral axis is 1.5" when N = 0 and M = 86 units,(which is approximately the ultimate moment with N = 0).

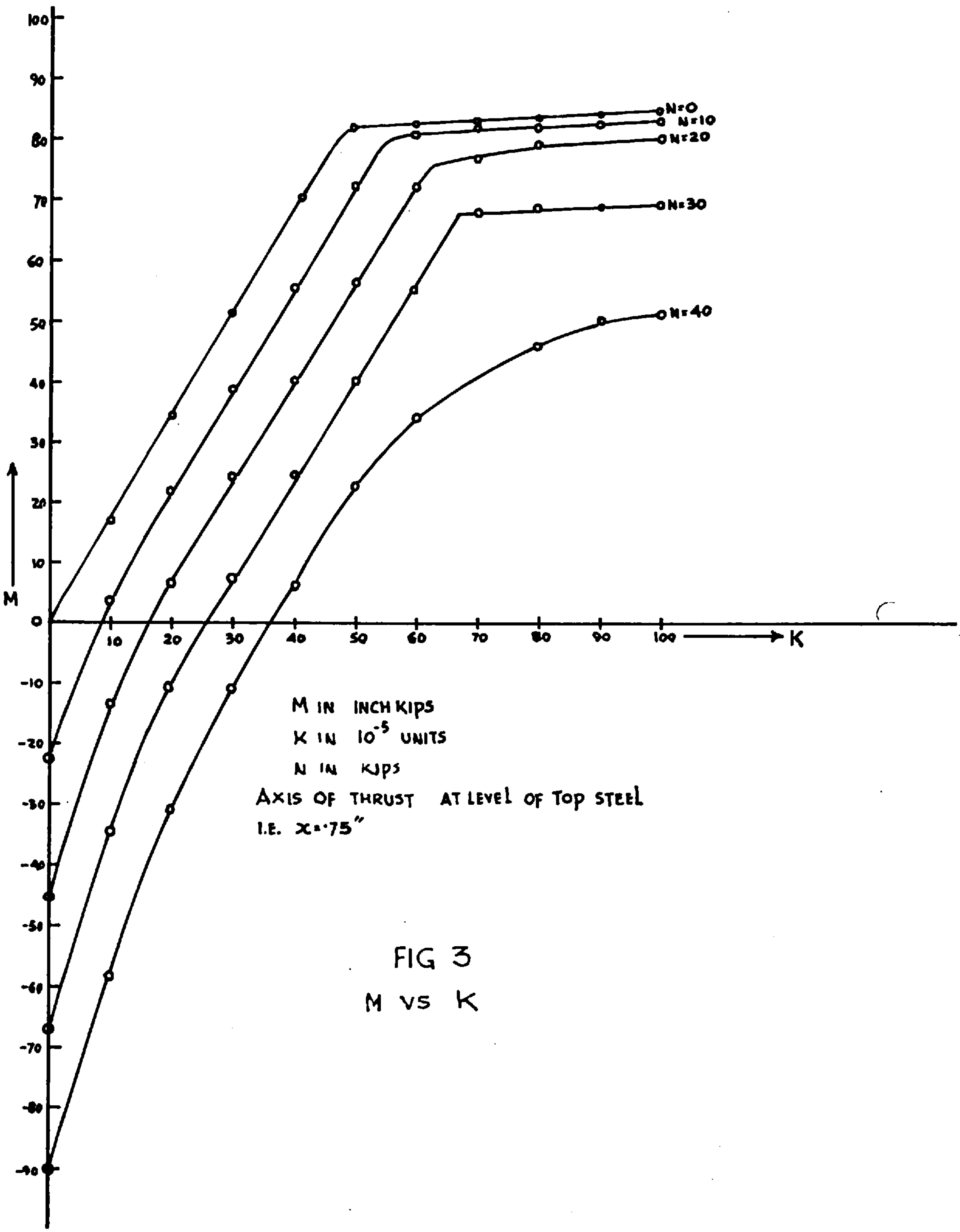

100
90
80
70
60
50
40
30
20
10
0
-10
-20
-30
-40
-50
-60
-70
-80
-90
M
10
20
30
40
50
60
70
80
90
100
K
N=0
N=10
N=20
N=30
N=40
M IN INCH KIPS
K IN 10^{-5} UNITS
N IN KIPS
AXIS OF THRUST AT LEVEL OF TOP STEEL
I.E. $x = \cdot 75''$

FIG 3
M vs K

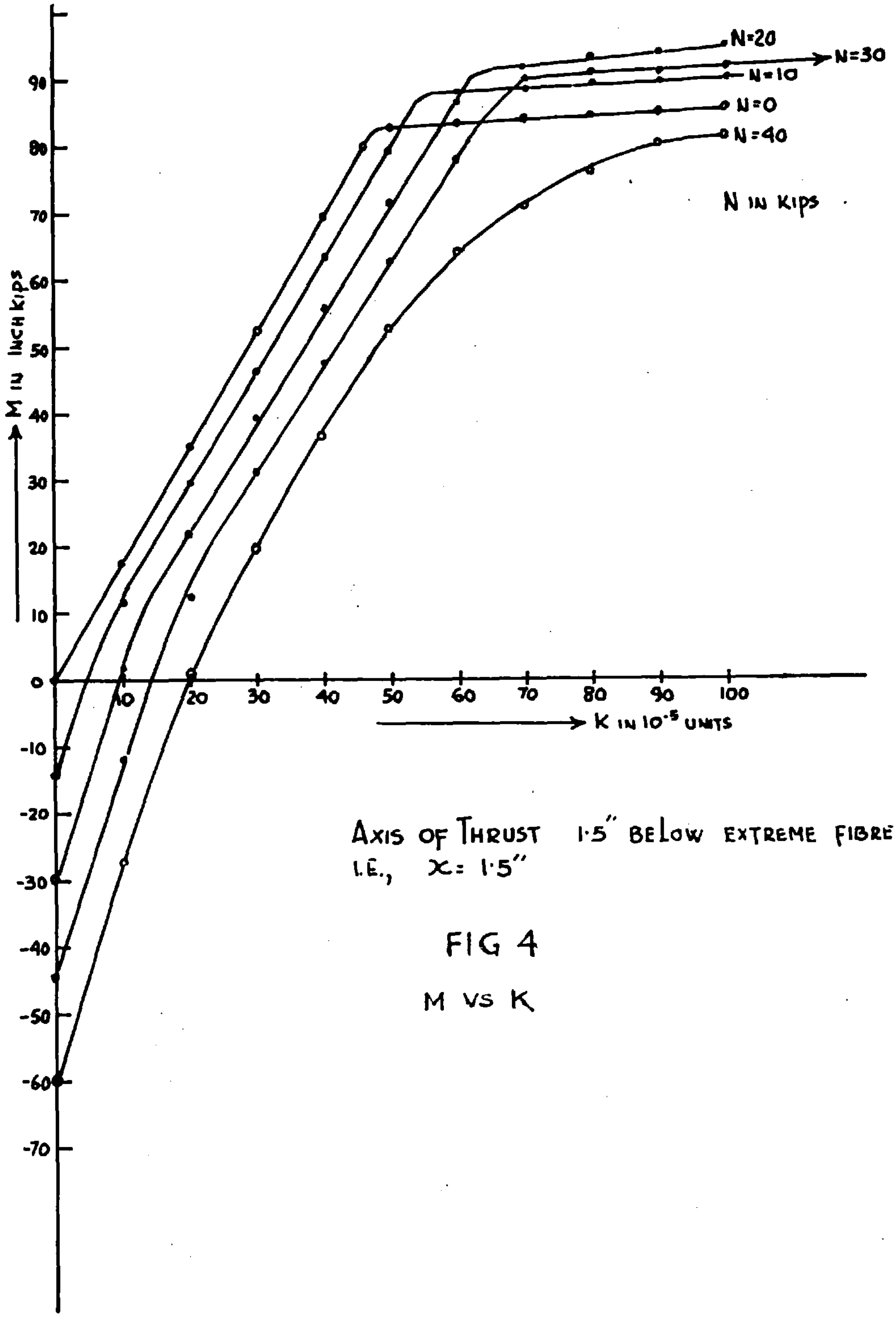
N=20
N=30
N=10
N=0
N=40
N IN KIPS
M IN INCH KIPS
K IN 10^-5 UNITS
90
80
70
60
50
40
30
20
10
0
-10
-20
-30
-40
-50
-60
-70
10
20
30
40
50
60
70
80
90
100
Axis of Thrust 1·5" below extreme fibre
i.e., x = 1·5"

FIG 4

M VS K

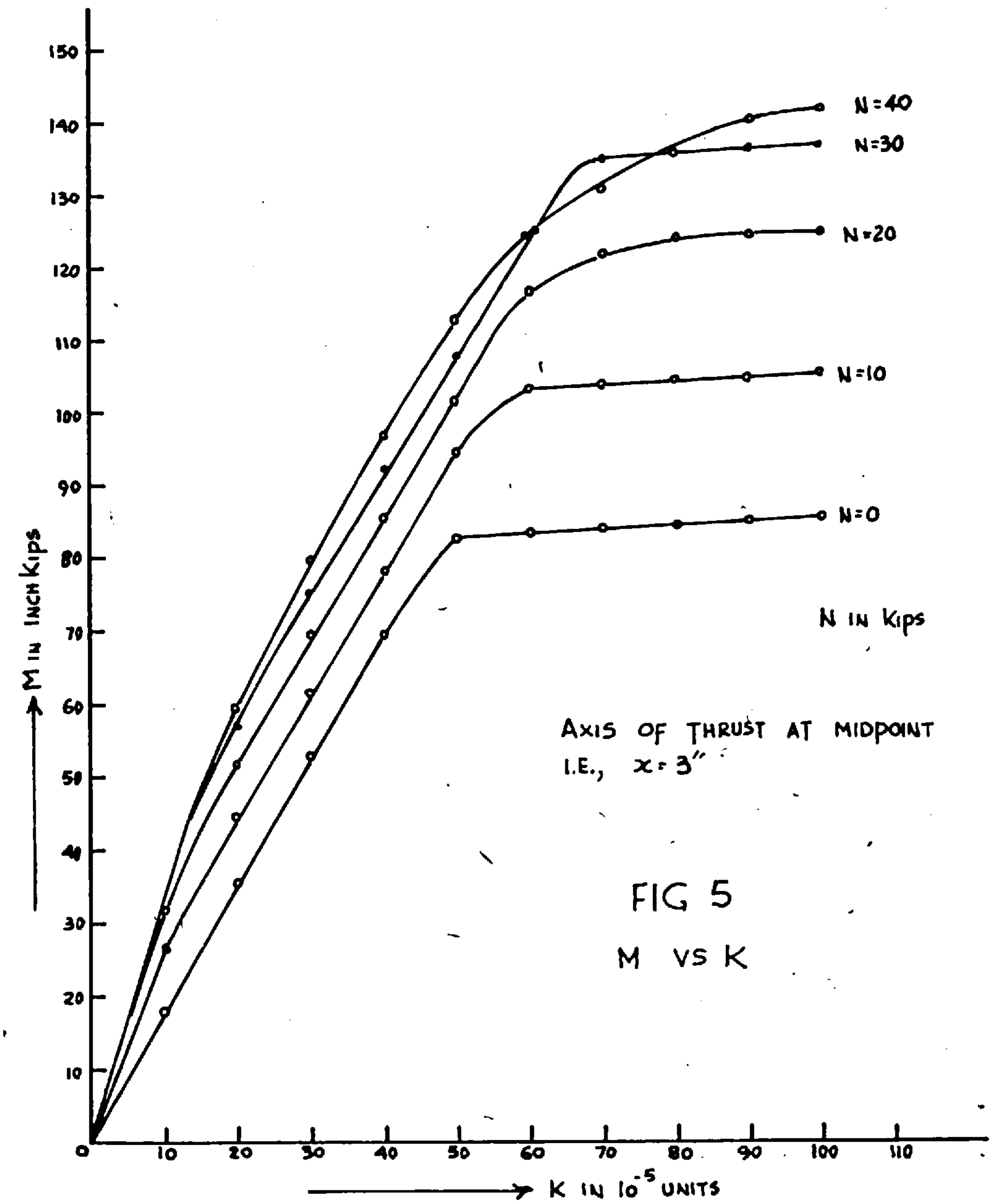
150
140
130
120
110
100
90
80
70
60
50
40
30
20
10
0
10
20
30
40
50
60
70
80
90
100
110
M IN INCH KIPS
K IN 10^{-5} UNITS
N=40
N=30
N=20
N=10
N=0
N IN KIPS
AXIS OF THRUST AT MIDPOINT
I.E., $x = 3''$

FIG 5

M VS K

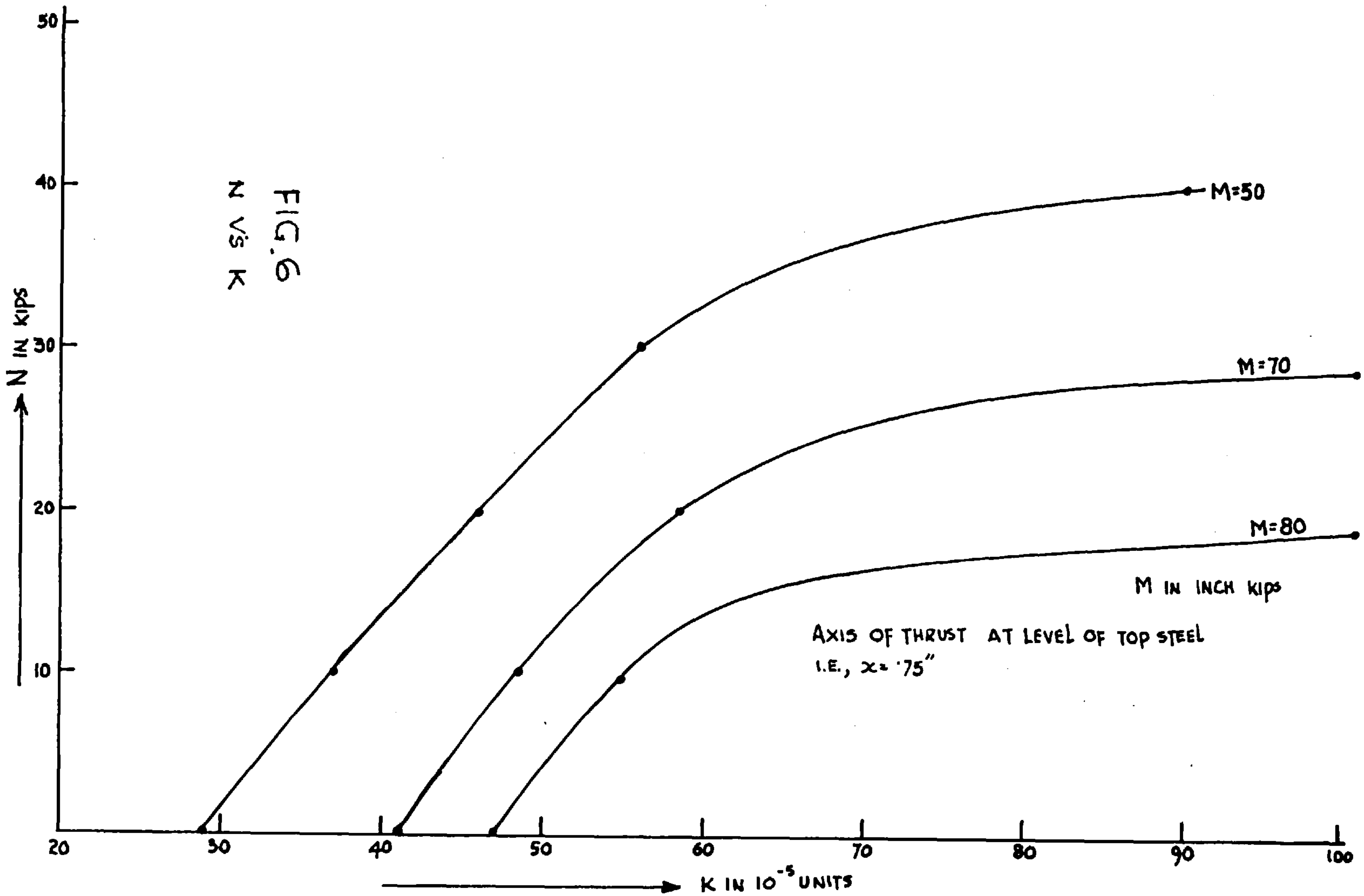

N IN KIPS
50
40
30
20
10
20
30
40
50
60
70
80
90
100
K IN 10^{-5} UNITS
M=50
M=70
M=80
M IN INCH KIPS
AXIS OF THRUST AT LEVEL OF TOP STEEL
I.E., x= ·75"

FIG. 6
N vs K

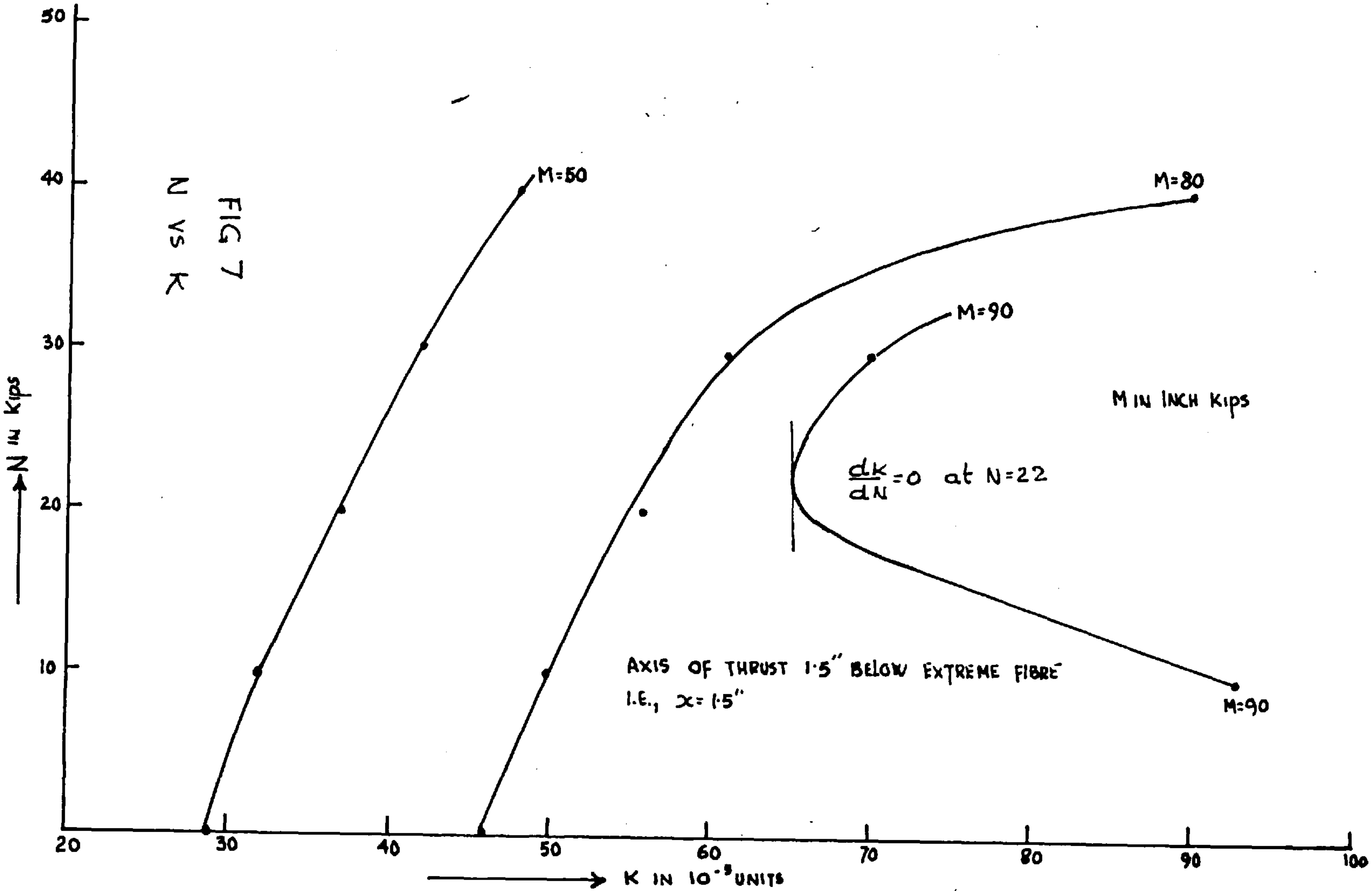

M=50
M=80
M=90
M=90
M IN INCH KIPS
$\frac{dK}{dN}=0$ at N=22
AXIS OF THRUST 1·5" BELOW EXTREME FIBRE
I.E., x= 1·5"
N IN KIPS
K IN 10^{-5} UNITS
50
40
30
20
10
20
30
40
50
60
70
80
90
100

FIG 7
N vs K

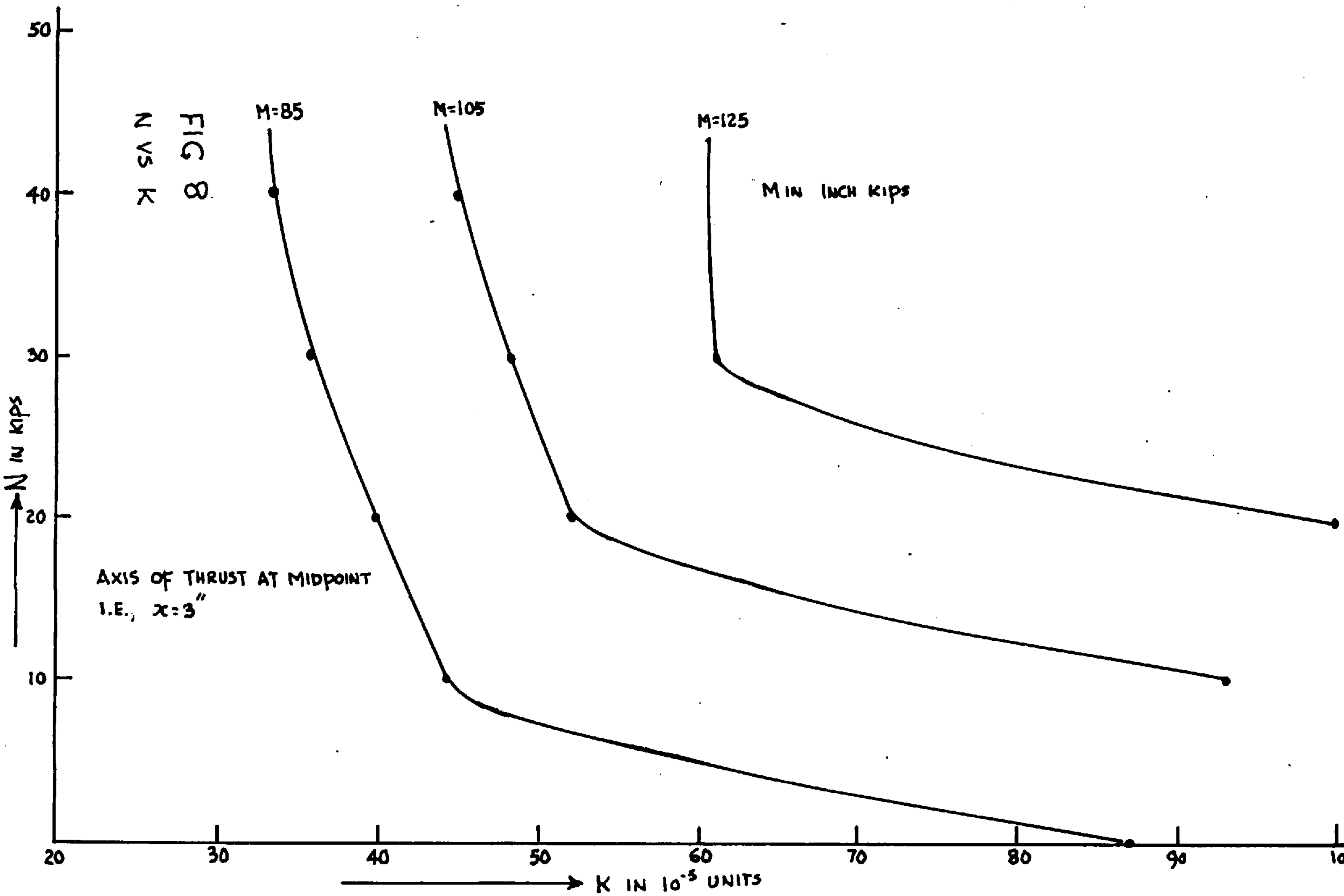
M=85
M=105
M=125
M IN INCH KIPS
AXIS OF THRUST AT MIDPOINT
I.E., x=3"
N IN KIPS
K IN 10^-5 UNITS
50
40
30
20
10
20
30
40
50
60
70
80
90
100

FIG 8
N VS K

APPENDIX 14.

RIB SHORTENING IN SECTIONS SUBJECTED TO PLASTICITY.

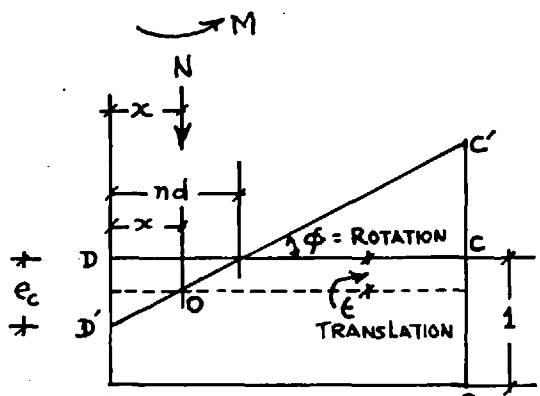

FIG. 1

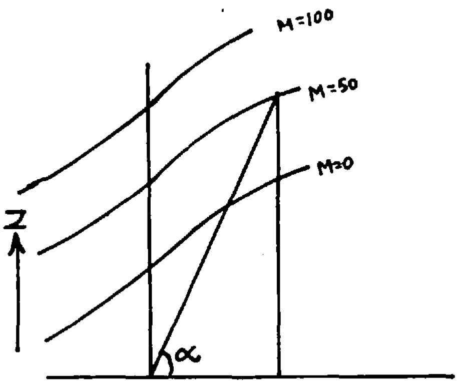

FIG 2

Let ABCD be an element of a member, having a length equal to unity, along the axis of the member. Let 'x' be the distance of the effective centroid from the face AD as defined earlier. Let the face CD assume a position C'D' by a rotation = Ø and a translation = ϵ , under the combined action of M and N acting at a distance of 'x' from AD.

As the element is of unit thickness, DD' = e_c

and $\tan \emptyset = \dfrac{e_c}{nd} = K$

The 'EI' value which is compatible with M & N is $\dfrac{M}{\tan \emptyset}$

The 'EA' " " " " "

" is $\dfrac{N}{\epsilon}$

where $\epsilon = e_c\left(1 - \dfrac{x}{nd}\right)$

It is possible to plot ϵ against N for different values of M as shown in Fig.2. The 'EA' value is then equal to tan α . In a rigorous analysis, this value of 'EA' should be used in integrals such as $\int \frac{n_i n_k}{EA} ds$, when deformations due to axial thrusts in cracked zones have to be taken into account.

APPENDIX - 15

FLOW DIAGRAM FOR CALCULATING MOMENT VS CURVATURE

ROUTINE 1
CALCULATES STRESS IN H.T STEEL, FOR A GIVEN STRAIN

ROUTINE 2
CALCULATES STRESS IN M.STEEL FOR A GIVEN STRAIN

ROUTINE 3
CALCULATES $\bar{C}_c$ FOR A GIVEN VALUE OF 'n_2'

ROUTINE 4
CALCULATES α & γ FOR A GIVEN VALUE OF 'e_c'

ROUTINE 5
CALCULATES 'e_{c2}' FOR GIVEN VALUES OF p'' & n_2

ROUTINE 6
CALCULATES EXTREME FIBRE STRESSES DUE TO PRESTRESS & ALSO 'e_{cp}'

ROUTINE 7
CALCULATES TOTAL COMPRESSION IN CONCRETE, TOTAL TENSION IN TENDONS AND MOMENT OF ALL FORCES INCLUDING AXIAL LOADS ABOUT FIBRE 2 — IN RECTANGULAR BEAMS
IT ASSUMES THAT $\bar{C}_c$, nd, & e_c ARE KNOWN
IT USES ROUTINES 1, 2, 4 & 6

ROUTINE 8
AS IN ROUTINE 7 BUT FOR I SECTIONS
IT USES ROUTINES 1, 2, 4, 6 & 7

ROUTINE 9
CALCULATES ULTIMATE MOMENT OF ANY SECTION (RECTANGULAR OR I)
AND USES ROUTINES 3, 5, 7 & 8

CONTINUED

ROUTINE 10
CALCULATES MOMENT FOR A GIVEN VALUE OF 'nd'. USES ROUTINES 7 & 8

ROUTINE 11
CALCULATES CURVATURE FOR A GIVEN VALUE OF MOMENT
USES ROUTINE 10

MAIN PROGRAMME

ENTRY 1 READ DATA WHICH DEFINES STRESS-STRAIN CHARACTERISTICS OF H.T. & MILD STEEL. READ VALUES OF 'e_p', STRAIN CORRESPONDING TO ·001 PROOF STRESS, AND ULTIMATE STRESS OF H.T STEEL. READ PROPERTIES OF CONCRETE SECTION, ECCENTRICITY OF TENDONS, CYLINDER STRENGTH, PERCENTAGE OF BINDERS AND THE GIVEN VALUE OF AXIAL LOAD, AND GIVEN SET OF MOMENTS

2 USE ROUTINE 9 TO DETERMINE VALUES OF n_2 AND M_2

3 USE ROUTINE 3 TO CALCULATE $\bar{C}_c$ CORRESPONDING TO n_2 FOUND IN 2

4 USE ROUTINE 11 TO CALCULATE VALUES OF CURVATURE CORRESPONDING TO MOMENTS WHICH NEARLY MATCH A GIVEN SET. STOP WHEN CALCULATED MOMENT IS NEARLY EQUAL TO M_2. PRINT OUT RESULTS

5 STOP

Flow Diagram of Routine 11

ENTRY 1 ASSUME A NEUTRAL AXIS DEPTH = OVERALL DEPTH 'D'. DECREASE IT IN STEPS OF ·1D. AT EACH STEP

2 JUMPDOWN TO ROUTINE 10 AND CHECK IF CALCULATED MOMENT IS ≥ GIVEN MOMENT

NO → (1 FOR FURTHER STEPS)

YES ↓

3 PUT 'nd' = ·1D + PREVIOUS VALUE WHEN IT LEFT 2 BUT NOW DECREASE IT IN STEPS OF ·01 D, AND

CONTINUED

4 JUMPDOWN TO ROUTINE 10 AND CHECK IF CALCULATED MOMENT IS ≥ GIVEN MOMENT
NO → 3 (FOR FURTHER STEPS)
YES ↓

5 PUT nd = ·01 D + PREVIOUS VALUE WHEN IT LEFT 4 BUT NOW DECREASE IT IN STEPS OF ·001 D &

6 JUMPDOWN TO ROUTINE 10 TO CHECK IF CALCULATED MOMENT IS ≥ GIVEN MOMENT
NO → 5 (FOR FURTHER STEPS)
YES ↓

7 CALCULATE CURVATURE FROM THE EQUATION $K = \frac{e_c}{nd}$
TAKE VALUE OF e_c AS OBTAINED IN ROUTINE 10
STORE THE VALUE OF CALCULATED MOMENT & CURVATURE FOR PRINTING.

8 RETURN TO MAIN PROGRAMME

FLOW DIAGRAM OF ROUTINE 10

ENTRY → 1 SELECT A SMALL VALUE OF STRAIN IN FIBRE 2 = ·0001. 'nd' IS KNOWN. START INCREASING THE VALUE OF e_c IN STEPS OF ·001 & AT EACH STEP

2 JUMPDOWN TO ROUTINE 7 OR 8 DEPENDING ON THE SECTION DO THE TOTAL TENSION + APPLIED THRUST IS ≤ COMPRESSION IN CONCRETE
NO → 1 (FOR FURTHER STEPS)
YES ↓

3 ASSUME e_c = PREVIOUS VALUE − ·001, BUT NOW INCREASE IT IN STEPS OF ·0001 AT EACH STEP

4 JUMPDOWN TO ROUTINE 7 OR 8 AND CHECK AS IN 2
NO → 3 (FOR FURTHER STEPS)
YES ↓

5 ASSUME e_c = PREVIOUS VALUE − ·0001, BUT NOW INCREASE IT IN STEPS OF ·00001. AT EACH STEP

6 JUMPDOWN TO ROUTINE 7 OR 8 AND CHECK AS IN 2
NO → 5 (FOR FURTHER STEPS)
YES ↓

7 STORE CALCULATED VALUES OF e_c AND MOMENT FOR USE IN ROUTINE 11

8 RETURN TO MAIN PROGRAMME

NOTE- FLOW DIAGRAM OF ROUTINE 9 IS ON THE SAME TECHNIQUE AND HAS BEEN OMITTED

APPENDIX 16.

Let the moments at all releases and at L, be the same and be equal to M_u at collapse (See Fig.1). Let the rotations represented by the shaded areas be A, B, C etc.

$$A = \frac{a}{2M_uM_c}(\phi_u \cdot M_c - \phi_c \cdot M_u)(M_u - M_c),$$

$$B = \frac{b}{2M_uM_c}(\phi_u \cdot M_c - \phi_c \cdot M_u)(M_u - M_c)$$

Let a_1 b_1 c_1 d_1 e_1 f_1 be the ordinates of the unit moment diagram at Release 1, corresponding to the position of C.Gs of A, B, C, D, E, F, and so on, then:

$$a_1 = 0 \qquad a_2 = \frac{a}{3h}\,\frac{M_u - M_c}{M_u} \qquad a_3 = 1 - \frac{a}{3h}\,\frac{M_u - M_c}{M_u}$$

$$b_1 = 0 \qquad b_2 = 1 - \frac{b}{3h}\,\frac{M_u - M_c}{M_u} \qquad b_3 = \frac{b}{3h}\,\frac{M_u - M_c}{M_u}$$

$$c_1 = \frac{c}{3h}\,\frac{(M_u - M_c)}{M_u} \qquad c_2 = 1 - \frac{c}{3h}\,\frac{M_u - M_c}{M_u} \qquad c_3 = 0$$

$$d_1 = 1 - \frac{d}{3h}\left(\frac{M_u - M_c}{M_u}\right) \qquad d_2 = \frac{d}{3h}\,\frac{M_u - M_c}{M_u} \qquad d_3 = 0$$

$$e_1 = 1 + \frac{e}{3h}\left(\frac{M_u - M_c}{M_u}\right) \qquad e_2 = \frac{e}{3h}\,\frac{M_u - M_c}{M_u} \qquad e_3 = 0$$

$$f_1 = 2 \qquad f_2 = 2 - \frac{f}{3h}\,\frac{M_u - M_c}{M_u} \qquad f_3 = 1 - \frac{f}{3h}\,\frac{M_u - M_c}{M_u}$$

Discontinuities caused by shaded areas are given by:

$$\left(\begin{array}{ll} \text{At Release } 1 = & -Cc_1 + Dd_1 + Ee_1 - Ff_1 \\ \text{" \quad " } 2 = & -Aa_2 + Bb_2 + Cc_2 - Dd_2 + Ee_2 - Ff_2 \\ \text{" \quad " } 3 = & Aa_3 - Bb_3 - Ff_3 \end{array}\right.$$

For the structure assume M_u = 91000 (average),

ϕ_u = 131 units of 10^{-5}

For releases 1, 2 and 3, assume M_c = 55000,

ϕ_c = 11 (units) of 10^{-5}

For the last hinge at L, assume M'_c = 30000,

ϕ'_c = 10 (units) of 10^{-5}

Note: above assumptions are based on m-k relations derived from a computer analysis described in Chapter 5.

$$A=B=C=D= \frac{27}{2} \times \frac{36000}{91000 \times 55000} \times \frac{(131 \times 55000 - 11 \times 91000)}{10^5} = .006$$

$$E = .012$$

$$F = \frac{54}{2} \times \frac{61000}{91000 \times 30000} \times \frac{(131 \times 30000 - 10 \times 91000)}{10^5} = .018$$

$a_1 = 0$	$a_2 = .066$	$a_3 = .934$
$b_1 = 0$	$b_2 = .934$	$b_3 = .066$
$c_1 = .066$	$c_2 = .934$	$c_3 = 0$
$d_1 = .934$	$d_2 = .066$	$d_3 = 0$
$e_1 = 1.132$	$e_2 = .132$	$e_3 = 0$
$f_1 = 2$	$f_2 = 1.776$	$f_3 = .776$

From above we obtain Rotation at Release 1 = -.017

" " " 2 = -.02

" " " 3 = -.0088

compare with rotations obtained by bilinear idealization which were:

For release 1 = - .01135

" " 2 = - .0227

" " 3 = - .01135

Note that the difference is not significant.

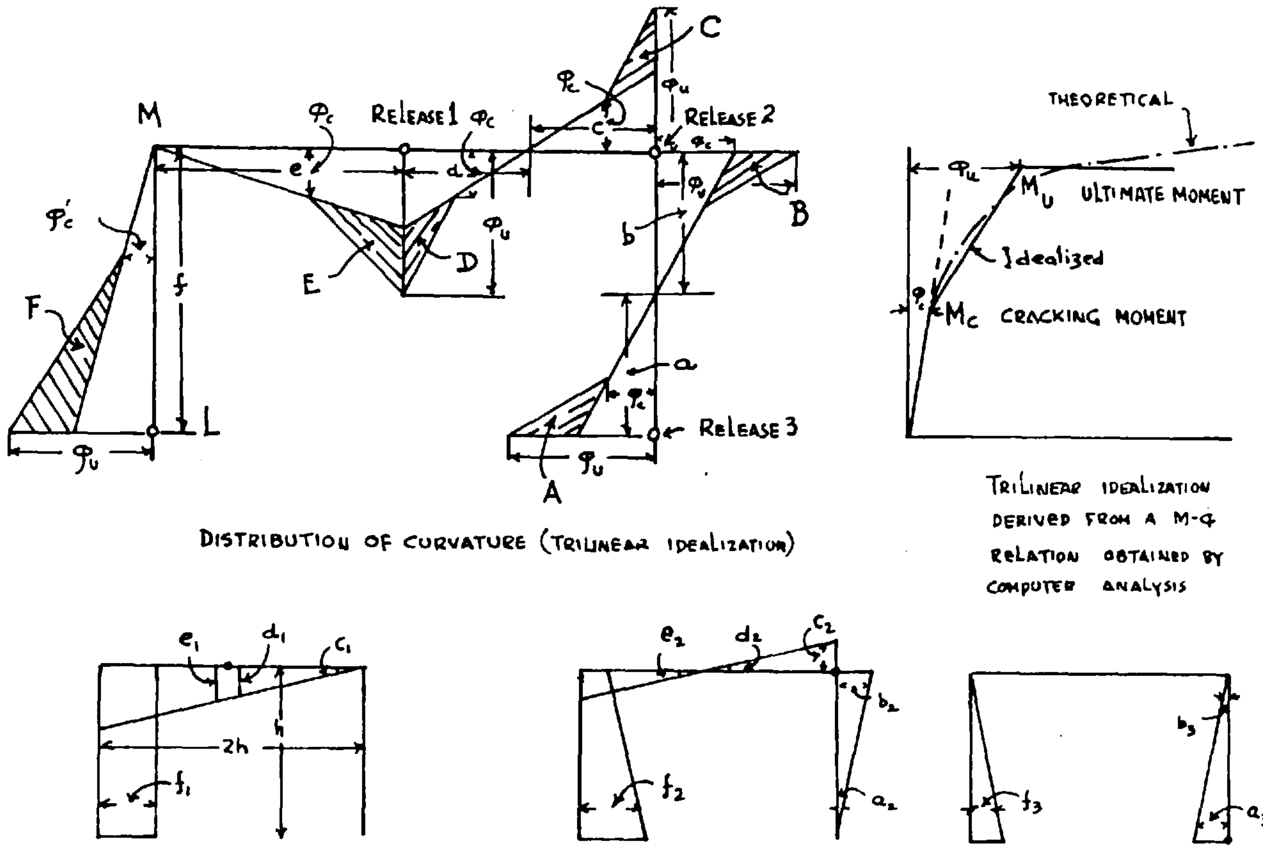

DISTRIBUTION OF CURVATURE (TRILINEAR IDEALIZATION)

TRILINEAR IDEALIZATION DERIVED FROM A M-φ RELATION OBTAINED BY COMPUTER ANALYSIS

UNIT MOMENT AT RELEASE 1

UNIT MOMENT AT RELEASE 2

UNIT MOMENT AT RELEASE 3

FIG 1

APPENDIX 17.

EFFECT OF INTERNAL STRESSES ON ROTATIONS IN FRAME 2.

Let the distribution of moments in the structure, before it is loaded, be as shown as under

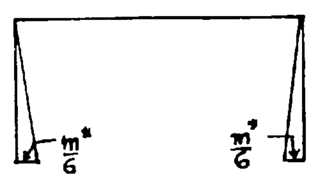

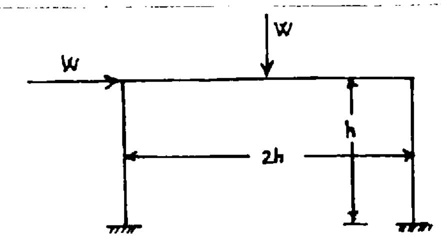

STRUCTURE & APPLIED LOADS

Stage 1. - At this stage, the first hinge forms at the foot of the right-hand column. The applied load W_1 is given by

$$.4125 W_1 h = \frac{5}{6} m^* \quad \text{or} \quad W_1 = \frac{2.02 m^*}{h}$$

The bending moment at the end of this stage is as under

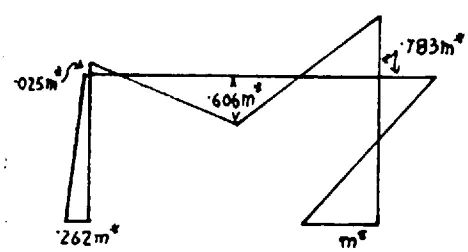

Stage 2. - At this stage, the second hinge forms at the top of the right-hand column. The additional load W_2 is given by

$$\frac{67}{158} W_2 h = (1 - .783) m^* \quad \text{from which } W_2 = \frac{.512 m^*}{h}$$

Total load at the end of this stage is $\frac{2.532 m^*}{h}$

The distribution of moment at the end of this stage is as under:-

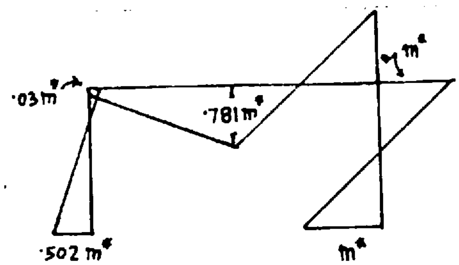

Stage 3. - At this stage, the third hinge forms at the centre of the transom. The additonal load W_3 is given by

$$\frac{23}{40} W_3 h = (1-.781)m^* \text{ or } W_3 = .381\frac{m^*}{h}$$

$$\text{Total load} = 2.913 \frac{m^*}{h}$$

The bending moment distribution at the end of stage 3 is as under:-

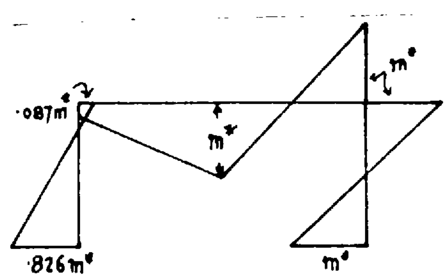

Stage 4. - At this stage the 4th hinge forms at the foot of the left-hand column. The additional load W_4 is given by

$$2W_4h = (1- .826)m^* \quad \text{or } W_4 = .087\frac{m^*}{h}$$

$$\text{Total load} = 3.000 \frac{m^*}{h}$$

Calculation of Rotations.

Rotations between any two stages are calculated by integrating the bending moment diagram due to a unit moment at the chosen release, and the change in the bending moment diagram due to the additional load acting.

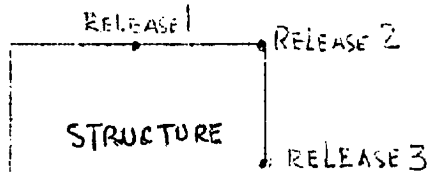

This is shown below:-

Rotations at stages →	Release 3	Release 2	Release 1
Between 1 and 2	$(-\frac{5}{6}+1x.342+\frac{2}{3}x.424).\frac{.512m^*h}{EI}$ $=-.21 \times \frac{.512m^*h}{EI}$ $=-.107\frac{m^*h}{EI}$	-	-
Between 2 and 3	$(-\frac{5}{6}+1x.575).\frac{.381m^*h}{EI}$ $= -.26x.\frac{381m^*h}{EI}$ $= -.\frac{099m^*h}{EI}$	$(-\frac{8}{3}+\frac{11}{3}x.575).\frac{.381m^*h}{EI}$ $= -.56x.381\frac{m^*h}{EI}$ $= -.\frac{214m^*h}{EI}$	-
Between 3 and 4	$-\frac{5}{6}x.087\frac{m^*h}{EI}=-.\frac{0725m^*h}{EI}$	$-\frac{8}{3}x.087\frac{m^*h}{EI}=-.\frac{232m^*h}{EI}$	$-\frac{23}{6}x.087\frac{m^*h}{EI}$ $=-.\frac{334m^*h}{EI}$
	Total $= -.\frac{278m^*h}{EI}$	$-.\frac{446m^*h}{EI}$	
Compare with rotations when internal moments are nil.	$-.\frac{166m^*h}{EI}$	$-.\frac{33m^*h}{EI}$	$-.\frac{166m^*h}{EI}$

APPENDIX 18.

In modern structures, redistribution may be necessary from the central span towards the supports, to economize on total quantity of steel. Take a continuous beam over three spans, with ends fixed (to simulate conditions existing in a multispan structure.)

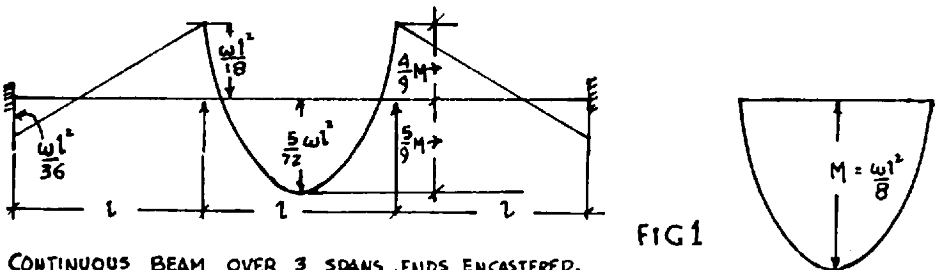

CONTINUOUS BEAM OVER 3 SPANS. ENDS ENCASTERED. U.D.L. IN CENTRE SPAN

FIG 1

FREE BM. DIAGRAM

Let it be required to reduce $\frac{5}{9}M$ by 30%.

Apply unit moment at the centre of middle span on the released structure and we get a bending moment distribution shown in diagram 1 of Fig. 2.

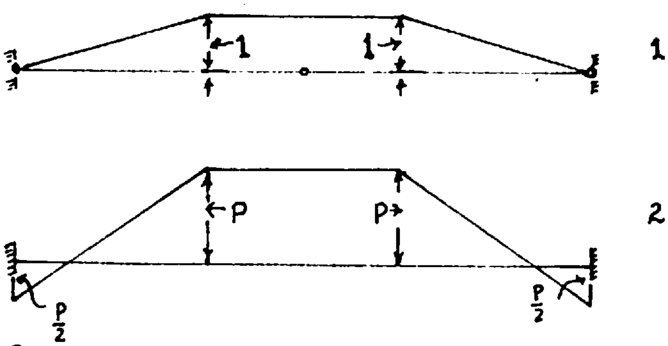

FIG 2

REDISTRIBUTION MOMENT ACTING ON THE STRUCTURE

Integrate diagram 1 with the distribution plastic moment shown in diagram 2.

we obtain $\frac{P\ell}{4EI} + \frac{P\ell}{EI} + \frac{P\ell}{4EI} = \frac{3}{2}\frac{P\ell}{EI}$

If P is 30% of $\frac{5}{9}M$, then required rotation

$$= \frac{3}{2}.\frac{1.5M}{9}.\frac{\ell}{EI} = \frac{M\ell}{4EI}$$

now $EI = \frac{mnd}{e_c}$, in this case 'm' $= \frac{5}{9}M$ so $EI = \frac{5}{9}\frac{Mnd}{e_c}$

Hence required rotation $= \frac{3}{2}.\frac{1.5}{9}.\frac{M}{M}.\frac{9}{5}.\frac{e_c}{nd}$

assuming $n = .5$

and $d = \frac{\ell}{25}$

$$= \frac{3}{2} \times .3 \times \frac{.002}{.5} \times 25$$

$= .045$ radians which is fairly high.

Note:- It will be difficult to attain this value when $n = .5$, without the use of binders.

LIST OF REFERENCES.

1. Amarakone A.M.N. 'Deformation characteristics of reinforced concrete columns subjected to bending' M.Sc. Thesis (London) 1963.

2. do. 'Limit design of Reinforced Concrete skeletal structures' Ph.D., Thesis (London) 1966

3. Arthanari S. Sundarasan 'Influence of temperature and Bi-axial stresses on creep in concrete', Ph.D., Thesis (London) 1966.

4. Baker A.L.L. 'Reinforced Concrete', Concrete Publications 1949.

5. do 'Ultimate load theory applied to the design of reinforced concrete and prestressed concrete frames'. Concrete Publications 1956.

6. do 'Recent research in Reinforced Concrete and its application to design' - journal of the I.C.E. Vo.35, structural paper No. 26 (Feb.51).

7. do. 'Further Research in Reinforced Comcrete and its application to ultimate load design.' Journal of the I.C.E. Vol.2 part III, Aug 53.

8. Baker A.L.L. 'A general equation for frame analysis'. - Concrete and Constructional Engineering - March 61.

9. do. 'Proposed co-ordination on inelastic deformation' C.E.B. Bulletin No.30.

10. do. 'The inelastic space frame' - a Concrete Publications Ltd. 1967

11. Baker and Amarakone 'Inelastic Hyperstatical frames - Analysis and application of International correlated tests, originally presented to the Hyperstatic Symposium of E.C.C. an Ankara in Sept. 64 and presented for disucssion at the Institute of Structural Engineers on 30.3.65.

12. Discussions on '11' at the meeting attended by the author.

13. Baker's letter No. CVE/ALLB dated 10.3.65, to all E.C.C. prestressed members - regarding Trilinear Idealization of prestressed members. (Now incorporated in '10).

14. Bremner T.W. 'Influence of reinforcement on the elastic and inelastic properties of reinforced concrete members' M.Sc. Thesis (London) 1963.

15. Burnett E.F.P. 'The ultimate load design of statically indeterminate concrete structures'. M.Sc. Thesis (London) 1963.

16. Burns Ned H., Chester P, Seiss F., 'Plastic Hinging in reinforced concrete.' Journal of the Structural Division proceedings of the A.S.C.E., Oct. 66.

17. Chan W.W.L. 'An investigation into characteristics of plastic hinges in reinforced concrete'. Ph.D., Thesis (London) 1954.

18. Chinwah. 'The strength and deformation characteristics of eccentrically loaded reinforced concrete columns'. M.Sc. Thesis (London 1965.

19. Cooke Nigel. 'The redistribution of bending moments in continuous prestressed concrete beams'. Ph.D., Thesis (Leeds) 1965.

20. Corley W. Gene. 'Rotational capacity of reinforced concrete beams.' Journal of the Structural Division Proceedings of the A.S.C.E. October 1966.

21. Cranston W.B. 'A computer method for inelastic analysis of plane frames.' March 1965. TRA/386 Cement and Concrete Assn.

22. Cranston W.B. 'Determination of moment axial load, curvature relations for structural members' TRA/395 June 1966, Cement and Concrete Association.

23. do. University of Newcastle, Department of Civil Engineering, International Symposium, July 1966. 'The use of Electronic digital computers in structural engineering'. Paper No. 4. 'A computer method of inelastic analysis of plane frames.'

24. Dastur 'An analytical and experimental investigation of the 'EI' values of prestressed and reinforced concrete beams'. M.Sc. Thesis, London 1960.

25. Edwards A.D. 'The elastic behaviour and ultimate strength of reinforced and prestressed concrete frames' Ph.D., Thesis, London 1965.

26. Evans and Benett. 'Prestressed Concrete'. Chapman & Hall Ltd., 1958.

27. Gupta , B.K., 'The ultimate strength of statically indeterminate prestressed concrete structures'. Ph.D., Thesis (London) 1967.

28. Guyon Y. 'Prestressed Concrete' Vol. I.

29. do. 'Prestressed Concrete' Vol. II.

30. Hernandez G. 'Strength of prestressed concrete beams with web reinforcement', Ph.D. Thesis, University of Illinois, May 1958.

31. Horne & Merchant. 'Stability of Frames'.

32. La Grange L.E. 'Moment redistribution in prestressed concrete beams and frames', Ph.D.Thesis (Cambridge) June 1961.

33. Leonhardt F. 'Prestressed concrete design and construction', Wilhelm Ernst & Sohn, second edition.

34. Macchi G. 'Proposed method of analysis based on the theory of imposed rotation'. C.E.B. Bulletin No. 21, January 1960.

35. Mullick S.K. 'Redistribution of moments in 2-span prestressed concrete beams', Magazine of concrete research Vo. 14, No. 42 - November 1962.

36. Morris P.B. 'Linear structural analysis', Thames and Hudson, 1958.

37. Moss-Morris A.L. 'An investigation of the factors affecting the collapse loads of reinforced concrete frames', Ph.D., Thesis (London).

38. Munro J. 'The elastic and limit analysis of planar skeletal structures', Civil Engineers and Public Works Review, May 1965.

39. Neal B.G. 'The plastic methods of structural analysis', Chapman and Hall (London) 1963.

40. Pietrzykowski J. 'The elastic plastic behaviour of prestressed concrete frames' - Magazine of Concrete Research, Vol.16, No. 48, September 1964.

41. Poologasoundranayagam, K. 'An analytical and experimental investigation of the formation and behaviour of plastic hinges in prestressed and reinforced concrete frames', Ph.D., Thesis, London 1960.

42. Poologasoundranayagam K and Tokarski E.W. 'The analysis of multi-storey frames by the plastic hinge method', Concrete publications.

43. Raina V.K. 'Ultimate moment distribution in continuous prestressed concrete beams', Ph.D., Thesis (London) 1966.

44. England & Ross 'Reinforced concrete under thermal gradients', Magazine of Concrete Research. Vol. 14, No. 40, March, 1962.

45. Sawyer, H.A. 'Elasti-plastic design of single span beams and frames' - Proceedings A.S.C.E., December 1955.

46. Somes U.F. 'Moment rotation characteristics of prestressed concrete members - Stage I', Rectangular Section. from his Ph.D. Thesis (London) 1966

47. Soliman M.T., 'Ultimate strength and plastic rotation capacity of reinforced concrete members ', Ph.D.Thesis (London) 1966.

48. Yu, C.W., 'An analytical investigation of the ultimate load design of reinforced concrete framed structures', Ph.D., Thesis, (London) 1954.

49. Report by Research Committee "Ultimate load design of concrete structures" proceedings I.C.E., February 1962.

50. Road Note No. 4, Department of Scientific and Industrial Research, Road Research Laboratory.